DOCTOR OF PHILOSOPHY

Innovative Topical Formulations from Bio-Based Polymers for Transdermal Drug Delivery

Froom, Richard

Award date:
2023

Awarding institution:
Bangor University

Innovative Topical Formulations from Bio-Based Polymers for Transdermal Drug Delivery

Richard Thomas Froom MChem

School of Natural Sciences
Bangor University

A thesis submitted to Bangor University in partial fulfilment
for the degree of Doctor of Philosophy

Ysgoloriaethau Sgiliau Economi Gwybodaeth
Knowledge Economy Skills Scholarships

Cronfa Gymdeithasol Ewrop
European Social Fund

Declaration to include in your thesis

I hereby declare that this thesis is the results of my own investigations, except where otherwise stated. All other sources are acknowledged by bibliographic references. This work has not previously been accepted in substance for any degree and is not being concurrently submitted in candidature for any degree unless, as agreed by the University, for approved dual awards.

Yr wyf drwy hyn yn datgan mai canlyniad fy ymchwil fy hun yw'r thesis hwn, ac eithrio lle nodir yn wahanol. Caiff ffynonellau eraill eu cydnabod gan droednodiadau yn rhoi cyfeiriadau eglur. Nid yw sylwedd y gwaith hwn wedi cael ei dderbyn o'r blaen ar gyfer unrhyw radd, ac nid yw'n cael ei gyflwyno ar yr un pryd mewn ymgeisiaeth am unrhyw radd oni bai ei fod, fel y cytunwyd gan y Brifysgol, am gymwysterau deuol cymeradwy.

Acknowledgements

Firstly, I would like to acknowledge KESS II for making this project possible. Without their funding and support I would not be in this position today, and I owe them a large deal of gratitude. I would particularly like to highlight Penny Dowdney for her constant support when required, and for her enthusiasm to ensure that PhD candidates have an enjoyable and fulfilling project. Penny goes above and beyond in her role, and I very much respect and appreciate what she does.

Secondly, I would like to thank Dr Hongyun Tai who gave me the opportunity to undertake my PhD.

It is important for me to highlight the influence of Dr Patrick Murphy who supported me upon Dr Tai's departure from Bangor University after the announcement of the closure of the Chemistry department. Patrick had no reason to act as an on-site supervisor, but not only supervised me, but went above and beyond to support me throughout a difficult final 9 months at the university. He taught me not just about chemistry, but about life, and he truly is a strong mentor who I firmly respect. If I only had a fraction of his understanding of chemistry, I would be in a fantastic position for the rest of my future career. I am also grateful to the Jamie, Joe and Daniel from the Patrick Murphy Group who supported me in my brief time with them.

I would like to thank the Bangor University School of Natural Sciences staff, especially those formerly of the School of Chemistry, for providing me with the facilities to perform my study. This includes the lecturers at the university for their constant influence on me as a chemist, and the technical staff for maintaining that the department was in a suitable condition to allow for me to complete my research.

I would like to extend my gratitude to my former company supervisor Alan Marsh from P&S Nano. Although they left the project in the early phases, they still played an important part in making the project possible and had a large influence on the project direction.

I am grateful to the entirety of the members of the Hongyun Tai Group, and the 501 office, who were there at any point throughout my project, for their support

throughout my project: Kenny, James, Mohammed, Sohad, Tom, Chester, Alex and David made my time in the department much more enjoyable. I would like to highlight the efforts of Dr Chester Blackburn for his facilitation of my growth, and his support when listening to problems I had encountered throughout my project, along with his influence over the manner in which I conducted myself as a researcher. Chester was a model researcher and set the standard I wished to adhere to as a chemist. I would also like to emphasise my gratitude to David Mondragon for his help with understanding how drug release can be quantified via UV analysis.

I would also like to express my gratitude for Dr Vera Thoss for allowing me to use her Centrifuge, and to Nicholas Welsby for training me to operate it. Thanks to Professor Igor Perepichka and his group for allowing me access to their 'Shimadzu UV-3600 UV' machine. Thanks to Dr Martina Lahmann for her insight into Copper Click Chemistry.

A special thank you to Ben Assinder, and the Bangor University School of Computer Science and Electronic Engineering, for their assistance in obtaining SEM images.

I would like to thank Dr. Chandra Senan, and Dr. Ian Ratcliffe from Glyndwr University, and for allowing access to the use of their Zetasizer 1000HS, and William Rhys Griffiths for his assistance in the work regarding stimuli responsive polymers.

Thank you to Wenxin Wang from University College Dublin for taking the time to influence the polymer selection for the stimuli responsive polymers research, and for his assistance in GPC analysis.

I would like to thank Rolf Kraehenbuehl for his assistance in obtaining Mass Spectrometry data for the compounds formulated in this chapter. I would also like to thank Graham J. Tizzard, and the UK National Crystallography Service, for allowing me to submit samples for X-Ray Crystallography analysis.

I would like to thank my family and friends. There is no chance that I would have been able to get this far in life without their constant love and support, whilst also motivating me to keep going with my project even in the bleakest hours. My father Robin, and my mother Cheryl, have constantly given me everything I need to succeed, and their unconditional support means the world to me. My brother Matthew has

always been able to bring the best out of me, knows when to tell me exactly what I need to hear, and can say exactly how it is whilst keeping spirits high. Thanks to my friends Gavin Williams, Jeff Simpkins, Alex Davies, Matthew Derby, Simon Lam, Liam Davies, and James Simpkins for being there when I needed them. A special thanks to my good friend Peter Huyton who deserves a special mention for his ability to keep me grounded, listening to me, and giving me much valued advice.

Finally, I would like to give a huge thank you to my loving partner, Claire Fuller. I met Claire whilst doing my thesis write-up, and her support throughout the long process has been nothing short of phenomenal. Claire motivated me to keep going when times were most difficult, and I couldn't have made it this far without her. I love her with all my heart.

A large thank you to you all from the bottom of my heart.

Declaration and Consent

Details of the Work

I hereby agree to deposit the following item in the digital repository maintained by Bangor University and/or in any other repository authorized for use by Bangor University.

Author Name: Richard Thomas Froom

Title: Innovative Topical Formulations from Bio-Based Polymers for Transdermal Drug Delivery

Supervisor/Department: Dr Patrick Murphy/School of Natural Sciences

Funding body (if any): Knowledge Economy Skills Scholarships 2 (KESS 2)

Qualification/Degree obtained: PhD in Chemistry

This item is a product of my own research endeavors and is covered by the agreement below in which the item is referred to as “the Work”. It is identical in content to that deposited in the Library, subject to point 4 below.

Non-exclusive Rights

Rights granted to the digital repository through this agreement are entirely non-exclusive. I am free to publish the Work in its present version or future versions elsewhere.

I agree that Bangor University may electronically store, copy or translate the Work to any approved medium or format for the purpose of future preservation and accessibility. Bangor University is not under any obligation to reproduce or display the Work in the same formats or resolutions in which it was originally deposited.

Bangor University Digital Repository

I understand that work deposited in the digital repository will be accessible to a wide variety of people and institutions, including automated agents and search engines via the World Wide Web.

I understand that once the Work is deposited, the item and its metadata may be incorporated into public access catalogues or services, national databases of electronic theses and dissertations such as the British Library’s EThOS or any service provided by the National Library of Wales.

I understand that the Work may be made available via the National Library of Wales Online Electronic Theses Service under the declared terms and conditions of use (http://www.llgc.org.uk/index.php?id=4676). I agree that as part of this service the

National Library of Wales may electronically store, copy or convert the Work to any approved medium or format for the purpose of future preservation and accessibility. The National Library of Wales is not under any obligation to reproduce or display the Work in the same formats or resolutions in which it was originally deposited.

Statement 1:

This work has not previously been accepted in substance for any degree and is not being concurrently submitted in candidature for any degree unless as agreed by the University for approved dual awards.

Signed Richard Thomas Froom (candidate)

Date 16/05/2023

Statement 2:

This thesis is the result of my own investigations, except where otherwise stated. Where correction services have been used, the extent and nature of the correction is clearly marked in a footnote(s). Other sources are acknowledged by footnotes giving explicit references. A bibliography is appended.

Signed Richard Thomas Froom (candidate)

Date 16/05/2023

Statement 3:

I hereby give consent for my thesis, if accepted, to be available for photocopying, for inter-library loan and for electronic repositories, and for the title and summary to be made available to outside organisations.

Signed Richard Thomas Froom (candidate)

Date 16/05/2023

NB: Candidates on whose behalf a bar on access has been approved by the Academic Registry should use the following version of **Statement 3:**

Statement 3 (bar):

I hereby give consent for my thesis, if accepted, to be available for photocopying, for inter-library loans and for electronic repositories after expiry of a bar on access.

Signed Richard Thomas Froom (candidate)

Date 19/05/2023

Statement 4:

Choose one of the following options

a) I agree to deposit an electronic copy of my thesis (the Work) in the Bangor University (BU) Institutional Digital Repository, the British Library ETHOS system, and/or in any other repository authorized for use by Bangor University and where necessary have gained the required permissions for the use of third party material.	YES
b) I agree to deposit an electronic copy of my thesis (the Work) in the Bangor University (BU) Institutional Digital Repository, the British Library ETHOS system, and/or in any other repository authorized for use by Bangor University when the approved bar on access has been lifted.	
c) I agree to submit my thesis (the Work) electronically via Bangor University's e-submission system, however I opt-out of the electronic deposit to the Bangor University (BU) Institutional Digital Repository, the British Library ETHOS system, and/or in any other repository authorized for use by Bangor University, due to lack of permissions for use of third party material.	

Options B should only be used if a bar on access has been approved by the University.

In addition to the above I also agree to the following:

1. That I am the author or have the authority of the author(s) to make this agreement and do hereby give Bangor University the right to make available the Work in the way described above.
2. That the electronic copy of the Work deposited in the digital repository and covered by this agreement, is identical in content to the paper copy of the Work deposited in the Bangor University Library, subject to point 4 below.
3. That I have exercised reasonable care to ensure that the Work is original and, to the best of my knowledge, does not breach any laws – including those relating to defamation, libel and copyright.

4. That I have, in instances where the intellectual property of other authors or copyright holders is included in the Work, and where appropriate, gained explicit permission for the inclusion of that material in the Work, and in the electronic form of the Work as accessed through the open access digital repository, or that I have identified and removed that material for which adequate and appropriate permission has not been obtained and which will be inaccessible via the digital repository.

5. That Bangor University does not hold any obligation to take legal action on behalf of the Depositor, or other rights holders, in the event of a breach of intellectual property rights, or any other right, in the material deposited.

6. That I will indemnify and keep indemnified Bangor University and the National Library of Wales from and against any loss, liability, claim or damage, including without limitation any related legal fees and court costs (on a full indemnity bases), related to any breach by myself of any term of this agreement.

Signature:

Date 16/05/2023

Abstract

The work detailed in this thesis details the development of bio-based polymer films designed for use in transdermal drug delivery.

This thesis is comprised of six chapters which all detail different aspects of the story of this work over the course of the three years of the project. Chapter one introduces the basis for the project and highlights the reasons for using bio-based polymers in transdermal films tailored for drug delivery, as well as the challenges faced in doing so. This chapter also covers the history of transdermal drug delivery, as well as the use of polymers in medicine including hydrogel formulation, the advantages of hyperbranching and stimuli-responsive polymers and the techniques used to synthesize them, methods for controlled drug delivery, and methods of transdermal medication formulation and trans dermal drug delivery.

Chapter two focusses on developing transdermal films using various methods, including the layer by layer technique, in order to determine which materials and development methods can be used to make films which exhibit desirable properties. This chapter also focusses on attempting to load and release drugs from the films in order to determine if they were capable of being used in transdermal drug delivery to patients using UV analysis to determine the effectiveness of the drug release from the films.

Chapter three looks at which drugs have been selected for use in the bio-based polymer transdermal films, explaining why galantamine has been chosen as a prime candidate. Galantamine has been commonly used in the treatment of Alzheimer's disease. Alzheimer's patients would benefit from the use of bio-based polymer transdermal films, as it would improve the ease of use, drug efficiency and patient comfortability. This chapter discusses which materials and material concentrations in the transdermal films have been used and how they affect the release profile of galantamine from the films, as well as exploring the optimal release media conditions. Various films were formulated, loaded with galantamine, and released under different conditions to determine which was the most favourable for use in transdermal drug delivery. Alginate and chitosan bio-based polymer films were of particular interest, with

assessing how altering the level of guluronic acid present in alginate effects galantamine release. Galantamine is commonly used in its galantamine hydrobromide form, but free base galantamine maybe more favourable in the use of transdermal drug delivery, prompting a release comparison between the two forms.

Chapter four shifts in focus to stimuli-responsive polymers and the formulation of galantamine prodrugs can be used in enhancing the release of drugs from films in transdermal drug delivery. Three reducible and dual responsive (pH and temperature) hyperbranched polymers were synthesized via Reversable Addition-Fragmentation Chain Transfer (RAFT) copolymerization of 2-(Dimethylamino)ethyl methacrylate (DMAEMA) and disulfanediylbis(ethane-2,1-diyl) diacrylate (DSDA) using varying ratios, subsequently polymers chains extended using N-isopropylacrylamide (NIPAM) to afford the temperature responsive properties to the polymers. 4-cyano-5-(((dodecylthio)carbonothioyl)thio)-4-methylpentanoic (CDTMA) was used as a RAFT agent. Galantamine hydrobromide was encapsulated within a selected hyperbranched polymer, which was loaded into a sodium alginate–chitosan transdermal film and used to assess its effect on the release of galantamine hydrobromide against a film where the polymer is absent. drug modification of galantamine is explored in an attempt to improve drug release and drug efficacy. (4a*S*,6*R*,8a*S*)-3-methoxy-11-methyl-4a,5,9,10,11,12-hexahydro-6H-benzo[2,3]benzofuro[4,3-cd]azepin-6-yl, commonly known as ‘memogain’ is a galantamine derived compound made through esterification of galantamine with benzoyl chloride. The resulting compound, memogain, has an increased lipophilicity as a result, which is assumed to give it an improved amount of release from bio-based polymer films into the skin, and also to improve its bioavailability in the brain. Conclusions are made on how using stimuli responsive polymers, and galantamine prodrugs, effect the rate of release and overall release of drugs from bio-polymer films.

Finally, chapter five features a conclusion based on the results of the work conducted in this thesis, and the future work which could be studied in the event this work were to be continued. The project aims and results are scrutinised and evaluated to determine the level of success of the project work. Appendices are provided in chapter six of the thesis.

List of Abbreviations

ACVA - 4,4′-Azobis(4-cyanovaleric acid)

AESO - Soybean Oil Epoxidized Acrylate

AIBN - Azobisisobutyronitrile

ATRA - Atom Transfer Radical Addition

ATRP - Atom Transfer Radical Polymerisation

CDTMA - 4-Cyano-5-(((Dodecylthio)Carbonothioyl)Thio)-4-Methylpentanoic Acid

CP - Cloud Point

CSIRO - Commonwealth Scientific and Industrial Research Organisation

Da - Dalton

DCC - N,N'-Dicyclohexylcarbodiimide

DCM - Dichloromethane

DDS - Drug Delivery System

DLS - Dynamic Light Scattering

DMAEMA - 2-(Dimethylamino)ethyl methacrylate

DMAP - Dimethylaminopyridine

DMF - Dimethylformamide

DMSO - Dimethylsulfoxide

DNA - Deoxyribonucleic Acid

DSDA - Disulfanediylbis(Ethane-2,1-Diyl) Diacrylate

DTT - Dithiothreitol

Eq - Equation

FRP - Free Radical Polymerisation

FTIR - Fourier Transform Infra-Red

G - α-L-Guluronate

GLT - Galantamine

GPC - Gel Permeation Chromatography

HCl - Hydrochloric Acid

HESI-II - Heated Electrospray Ionisation

HBP - Hyperbranched Polymer

HBr – Hydrobromide

IMS - Industrial Methylated Spirits

IR – Infra Red

IUPAC - International Union of Pure and Applied Chemistry

LbL - Layer by Layer technique

LC-MS - Liquid Chromatography Mass Spectrometry

LCST - Lower Critical Solution Temperature

M - (1,4)-linked β-D-Mannuronate

Mn - Number Averaged Molecular Weight

MOPP - Nitrogen Mustard Combined with Mechlorethamine, Vincristine, Procarbazine, and Prednisone

MOPP-ABV - Nitrogen Mustard Combined with Mechlorethamine, Vincristine, Procarbazine, and Prednisone (MOPP), combined with Adriamycin bleomycin, and vinblastine

MS - Mass Spectrometry

MVM - Multi Vinyl Monomer

NFT - Neurofibrillary Tangle

NIPAM - N-Isopropylacrylamide

NMR - Nuclear Magnetic Resonance

PDD - Poly(DMAEMA-DSDA)

PDDN - Poly(DMAEMA-DSDA)-PNIPAM

PEG - Polyethylene glycol

PEGDA - PEG Diacrylate

PET - Polyethylene Terephthalate

PHA - Poly(Hydroxy Alkanoates)

PLA - Polylactides

PMMA - Poly Methyl Methacrylate

QT - Pentaerythritol Tetrakis(3-Mercaptopropionate)

RAFT - Reversible Addition Frag-mentation chain-Transfer Polymerisation

RBF - Round Bottom Flask

RI - Refractive Index

RPM - Rotations Per Minute

SEM - Scanning Electron Microscopy

SS - Stock Solution

TEA - Triethylamine

THF - Tetrahydrofuran

TLC - Thin Layer Chromatography

UV - Ultra-Violet

UV-VIS - Ultraviolet Visible Spectroscopy

Đ - Dispersity

List of Figures

List of Tables

Table of Contents

Chapter 1 – Thesis Introduction

1.1 Alzheimer's Disease

Alzheimer's disease is a neurological disorder which causes the deterioration of a person's memory, thinking skills, behaviour and cognitive abilities[1]. Clinical Alzheimer's disease has been defined as a disease which causes dementia[2]. Dementia itself is not a specific disease, it is a general term which refers to memory impairment and the inability to make decisions which affects everyday activities[3]. Alzheimer's is the leading cause of dementia in developed countries[4] with Alzheimer's accounting for 60-70% of dementia cases[5]. There is no cure for Alzheimer's Disease, however there is medicine and techniques available which aid in slowing the degradation of a person suffering with Alzheimer's symptoms[6]. This chapter discusses the history and causes of Alzheimer's disease, the battle to help those suffering with the disease, including medicines and therapeutic approaches, and the discussion of transdermal drug delivery as a preferable drug delivery method.

1.1.1 The History of Alzheimer's Disease

Dementia itself has been present in the entirety of human history. Even as far back as 2000 BC, the ancient Egyptians were aware that memory disorders could occur in the elderly, even citing that judgement could be impaired by old age. In the 2nd century, the Hellenistic Empire wrote about dementia, and similar mental disorders, noting that they were irreversible cognitive impairments. References to dementia like symptoms are also seen in Greek and Roman literature. The term dementia is believed to have first been used in 1797 by physician Philippe Pinel, though it could have been earlier. Pinel was one of the earliest to give a detailed assessment of what dementia entails, and the symptoms of those who suffer with it[7].

In 1906, Dr Alois Alzheimer identified changes in the brain tissue of a woman, Auguste Deter, who had died with the cause being cited as a mental illness. Her symptoms included those commonly associated with Alzheimer's as we know it today: memory loss and cognitive difficulties. Upon examination of the deceased woman's brain, Dr Alzheimer was able to determine that her brain contained abnormal clumps and bundles of fibres, which are now referred to as amyloid plaques, and neurofibrillary tangles[8].Dr Alzheimer would go on to publish descriptions of patients who had suffered similar fates to Auguste Deter. In 1910, Emil Kraepelin was the first to use the name 'Alzheimer's Disease' when classifying patients who exhibited the pathological features first identified by Dr Alzheimer[9]. Due to Auguste Deter being only 51 years old at her time of death, Alzheimer's Disease was branded as a "presenile dementia" in order to ensure it was easily distinguished from senile dementias related to ageing. However, it was later determined that tangles were also present in elderly patients exhibiting symptoms of dementia[10]. In 1976, a neurologist named Robert Katzman stated that presenile and senile Alzheimer's types should no longer be distinguished[11].

By 1984, the National Institute of Neurological and Communicative Disorders and Stroke, along with the Alzheimer's Disease and Related Disorders Association, detailed the most commonly used diagnosis for Alzheimer's disease[12] stating that neuropsychological testing be used as a clinical technique to confirm its presence in a patient. This included a histopathological confirmation with a microscopic examination of the patient's brain tissue[13]. The resulting findings meant that by the mid 1980s, Alzheimer's was known to be the leading cause of dementia in elderly sufferers[14].

1.2 Causes of Alzheimer's Disease

1.2.1 Amyloid Beta (Aβ) Accumulation - The Amyloid Hypothesis

The formation of neurofibrillary tangles, and amyloid plaques as a result of large quantities of amyloid beta (Aβ) accumulation, causes the brain to progressively lose

function[15]. Aβ consists of up to 42 toxic amino acids, and is produced by the cleavage of a transmembrane protein named the Amyloid Precursor Protein - a protein which can penetrate a neuron's membrane - which is first cleaved by β-secretase, and again by γ-secretase, resulting in Aβ formation [Figure 1- 1][16][17]. When Aβ molecules clump together the result is oligomers which exhibit flexible and soluble properties[17]. These oligomers are both neurotoxic, and toxic to nerve cells[18]. The result of Aβ accumulations is a toxic cascade leading to mass cell death, disruption of brain cell activity, and then interruption of protein function which causes the degradation of brain function and eventually leads to the brain shrinking in size [Figure 1- 2][21][19]. The Amyloid hypothesis is believed to be the leading hypothesis for Alzheimer's pathophysiology due to the interpretation of the relation between amyloid plaque formation and brain functionality degradation[20].

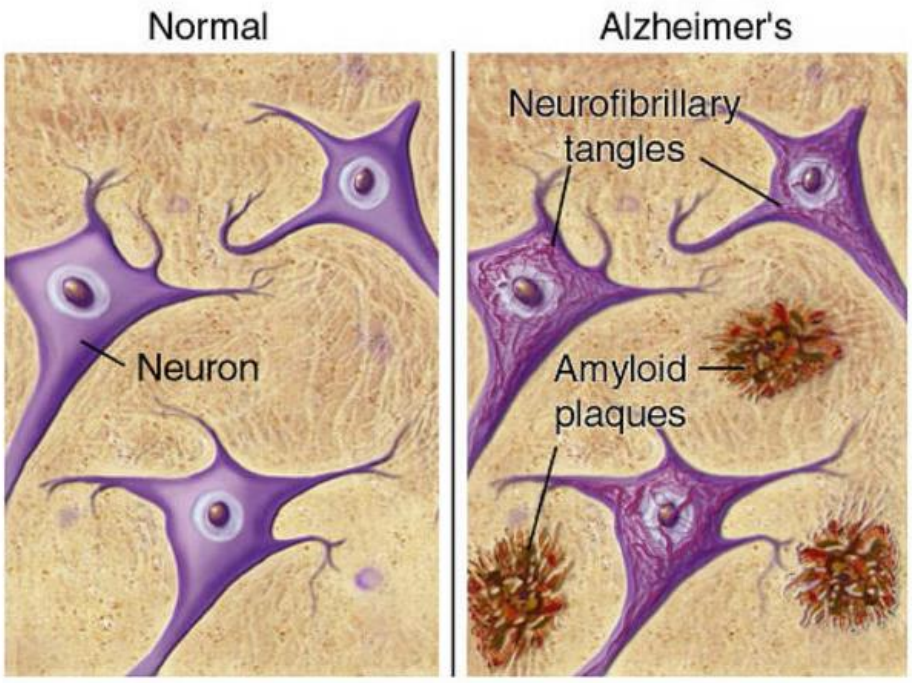

Figure 1- 1: A diagram depicting the appearance of neurons in a normal brain (left) against a brain of a person with alzheimer's (right)[17].

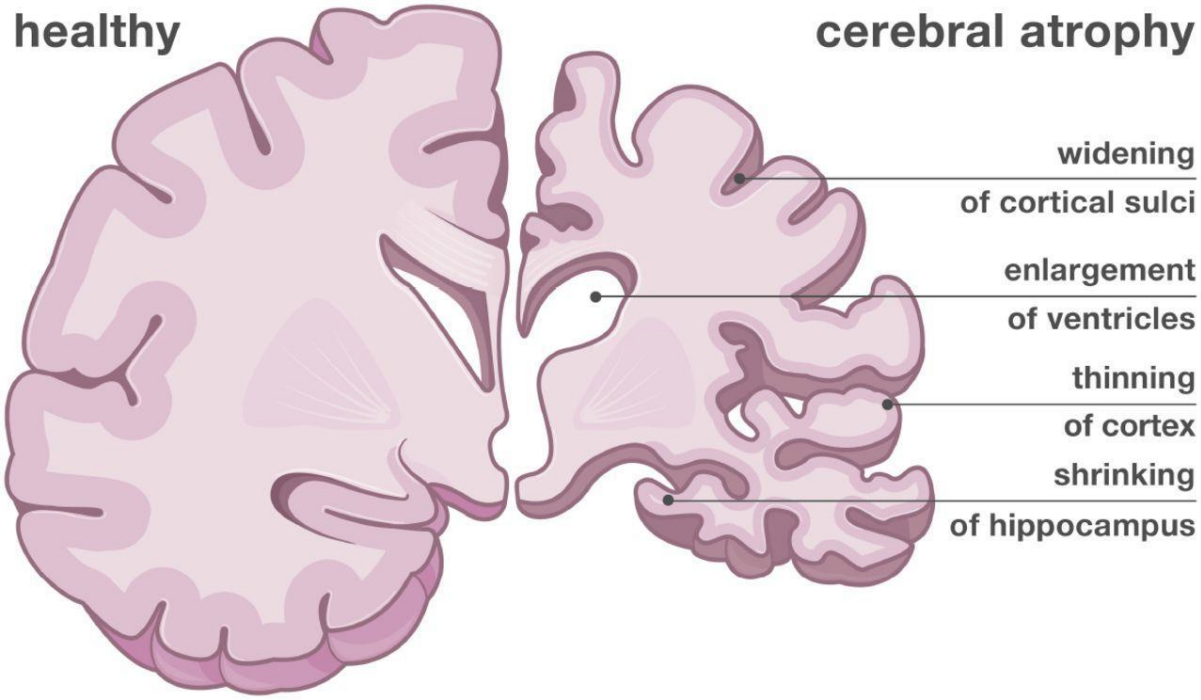

Figure 1- 2: A diagram illustrating the effect of cerebral atrophy resulting from Alzheimer's disease[21].

1.2.2 The Tau Hypothesis

The Tau hypothesis is a less supported alternative to the Amyloid hypothesis[22]. Tau proteins are soluble proteins found in neurons, and are a group of six protein isoforms consisting of between 352 to 441 amino acids[23]. Tau proteins are microtubule-associated proteins associated with ensuring the functionality of the cytoskeletal network in terms of microtubule assembly[24].The basis for the Tau hypothesis is that hyperphosphorylated tau proteins pair together with tau threads resulting in paired helical filaments[25]. When the amount of paired helical filaments increases, it causes the formation of neurofibrillary tangles within nerve cells[26]. This leads to microtubules disintegrating, which causes structural degradation of cell cytoskeletons, which leads the neurons transport system to fail [Figure 1- 4][27].

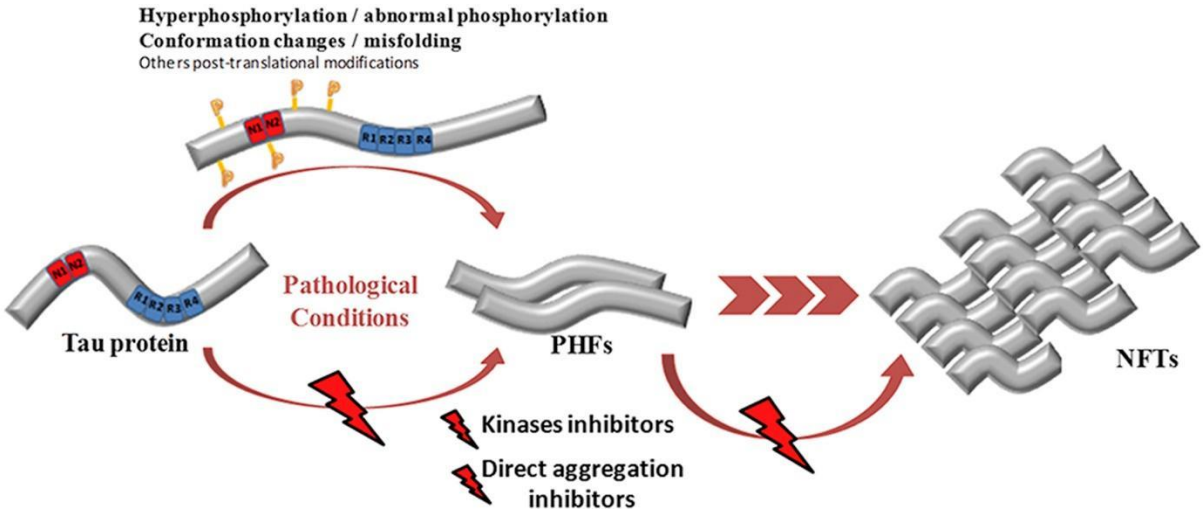

Figure 1- 3: Hyperphosphorylation of tau proteins, leading to paired helical filaments (PHFs) which clump to form Neurofibrillary Tangles (NFTs)[28].

1.2.3 Genetic Inheritance

Although most cases are not linked to inheritance, some cases of Alzheimer's disease can be linked to being genetically inherited, typically resulting in early onset Alzheimer's types referred to as early-onset familial Alzheimer's disease[29]. Mutations in presenilin proteins PS1 and PS2, along with the amyloid precursor protein are often found in cases of early-onset familial Alzheimer's disease [Figure 1- 4][30]. Mutations in these genes result in Aβ production, leading to amyloid plaque build-up[31].

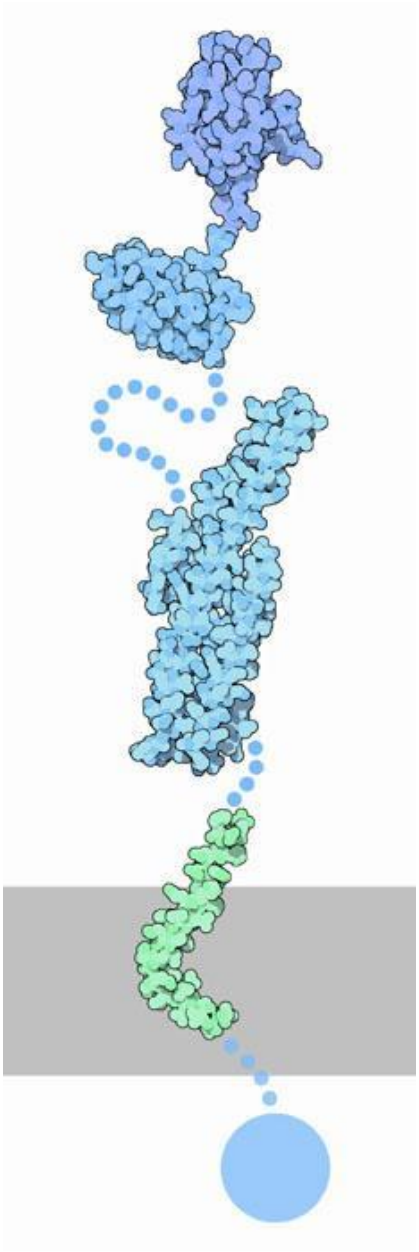

Figure 1- 4: The amyloid-beta precursor protein. Flexible portions that are not included in the structures are shown with dots, and the membrane is shown schematically in grey[30].

1.2.4 Alternative Theories

The inflammation hypothesis works on the understanding that astrocytes and reactive microglia will surround amyloid plaques and tau proteins, release pro-inflammatory cytokines, and promote their spread[32]. The key argument against the

inflammation hypothesis is that the use of anti-inflammatory drugs has not shown to be beneficial in the fight against Alzheimer's disease[32].

The cholinergic hypothesis states that Alzheimer's disease is linked to damaged acetylcholine neurotransmitters [Figure 1- 5], resulting in cognitive decline[33]. Acetylcholine is an important neurotransmitter which affects memory and cognitive function[34]. This hypothesis reasoned that cholinesterase inhibitors would be crucial in the treatment of Alzheimer's disease, and while they do slow down the onset effects of Alzheimer's disease, none have been found which prevent it entirely[32][35].

Another hypothesis given consideration is the oxidative stress hypothesis, with oxidative stress considered to be an important factor in the pathogenesis of Alzheimer's disease[36]. The reasoning is that the brain exhibits mitochondrial respiration[37]. When the mitochondria is exposed to stressful conditions ROS formation is increased by the mitochondria's electron transport system, causing mitochondrial dysfunction which results in neurodegeneration[38][39]. Oxidative stress also results in the imbalance of oxidants and antioxidants, which in turn affects the balance of transition metals within the brain, such as copper, iron and zinc which all affect cognitive regions of the brain[39]. Copper and zinc can bind to Aβ and its precursor protein, giving it an important role in neurodegeneration[39]. It is reasoned that smoking[40], and exposure to air pollution[41], are two common factors which can make someone more susceptible to exhibiting oxidative stress, and are therefore linked to increasing the risk factor of developing Alzheimer's disease in the later stages of a person's life.

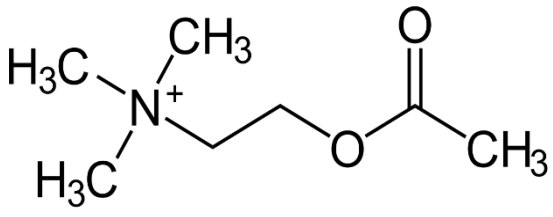

Figure 1- 5: The chemical structure of acetylcholine.

1.2.5 Traumatic Brain Injury

There is a link between people who suffer traumatic brain injuries and an increased likelihood of developing Alzheimer's disease in later life. Although not fully understood, it is believed that traumatic brain injury induced neurovascular damage can result in the acceleration of Aβ production[42]. Athletes who compete in heavy contact sports such as Rugby, American Football and Boxing have been found to have an increased risk of forming Alzheimer's disease like dementias in later life, due to receiving multiple head injuries and concussions[43].

1.2.6 Increased Likelihood of Developing Alzheimer's Disease with Age

It is recognised that Alzheimer's Disease is more prevalent in the elderly[44]. It is believed that the reason for this is that tau proteins are able to spread at a faster rate in elderly brains[45]. Researchers have posed that tau protein deposition begins within the anterolateral entorhinal cortex, and the presence of Aβ facilitates the spread of tau proteins allowing it to reach the neocortex, which some scientists suggest is where Alzheimer's disease begins[46]. The simplest answer as to why the risk of developing Alzheimer's disease increases with age is because Aβ deposition and tau aggregation is more prevalent in elderly brains as they accumulate as humans age[47]. It should be noted that avoiding the formation of Aβ and tau as age increases is unavoidable for most people as they get older, though it does not mean that it will result in developing Alzheimer disease, or any form of dementia[47][48].

1.3 Symptoms of Alzheimer's

1.3.1 Earliest Symptoms

The earliest symptoms of Alzheimer's disease include short-term memory loss, and an increased amount of apathy. It has been recognised that patients exhibiting the earliest symptoms of Alzheimer's have issues with acquiring and remembering recently learned information, whilst also struggling with abstract thinking and planning[49]. Apathy is seen as the most common behavioural change in patients developing the disease, and is a direct link to cognitive decline, and the lowering of daily function[50]. The name given to the preclinical stage of Alzheimer's disease is Mild Cognitive Impairment which is diagnosed in patients suffering memory loss, and has over 90% association with Alzheimer's disease[51].

1.3.2 Early stages

Patients in the early stages of Alzheimer's disease will see their ability to retain new information decrease, while problems with their memory increase. Some may also exhibit new difficulties with movement, language and possibly impaired perception[52]. It is recognised that in the early stages, memories formed more recently by patients are more likely to deteriorate than memories and facts learned by the patient earlier in their life[53]. Issues with language can become more apparent[54]. Patients will exhibit a shrunken vocabulary, and find it more difficult to express ideas, or conceptions, through vocabulary or in a written form[54]. Patients in the early stages of the disease can still complete everyday tasks, and interact with other people, though they may require support with more complex activities[55].

1.3.3 Middle stages

Patients in the middle stages of the disease experience further difficulties when performing basic tasks, requiring them to have a greater amount of support[56]. Vocabulary also deteriorates further, and can result in patients using incorrect substitutions of words or phrases, whilst also seeing their ability to read and write become more hindered[57]. Motor skills become more difficult, which naturally increases the likelihood of an accident when attempting complex movements[58]. It is at the middle stages where long-term memory becomes hindered, and results in patients potentially failing to recognise faces of those who have been consistently present in their lives[59]. As Alzheimer's disease progresses, behavioural changes in patients may become increasingly apparent, with emotional outbursts becoming more common, including crying, aggression, frustration and irritability[60]. Another common symptom of behavioural change in the middle stages is wandering, where a patient will roam, which can result in them becoming lost due to confusion of their location[61]. Some patients have been reported to have exhibited delusional symptoms such as experiencing hallucinations and illusions[62]. Perhaps the most difficult symptom of all during the middle stages is that patients lose their understanding of their diagnosis resulting in a loss of realising their limitations and ability to recognise their ongoing deterioration[57].

1.3.4 Later stages

Patients in the later stages of Alzheimer's disease struggle to perform the simplest of tasks, and are completely dependent on carers[63]. A patient's vocabulary will have drastically reduced to basic phrases, a limited amount of words, or in some cases no speech at all, but still may be able to give emotional prompts and responses[64]. Apathy and exhaustion become far more prevalent in the later stages, which leads to a loss of muscle mass, often resulting in late stage patients spending the majority of their time in bed[57]. Cerebral apathy occurs as a result of damage to neurons, which causes brain shrinkage [Figure 1- 6]. Alzheimer's does not usually

cause death directly, but does instead cause patients to become more susceptible to infection, including pneumonia, and other illnesses, leading to the death of a patient with Alzheimer's disease[65].

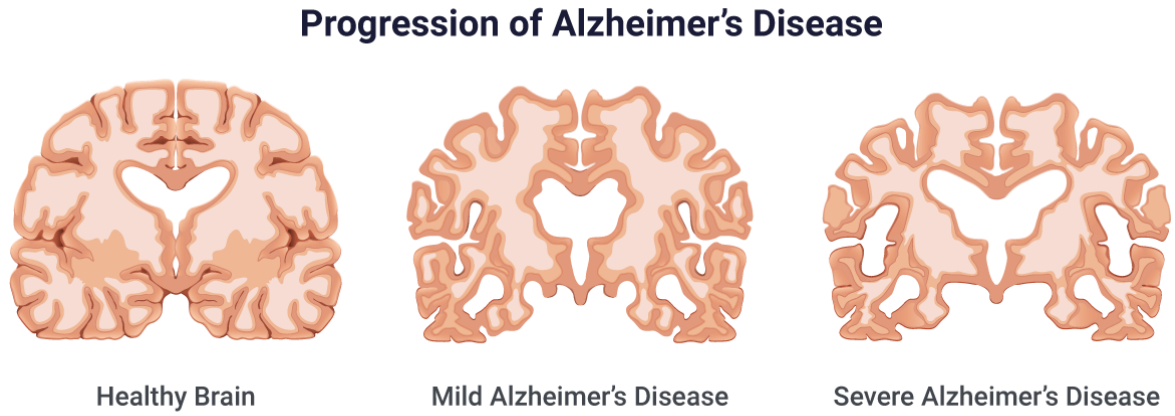

Figure 1- 6: The progression of the brain through the stages of Alzheimer's disease[57].

1.4 Pharma Company's Therapies for Alzheimer's

1.4.1 The Dementia Consortium

In 2013 Alzheimer's Research UK, the UK's leading dementia research charity, partnered with MRC Technology and pharmaceutical companies, Eisai and Lilly, to found the 'Dementia Consortium'. To date, there are eight members of Dementia Consortium: Alzheimer's Research UK, Evotec, along with pharmaceutical companies Johnson & Johnson, Abbvie, MSD, Eisai, Lilly, and Astex Pharmaceuticals. The consortium set out to bring together Alzheimer's disease experts from the private sector, charities, and academia in order to identify and develop drug targets and therapies for the treatment of the disease. The Dementia Consortium members contribute drug discovery resources, project funding, and tools which allow them to support small molecule and antibody-based techniques with the goals of identifying

drug candidates or therapies to prevent Alzheimer's, combat the symptoms of the disease, and ultimately to cure the disease. The consortium also donates funding to research into drug discovery for frontotemporal dementia and neurodegeneration-associated cognitive defects, dementia with Lewy bodies, plus Parkinson's disease, Huntington's disease and amyotrophic lateral sclerosis[66][67].

1.4.2 The Leading Companies in the Development of Alzheimer's Drugs

There are many large pharmaceutical companies putting resources into Alzheimer's drug development. As of September 2019, there are six companies with drugs in phases 1, 2 and 3 of clinical trials. Lilly has six drugs in Alzheimer's clinical trials, with two in phase 1, two in phase 2, and two in phase 3 trials. Biogen has five drugs - two in phase 1, one in phase 2, and two in phase 3 trials. Roche has three drugs - two in phase 2, and one in phase 3. Esiai, in collaboration with Biogen, has one drug in phase 3 trials[68].

In May 2022, it was published in a paper that there are currently 143 drugs in development for the treatment of Alzheimer's disease. The pipeline showed 30 drugs in phase 1 clinical trials, 82 drugs in phase 2, and 31 drugs in phase 3. Of these drugs,

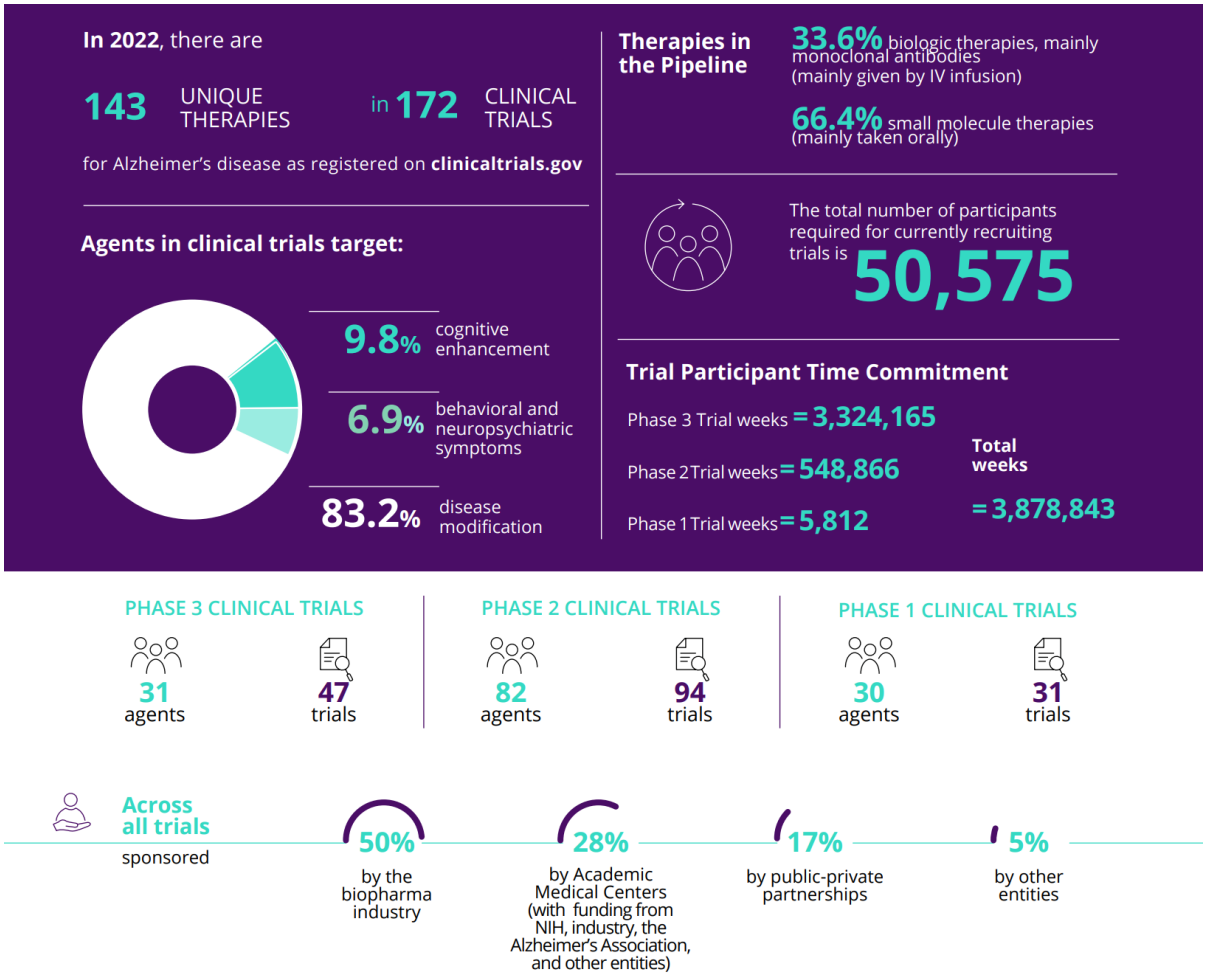

Figure 1- 7: An info graphic of the Alzheimer's disease drug development pipeline as of May 2022[69].

83% were designed for use as disease-modifying therapies, 10% as symptomatic cognitive enhancing treatments, and 7% as treatment of neuropsychiatric symptoms [Figure 1- 7][69].

1.4.3 Management of Alzheimer's Disease

There is currently no effective medication for the prevention of Alzheimer's disease, nor is there any medication which can impede the cognitive can impede the cognitive degradation resulting from disease progression[70]. There are medications used to help hinder cognitive degradation along with advice to aid in delaying Alzheimer's disease surfacing in people at higher risk.

1.4.3.1 Acetylcholine Inhibitors

Currently the most effective medications to hinder cognitive degradation are classified as acetylcholine inhibitors or cholinesterase inhibitors. The three most effective acetylcholine inhibitors currently on the market are donepezil, rivastigmine, and galantamine[71]. Galantamine and donepezil are labelled as short acting or reversible agents, whereas rivastigmine is labelled as an intermediate-acting or pseudo irreversible agent[71]. Tacrine was the first acetylcholine inhibitor, but due to tarcine's hepatotoxicity, the drug has been withdrawn from use[71]. It is recognised that the efficacy of the listed acetylcholine inhibitors are similar, with all of them being deemed as having mild benefits as drugs for treatment of the disease[71]. Currently pharmaceutical companies are working to improve the pharmacological activity of the acetylcholine inhibitors, whilst also attempting to eliminate the gastrointestinal side effects[71].

Acetylcholinesterase inhibitors work by inhibiting an enzyme named Acetylcholinesterase [Figure 1- 8] [72]. By inhibiting Acetylcholinesterase, the breakdown of acetylcholine is prevented[73]. Acetylcholine works as both a neurotransmitter and a neuromodulator[74]. By preventing the breakdown of acetylcholine in patients with Alzheimer's disease, it can result in the hindering of cognitive degradation as there is more acetylcholine available than there would be without the use of acetylcholinesterase inhibitors[75].

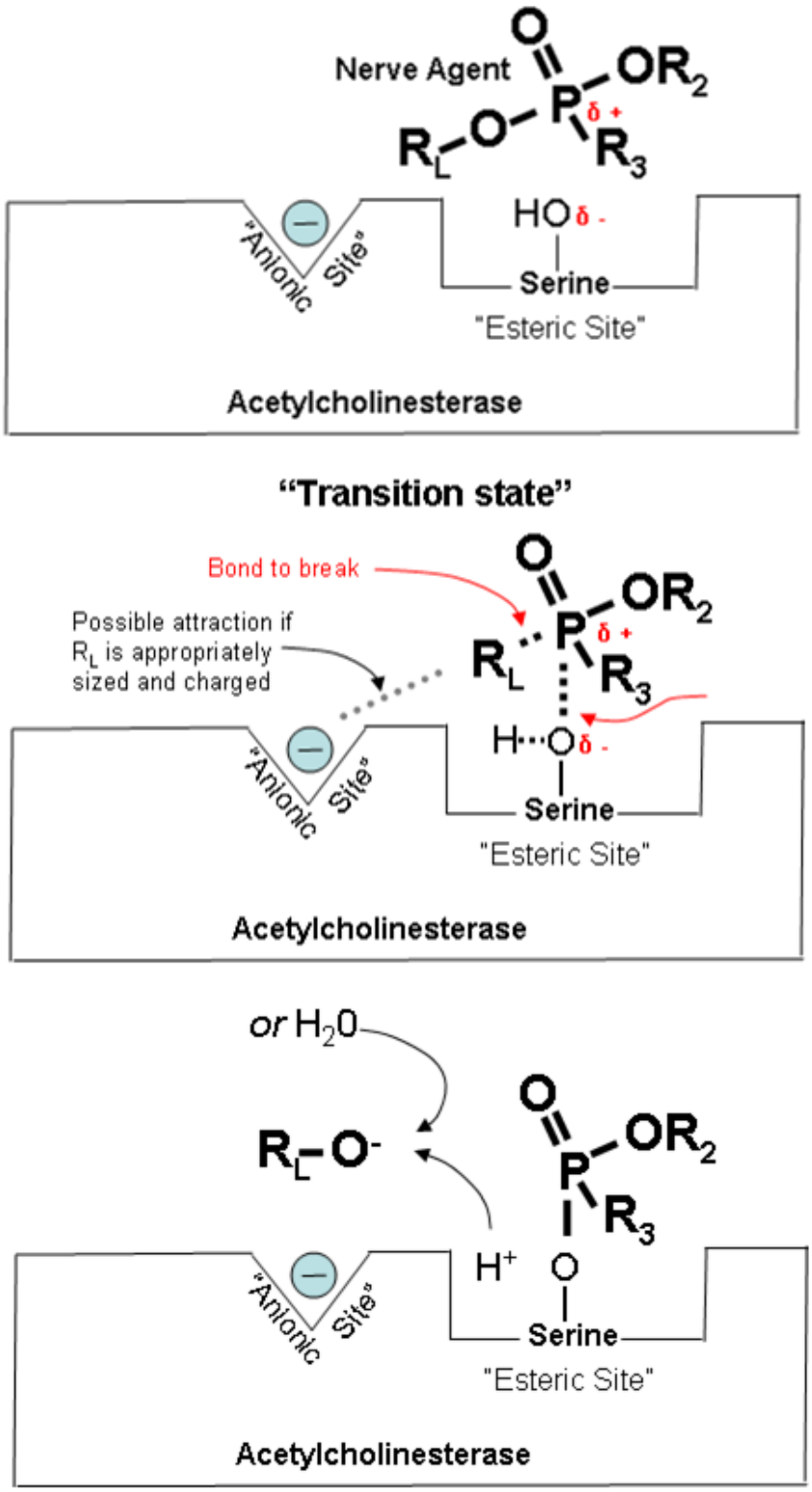

Figure 1- 8: An acetylcholinesterase inhibitor (in this example, a nerve agent) binds to the serine hydroxyl group on acetylcholinesterase. The result is the prevention of acetylcholine from being broken down by acetylcholinesterase[76].

1.4.3.2 Memantine

Memantine [Figure 1- 9] is a non-competitive N-methyl-d-aspartate (NMDA) modulator/antagonist used to medicate patients in the moderate to severe stages of Alzheimer's disease[77]. It was originally designed to combat influenza[78]. Memantine blocks the glutamatergic system's NMDA receptors, resulting in the inhibition of overstimulation by glutamate[79]. There is evidence that glutamate can affect the neurodegenerative process in dementia. Patients with Alzheimer's disease exhibit increases in glutamate, leading to the theory there is a link between NMDA activation and the increased production of Aß and tau protein production[80]. Memantine has been seen to have small benefits in patients in the later stages of Alzheimer's disease which lends weight to the theory that blocking the production of glutamate does hinder neurodegeneration[81]. Memantine has been seen to assist in the elimination of damaged mitochondria from neuronal modules, meaning it could further aid in the treatment of neurodegeneration[82]. Side-effects of using memantine include fatigue, headaches, dizziness, hallucinations and confusion[83]. Acetylcholine inhibitors are often prescribed along with memantine in a view that, in combination, they will have a greater effect[83][84]. Acetylcholine inhibitors can reduce the production of proinflammatory cytokines which can also reduce NMDA receptor expression[83]. Though the combination of memantine and acetylcholine inhibitors is seen as clinically beneficial, the difference is seen to be marginal in patients[84].

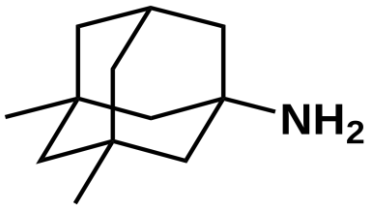

Figure 1- 9: The chemical structure of memantine.

1.4.3.3 EGb 761

EGb 761 is an extract of Ginko Biloba [Figure 1- 10], a species of tree found locally in China[85]. The extract has been used to treat Alzheimer's disease as well as other neuropsychiatric disorders[86]. EGb 761 is a free radical scavenger, a serotonin modulator, improves mitochondrial function, and is recognised as neuroprotective[87]. Though it cannot prevent the progression of dementia, the use EGb 761 has seen patients' cognitive function improve, and also can give patients a greater quality of daily living[88]. EGb 761 works by blocking the pathological cascade of Aß caused events, such as mitochondrial disfunction and reactive oxygen species germination, which prevents neurotoxicity. The extract also protects against Aß-induced apoptosis and neurotoxicity[89]. EGb 761 is seen to be most beneficial in patients in the mild to moderate stages of Alzheimer's disease[88].

Figure 1- 10: A Ginko Biloba Leaf (Left) and EGb 761 Extract (Right)[85].

1.4.3.4 Suvorexant

Suvorexant, [Figure 1- 11] known more commonly by its commercial name 'Belsmora' is an orexin antagonist prescribed to treat Insomnia[90]. Suvorexant has been used as a drug to tackle the non-cognitive symptoms of Alzheimer's disease, focusing on the behavioural and psychological aspects of the disease[91]. Orexins, also referred to as hypocretins, are excitatory neurotransmitters which promote wakefulness[92]. They are secreted in the lateral hypothalamus by orexin-containing neurons[92][93].

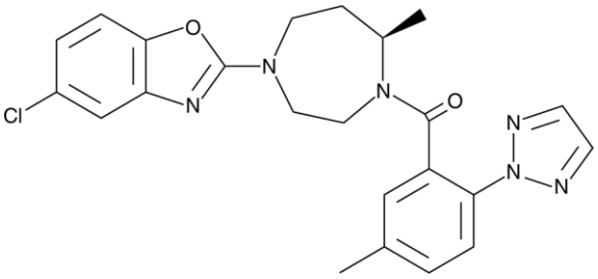

Figure 1- 11: The Chemical Structure of Suvorexant.

Suvorexant negates orexin from stimulating histaminergic neurons, which antagonizes wakefulness[92]. Due to the body clearing amyloid-ß from the brain more optimally whilst the body is asleep, there have been suggestions that suvorexant may aid in reducing the risk of forming Alzheimer's disease[92]. Suvorexant has also been used in patients suffering with mild to moderate Alzheimer's disease to aid in reducing delirium[94]. It has been theorised that orexinergic output increases with the progression of Alzheimer's disease as neurotransmitter network imbalance affects the regulation of a patient's sleep schedule[94]. Studies have shown that Suvorexant does improve patients' sleep time and sleep cycles[95].

1.4.3.5 Psychosocial Management and Interventions

The use of psychosocial interventions in patients with Alzheimer's disease is to aid in the reduction of problematic behaviour, cognitive deficits and difficulties with emotional control[96].

Behavioural modification is an approach used to aid in behavioural change by utilising respondent and operant conditioning[97]. The approach has shown little success as a technique to improve overall function[98] though it has been shown to help in preventing urinary incontinence[99]. Studies have been conducted researching how music can reduce problematic behaviour, with results showing that music therapy can be effective[100].

Cognitive-oriented treatments are used to aid in reducing cognitive defects[101]. The two main techniques used are reality orientation and cognitive retraining. Reality orientation uses familiarities relevant to a patient such as people, places and presentation of time information in order to help the patient better understand their surroundings[102]. Cognitive retraining aims to exercise mental abilities in hope it will improve impaired capacities. Studies have reported that both techniques have shown the cognitive capacities can be moderately improved when used[103].

Emotion-oriented interventions have proven to be mostly ineffective in patients suffering with Alzheimer's disease. The two most prevalent techniques of this classification are reminiscence therapy and simulated presence therapy. Reminiscence therapy attempts to utilise patients' past experiences by using sound, such as music or familiar noises, and objects, such as personal belongings and photographs[104]. A study has shown that reminiscence therapy has minimal efficacy and is likely to not be of clinical significance[104]. Simulated presence therapy utilises patients' pre-disease emotional attachments and consists of playing vocal recordings of the patients' close friends and family. Studies would suggest simulated presence therapy could be the most effective emotion-oriented intervention as it could reduce some problematic behaviours[105].

The final psychosocial intervention is stimulation-oriented, which uses recreational activities such as exercise, art, and the use of pets[106]. Stimulation-

oriented intervention has been linked to modest improvements in patients' mood, behaviour, and potentially even function. The most common reason for the use of stimulation-oriented intervention is to change a patients' routine[107].

1.4.4 Reasons for Lack of Treatments and Obstacles Preventing Progress

Discovering a cure for Alzheimer's disease is a struggle for researchers for a multitude of reasons. Neurodegenerative diseases in general are hard to diagnose[108]. There are many diagnostic tests and methods used to exclude other potential causes for dementia-linked symptoms[108]. It is difficult for drugs to enter the brain as a result of the brain's blood supply being mostly separate to that of the rest of the human body[109]. Ultimately, we still don't know the true cause of Alzheimer's disease[110]. A large part of the difficulty in determining effective treatments is that dementia-linked diseases are not just singular diseases – they are a multitude of complex health issues, each with their own causes[111.

The expense of developing drugs to help treat Alzheimer's disease is costly, which both dissuades companies from attempting to develop a drug, and causes companies which are researching treatments to leave the area[112]. Lead time to develop a drug is long, and failed attempts are proven to be very costly[113]. A large amount of funding for Alzheimer's research is provided by pharmaceutical companies[114] so when a company decides to stop funding the research area, it can have a substantial effect on the amount of drug development taking place.

In order for a drug to be effective in the treatment of Alzheimer's disease, it must efficiently cross the blood-brain barrier [Figure 1- 12] [115][118]. This is difficult as one of the functions of the blood-brain barrier is to protect against toxins, and disease-causing pathogens, which can be found in the blood[116]. Whilst the blood-brain barrier's efficiency for protecting the brain in this capacity is very beneficial to the brain's health, the main detriment is that the blood-brain barrier will prevent drugs from getting to the brain, which is the objective for every Alzheimer's targeting drug [117].

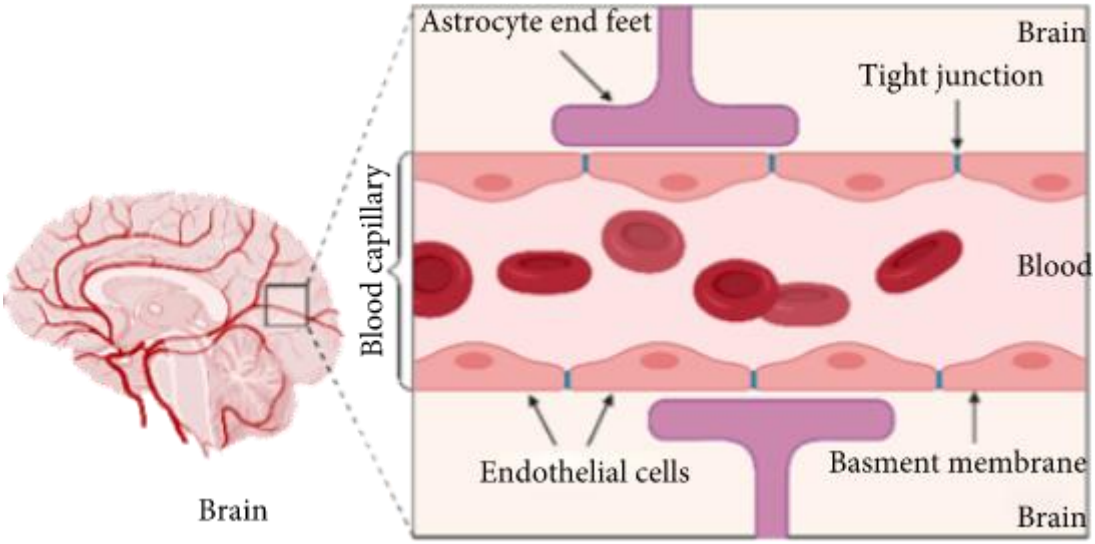

Figure 1- 12: A simple diagram of the blood-brain barrier[118].

1.5 Patient Adherence to Therapies

One of the most discussed topics in medicine today is how to improve patient adherence with medicine that requires a course of administration. This has led to an increased focus on researching and developing long-acting therapies, including strategies that allow for the therapeutic window of drugs to be maintained for a minimum of one month[119].

1.5.1 Issues with Patient Adherence

It is important to recognise that a patient's adherence to a prescribed therapy is imperative to the treatment being a success[120]. If a patient fails to adhere to their therapy, it can have serious repercussions to themselves, whilst also having a detrimental effect on the healthcare system[120]. If a patient does not follow their prescribed treatment, the result can lead to their disease worsening, them putting their own life at risk, and also health care costs increasing[120]. It is unfortunate that nonadherence and noncompliance to therapies is a regular occurrence[121]. There are multiple reasons that patients use in order to avoid their prescribed treatments[121].

Disbelief that the treatment is working, adverse side-effects, depression and worry, prescription costs, lack of trust, lack of symptoms and religious beliefs are the most common reasons for nonadherence[121][122][123]. It is believed that better patient adherence will result in increased control and prevention of diseases, whilst also saving the health care sector money and lowering the hospitalisation rate[124][125].

The use of oral medications is the most common method of drug delivery, with oral medications being used to treat a multitude of diseases[126]. One of the biggest disadvantages to the oral route is that pharmacokinetic properties can often lead to short half-lives, with the result being more frequent doses to ensure a patient remains in the therapeutic window[127]. The therapeutic window is defined as “the dose range of a drug that provides safe and effective therapy with minimal adverse effects,” meaning that dropping below the range will result in a drug being ineffective, whereas going above the range can result in increased adverse side effects[128]. A common reason for patients to become non-adherent with oral medications is because they forget to take their prescribed doses[120]. As oral medications often require daily, or even multiple daily doses, it can be difficult for patients to remember to take their medications resulting in them dropping below the therapeutic window, and putting themselves at further risk of their disease worsening[120]. Patients may actively avoid taking their oral medications due to the taste, texture, or in the case of tablets, the size of the medication[129][130].

1.5.2 Patient Adherence to Antibiotics and Immunosuppressants

A strong example for the importance of patient adherence is the patient adherence to antibiotics. Patient non-adherence to antibiotics is a large societal issue. Bacterial resistance to antibiotics is a significant challenge which is hindered through patient non-adherence[131]. A result of patients not taking their prescribed antibiotics is an increase in the resistance to antibiotics[132]. Prescribed antibiotics courses for acute cases tend to have a course range of 5 to 10 days, yet patients still do not take doses on time, miss doses, or do not finish their course of antibiotics[132]. Patients who do neglect their prescribed course of antibiotics threaten the treatment's efficacy, risk dropping out of the therapeutic window, and contribute to increased bacterial

resistance as a result of failing to eliminate the organism the antibiotics were prescribed to remove[132].

A study was carried out in October 2012 in which 428 patients were invited to take part in tracking their antibiotic-taking behaviour. From this study it was recorded that 42.7% of patients achieved what the study defined as “acceptable adherence” or higher, whilst 57.2% of patients were deemed to be in the levels of “declining to non-adherence”[133]. Knowing the risks and negative effects of non-adherence to antibiotics, we need to ask why patient adherence to antibiotic courses is so low? It is known that patient adherence is better with shorter-term courses of antibiotics which consist of lower treatment lengths and fewer required doses[132]. Reasons why longer-term courses of antibiotics result in lower patient adherence can be largely put down to forgetfulness, or patients claiming they are too busy to take them[134]. When looking more broadly at adherence over any term of prescription, reasons for patients consciously non-adhering can include patients believing that their condition is improving or that they have fully recovered, and so do not end their prescribed course of antibiotics, or in some cases do not even start the course[134]. Some patients' motives for refusing to adhere to their prescribed courses of antibiotics include patients believing that their symptoms are not severe enough to warrant treatment, despite the advice of a physician[135]. Another motive for refusal includes patients being concerned about bacterial resistance with patients believing that the antibiotics they are prescribed are ineffective and will only result in increased bacterial resistance[135]. Other motives include worries over prolonged illness and side-effects, and a lack of trust in the prescriber[135].

It is hard to digest some of the reasons patients give for the refusal of antibiotic treatment, as although they believe they are doing the correct thing, they are putting themselves at risk of further worsening of disease, to which the end result can be sometimes physically crippling, or even fatal[135].

Patient non-adherence is even seen in the most extreme of cases, such as after an organ transplant. Should patients not adhere to immunosuppression, the result can be severe. Failure to follow the prescribed treatment after an organ transplant often causes graft loss, late acute rejection episodes, organ loss, hospital readmissions, and death[136][137]. For something so serious as an organ transplant, it would be assumed

that patient adherence would be high, however, even in this case, nonadherence has been observed at as high as 20% to 50%[136][138]. When considering that 10% to 20% of patients awaiting an organ transplant die while waiting for a donor to become available[137] and that 25% of organ transplant related deaths are a result of patient poor adherence to immunosuppressive therapies[138] why are patients still struggling to follow their prescribed treatments? Studies have shown that there is a link between post-transplant therapy non-adherence and psychological vulnerabilities, including anxiety, the development of depression and social complications[137]. When all of this is considered, it can be determined that patient lifestyle has a huge effect on adherence[137] and that patient adherence is a large societal issue which requires the modification and determination of new methods to aid in increased adherence.

1.5.3 Dementia Patient Adherence to Therapies

For patients suffering with dementia, being prescribed treatments with a high level of drug exposure is considered to be standard rather than a rarity[139]. As the stages of dementia progress, so does the level of impaired memory and other cognitive impairments in patients[139], which contributes negatively to patient adherence[139]. The results of an American study conducted on dementia patients being discharged from hospitals showed that dementia patients had between a 20% to 30% chance of taking more medication than that which was prescribed to them by a physician, whilst as much as 31% of patients took less medication than that was prescribed to them[139][140]. The overall result of the study indicated that just over half of the patients were already showing various degrees of non-adherence after only 2 weeks of their course of treatment[140]. The largest reasons for non-adherence are believed to be deteriorating cognition, poor education, and patients having difficulties with having to track and take multiple prescribed medications[140]. It is more prevalent for older patients suffering with dementia to have larger levels of non-adherence, although this is not necessarily directly linked to dementia, as this is also a common trend in various types of chronic diseases as a result of geriatric conditions[139].

One strategy that has been discussed is to prescribe as few medicines and doses as possible in order to help patients to remember to take the remaining medicines

prescribed to them[139]. However, an issue with reducing prescribed medicines and doses will be treatment efficacy[139] [141]. At the point of which a patient's dementia has progressed to the stage where they become reliant on a caregiver's assistance to aid in the administration and tracking of medications, adherence levels can then be affected as a result of the caregiver's level of involvement and persistence on aiding the patient with their medication[141]. Caregiver assisted adherence can also vary depending on a patient's level of contact with the health service, ability to fund a caregiver, or the amount of voluntary caregiving accessible to the patient from family members and the community[141]. When exploring behavioural issues with patient adherence, there is the potential for patients to refuse the help of a caregiver, and even become aggressive towards the caregiver when the caregiver attempts to aid the patient with their medication[142]. In the event that a patient is admitted to hospice care, the likelihood of the patient's relatives choosing to discontinue therapies and treatments is largely increased[141].

When looking at persistence levels with Alzheimer related drugs, studies have shown that patients are more persistent with once-daily doses of donepezil capsules and extended release galantamine than with twice-daily doses of rivastigmine capsules[141]. It has also been seen that persistence is higher with galantamine when compared to donepezil[141].

Patients and caregivers are encouraged to adopt a routine to aid with adherence[143]. Pill boxes, envelopes and other methods of organising doses are adopted in order to help inform the patient or caregiver about whether a dose has been taken[139]. Diary entries and log-taking is encouraged to see what medications are required to be taken and when they should be consumed[144].

1.5.4 Technologies Aiming to Address Patient Adherence

Addressing issues with patient adherence has been a constant battle for physicians throughout the ages. In the modern age, there have been new advancements in technology which have presented the opportunity for new methods of technology-aided assistance to help aid in improving patient adherence.

1.5.4.1 Text Message Reminders

Although the ability to send text messages to mobile phones can no longer be considered to be cutting-edge technology, it is only since the beginning of the previous decade that text message reminders have been sent to patients in an effort to help them to remember to follow their prescribed treatments[145].

A study conducted in 2016 involving 2742 chronically ill patients, where patients were sent text message reminders to remind them to follow their prescribed medication, showed that patient adherence rose from 50.0% to 67.8%[146]. This shows that even technology as old and as simple as text message reminders can improve patient adherence, and save resources as a result of patients' recoveries improving[146].

1.5.4.2 Smartphone Applications

A relatively new advancement in technology is the use of smartphones and their applications[147]. The first smartphone was the Apple iPhone, which was released in 2007[147]. As of the end of 2020 it was estimated that 5 billion people own a smartphone[148]. Smartphones allow users to download applications, more commonly known as ‘apps’, to their smartphones for various applications such as tracking medication[149].

In 2018, a study conducted by a team at Imperial College London was attempted to identify useful apps available to the public via the leading app stores[150]. The team screened 5881 apps and found 420 free apps which utilised at least one of the listed strategies, and 22 free apps that had incorporated all three strategies to aid with adherence[150]. As of February 2021 the four leading free apps for aiding with patient adherence were Medisafe, MyTherapy, Meds on Time and Médi'rappel[151].

In 2021 a study was conducted on assessing the effect of using a mobile health app on patient adherence to hypertension treatment[152]. 49 participants were given an app to track their adherence. Before using the app, 8% were non-adherent, 64% were partial adherents and 28% were adherent to the treatment. After 12 weeks of using a mobile health app 0% were non-adherent, 8% were partial adherents and 92% were

adherent to the treatment[152]. Although this is just one study, it does suggest that using mobile phone applications to aid with therapies can improve patient adherence.

1.5.4.3 Smart Pillboxes

Conventional pillboxes use letter or number coded plastic racks to help patients organise and track their prescribed medications, but it has been seen that patients still struggle with adherence when using a conventional pillbox[153]. A smart pill box [Figure 1- 13] is able to dispense medicines at required times via micro control, and can give signals when it needs to be opened, has been opened too early, or opened too late[154]. The latest models of smart pillboxes are able to connect to the internet using Bluetooth allowing the patient to receive alerts about the medication via the smart pillbox's corresponding mobile phone application[154]. Caregivers and physicians can also better track patient adherence through receiving information from their patient's smart pillbox, sending data to the caregivers' and physicians' mobile phone tracking apps[154]. The use of smart technologies, including the use of a smart pillbox, have been proven to help patients better track their medication, and therefore, improve patient adherence[155].

Figure 1- 13: A Hero Automatic Smart Pillbox and mobile phone application.

1.5.4.4 Telemedicine

Telemedicine is the remote treatment and diagnosis using telecommunications technology[156]. Phone calls, video calls and other types of telecommunication between a patient and physician help to improve adherence in patients struggling with chronic

diseases[157]. During the Covid-19 pandemic, telemedicine was useful for elderly patients who were unable to leave their home[158].

1.5.4.5 Ingestible Sensors

Ingestible sensors such as smart pills are seen as a breakthrough technology for helping to combat patient non-adherence. Ingestible pills are able to monitor the exact time a drug has been taken[159]. They are easy to swallow, and upon reaching the stomach, a reaction with the stomach fluid takes place, which sends a signal to the receiver, often an adhesive patch, which will then send a signal via Bluetooth to a mobile device [Figure 1- 14][159].

Diagnostic smart pills are small, easy-to-swallow ingestible capsules containing an edible electronic element which is activated in the stomach [Figure 1- 15][160]. Once the element is activated, the smart pill can transmit signals to a receiver which can connect and send data to a smartphone informing patients that it is time to adhere to their prescribed treatment[160][161]. Therapeutic smart pills can be ingested in the same way as diagnostic smart pills, but instead respond to their environment and release medication upon responding to stimuli[160].

Ingestible sensors, often combined with an adhesive patch[161], are capable of physical sensing, pressure sensing, temperature sensing, pH sensing, chemical and biological sensing, and are able to detect haemoglobin[160]. Ingestible sensors should leave the body in less than 72 hours[162].

Although ingestible sensors are promising and show a large amount of potential, the cost factor for manufacturing ingestible sensors is high, and they do occasionally have reliability issues[162]. At current, there are a lack of studies regarding how effective ingestible sensors are at changing patient adherence[161], though once made more cost-effective, ingestible sensors do hold a large amount of promise for improving patient adherence[161].

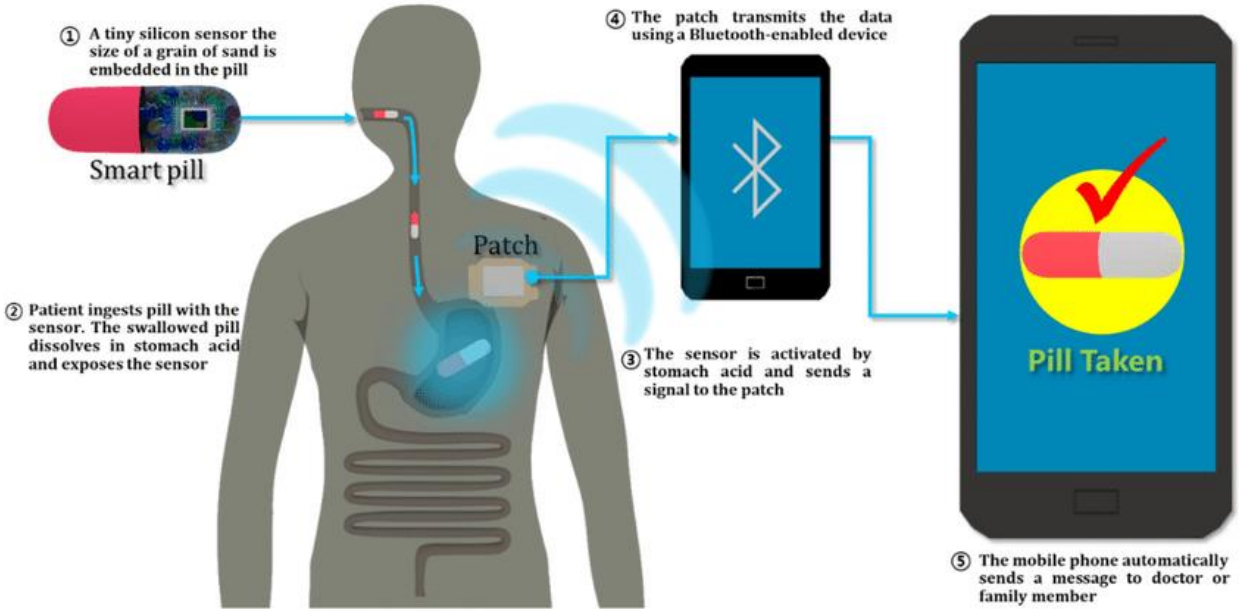

Figure 1- 14: A diagram demonstrating how a smart pill, coupled with an adhesive patch, transmits data via bluetooth to a patients mobile phone application, and notifies whoever is tracking the medication[159].

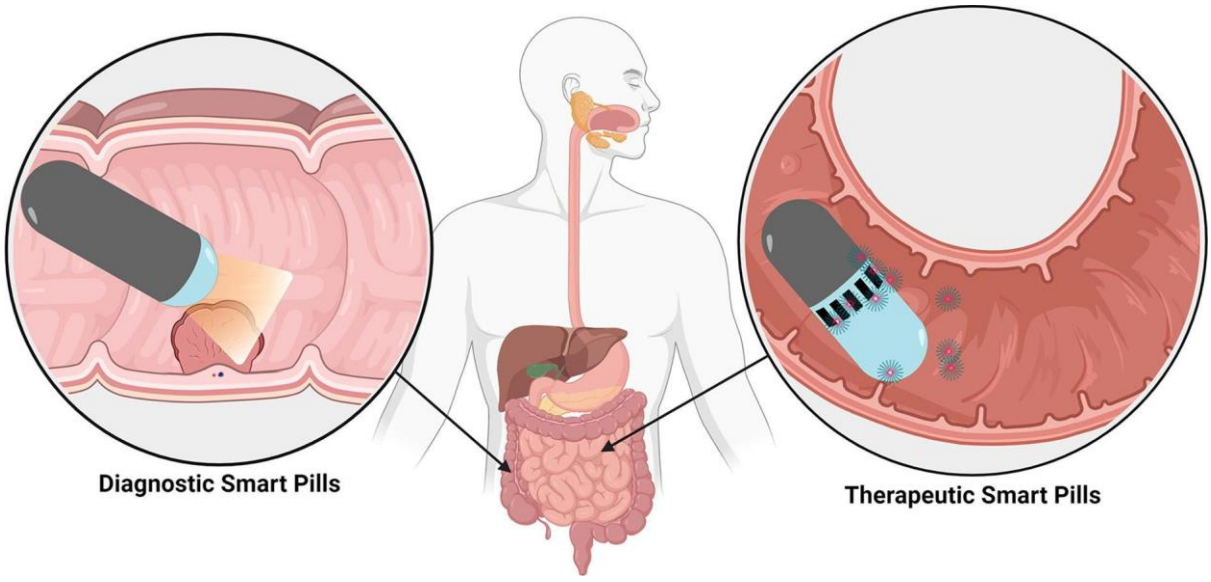

Figure 1- 15: A diagram demonstrating the actions of a diagnostic smart pill (Left) and a therapeutic smart pill (right) in the small and large intestine[160].

1.5.5 Patient Adherence to Transdermal Patches

Use of a long acting transdermal patch, especially in the case of patients suffering with Alzheimer's disease, has been seen to aid with patient adherence when switching from oral drug delivery methods[163][164]. Cognitive impairment will affect a patient's ability to read labels, follow a routine, differentiate between tablets and manage their own medications[163]. This combined with behavioural issues faced by caregivers, who themselves can also suffer from human error when assisting an Alzheimer's patient with their medication, has resulted in non-adherence levels as high as 42% in patients with Alzheimer's disease as of 2013[163][165]. Using a long-acting transdermal patch to deliver acetylcholinesterase inhibitors, such as rivastigmine and galantamine, could help to reduce the difficulties faced by Alzheimer's patients and their caregivers. Moreover, it could also benefit patients who suffer from other types of chronic diseases[165].

1.6 Transdermal Drug Delivery

Being able to deliver drugs painlessly through the skin has been seen as advantageous to that of oral consumptions of drugs. The reasons for this include patients being dissuaded from swallowing tablets or forgetting to take their medication. Transdermal drug delivery also bypasses the gastrointestinal tract, and avoids gastrointestinal irritation and first-pass inactivation and metabolism occurring in the liver[166]. Drugs also avoid being broken down by stomach acids. There are a multitude of benefits to using transdermal drug delivery over oral drug delivery, which includes prolonged and continuous drug delivery, a higher amount of bioavailability, a reduction of drug side reactions in the human body, and improved therapy as a result of maintenance of drug concentrations in plasma[167].

As the skin is a fantastic barrier for molecular transport, it is often a struggle for multiple types of drugs to be delivered through the skin. However, the same can happen with regards to oral delivery, and alternative methods of delivery must be considered. The transdermal delivery method offers a large amount of advantages[168]:

1. The surface area of the human skin is a readily large and accessible surface for delivery (between 1.5 and 2.0 m^2 in adults).
2. Transdermal patches provide a harmless and comfortable method of drug delivery, allowing for prolonged drug release.
3. A sustained release of drugs that have short biological half-lives, which would usually require frequent doses when consumed orally.

As transdermal drug delivery is designed for prolonged and sustainable drug delivery over large time periods, tolerance inducing drugs, and drugs which need Chrono pharmacological management are currently unsuitable for delivery via transdermal methods. Transdermal drug delivery can be used as an alternative to injections, where the main advantage is avoiding the pain of an injection, beneficial to those who have a phobia of needles[169].

The route a drug needs to follow through the topical administration route of using a transdermal patch involves transport across the stratum corneum [Figure 1-16][169][170]. This involves diffusion through intercellular lipids through a route which winds around the corneocytes, where molecules then travel through the lipid head group regions if they are hydrophilic and through the lipid tail group regions if they are lipophilic. The transport route is restricted by solubility and structural requirements in order to allow diffusion within the stratum corneum lipid bilayers.

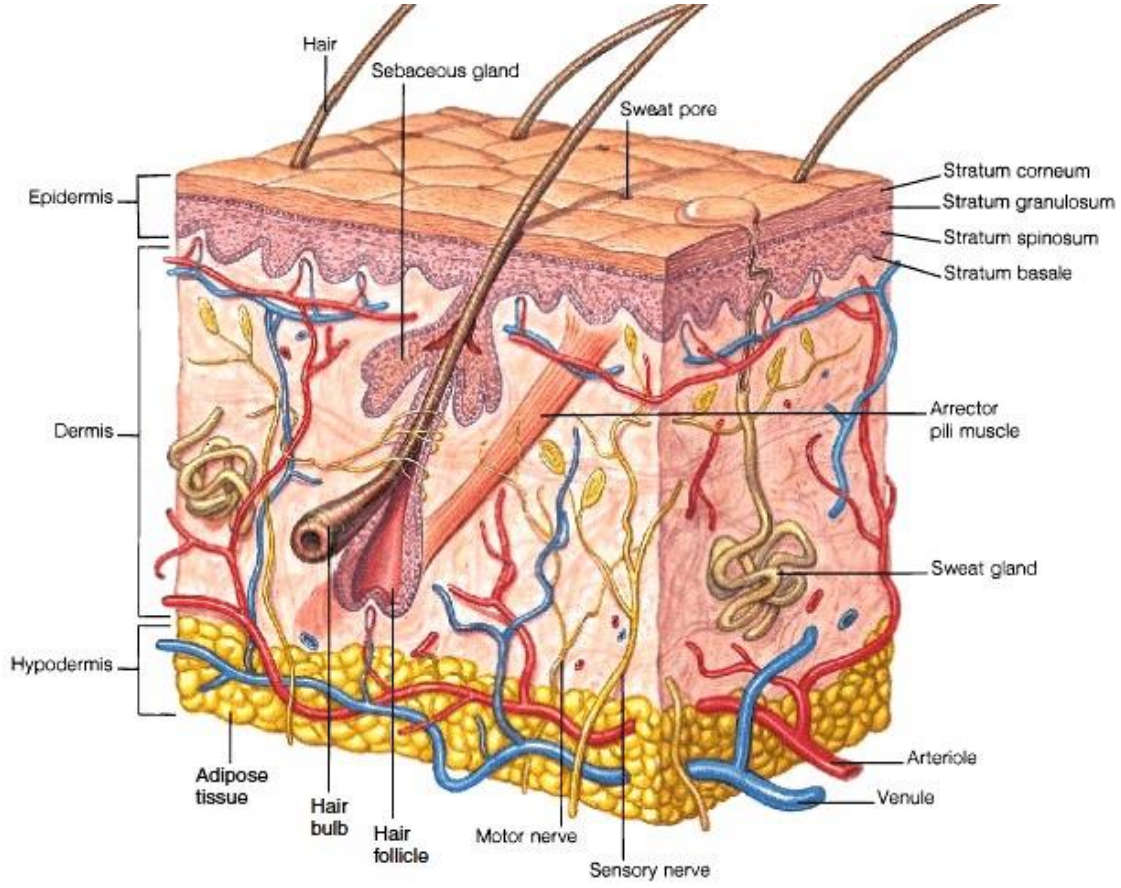

Figure 1- 16: The cross-section of the human skin, the barrier for transdermal drug delivery[170].

In a sense, the use of transdermal drug delivery methods can be argued to be a drug delivery method as old as mankind itself. Topological remedies such as bandages, ointments, herbal remedies, salves and balms have been used for centuries. Ancient civilisations were renowned for using oils, fats and perfumes to make creams and other dermatological remedies for use as medicines[171]. Later, the invention of plasters and medical tapes were used to adhere to human skin to aid in the reparation of surface wounds. Following that, the introduction of patches offered an exciting opportunity for drug delivery, introducing transdermal patches. At the time, new transdermal patches proved to be beneficial in reducing side-effects from drugs originally developed by alternative delivery methods[172]. It is often that when the use of transdermal patches is discussed, thoughts are drawn to perhaps the most famous transdermal patch of all, the nicotine patch, used to combat the desire to smoke cigarettes[173].

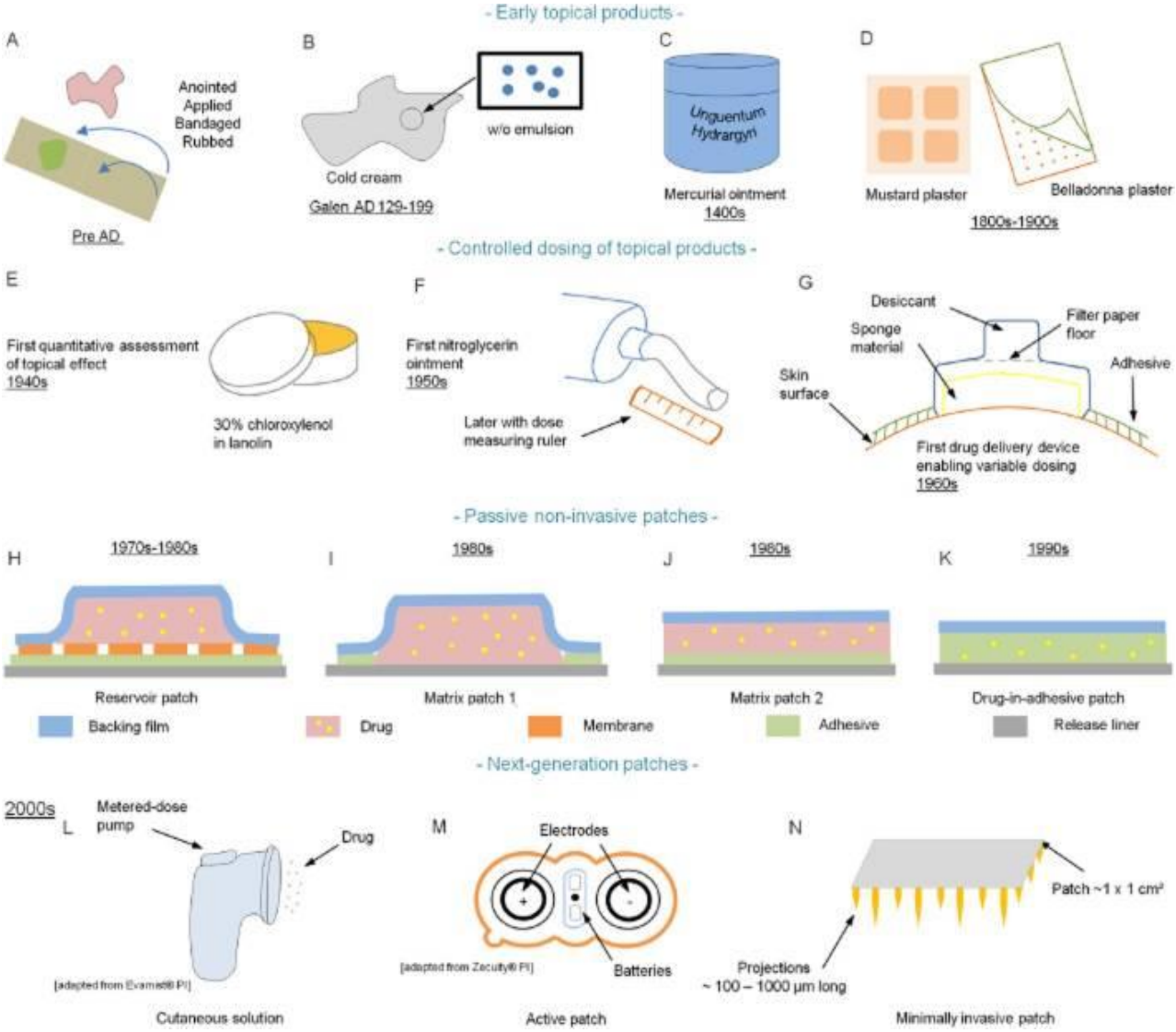

Figure 1- 17: The history of transdermal patch development: (A) Ancient era products; (B) Galen's cold cream; (C) Mercurial ointment; (D) Mustard and belladonna plasters; controlled dosing of topical products. (E) First quantitative systemic delivery (Zondek's System). (F) Individualized delivery system: nitroglycerin ointment. (G) Topical delivery device (Wurster & Kramer's system). Passive non-invasive patches. (H) First patch system – the reservoir – introduced for scopolamine, nitroglycerin, clonidine and oestradiol. (I, J, K) Other types of patches – matrix and drug-in-adhesive (e.g. Fentanyl and nicotine patches). Next-generation patches. (L) Cutaneous solutions (e.g. Patchless patch®, Evamist®). (M) Active patches (e.g. Iontophoresis, Zecuity®). (N) minimally invasive patches (e.g. Microneedles, Nanopatch®)[174].

There are four types of patches [Figure 1 – 17] which rely on the use of adhesive based systems[174].

1. Reservoir patches.
2. A first-generation matrix patch (Matrix patch 1).
3. A second-generation matrix patch (Matrix patch 2).
4. Drug in adhesive patches.

Although the patches share common similarities [Figure 1-18], it should be noted that each patch is a successor of the one made prior to it, with the drug in adhesive patches being the result of constant research into improving patch efficiency, which has taken scientists decades to reach[175]. Transdermal patches are often comprised of four key components which include the backing layer, the loaded drug, the patch adhesive and the release liner[176]. The reservoir patch consists of a membrane located between the adhesive, and the dissolved drug in eluent, as a result of being the first transdermal patch commercially available, where initially researchers believed it would increase the control over the drug release – this was later found to not be the case[174][177]. Matrix 1 and 2 patches consisted of a drug layer of a semisolid matrix which incorporated drug solutions in an adhesive polymer layer. In the matrix patch types, the adhesive layers in these patches surrounded the drug layer, the matrix is applied to the surface of the human skin and the drug is released with the matrix controlling the rate of drug delivery[178]. The drug in adhesive patches is the most efficient transdermal patch in use in the modern day due to its superb efficacy, and in patient compliance, and it removes the need to add eluent for transporting the incorporated drugs. The drug in adhesive patch diffuses drugs from the transdermal patch at a controlled rate upon contact with the surface of skin[179].

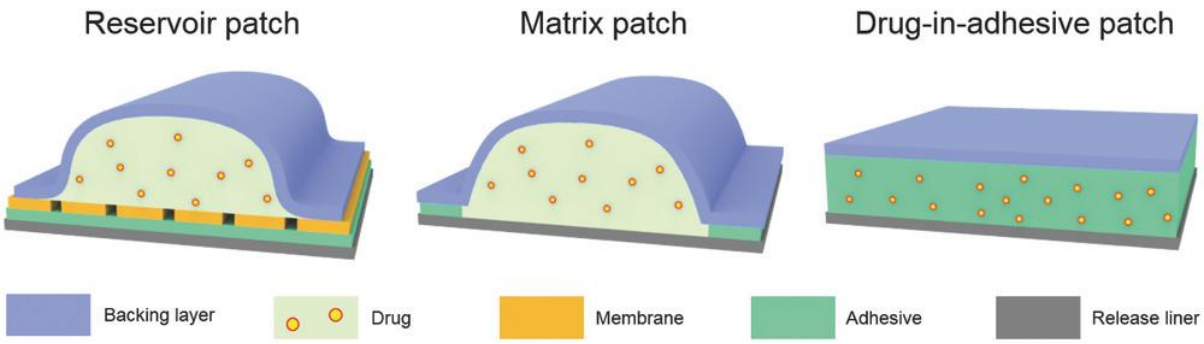

Figure 1- 18: The structures of the four types of transdermal patches showing the differences between the reservoir patch, matrix patch, and drug-in-adhesive patch systems[180].

1.6.1 Transdermal Microneedles

The main drawbacks of the transdermal patches have been the occurrence of rash outbreaks and allergic reactions occurring in patients due to the chemicals present in the patch adhesives[181]. To combat the allergic responses, the use of microneedles has been devised as a new innovative method for transdermal drug delivery. The use of microneedles removes the requirement for an adhesive layer to adhere to the surface of the skin, as microneedles are able to adhere to the skin through penetrating the surface by a low number of micrometres, into the stratum corneum[182]. Although the microneedles penetrate the surface of the skin, patients have been found to feel no discomfort, and the microneedles are able to dissolve in the body as they are biocompatible, which allows for the transdermal film's backing layer to be safely peeled from the patient's skin without causing any damage[183].

The microneedle approach is able to utilise various therapeutic agents which included anti-cancer treatments, macromolecules such as proteins and peptides, as well as hydrophilic and hydrophobic compounds. It is a route which provides improved bioavailability for drugs being delivered through the skin through the 10–15 μm stratum corneum, which forms a barrier blocking exogenous substance and limits the possibilities of drugs which can be delivered therapeutically through the skin. Microneedles, which are completely soluble in the human body, can be used to overcome this barrier, and provides a more therapeutic device tailored to delivering

drugs through the human skin layers. Providing routes to overcome limitations found in typical transdermal patches, microneedles also offer a reduction in cost and sharp waste[184].

Microneedles offer distinct advantages in terms of being able to deliver larger molecular sized drugs, faster healing at the injection site, improved drug efficacy and release, ease of administration [Figure 1- 19], deliver increased drug doses, and cause no disruption of nerve endings. The needles themselves are often made of polysaccharides, so that upon dissolving into the human body, no harm would come to the patient as a result. Microneedles have also been used in the cosmetic industry to treat acne and wrinkles, hide scarring, and improve skin-tone[185].

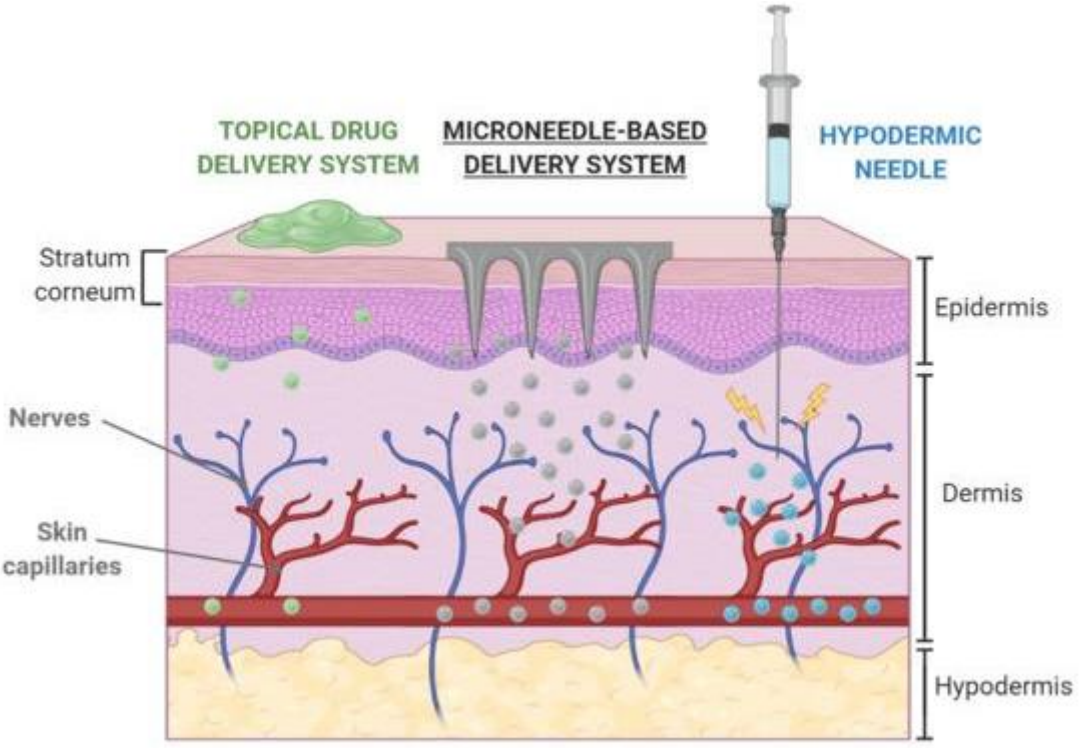

Figure 1- 19: A comparison of the microneedle deliver system with that of topological and needle drug delivery methods[186].

1.6.2 Adhesion in Transdermal Patches

There are various methods of adhesion. Chemical adhesion occurs through physical chemical bonds forming between materials, through penetration, or through intermolecular interactions involving Van der Waals forces which occurs through the attraction and repulsion of weak, non-covalent, intermolecular forces between molecules[187]. Although Van der Waals forces are generally weak interactions occurring between molecules, when a large amount of Van der Walls interactions occur between 2 materials, the large number of interactions promotes the capability for adhesion[188].

It is important that when formulating the adhesive layer, the adhesive layer does not limit the overall drug delivery from transdermal methods. It is also imperative that the selected adhesive be renewable[189]. In order for adhesion to occur between a transdermal material and the skin, the transdermal material must contain hydrophobic properties which are capable of interacting with the human skin, whilst also reducing solubility. Furthermore, they must also contain hydrophilic properties to allow for actions as a drug carrier for drugs to pass through the adhesive layer. Common adhesives in transdermal patches include silicones, acrylics [Figure 1- 20] and poly isobutylene blends. Of these, the acrylic adhesive offers the largest amount of versatility as they can easily be manipulated through altering the monomer functionality in molecules of varying sizes, depending on the requirements of the adhesive[190]. Acrylate monomers contain a carbonyl group, typically an ester functional group, and an adjacent carbon-carbon double bond, which is the biggest drawback of acrylates as they are UV sensitive[191].

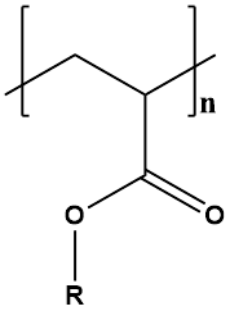

Figure 1- 20: The structure of a polyacrylate polymer.

Polyacrylate polymers rely on Van der Walls forces to achieve adhesion. Due to its ability to cross-link with other polymers and through Van der Waals forces, the strong adhesion of acrylates makes it one of the most desirable and used polymers today[192]. Acrylates' ability to freely crosslink is a huge asset to aid its strong adhesion, as is their low glass transition temperatures. Multiple crosslinking methods are available for acrylates, with UV crosslinking and Michael addition crosslinking being the most common approaches used[193]. Michael addition crosslinking relies on the use of an intermediate compound to crosslink different polymers, or even to react between polymer chains in the same molecule. Michael addition reactions occur via nucleophilic addition of a nucleophile on the β carbon in an α, β – unsaturated carbonyl compound [Scheme 1- 1]. The reaction has been accepted as a "click" reaction[194] due to the ability to react promptly in mild conditions. Michael addition can result in a large amount of crosslinking [Figure 1- 21] which can be used to form hydrogels. As previously discussed, hydrogels consist of multiple polymeric chains resulting in hydrophilic macromolecules[195]. Hydrogels formed through crosslinking are commonly found in most adhesives used for transdermal drug delivery as they are capable of tolerating biological conditions, whilst being able to hold large amounts of drug loaded solutions which can be delivered through the skin[196].

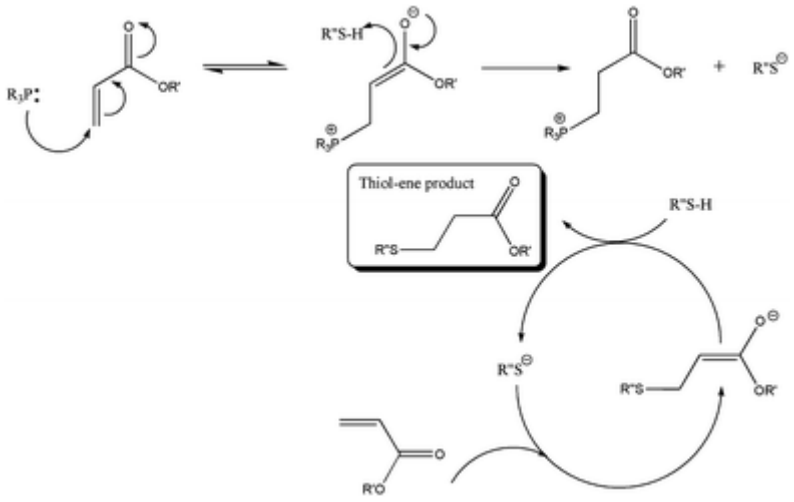

Scheme 1- 1: The Michael Addition mechanism for the reaction between thiols and acrylates[197].

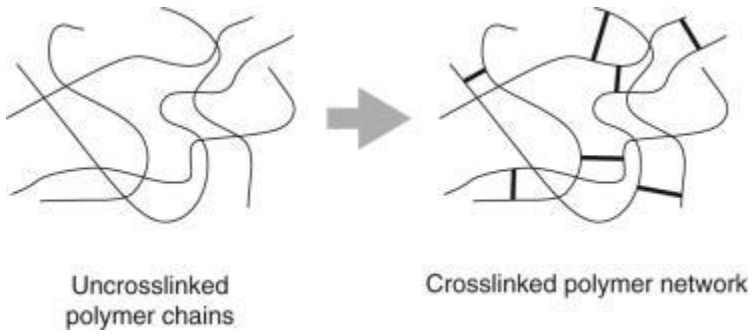

Figure 1- 21: Polymer chains becoming crosslinked to form a crosslinked polymer network[198].

1.6.3 Bio-based Polymers in Green Chemistry and Medicine

To define what makes a bio-based polymer, a bio-based polymer, or a bio-based plastic, is a material where the polymer consists of materials obtained from renewable sources. The majority of bio-based polymers use materials extracted from plants, and very often have low carbon footprints making them preferential due to being environmentally friendly. Due to the constant threat of fossil resources being depleted throughout the planet, and the increasing fear of the effects of global warming caused by fossil fuels, bio-based polymers have been seen as a potential greener substitute for fossil materials[199].

Bio-based polymers [Figure 1- 22] in chemistry are desirable for their functionality and biodegradability. They have a variety of applications, and have been used in multiple different aspects including agriculture[200], packaging[201], alternatives to fossil-fuels[202], electrochemical[203] applications and use in medicinal chemistry[204]. Bio-based polymers, or bio-based plastics can be petroleum based, renewable based, or a mixture of both petroleum and material obtained from renewable sources. In the 1980s, the damaging effects of fossil-based industrial processes on the environment had reached a critical level, and resulted in companies turning to biodegradable polymers including polylactides (PLA) and poly(hydroxy alkanoates) (PHA) in order to reduce the amount of industrial waste being produced[205].

From the latter end of the 20th century, the polymer industry has struggled with the ever-increasing amount of fossil fuel depletion, and global warming. Bio-based polymers were viewed as a promising solution as a suitable replacement to the fossil based materials being used at the time. Biomass feedstocks were seen as a possible sustainable resource. It is possible for biomass feedstocks to be converted into materials for use in polymer production, and the formation of bio-based polymers, and is still an emerging prospect in polymer science today[207].

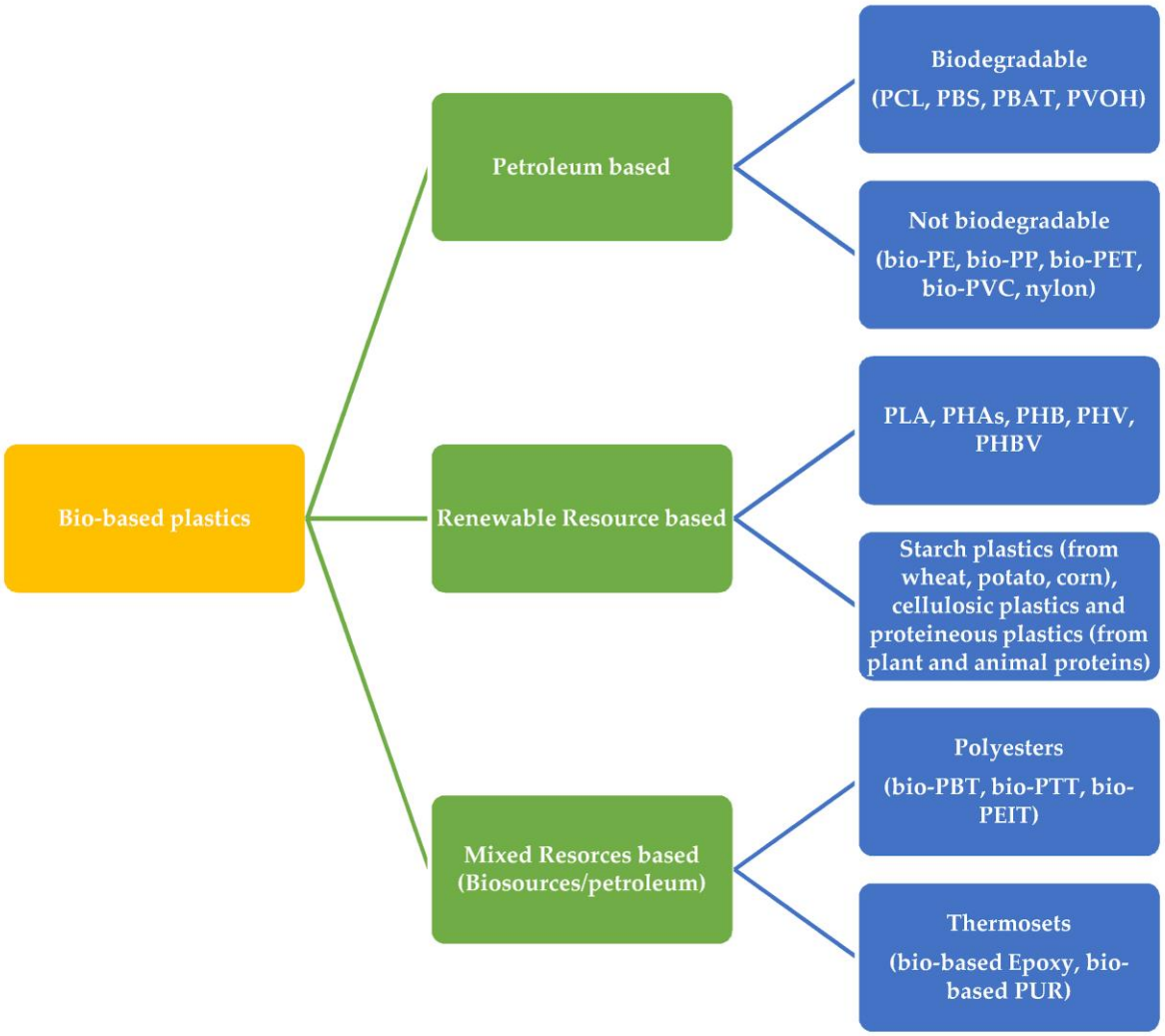

Figure 1- 22: Types of bio-based polymers and the sources of the bio-materials[206].

Biopolymers are natural polymers made by plants, animals and also from microorganisms [Figure 1- 23]. Biopolymers are known for their fantastic biodegradability, with some exceptions such as wood. Unlike biopolymers, artificially synthesized bio-based polymers cannot be classed as a biopolymer, which is the key difference in the classification between the two polymer types[208].

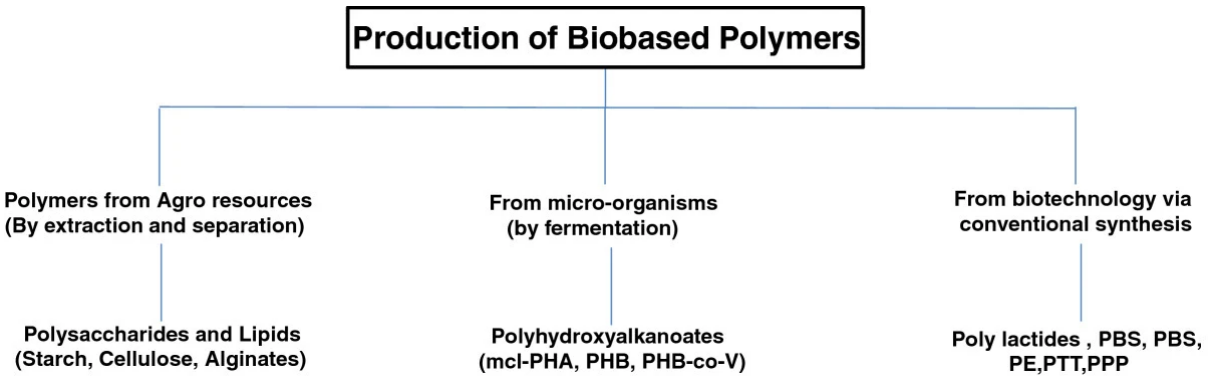

Figure 1- 23: The production of bio-based polymers[209].

First generation bio-based polymers were derived from agricultural feedstocks including potatoes, corn, sugarcane and many more carbohydrate based feedstocks[210]. As the interest in bio-based polymers increased, bio-based polymers' focus moved away from agriculture and towards technological advancement in biotechnology. Bio-based polymers are formed by bacterial fermentation through the synthesis of monomers derived from renewable resources, but can also be found in nature in proteins, polysaccharides and nucleic acids. There are 3 principle methods for the industrial production of bio-based polymers [Figure 1- 23][211].

1. Partially modifying natural bio-based polymers for desired functionality.
2. Using fermentation followed by polymerisation.
3. Direct production from bacteria.

Biopolymers have become prominent materials for the use in a variety of medical applications, due to their biodegradability, biofunctionality and biocompatibility. These properties make them prime candidates for use as vehicles for drug delivery for skin healing, skin grafting and in skin regeneration techniques. Biopolymer materials can be synthesized to be hydrolytically sensitive biocellulosics, polyesters and their amides, polypeptides, furan-based polymers, polyphosphazenes, polyanhydrides, polyurethanes and pseudo-polyamino acids, polysaccharides, and more. These polymers are capable of being used to synthesise hydrogels, spun into fibres and turned into fibrous scaffolds, for the use in the medical sector[212]. Biopolymers have been used to create three-dimensional scaffold structures with suitable biocompatibility and porous structures to make them suitable for use in the regeneration of human skin tissue. Their properties are optimised to support cells with

the ability to invoke tissue regeneration, whilst also being able to degrade post enzyme release from the cells in the scaffold, and meeting the requirements of being a suitable delivery vehicle with mass transport properties[213]. More recently, biopolymers have been researched for their use in transdermal drug delivery due to their biocompatibility, where drugs are delivered systemically from the biopolymers onto healthy human skin[214].

1.6.4 Selecting Biopolymer Materials for Transdermal Drug Delivery

Biopolymers have offered plenty of advantages for use in the drug delivery devices, such as transdermal drug delivery. Being biodegradable, cost effective, patient friendly, and offering enhanced therapeutic efficacy, attention has turned towards using them in transdermal drug delivery to reduce waste and to create more effective drug carriers. It is important that the materials chosen can grant an effective and controlled drug delivery, whilst the materials allow for the formation of gels or films consisting of properties making them durable, versatile, flexible, and being of a size that is comfortable for patients - preferably thin. Various materials have been explored for their potential to be used to create transdermal gels or films. Biopolymer films or gels must be able to load drugs and release them once placed in contact with the surface of human skin. Solvent evaporation [Figure 1- 24] from the films or gels will occur once the drug release has concluded[215].

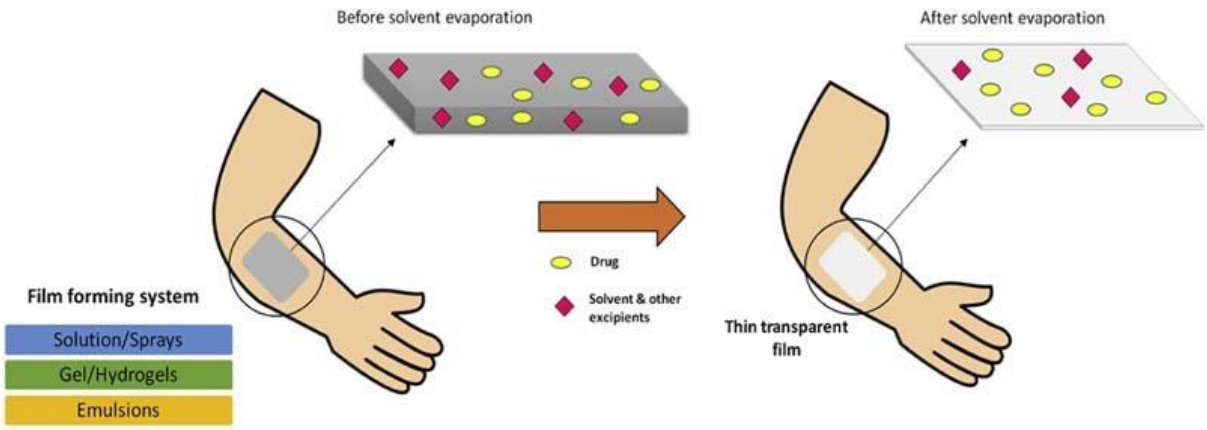

Figure 1- 24: Solvent evaporation from a biopolymer film upon contact with skin to release drugs[215].

1.7 Project Aim and Objectives

This introduction was written to give an insight into Alzheimer's disease, the treatments available to patients suffering with Alzheimer's disease, what pharma companies are doing in relation to combatting the disease, patient adherence to treatments and technologies aimed to improve adherence, the use of transdermal drug delivery, the advantages of transdermal drug delivery, and the use of bio-based polymers in the formulation of transdermal drug delivery systems. Transdermal drug delivery offers a variety of benefits including prolonged and continuous drug delivery, a higher level of bioavailability, a reduction of drug side reactions in the human body, and improved therapy as a result of maintenance of the drug concentration in the plasma. Bio-based polymers have been explored for their use as materials to formulate transdermal films which are biodegradable, biocompatible, cost effective, patient friendly, and can offer enhanced therapeutic efficacy. Enhancing the properties of the bio-based transdermal films and modifying the drugs which have been selected to be delivered, are important factors for improving biocompatibility and drug solubility for a more effective drug release and absorption.

Bio-based polymer-formulated transdermal patches can offer a large number of benefits to Alzheimer's patients, and their caregivers, as they can aid with adherence whilst being easily administered. They can be long-acting drug delivery systems which offer the benefits of not requiring multiple doses, which is highly beneficial to patients and caregivers who are prone to forgetting to take their medication, whilst also being harmless to the patient if the patch is forgotten to be removed. Using bio-based polymer-formulated transdermal patches could improve patient adherence, comfort, and improve the therapeutic efficacy of the prescribed medication. This brings us to the aims of this project.

1. To develop a method for formulating a bio-based polymer transdermal drug delivery system capable of loading and releasing drugs. This will include testing various bio-based polymeric materials which follow the criteria outlined in the introduction for use in transdermal drug release. These films must be biodegradable, biocompatible, malleable, capable of governing controlled drug release, and be a non-irritant to human skin. An efficient technique capable of

formulating a bio-based transdermal film must be determined.

2. An acetylcholinesterase inhibitor must be selected as a candidate drug for transdermal drug delivery as this will be highly beneficial for use in the treatment of patients suffering with Alzheimer's Disease. One aim will be to load and release acetylcholinesterase inhibitor from a bio-based polymer formulate transdermal film and analyse the effects of altering the film properties and release conditions for the optimal release of galantamine in its release media.

3. To utilise methods of drug modification to improve drug release and drug hydrophobicity. Increase drug solubility and lipophilicity resulting in improved drug release, a reduction in drug side-effects, a reduction in dosage amount or dosage frequency, and increased biocompatibility.

These objectives outline the direction for the project over its three-year timeline, with the results of the project research thoroughly discussed and presented in the chapters which make up this thesis. The project aims to build on already existing research in the areas of transdermal drug delivery and polymers used in medicine, whilst outlining new methodologies for improving transdermal drug delivery for medicines, and determining optimal conditions and parameters for improved drug release.

References

1. X. Y. Chen, Y. F. Du. L. Chen, *Frontiers in Molecular Neuroscience.,* 2019, **11**, 1-13
2. J. W. Ashford, *Journal of Molecular Neuroscience*, 2004, **23**, 157-164
3. A. S. Henderson, A. F. Jorm, M. Maj, N. Sartorius, *Dementia,* John Wiley & Sons Ltd, Hoboken, New Jersey, United States, 2nd edn, 2002, vol. 3, ch. 2, pp. 1-68
4. D. A. Casey, D. Antimisiaris, J. O'Brien, *Pharmacy and Therapeutics.,* 2010, 208-211
5. J. Harashish, B. Bhatt, S. Shashikantha, S. M. Jagbir, *Human Vaccines & Immunotherapeutics,* 2014, **10**, 2741-2743

6. R. V. Rao, O. Descamps, V. John, D. E. Bredesen, *Alzheimer's Research & Therapy*, 2012, **4**, 1-9
7. H. J. Möller, M.B. Graeber, *European Archives of Psychiatry and Clinical Neuroscience*, 1998, **248**, 111-122
8. H. D. Yang, D. H. Kim, S. B. Lee. L. D. Young, *Dementia and Neurocognitive Disorders*, 2016, **15**, 115-121
9. F. Boller, M. M. Forbes, *Journal of the Neurological Sciences*, 1998, **158**, 125-133
10. K. Miyoshi, *Psychogeriatics*, 2009, **9**, 67-72
11. W. G. Rosen, R. D. Terry, P. A. Fuld, R. Katzman, A. Peck, *Annals of Neurology*, 1980, **7**, 486-488
12. G. McKhann, D. Drachman, M. Folstein, R. Katzman, D. Price, E. M. Stadlan, *American Academy of Neurology*, 1984, **34**, 939
13. D. Blacker, M. S. Albert, S. S. Bassett, *Arch Neurol.*, 1994, **51**, 1198-1204
14. D. S. Knopman, R. C. Petersen, C. R. Jack, *Neurology*, **92**, 1053-1059
15. C. Tackenberg, L. Kulic, R. M. Nitsch, *PLOS ONE*, 2020, **15**, 1-14
16. J. H. K. Tam, S. H. Pasternak, *Canadian Journal of Neurological Sciences*, 2014, **39**, 286-298
17. A. De Loof, L. Schoofs, *Neuroscience*, 2019, **3**, 1-26
18. C. Hass, D. J. Selkoe, *Nature Reviews Molecular Cell Biology*, 2007, **8**, 101-121
19. S. J. Henderson, C. Andersson, R. Narwal, J. Janson, T. J. Goldschmidt, P. Appelkvist, A. Bogstedt, A. Steffen, U. Haupts, J. Tebbe, P. O. Freskgård, L. Jermutus, M. Burrell, S. B. Fowler, C. I. Webster, *Brain*, 2014. **137**, 553-564
20. Y. Chen, S. Zhao, Z. Fan, Z. Li, Y. Zhu, T. Shen, K. Li, Y. Yan, J. Tian, Z. Liu, B. Zhan, *Alzheimer's Research & Therapy*, 2021, **13**, 1-13
21. T. C. Harris, R. de Rooij, E. Kuhl, *Annals of Biomedical Engineering*, 2018, **47**, 1941-1959
22. A. Mudher, S. Lovestone, *Trends in Neuroscience*, 2002, **25**, 22-26
23. E. Mohandas, V. Rajmohan, B. Raghunath, *Indian J Psychiatry*, 2009, **51**, 55-61
24. R. K. Garg, H. S. Malhotra, N. Kumar, *Multiple Sclerosis,* Academic Press, Cambridge, Massachusetts, United States, 2nd edn, 2016, vol. 19, ch. 8, pp. 201-248

25. E. Mendelkow, M. Von Bergen, J. Biernat, E. M. Mandelkow, *Brain Pathology*, 2007, **17**, 83-90
26. A. J. Dregni, P. Duan, H. Xu, L. Changolkar, N. E. Mammeri, V. M. Y. Lee, M. Hong, *Nature Communications*, 2022, **13**, 1-11
27. K. Iqbal, A. C. Alonso, S. Chen, M. O. Chohan, E. El-Akkad, C. X. Gong, S. Khatoon, B. Li, F. Liu, A. Rahman, H. Tanimukai, I. Grundke-Iqbal, *Biochimica et Biophysica Acta (BBA) - Molecular Basis of Disease*, 2005, **1739**, 198-210
28. M. Jouanne, S. Rault, A. S. Voisin-Chiret, *European Journal of Medicinal Chemistry*, 2017, **139**, 153-167
29. L. Wu, P. Rosa-Neto, G. Y. R. Hsiung, A. D. Sadovnick, M. Masellis, S. E. Black, J. Jia, S. Gauthier, *Canadian Journal of Neurological Sciences*, 2014, **39**, 436-445
30. G. Thinakaran, *Journal of Clinical Investment*, 1999, **104**, 1321-1327
31. Sarah Tomlin, *Nature*, 1999, **399**, 23-23
32. X. Du, X. Wang, M. Geng, *Translational Neurodegeneration*, 2018, **7**, 1-7
33. A. V. Terry, J. J. Buccafusco, *Journal of Pharmacology and Experimental Therapeutics*, 2003, **306**, 821-827
34. M. G. Baxter, J. L. Crimins, *Neuron*, **98**, 2018, 1064-1066
35. T. C. dos Santos, T. M. Gomes, B. A. S. Pinto, A. L. Camara, A. M. A. Paes, *Frontiers in Pharmacology.,* 2018, **9**, 1-14
36. Y. Zhao, B. Zhao, *Oxidative Medicine and Cellular Longevity*, 2013, **2013**, 1-10
37. J. Yao, R. W. Irwin, L. Zhao, R. D. Brinton, R. T. Hamilton, R. D. Brinton *Pharmacology and Pharmaceutical Sciences*, 2009, **106**, 14670-14675
38. W. J. Huang, Z. Zhang, W. W. Chen, *Biomedical Reports*, 2016, **4**, 519-522
39. G. Grasso, A. M. Santoro, V. Lanza, D. Sbardella, G. R. Tundo, C. Ciaccio, S. Marini, M. Coletta, D. Milardi, *Coordination Chemistry Reviews*, 2017, **347**, 1-22
40. R. Wadhwa, K. R. Paudel, M. Mehta, S. D. Shukla, K. Sunkara, P. Prasher, N. Panth, R. Goyal, D. K. Chellappan, G. Gupta, P. M. Hansbro, A. A. A. Aljabali, M. M Tambuwala, D. Kamal, *CNS & Neurological Disorders*, 2020, **19**, 698-708
41. P. V. Moulton, W. Yang, *Journal of Environmental and Public Health*, 2011, **2012**, 1-9
42. J. Ramos,Cejudo, T. Wisniewski, C. Marmar, H. Zetterberg, K. Blennow, M. J. de Leon, S. Fossati, *EBioMedicine*, 2018, **28**, 21-30

43. G. D. Batty, U. M. Kujala, S. J. Sarna, C. A. Valencia-Hernández, J. Kaprio, *https://www.medrxiv.org/content/10.1101/2022.05.24.22275500v3,* 22/09/2022, **1**, 1-19, (accessed 22/09/2022)
44. M. E. A. Vilatela, M. López-López, P. Yescas Gómez, *Archives of Medical Research*, 2012, **43**, 622-631
45. S. Wedmann, R. E. Bennet, L. Delorme, A. B. Robbins, M. Hu, D. McKenzie, M. J. Kirk, J. Schiantarelli, N. Tunio, A. C. Amaral, Z. Fan, S. Nicholls, E. Hudry, B. T. Hyman, *Science Advances*, 2019, **5**, 1-10
46. X. Chen, K. E. Cassady, J. N. Adams, T. M. Harrison, S. L. Baker, W. J. Jagust, *Journal of Neuroscience*, 2021, **41**, 366-375
47. K. Zhang, H. Mizuma, X. Zhang, K. Takahashi, C. Jin, F. Song, T. Gao, Y. Kanayama, Y. Wu, Y. Li, L. Ma, M. Tian, H. Zhang, Y. Watanabe, *European Journal of Nuclear Medicine and Molecular Imaging*, 2021, **48**, 3859-3871
48. A. Delacourte, N. Sergeant, A. Wattez, C. A. Maurage, F. Lebert, F. Pasquier, J. P. David, *Experimental Gerontology*, 2002, **37**, 1291-1296
49. H. Jahn, *Dialogues in Clinical Neuroscience*, 2013, **15**, 445-454
50. A. M. Landes, S. D. Sperry, M. E. Strauss, D. S. Geldmacher, *Journal of the American Geriatrics Society,* 2001, **49**, 1700-1707
51. A. Atri, *Medical Clinics of North America*, 2019, **103**, 263-293
52. H. Förstl, A. Kurz, *European Archives of Psychiatry and Clinical Neuroscience*, 1999, **249**, 288-290
53. A. Bahar-Fuchs, L. Clare, B. Woods, *Cochrane Database of Systematic Reviews*, 2013, **6**, 1-84
54. G. Hirst, V. W. Feng, *English Studies*, 2012, **93**, 357-370
55. E. Steeman, B. D. De Casterelé, J. Godderis, M. Grypdonck, *Journal of Advanced Nursing*, 2006, **54**, 722-738
56. R. M. Tappen, C. Williams, S. Fishman, T. Touhy, *Journal of Nursing Scholarship*, 1999, **31**, 121-125
57. E. M. Frank, *Journal of the South Carolina Medical Association.*, 1994, **90**, 417-423
58. Q. Cheng, M. Wu, Y. Wu, Y. Hu, W. R. Kwapong, Z, Shi, Y. Fan, X. Yu, J. He, Z. Wang, *Frontiers in Aging Neuroscience*, 2020, **12**, 1-8
59. R. Hoveida, H Alaei, S. Oryan, K. Parivar, P. Reisi, *Behavioural Brain Research*, 2011, **216**, 270-274

60. A. M. Palmer, *Trends in Pharmacological Sciences*, 2002, **23**, 426-433
61. L. Mangini, J. Y. Wick, *The Consultant Pharmacist*, 2017, **32**, 324-331
62. R. T. Gottersman, A. Kociolek, K. Fernandez, S. Cosentino, D. P. Devanand, Y. Stern, Y. Gu, *Journal of Alzheimer's Disease*, 2021, **81**, 1131-1139
63. T. McLaughlin, H. Feldman, H. Fillit, M. Sano, F. Schmitt, P. Aisen, C. Leibman, L. Mucha, J. M. Ryan, S. D. Sullivan, D. E. Spackman, P. J. Neumann, J. Cohen, Y. Stern, *Alzheimer's & Dementia*, 2010, **6**, 482-493
64. K. Forbes-McKay, M. F. Shanks, A. Venneri, *Acta Neuropsychiatrica*, 2013, **25**, 320-327
65. Alzheimer's Association, *Alzheimer's & Dementia*, 2016, **12**, 459-509
66. Dementia Consortium Launched in U.K., https://www.genengnews.com/news/dementia-consortium-launched-in-u-k/ , (accessed October 2018)
67. Dementia Consortium, https://www.alzheimersresearchuk.org/research/for-researchers/research-opportunities/drug-discovery/dementia-consortium/#:~:text=The%20Dementia%20Consortium%20provides%20funding,%26%20Johnson%2C%20Lilly%20and%20MSD. , (accessed July 2022)
68. C. W. Burke, *Alzheimer's Report*, https://www.biospace.com/article/alzheimer-s-disease-insight-report-current-therapies-drug-pipeline-and-outlook/ ,(accessed September 2019)
69. J. Cummings, G. Lee, P. Nahed, M. E. Z. N. Kambar, K. Zhong, J. Fonseca, K. Taghva, *Translation Research & Clinical Interventions*, 2022, **8**, 1-24
70. J. Rasmussen, H. Langerman, *Degenerative Neurological and Neuromuscular Disease.*, 2019, **9**, 123-130
71. G. Marucci, M. Buccioni, D. D. Ben, C. Lambertucci, R. Volpini, F. Amenta, *Neuropharmacology*, 2021, **190**, 1-15
72. T. Khuanjing, S. Palee, S. C. Chattipakorn, N. Chattipakorn, *Acta Physiologica*, **228**, 1-12
73. P. K. Mukherjee, V. Kumar, M. Mai, P. J. Houghton, *Phytomedicine*, **14**, 289-300
74. G. M. Kapalka, *Science Direct*, 2010, **1**, 379-403
75. R. Singh, N. M. Sadiq, *StatPearls*, StatPearls Publishing, Tampa, Florida, United States, 1st edn 2022, vol. 2022, Ch. Cholinesterase Inhibitors, pp. 1-5

76. S. W. Wiener, R. S. Hoffman, *Journal of Intensive Care Medicine*, 2004, **19**, 22-37
77. J. Weller, A. Budson, *F1000 Research.*, **7**, 2018, 1-9
78. S. A. Lipton, *Current Drug Targets*, **8**, 2007, 621-632
79. J. L. Molinuevo, A. Lladó, L. Rami, *American Journal of Alzheimer's Disease & Other Dementias*, 2005, **20**, 77-85
80. N. W. Hu, T. Ondrejcak, M. J. Rowan, *Pharmacology Biochemistry and Behavior*, 2012, **100**, 855-862
81. R. McShane, M. J. Westby, E. Roberts, N. Minakaran, L. Schneider, L. E. Farrimond, N. Maayan, J. Ware, J. Debarros, *Cochrane Database of Systematic Reviews*, 2019, **3**, 1-291
82. M. M. Koola, *Psychiatry Research*, 2020, **293**, 1-8
83. N. Mimica, P. Presečki, *Psychiatria Danubina*, 2009, **21**, 108-113
84. P. Raina, P. Santaguida, A. Ismaila, C. Patterson, D. Cowan, M. Levine, L. Booker, M. Oremus, *Annals of Internal Medicine,* 2008, **148**, 379-397
85. T. Y. Wu, C. P. Chen, T. R. Jinn, *Taiwanese Journal of Obstetrics and Gynecology*, 2011, **50**, 131-135
86. N. Kandiah, P. A. Ong, T. Yuda, L. L. Ng, K. Mamun, R. A. Merchant, C. Chen, J. Dominguez, S. Marasigan, E. Ampil, V. T. Nguyen, S. Yusoff, Y. F. Chan, F. M. Yong, O. Krairit, C. Suthisisang, V. Senanarong, Y. Ji, R. Thukral, R. Ihl, *CNS Neuroscience & Therapeutics*, 2019, **25**, 288-298
87. N. Bachinskaya, R. Hoerr, R. Ihl, *Neuropsychiatric Disease and Treatment*, 2011, **7**, 209-215
88. N. Kandiah, P. A. Ong, T. Yuda, L. L. Ng, K. Mamun, R. A. Merchant, C. Chen, J. Dominguez, S. Marasigan, E. Ampil, V. T. Nguyen, S. Yusoff, Y. F. Chan, F. M. Yong, O. Krairit, C. Suthisisang, V. Senanarong, Y. Ji, R. Thukral, R. Ihl, *CNS Neuroscience & Therapeutics*, 2019, **25**, 288-298
89. K. McKeage, K. A. Lyseng-Williamson, *Drugs & Therapy Perspectives*, 2018, **34**, 358-366
90. L. P. H. Yang, *Drugs*, 2014, **74**, 1817-1822
91. M. Moline, S. Thein, M. Bsharat, N. Rabbee, M. Kemethofer-Waliczky, G. Filippov, N. Kubota, S. Dhadda, *The Journal of Prevention of Alzheimer's Disease,* 2021, **8**, 7-18
92. D. F. Kripke, *F1000 Research*, 2015, **4**, 456

93. C. Wang, Q. Wang, B. Ji, Y. Pan, C. Xu, B. Cheng, B. Bai, J. Chen, *Frontiers in Molecular Neuroscience*, 2018, **11**, 220
94. T. Hanazawa, Y. Kamijo, *Clinical Psychopharmacology and Neuroscience*, **17**, 547-550
95. W. J. Herring, P. Ceesay, E. Snyder, D. Bliwise, K. Budd, J. Hutzelmann, J. Stevens, C. Lines, D. Michelson, *Alzheimer's and Dementia*, 2020, **16**, 541-551
96. P. V. Rabins, D. Blacker, B. W. Rovner, T. Rummans, L. S. Schneider, P. N. Tariot, D. M. Blass, J. S. McIntyre, S. C. Charles, D. J. Anzia, I. A. Cook, M. T. Finnerty, B. R. Johnson, J. E. Nininger, B. Schneidman, P. Summergrad, S. M. Woods, J. Berger, C. D. Cross, H. A. Brandt, P. M. Margolis, J. P. D. Shemo, B. J. Blinder, D. L. Duncan, M. A. Barnovitz, A. J. Carino, Z. Z. Freyberg, S. H. Gray, T. Tonnu, R. Kunkle, A. B. Albert, T. J. Craig, D. A. Regier, L. J. Fochtmann, *The American Journal of Psychiatry*, 2007, **164**, 5-56
97. A. E. Kazdin, *History of Behavior Modification: Experimental Foundations of Contemporary Research*, University Park Press, Maryland, United States, 1st edn, 1978, vol 1. ch. 4, pp. 87 - 118
98. C. M. C. Bottino, I. A. M. Carvalho, A. M. Alvarez, A. M. M. A. Alvarez, R. Avila, P. R. Zukauskas, S. E. Z. Bustamante, F. C. Andrade, S. R. Hototian, F. Saffi, C. H. P. Câmargo, *Clinical Rehabilitation*, 2005, **19**, 861-869
99. R. S. Doody, J. C. Stevens, C. Beck, R. M. Dubinsky, J. A. Kaye, L. Gwyther, R. C. Mohs, L. J. Thal, P. J. Whitehouse, S. T. DeKosky, J. L. Cummings, *Neurology,* 2001, **8**, 1154-1166
100. I. Abraha, J. M. Rimland, F. M. Trotta, G. Dell'Aquila, A. Cruz-Jentoft, M. Petrovic, A. Gudmundsson, R. Soiza, D. O'Mahony, A. Guaita, A. Cherubini, *BMJ Open*, 2017, **7**, 3-28
101. H. Amieva, P. H. Robert, A. S. Grandoulier, C. Meillon, J. De Rotrou, S. Andrieu, C. Berr, B. Degranges, B. Dubois, C. Girtanner, M. E. Joël, B. Lavallart, F. Nourhashemi, F. Pasquier, M. Rainfray, J. Touchon, C. Chêne, J. F. Dartigues, *International Psychogeriatrics*, 2015, **28**, 707-717
102. O. Zanetti, M. Oriani, C. Geroldi, G. Binetti, G. B. Frisoni, G. Di Giovanni, L. P. De Vreese, *Age and Ageing*, 2002, **31**, 193-196
103. A. Spector, L. Thorgrimsen, B Woods, L. Royan, S. Davies, M. Butterworth, M. Orell, *The British Journal of Psychiatry*, 2003, **183**, 248-254

104. B. Woods, L. O'Philbin, E. M. Farrell, A. E. Spector, M. Orrell, *The Cochrane Database of Systemic Reviews*, 2018, **3**, 193-196
105. J. Zetteler, *Aging & Mental Health*, 2008, **12** 779-785
106. Y. Cai, L. Li, C. Xu, Z. Wang, *World Views on Evidence-Based Nursing*, 2020, **17**, 253-331
107. P. V. Rabins, D. Blacker, B. W. Rovner, T. Rummans, L. S. Schneider, P. N. Tariot, D. M. Blass, J. S. McIntyre, S. C. Charles, D. J. Anzia, I. A. Cook, M. T. Finnerty, B. R. Johnson, J. E. Nininger, B. Schneidman, P. Summergrad, S. M. Woods, J. Berger, C. D. Cross, H. A. Brandt, P. M. Margolis, J. P. D. Shemo, B. J. Blinder, D. L. Duncan, M. A. Barnovitz, A. J. Carino, Z. Z. Freyberg, S. H. Gray, T. Tonnu, R. Kunkle, A. B. Albert, T. J. Craig, D. A. Regier, L. J. Fochtmann, *The American Journal of Psychiatry*, 2007, **164**, 5-56
108. P. Colligris, M. H. P. de Lara, B. Colligris, J. Pintor, *Journal of Ophthalmology*, 2018, **2018**, 1-12
109. W. M. Pardridge, *Journal of Cerebral Blood Flow & Metabolism*, 2012, **32**, 1959-1972
110. L. Shrestha, B. Shrestha, N. M. Rawal, *Gerontology and Geriatric Medicine*, 2022, **8**, 1-5
111. S. Walsh, I. Govia, L. Wallace, E. Richard, R. Peters, K. J. Anstey, C. Brayne, *Comment*, 2022, **3**, 6-8
112. T. Daly, M. Houot, A. Barberousse, A. Petit, S. Epelbaum, *Journal of Alzheimer's Disease Reports*, 2021, **5**, 637-645
113. S. Y. Pan, S. Pan, Z. L. Yu, D. L. Ma, S. B. Chen, W. F. Fong, Y. F. Han, K. M. Ko, *The Journal of Pharmacy and Pharmaceutical Sciences*, 2010, **13**, 450-471
114. J. Cummings, J. Bauzon, G. Lee, *Translational Research & Clinical Interventions*, 2021, **7**, 1-7
115. W. A. Banks, *Advanced Drug Delivery Reviews*, 2012, **64**, 629-639
116. R. Daneman, A. Prat, *Cold Spring Harbor Perspectives in Biology*, 2015, **14**, 1-23
117. H. Brzica, W. Abdullahi, K. Ibbotson, P. T. Ronaldson, *Journal of Central Nervous System Disease*, 2017, **9**, 1-12
118. A. Alahmari, *Neural Plasticity*, 2021, **2021**, 1-10

119. A. Shakil, F. Y. Hern, C. Liu, K. Temburnikar, P. Chambon, N. Liptrott, T. O. McDonald, M. Neary, A. Owen, C. F. Meyers, S. P. Rannard, *Journal of Materials Chemistry B*, 2022, **10**, 4395-4404
120. B. Jimmy, J. Jose, *Oman, Medical Journal*, 2011, **26**, 155-159
121. A. R. Scialli, K. Saavedra, A. Fugh-Berman, *The Journal of Scientific Practice and Integrity*, 2021, **3**, 1-10
122. F. Dobbels, R. V. Damme-Lombaert, J. Vanhaecke, Sabin De Geest, *Pediatric Transplantation*, 2005, **9**, 381-390
123. R. N. Kisenyi, J. K. Muliira, E. Ayebare, *Journal of Religion and Health*, 2011, **52**, 307-317
124. J. Bourbeau, S. J. Bartlett, *Thorax*, 2008, **63**, 831-838
125. A. O. Iuga, M. J. McGuire, *Risk Management and Healthcare Policy*, 2014, **7**, 35-44
126. M. S. Alqahtani, M. Kazi, M. A. Alsenaidy, M. Z. Ahmad, *Frontiers in Pharmacology.*, 2021, **12**, 1-21
127. G. Fuller, M. Manford, *Neurology*, Churchill Livingston, London, United Kingdom, Third Edition, 3rd edn, 2010, ch. Parkinson's disease and other akinetic rigid syndromes II, pp. 90-91
128. A. Caraceni, C. Martini, E. Zecca, E. Fagnoni, *Handbook of Clinical Neurology*, 2012, **104**, 391-415
129. J. A. Mennella, A. C. Spector, D. R. Reed, S. E. Coldwell, *Clinical Therapeutics*, 2013, **35**, 1225-1246
130. G. Garg, P. Sharma, *International Journal of Pharmaceutical Sciences Review and Research*, 2010, **4**, 87-96
131. C. Treibich, B. Ventelou, *European Journal of Public Health*, 2017, **27**, 978-980
132. C. Jackson, R. J. Lawton, D. K. Raynor, P. Knapp, M. T. Conner, C. J. Lowe, S. J. Closs, *Patient Education and Counseling*, 2006, **61**, 212-218
133. C. Llor, S. Hernández, C. Bayona, A. Moragas, N. Sierra, M. Hernández, M. Miravitlles, *International Journal of Infectious Diseases*, 2013, **17**, 168-172
134. M. Fernandes, A. Liete, M. Basto, M. A. Nobre, N. Vieira, R. Fernandes, P. Nogueira, P. Jorge, *International Journal of Clinical Pharmacy*, 2014, **36**, 86-91
135. A. Bagnulo, M.T. M. Sastre, L. Kpanake, P. C. Sorum, E. Mullet, *BMC Public Health*, 2019, **19**, 1-9

136. K. Laederach-Hofmann, B. Bunzel, *General Hospital Psychiatry*, 2000, **22**, 412-424
137. J. R. Maldonado, *The American Journal of Bioethics*, 2019, **19**, 1-8
138. G. Germani, S. Lazzro, F. Gnoato, M. Senzolo, V. Borella, G. Rupolo, U. Cillo, P. Rigotti, G. Feltrin, M. Loy, A. Martin, G. C. Sturniolo, P. Burra, *Transplantation Proceedings*, 2011, **43**, 318-323
139. S. Arlt, R. Lindner, A. Rösler, W. von Renteln-Kruse, *Drugs & Aging*, 2008, **25**, 1033-1047
140. S. L. Gray, J. E. Mahoney, D. K. Blough, *The Annals of Pharmacotherapy*, 2001, **35** 539-545
141. C. J. Maxwell, K. Stock, D. Seitz, N. Herrmann, *Canadian Journal of Psychiatry*, 2014, **59**, 624-631
142. M. Lee, J. H. Ryoo, C. Campbell, P. J. Hollen, I. C. Williams, *Journal of Clinical Nursing*, 2019, **28** 23-24
143. V. van der Wardt, J. Hancox, D. Gondek, P. Logan, R. das Nair, K. Pollock, R. Harwood, *Preventive Medicine Reports*, 2017, 38-45
144. J. M. Bruce, L. M. Hancock, P. Arnett, S. Lynch, *Journal of Behavioral Medicine*, 2010, **33**, 219-227
145. K. F. Foreman, K. M. Stockl, L. B. Le, E. Fisk, S. M. Shah, H. C. Lew, B. K. Solow, B. S. Curtis, *Clinical Therapeutics*, 2012, **34**, 1084-1091
146. 5 ways technology can help improve medication adherence, https://digitalhealthcentral.com/2021/09/15/how-to-improve-medication-adherence/#:~:text=%205%20ways%20technology%20can%20help%20improve%20medication,during%20the%20Covid%20pandemics%2C%20but%20telemedicine...%20More%20, 15th September 2021
147. J. D. Akkara, A. Kuriakose, *Kerala Journal of Ophthalmology*, 2018, **30**, 138-144
148. A. Z. Dawson, R. J. Walker, J. A. Campbell, T. M. Davidson, L. E. Egede, *MHealth*, 2020, **6**, 1-17
149. A. Choi, A. W. Lovett, J. Kang, K. M. Lee, L. Choi, *Advances in Pharmacology and Pharmacy*, 2015, **3**, 64-74
150. I. Ahmed, N. S. Ahmad, S. Ali, S. Ali, A. George, H. S. Danish, E. Uppal, J. Soo, M. H. Mobasheri, D. King, B. Cox, A. Darzi, *JMR mHealth and uHealth*, 2018, **6**, 1-13

151. C. Backes, C. Moyano, C. Rimaud, C. Bienvenu, M. P. Schneider, *Frontiers in Medical Technology*, **2**, 2021, 1-11
152. S. S. Volpi, D. Biduski, E. A. Bellei, D. Tefili, L. McCleary, A. L. S. Alves, A. C. B. De Marchi, *PeerJ*, 2021, **9**, 1-16
153. N. Zelikovsky, A. P. Schast, J. Palmer, K. E. C. Meyers, *Pediatric Transplantation*, 2008, **12**, 300-308
154. P. K. N. J. Najeeb, A. Rimna, K. P. Safa, M. Silvana, T. K. Adarsh, *2018 International Conference on Emerging Trends and Innovations In Engineering And Technological Research*, 2018, **1**, 1-5
155. M. Aldeer, M. Javanmard, R. P. Martin, *Applied System Innovation*, 2018, **1**, 1-27
156. J. Craig, V. Petterson, *Journal of Telemedicine and Telecare*, 2005, **11**, 3-9
157. J. M. Bingham, M. Black, E. J. Anderson, Y. Li, N. Toselli, S. Fox, J. R. Martin, D. R. Axon, A. Silva-Almodóvar, *The Annals of Pharmacotherapy*, 2021, **55**, 637-649
158. A. K. C. Wong, F. K. Y. Wong, K. K. S. Chow, *JAMA Network Open*, 2021, **4**, 1-13
159. K. Guk, G. Han, J. Lim, K. Jeong, T. Kang, E. K. Lim, J. Jung, *Nanomaterials*, 2019, **9**, 1-23
160. G. Cummins, *Advanced Drug Delivery Reviews*, 2021, **177**, 1-22
161. A. Alipour, S. Gabrielson, P. Baldev, *Pharmacy*, 2020, **8**, 1-11
162. K. Kalantar-Zadeh, N. Ha, J. Z. Ou K. J. Berean, *ACS Sensors*, 2017, **2**, 468-483
163. H. Tian, S. Abouzaid, W, Chei, K. H. Kahler, E. Kim, *Alzheimer Disease & Associated Disorders*, 2013, **27**, 183-186
164. G. Adler, B. Mueller, K. Articus, *The International Journal of Clinical Practice*, 2014, **68**, 465-470
165. G. Small, B. Dubois, *Current Medical Research and Opinion*, 2007, **23**, 2705-2713
166. S. Scheindlin, *Molecular Interventions*, 2004, **4**, 308-312
167. D. Patel, S. A. Chaudhary, B. Parmar, N. Bhura, *The Pharma Innovation*, 2012, **1**, 66-75
168. A. Naik, Y. N. Kalia, R. H. Guy, *Pharmaceutical Science & Technology Today*, 2000, **3**, 318-326

169. M. R. Prausnitz, R. Langer, *Nature Biotechnology*, 2008, **26**, 1261-1268
170. V. R. Karuppiah Ramachandran, K. Zhang, N. Meratnia, P. Havinga, *Proceedings of the 10th EAI International Conference on Body Area Networks*, 2015, **2**, 1-7
171. F. J. González-Minero, L. Bravo-Díaz, *Cosmetics*, 2018, **5**, 1-9
172. N. Mimica, *Psychiatria Danubina*, 2009, **21**, 108-113
173. M. C. Fiore, S. S. Smith, D. E. Jorenby, *The Journal of the American Medical Association*, 1994, **271**, 1940
174. M. N. Pastore, Y. N. Kalia, M. Horstmann, M. S. Roberts, *British Journal of Pharmacology*, **172**, 2179-2209
175. Y. Hu, Y. Wu, X. Xia, W. Liang, J. Gao, *Drug Delivery*, 2010, **18**, 84-89
176. Y. Wang, D. J. Burgess, *Drug-Device Combination Products*, Woodhead Publishing, United Kingdom, 1st edn, 2010, ch. 1, 3-28
177. S. Dhiman, T. G. Singh, A. K. Rehni, *International Journal of Pharmacy and Pharmaceutical Sciences*, 2011, **3**, 26-34
178. L. Margetts, R. Sawyer, *Continuing Education in Anaesthesia Critical Care & Pain*, 2007, **7**, 171-176
179. W. Weng, P. Quan, C. Liu, H. Zhao, L. Fang, *Journal of Pharmaceutical Sciences*, 2016, **105**, 3153-3161
180. I. Hwang, H. N. Kim, M. Seong, S. Lee, M. Kang, H. Yi, W. G. Bae, M. K. Kwak, H. E. Jeong, *Advanced Healthcare Materials*, 2018, **7**, 1-20
181. M. Murphy, A. J. Carmichael, *American Journal of Clinical Dermatology*, 2000, **1**, 361-368
182. B. Chen, J. Wei, C. Iliescu, *Sensors and Actuators B: Chemical*, 2010, **145**, 54-60
183. J. W. Lee, S. Choi, E. I. Felner, M. R. Prausnitz, *Small*, 2011, **7**, 531-539
184. R. Ali, P. Mehta, M. S. Arshad, I. Kucuk, M. Chang, Z. Ahmad, *American Association Of Pharmaceutical Scientists*, *Sci. Tech.*, 2019, **21**, 1-14
185. S. H. Bariya, M. C. Gohel, T. A. Mehta, O. P. Sharma, *Journal of Pharmacy and Pharmacology*, 2011, **64**, 11-29
186. A. J. Guillot, A. S. Cordeiro, R. F. Donnelly, M. C. Montesinos, T. M. Garrigues, A. Melero, *Pharmaceutics*, 2020, **12**, 569
187. Y. Liu, Y. Huang, X. Duan, *Nature*, 2019, **567**, 323-333,

188. F. W. DelRio, M. P. de Boer, J. A. Knapp, E. D. Reedy, P. J. Clews, M. L. Dunn, *Nature Materials*, 2005, **4**, 629-634
189. K. Sharma, V. S. Mahalwal, *International Journal of Drug Development & Research*, 2011, **3**, 85-103
190. A. Mignon, J. Vermeulen, G. Graulus, J. Martins, P. Dubruel, N. De Beilie, S. Van Vilerberghe, *Carbohydrate Polymers*, 2017, **168**, 44-51
191. F. Dong, S. Magnanty, S. J. Meschter, J. Cho, *Progress in Organic Coatings*, 2018, **114**, 58-67
192. J. Liu, X. Jio, F. Cheng, Y. Fan, Y. Wu, X. Yang, *Progress in Organic Coatings*, 2020, **144**, 1-9
193. W. E. Hennink, C. F. Van Nostrum, *Advanced Drug Delivery Reviews*, 2012, **64**, 223-236
194. X. Sui, L. Van Ingen, M. A. Hempenius, G. J. Vancso, *Macromolecular Rapid Communications*, 2010, **31**, 2059-2063
195. C. Löwenberg, M. Balk, C. Wischke, M. Behl, A. Lendlein, *Accounts of Chemical Research*, 2017, **50**, 723-732
196. A. Ahsan, W. Tian, M. A. Farooq, D. H. Khan, *International Journal of Polymeric Materials and Polymeric Biomaterials*, 2020, **1**, 1-11
197. G. Li, R. K. Randev, A. H. Soeriyadi, G. Rees, C. Boyer, Z. Tong, T. P. Davis, C. R. Becer, D. M. Haddleston, *Polymer* Chemistry, 2010, **1**, 1196-1204
198. H. M. C. De Azeredo, M. F. Rosa, M. De Sá, M. Souza Filho, K. W. Waldron, *Advances in Biorefineries*, Woodhead Publishing, United Kingdom, 1st edn, 2014, ch. 26, pp. 819-874
199. S. Walker, R. Rothman, *Journal of Cleaner Production*, 2020, **261**, 1-15
200. S. N. Raj, S. N. Lavanya, J. Sudisha, H. S. Shetty, *Biopolymers*, 2011, **1**, 459-481
201. M. J. Fabra, A. López-Rubio, J. M. Lagron, *Smart Polymers and their Applications*, 2014, **1**, 476-509
202. M. Fasciotti, *Sustainable Chemistry and Pharmacy*, 2017, **6**, 82-89
203. M. Rayung, M. M. Aung, S. C. Azhar, L. C. Abdullah, M. S. Su'ait, A. Ahmad, S. N. A. M. Jamil, *Materials*, 2020, **13**, 838
204. J. Fernández, A. Larrañaga, A. Etxeberria. J. Sarasua, *RSC Advances*, 2016, **6**, 22121-22136

205. Y. F. Tsang, V. Kumar, P. Samadar, Y. Yang, J. Lee, Y. S. Ok, H. Song, K. Kim, E. E. Kwon, Y. J. Jeon, *Environment International*, 2019, **127**, 625-644
206. V. Siracusa, I. Blanco, *Polymers*, 2020, **12,** 1641
207. T. Iwata, *Angewandte Chemie International Edition*, 2015, **54**, 3210-3215
208. M. Jahangeer, S. A. Qamar, Z. Mahmood, M. Asgher, *Life Science Journal of Pakistan*, 2019, **1**, 33-40
209. R. P. Babu, K. O'Connor, R. Seeram, *Progress in Biomaterials*, 2013, **2**, 1-16
210. L. Chen, R. E. O. Pelton, T. M. Smith, *Journal of Cleaner Production*, 2016, **137**, 667-676
211. H. Nakajima, P. Dijkstra, K. Loos, *Polymers*, 2017, **9**, 523
212. N. C. Iheaturu, I. V. Diwe, B. Chima, O. O. Daramola, E. R. Sadiku, *Green Biopolymers and their Nanocomposites*, ed. D. Gnanasekaran, Springer, Singapore, 1st edn, 2019, ch. 10, pp. 233-250
213. E. Campodoni, E. B. Heggest, A. Rashad, G. B. Ramírez-Rodríguez, k. Mustafa, K. Syverud, A. Tampieri, M. Sandri, *Materials Science and Engineering: C*, 2019, **94**, 867-878
214. A. Alkilani, M. T. McCrrudden, R. Donnelly, *Pharmaceutics*, 2015, **7**, 438-470
215. K. Kathem, H. Kathpalia, *Asian Journal of Pharmaceutical Sciences*, 2017, **12**, 487-497

Chapter 2 – Formulation, Property Testing and Drug Loading of Bio-based Polymer Transdermal Films.

2.1 Overview

The study of transdermal drug delivery systems has been a topic which has been explored for the past 50 years. The use of bio-based polymers for transdermal drug delivery would be an ideal solution, due to their non-toxic and safe nature. Transdermal films with the ability to load and release drugs, while meeting a criteria of being thin, having a consistent and homogenous shape, and being flexible, were synthesised. Explored approaches included Michael addition through linking thio and acrylate groups, and the Layer by Layer (LbL) technique which utilised electrostatic interactions of charged bio-materials.

2.2 Introduction

The concept of transdermal drug delivery systems has been contemplated for almost 50 years[1]. Transdermal drug delivery carries the potential to be an alternative to oral delivery as it can be more efficient as a result of reducing first-pass metabolism. It is also a more comfortable alternative to having an injection[2]. More recently, the possibility of creating transdermal gels and films for transdermal drug delivery has been explored. It's hypothesised that bio-based polymer films which are thin, flexible, homogenous, non toxic and durable, can be fabricated with the ability to load and release drugs.

Bio-based polymers have been sought after due to being non-toxic and being safer for use on human skin. Bio-based polymers are also good for the enviornment as they are made from renewable resources and can be completely biodegradeable. By using bio-based polymers, we can reduce the amount of fossil fules being used, and help preserve the enviornment[3].

Soybean oil has been used in dermatology[4], but has more recently seen use as pressure sensitive adhesives due to the fact that it can be easily obtained and fucntionalised[5]. Acrylated Soybean oil can be cross-linked with other polymers containing thiol groups in order to create lipophilic based hydrogels[6]. As human skin is also lipophilic, it allows for the hydrogel to bond easily to the surface of the skin.

Dextran is a straight chain polysaccharide which is both biodgradeable and biocompatable making it a promising prospect for a variety of uses in biomedical applications. Modifications can be made to the hydroxyl functionality within dextran, which can allow for crosslinking, and therefore gain adhesive properties as a result. Thiolating dextran allows for the crosslinking with acrylates to form hydrogels [Scheme 2- 1][7].

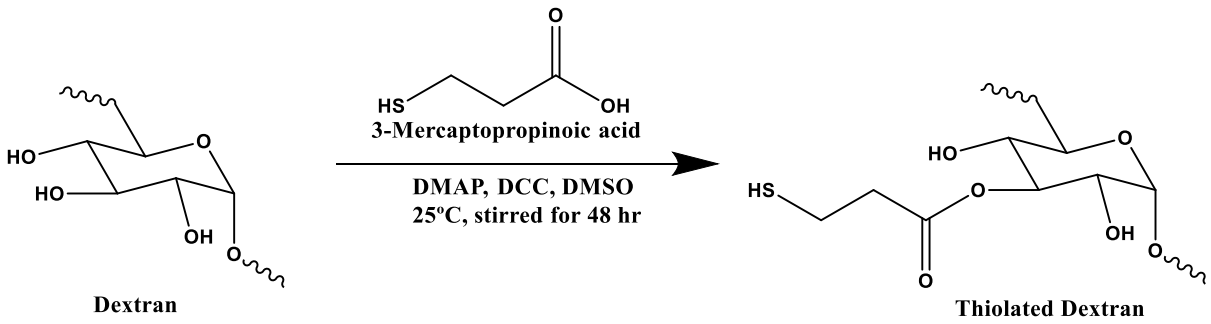

Scheme 2- 1: Synthesising thiolated dextran using dextran and 3-mercaptopropionic acid.

Crosslinking with polyethylene glycol (PEG) is explored due to its nonadhesive properties towards proteins[8]. PEG was acrylated to form PEG diacrylate (PEGDA) in order for cross-linking to occur through the process of Micheal addition [Scheme 2- 2]. PEGDA also has shown promising results for biospecific tissue resurfacing.

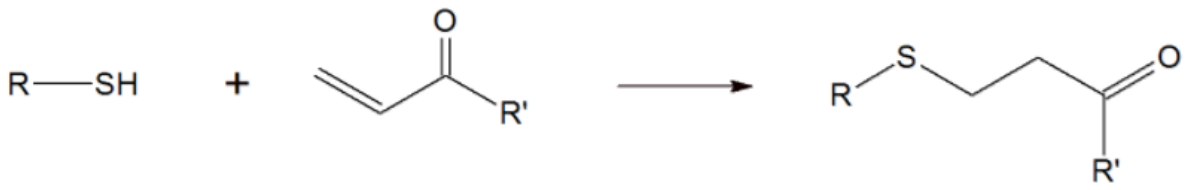

Scheme 2- 2: Thiol Michael Addition with an acrylate group, where R and R' are different carbon chains.

Sodium alginate is another natural polysaccharide which is a derivative from algae. Its unbranched chains consists of d-mannuronate (M) and l-guluronate (G) residues covalently linked with (1-4) glycoside bonds. It has previously been used for encapsulated drug delivery due to its ability to swell up to 300x its own weight and release molecules[9].

Chitosan has been explored as a material with the ability to extend the corneal residence time of drugs. Chitosan–alginate polymeric complex can be formed due to ionic interaction between the carboxylate groups of alginate and the ammonium groups of chitosan. The formed films are biocompatible, biodegradable, non-toxic, and capable to sustain the release of drugs more efficiently than either alginate or chitosan can without each other[10].

2.3 Experimental

2.3.1 Materials and Methods

Soybean oil epoxidized acrylate (100%) (AESO), pentaerythritol tetrakis(3-mercaptopropionate) (95%) (QT), triethylamine (99%) (TEA), 40kDa dextran, PEG Diacrylate (PEGDA), Methanol (99.8%), 3-mercaptopropionic, 4-(dimethylamino)pyridine, 1,3- dicyclohexylcarbodiimide, dimethyl sulfoxide (DMSO), Industrial Methylated Spirits (IMS), sodium alginate (Low viscosity) (100%), chitosan (90%), acetic acid glacial (99.5%), hydrochloric acid (37%) (HCl) all purchased from Sigma-Aldrich. Fused granular calcium chloride purchased from Fischer Science.

Polyethylene terephthalate (PET) were sheets kindly donated by various supplyers, and cut to size using a pair of scissors and a 15 cm ruler (subdivision 0.1 cm).

2.3.2 Michael Addition of AESO and QT

Ratios of 4:1, 2:1 and 1:1 AESO:QT were prepared for cross linking. Soybean oil epoxidized acrylate (250.0 mg, 0.20 mmol) samples were added to three pentaerythritol tetrakis(3-mercaptopropionate) samples and were prepared on glass slides of the dimensions 7.5 cm x 2.5 cm. (25.0 mg, 0.05 mmol), (49.0 mg, 0.10 mmol) and (98.0 mg, 0.20 mmol) respectively at room temperature. Triethylamine (56 µL, 0.04 mmol), (84 µL, 0.06) and (102 µL, 0.074) was added to the respective 4:1, 2:1 and 1:1 AESO:QT samples in order to provide a base for the reaction to occur. The reaction was monitored for 7 hours at 38ºC in an oven. The resulting gels were then washed with 1:1 methenol:deionised water (5 mL), and dried in 'Thermo Scientific Hereaus vacumm oven' for 24 hours.

The experiment was repeated with DMSO (0.35 mL) added at room temperature to each sample after the addition of triethylamine, in order to assess how the solvent would affect the gel's properties.

2.3.3 Thiolation of 40kDa Dextran

3-mercaptopropionic acid (638.0 mg, 6.01 mmol), 4-dimethylaminopyridine (1100.0 mg, 9.00 mmol), and *N*,*N*′-Dicyclohexylcarbodiimide (911.0 mg, 4.41 mmol) was dissolved in 50 mL DMSO. The resulting mixture was purged with nitrogen for 20 minutes and stirred at 300 rpm at room temperature. 40 kDa dextran (3 g, 0.075 mmol) was then added to the solution, and the mixture was purged with nitrogen for a further 10 minutes at room temperature. The mixture was heated to 25ºC and left to stir for 48 hours. The resulting mixture was stored and cooled to 0ºC in a refrigerator for 16 hours. An off-white solution was observed. The resulting mixture was precipitated into

a stirring solution of cold industrial methylated spirits (400 mL). The precipitate in solution was centrifuged at 20ºC for 30 minutes at 3500 rpm using a 'Heraeus Megafuge 16R' centrifuge. The industrial methylated spirits were decanted from the centrifuge tubes, and the remaining white solid was collected for drying. The solid was dried in an oven at 20 ºC for 48 hours resulting in a white solid. The product was redissolved, vacuum filtered, and precipitated out into a stirring solution of cold industrial methylated spirits (1 L). The precipitate in solution was centrifuged again at 20ºC for 30 minutes at 3500 rpm. The industrial methylated spirits was decanted from the centrifuge tubes, and the remaining white solid was collected. The product was placed in a 'Thermo Scientific Hereaus Vacumm Oven' which was heated to 37.5ºC, and reduced to 50 mbar pressure, and left for 48 hours. The product was then dried to afford the desired product (2.34 g, 64.21%) [Table 2- 1] as a white solid. The product was analysed via NMR analysis, using D_2O as the solvent. [Figure 2- 1]

The above experiment was repeated to observe the effect of leaving the initial reaction mixture to stir at 25ºC for only 24 hours instead of 48 hours, after being purged with nitrogen. The product was then dried to afford the desired product (2.10 g, 57.84%) [Table 2- 1] as a white solid.

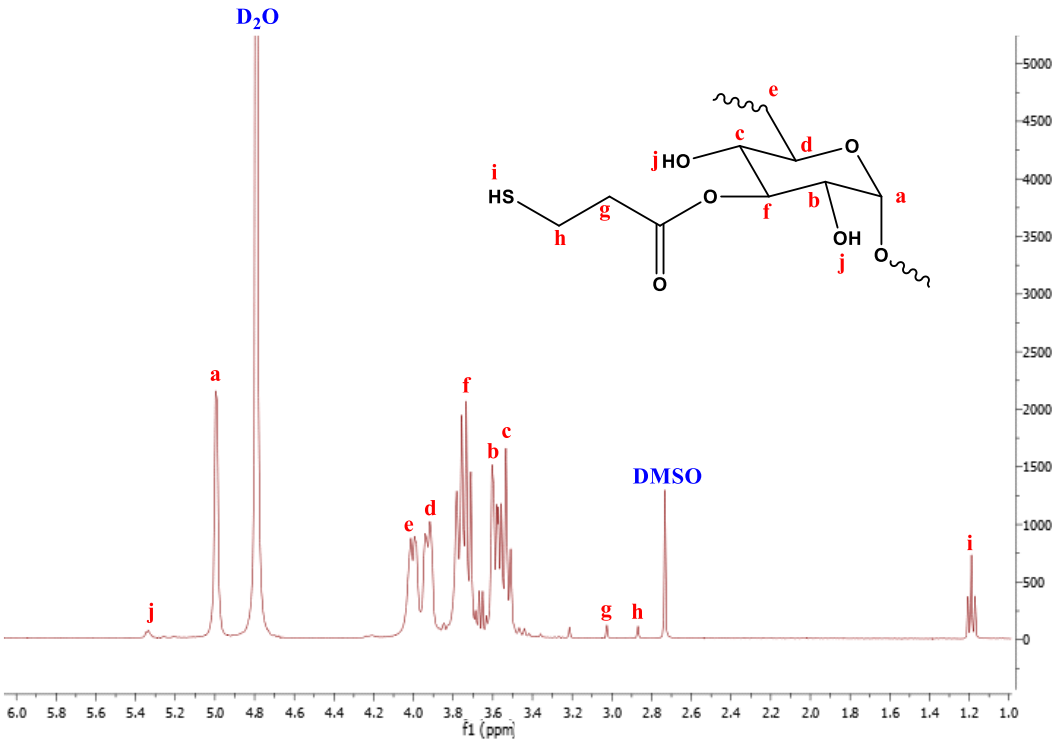

Figure 2- 1: The ^{1}H NMR spectrum for the 48 hour reaction of thiolated dextran in D_2O.

Table 2- 1: Weights and yields of thiolated dextran after the 24 hour and 48 hour reactions.

Time (hours)	Weight (g)	Yield (wt. %)
24	2.10	57.84
48	2.34	64.21

The NMR spectra of both the 48 hour and 24 hour products showed the appearance of singlets at ~2.9 ppm and ~3.0 ppm [Figure 2- 1] indicating that the thiolation of dextran had occurred. The resonances within the NMR spectra of 48 hour reactions are more intense than that of the 24 hour reaction, indicating that a greater amount thiolation has occurred[11].

2.3.4 Michael Addition of Thiolated Dextran with PEGDA

Thiolated 40 kDa dextran was used in attempted Michael addition with PEG diacrylate (700 Mn), in 1:1 ratio.

To a solution of 40 kDa thiolated dextran (100 mg, 2.5 µmol) and PEGDA ($Mn=700 g mol^{-1}$, 120 mg, 0.17 mmol) in water (1 mL) was added triethylamine (0.12 mmol). The solution was placed on PET slide, and incubated in a vacuum oven for 12 hours at 38ºC. A milky white, translucent, thin crust like film formed on the PET slide.

2.3.5 Layer by Layer Film Experiments Using Sodium Alginate with Calcium Chloride

The layer by layer film formulation relies on the ionic interaction of two biopolymers consisting of opposingly charged components - in this case sodium alginate (positively charged) and calcium chloride (negativley charged).

Two solutions were prepared. 3% sodium alginate solution, and 5% calcium chloride ($CaCl_2$) solutions were prepared by dissolving 1.5 g of sodium alginate in 50 ml of deionised water, and 2.5 g of $CaCl_2$ in 50 ml of deionised water. Solutions were made up in a 50 ml volumetric flask and stirred at 300 rpm for 3 hours.

A 7.5 cm x 2.5 cm PET slide was cut. The slide was cleaned using deionised water, then submerged in industrial methylated spirit for 1 hour. After drying in air, the PET slide was submerged vertically in a centrifuge tube containing a 3% sodium alginate solution for 15 minutes. The sodium alginate covered slide was then dried for 12 hours. The slide was then transferred to the 5% $CaCl_2$ solution for 15 minutes using the same method. The process was repeated once, and then the resulting gel was dried using a light flow of nitrogen from a hose, resulting in a film thin, flexible, translucent, homogenous film.

The sodium alginate/calcium chloride multi-layer film experiment was repeated changing the time parameters for time spent submerged in each solution [Table 2- 2]. PET slides were submerged vertically in each 50 mL solutions once each for 2 minutes, in order to determine the difference in thickness[12].

2.3.6. Layer by Layer Film Experiments Using Sodium Alginate with Chitosan

The layer by layer film formulation relies on the ionic interaction of two biopolymers consisting of opposingly charged components - In this case sodium alginate (positively charged) and chitosan (negativley charged) [Figure 2- 2].

A 3% soduim alginate solution was prepared by dissolving sodium alginate (1.5 g) in deionised water. A pH 4 actic acid solution was prepared by adding concentrated acetic acid dropwise to 50 mL of deionised water, using a 'Thermo Scientific Orion Star A111' pH meter to determine when pH 4, approximate concentration of $1x10^{-3}mol/d^3$, had been reached. A 5% chitosan solution was prepared by dissolving chitosan (2.5) g in 50 mL of the prepared pH 4 acetic acid solution in a 50 mL chonical flask, and stirred for 24 hours. A 7.5 cm x 2.5 cm PET slide was cut, cleaned with deionise water, then submerged in industrial methylated spirit for 1 hour, dried in air,

and then submerged in the 3% sodium alginate solution for 5 minutes. The sodium alginate coated PET slide was then removed, and placed in the 5% chitosan solution for 5 minutes. The PET slide was then removed, and left to dry in air for 12 hours.

A 3% chitosan solution was made up by dissolving chitosan 1.5 g in the pH 4 acetic acid solution (50 mL) using the same method used to make the 5% solution. This was used to determine the effect on thickness of the films when changing the conecntration of chitosan[13].

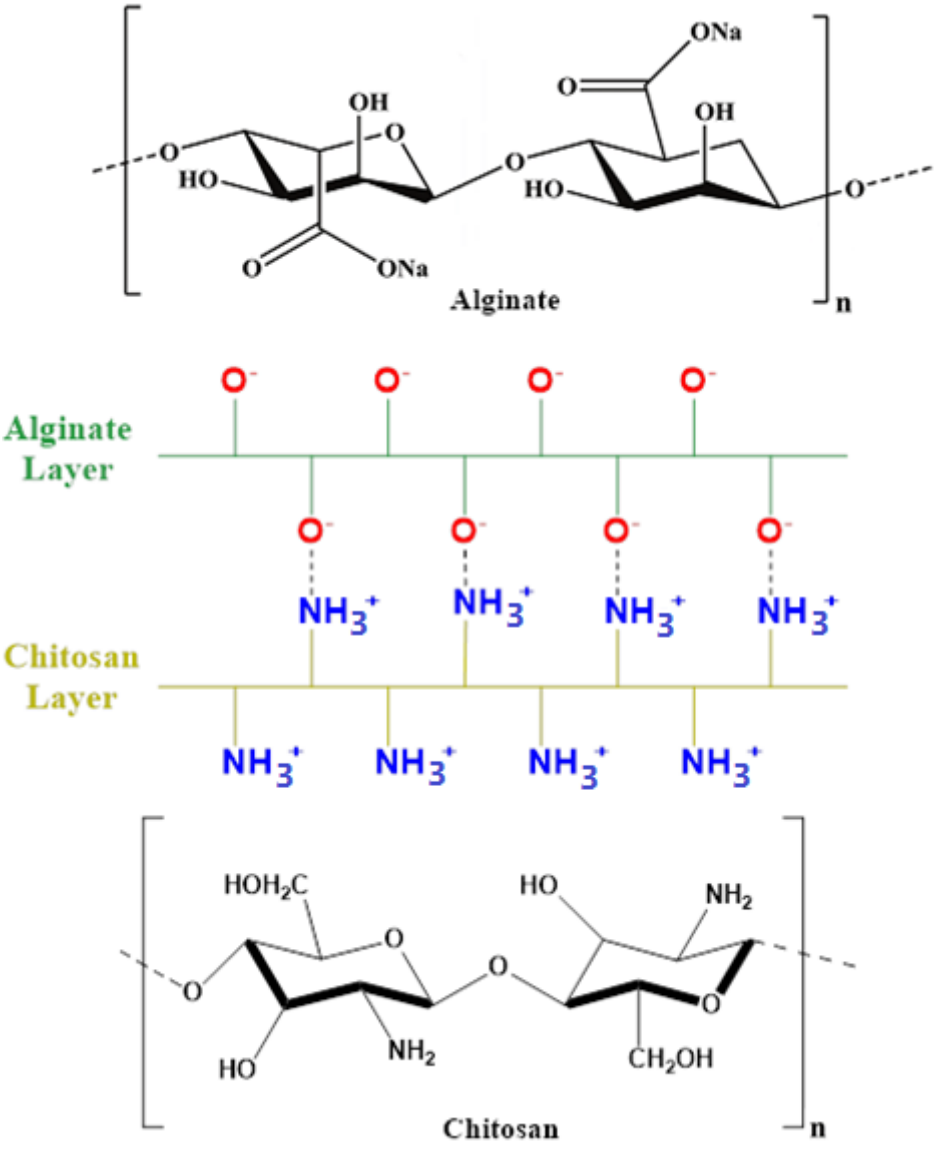

Figure 2- 2: Digram representing the electrostatic interactions between alginate and chitosan in the LbL technique.

2.3.7 Swelling studies of Sodium Alginate Films

Swelling tests were carried out on sixteen films. These films were created using the LbL technique. Both 2% and 3% solutions of sodium alginate in water were prepared. 3% and 5% solutions of calcium carbinate in water were prepared. 3% and 5% solutions of chitosan in pH 4 acetic acid were prepared. Eight of the films were made using 3% sodium alginate solutions with either 3% or 5% calcium chloride or chitosan, in either a 1 double layer or 2 double layer film system. Eight films of different compositions were submerged in each solution once for 5 minutes each to generate films consisting of 1 double layer. The other eight films were submerged in each solution twice for 2.5 minutes each to generate films consisting of 2 double layers. Each LbL process lasted a total of 10 minutes with 12 hour drying breaks between each submersion.

Sixteen 7.5 cm x 2.5 cm PET slides were created, weighed, and then used to hold each individual multi-layer film. The resulting films were then left to air dry, and then weighed before the swelling test. Each film (on its PET slide) was fully submerged in 20 mL deionised water for 1 minute, weighed, submerged for a further 4 minutes, and then weighed again. After each withdrawal, the swollen films were dried using kimtech science wipes in order to remove any residual water. It was possible to determine the percentage increase of the films' weight, therefore showing how much water each film combination could hold.

2.3.8 Determining Film Thickness of Sodium Alginate/Chitosan Films

Eight films formulated using sodium alginate and chitosan were created using biopolymer solutions of various concentrations. 2% and 3% sodium alginate solutions, and 3% and 5% chitosan solutions were used to create films which were tested to determine their film thickness. Eight 7.5 cm x 2.5 cm PET slides were cut and submerged vertically in solutions of sodium alginate and chitosan. Four films were consisting of a 1 double layer system were created, where the slide sat in each solution

for 5 minutes, with 1 hour of drying time between submersions. Four 2-layered films were created where the slide sat in each solution for 2.5 minutes, with 1 hour of drying time between submersions. Films were left to dry for 12 hours, and then weighed. After weighing, film thickness was tested using a micrometer (subdivision 0.01 mm).

2.4 Results and discussion

2.4.1 Gelation via Crosslinking AESO with QT

Gelation was attempted using acrylated groups from AESO[16], and crosslinking it with QT's thiol groups through Michael Addition, using TEA as the base to catalyse the reaction. The initial ratio of AESO:QT used was 4:1. Samples both with and without DMSO as a solvent were synthesized to to assess the effect of DMSO on the gelation and the gel's properties. The resulting gels were non-homgenous, soft and malliable, easily broken and flexible. The gelation with DMSO resulted in increased toughness of the gel, but were also more brittle.

Gelation was attempted again using a 1:1 ratio, where the amount of QT was increased. The result was gels with similar properties for both with and without DMSO, with the only difference being that the gels had an increase thickness.

Gelation was attempted once more using a 2:1 ratio, where the equivalents of QT were decreased, however there were no changes in the properties. The result was a gel thicker than the 4:1 ratio, but thinner than the 1:1 ratio.

This led to the understanding that increasing the amount of QT increases the amount of film thickness due to an increased amount of cross linking resulting in more gelation. The use of DMSO only made the films more brittle, as a result of interaction with the QT's thiol groups. At this point, soybean oil crosslinked with QT's candidacy to be used as a transdermal adhesive was put on hold, and the option to explore other materials was favoured.

2.4.2 Thiolated Dextran with PEGDA

Gelation was attempted using thiolated 40 kDa dextran, and crosslinking it with PEGDA (Mn=700gmol^{-1}) through Michael addition[17], using TEA as the base to catalyse the reaction. The ratio used was 1:1.

The reactants were applied to a 7.5 cm x 2.5 cm PET slide. After the experimental was completed, the contents were removed from the oven. What was observed was a milky white, translucent, thin crust like film [Image 2- 1]. It was apparent that the composition had no adhesion. The product was easily removed from the PET slide.

Instead of trying to improve the gelation of dextran with PEGDA, this biopolymer combination was paused due to more promising films being seen using sodium alginate with $CaCl_2$ and chitosan, using the LbL technique[18].

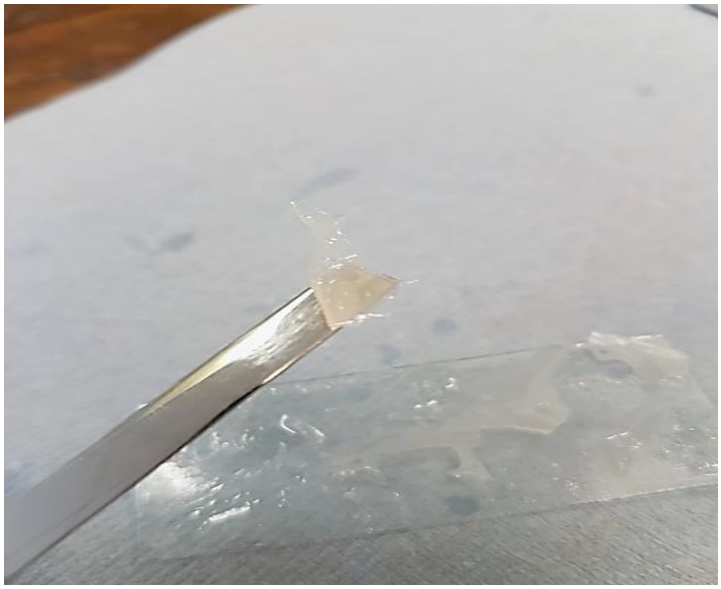

Figure 2- 3: Thin translucent crust formed from crosslinking thiolised 40 kDa dextran with PEGDA(Mn = 700gmol^{-1}).

2.4.3 Using the Layer by Layer technique to Create Films Consisting of Sodium Alginate and Calcium Chloride.

Using LbL, films consisting of sodium alginate and calcium chloride were created through electrostatic attraction. A solution of 3% sodium alginate, carrying a negative charge, was the first coating on the PET slide and comprised the bottom layer of the film. A 5% solution of calcium chloride was then coated on top, and the result was a thin, flexible, translucent, homogenous film in the shape of a rectangle.

Experiments to determine how submerge time affected the film thickness were carried out. A PET slide was submerged in each solution for 15 minutes, and then a second slide was submerged for only 2 minutes in each solution using the same procedure.

The difference in thickness could be determined visibly [Figure 2- 3]. It was apparent that a longer submerge time resulted in an increased film thickness. The 15 minute film also began to lose it's homgenity, as the film was much thicker in the centre than it was on the sides.

Figure 2- 4: Sodium alginate/$CaCl_2$ films after air drying. The 15 minute submerged film (top) and the 2 minute submerged film (bottom) showing visible differences in film/gel thickness and homogenity.

2.4.4 Using the Layer by Layer Technique to Create Films Consisting of Sodium Alginate and Chitosan.

LbL was used to create a sodium alginate and chitosan comprised film, again using the electrostatic attraction. A solution of negatively charged 3% sodium alginate coated the surface of the PET slide, and was then coated with a layer of positively charged 5% chitosan solution.

The result was another homogenous thin film coating on the PET slide. The film was partially removed from the slide in order to determine its properties. The film was thin, homogenous, flexible, transparent, strong and durable, and exhibited a plastic like texture [Figure 2- 4].

A solution of 3% chitosan was prepared in pH 4 acetic acid in deionised water (50 mL). This was made in order to determine the difference between that and using a 5% chitosan solution. A new solution on 3% sodium alginate (low viscosity) was also prepared. A 2-layer film was made by submerging a PET slide in the 3% sodium alginate solution for 5 minutes, followed by 12 hours of drying in air, then the PET slide being submerged in 3% chitosan for 5 minutes, and finally left to dry for 12 hours in air. This process was then repeated with the amount of time submerged reduced to 2.5 minutes in each solution.

Using 3% chitosan, as opposed to 5%, resulted in a thinner film as the end product. The amount of time for the slide to be submerged in each solution is a direct factor in the outcome of film thickness.

Figure 2- 5: Thin multi-layer film coating of sodium alginate and chitosan on a PET slide.

2.4.5 Swelling Studies of Sodium Alginate Films Comprised with Calcium Chloride or Chitosan

Swelling tests[19] were carried out on sixteen multi-layer films. Four 2-layered films consisting of alternating sodium alginate and $CaCl_2$ layers, four 4-layered films consisting of sodium alginate and $CaCl_2$, four 2-layered films consisting of alternating sodium alginate and chitosan layers, four 4 layered films consisting of sodium alginate and chitosan. See [Table 2- 2] for film composition. 2-layer films were submerged in each solution once for 5 minutes - 4-layer films were submerged in each solution twice for 2.5 minutes. Films were dried for 12 hours in air between each submersion. All films spent a total of 10 minutes submerged, and were fully dry before being subjected to swelling tests.

Table 2- 2: Bio-based polymer multi-layer film contents, number of layers within each film, and time spent submerged in sodium Alginate, and chitosan or calcium chloride solutions per layer.

Film Number	Multi-Layer Film Contents	Number of layers in the Film	Time Submerged in Each Solution Per Layer (Min)
1	2% sodium alginate + 3% chitosan	2	5.0
2	3% sodium alginate + 3% chitosan	2	5.0
3	2% sodium alginate + 5% chitosan	2	5.0
4	3% sodium alginate + 5% chitosan	2	5.0
5	2% sodium alginate + 3% $CaCl_2$	2	5.0
6	3% sodium alginate + 3% $CaCl_2$	2	5.0
7	2% sodium alginate + 5% $CaCl_2$	2	5.0
8	3% sodium alginate + 5% $CaCl_2$	2	5.0
9	2% sodium alginate + 3% chitosan	4	2.5
10	3% sodium alginate + 3% chitosan	4	2.5
11	2% sodium alginate + 5% chitosan	4	2.5
12	3% sodium alginate + 5% chitosan	4	2.5

13	2% sodium alginate + 3% $CaCl_2$	4	2.5
14	3% sodium alginate + 3% $CaCl_2$	4	2.5
15	2% sodium alginate + 5% $CaCl_2$	4	2.5
16	3% sodium alginate + 5% $CaCl_2$	4	2.5

The swelling test results were tabulated. Contents, number of times transferred to a new solution, time submerged in each solution, dry film weight, swollen film weight after 1 and 5 minutes percentage increase were all included in [Table 2- 3].

Table 2- 3: The contents, weight dry film, swollen weights at each time and percentage weight increase.

Film Number	Weight of Dry Film (mg)	Weight of Swollen Film After 1 min (mg)	Weight of Swollen Film After 5 Mins (mg)	% Weight Increase After 1 min of Swelling	% Weight Increase After 5 Mins of Swelling
1	37.7	2163.7	2884.8	5639.26	7551.99
2	26.0	1593.1	2219.7	6027.31	8437.31
3	63.3	2946.2	5810.2	4554.34	9078.83
4	20.3	860.4	1239.0	4138.42	6003.45
5	49.2	106.9	106.0	117.28	115.45
6	40.4	114.6	182.4	183.66	351.49
7	69.2	113.3	172.8	63.73	149.71
8	61.9	116.1	188.0	87.56	203.72
9	68.2	2851.3	5445.3	4080.79	7884.31
10	74.1	4480.6	6336.2	5946.69	8450.88
11	19.2	1048.3	1513.8	5359.90	7784.38
12	40.4	1956.4	3304.0	4742.57	8078.22
13	84.6	190.7	195.9	125.41	131.56
14	59.4	247.3	286.6	316.33	382.49
15	91.9	149.5	157.9	62.68	71.82
16	116.8	211.2	261.3	80.82	123.72

All of the films had the capability to absorb water, but some were more absorbent than others. The number of layers had a negligible effect on the amount of swelling that occurred. This leads to the conclusion that the amount of swelling must be time dependent, as the total time for the films being submerged was 10 minutes.

Sodium alginate and chitosan comprised films held a much higher volume of water than the sodium alginate and calcium chloride comprised films. Increasing the percentage of chitosan, in the sodium alginate/chitosan films, reduces how much water can be held by the film [Figure 2- 6].

Figure 2- 6: Swollen sodium alginate/chitosan film (Left). swollen sodium alginate/calcium carbonate film (right) both after drying in air.

Increasing the percentage of sodium alginate increased the amount of water held for most of the films. Increasing the amount of calcium carbonate, in the sodium alginate/calcium carbonate films, decreases the amount of water that could be held by the films.

Although holding far less water, the sodium alginate + calcium chloride films maintained the shape of the PET slide more than the sodium alginate/chitosan films, most likely due to increased swelling.

The results would suggest that sodium alginate is the most water absorbent material, followed by chitosan, and finally calcium chloride. Films comprising of more sodium alginate will absorb greater volumes of solution.

2.4.6 Analysing Film Thickness of Sodium Alginate/Chitosan Films

Eight films were created using different combinations of 2% and 3% sodium alginate solutions with 3% and 5% chitosan solutions, to determine film thickness. Four 2-layer films, of alternating sodium alginate and chitosan layers, were created where the PET slide was submerged in the sodium alginate and chitosan solutions for 5 minutes, with 12 hours of air drying between each submersion. Four 4-layered films were created where the slide sat in each solution for 2.5 minutes. The films were left to dry for 12 hours, and then weighed. After weighing, film thickness was tested.

The data in [Table 2- 4] shows that the 2 double layer films appeared to weigh more and resulted in thicker films. All films were measured using a micrometre (subdivision 0.01 mm) and were 0.07 mm (70 micrometres) or thinner. Film weight does not appear to have an overall effect, which indicates that the film thickness is primarily linked to the number of layers comprised in the film. Increasing the percentage concentration of sodium alginate appears to increase film thickness. Increasing the concentration of chitosan appears to have no effect on the thickness[20].

Table 2- 4: Film contents, weight of films and film thickness.

Film Contents	Number of Layers	Time Submerged in Each Solution	Weight of PET Slide (mg)	Weight of Dry Film (mg)	Film Thickness (mm)
2% Sodium Alginate 3% Chitosan	2	5 minutes	264.3	24.8	0.04
3% Sodium Alginate 3% Chitosan	2	5 minutes	309.1	26.1	0.04
2% Sodium Alginate 5% Chitosan	2	5 minutes	585.5	22.4	0.03
3% Sodium Alginate 5% Chitosan	2	5 minutes	274.4	25.5	0.05
2% Sodium Alginate 3% Chitosan	4	2.5 minutes	584.0	31.5	0.06
3% Sodium Alginate 3% Chitosan	4	2.5 minutes	551.3	53.3	0.07
2% Sodium Alginate 5% Chitosan	4	2.5 minutes	287.1	36.1	0.06
3% Sodium Alginate 5% Chitosan	4	2.5 minutes	630.9	64.4	0.06

2.5 Conclusion

Bio-based polymers were used to create gels and films as candidates to be used as transdermal drug delivery systems.

Gels made from crosslinking AESO with QT yielded gels that were soft, malleable and flexible, but did not meet the full criteria desired as the gels were not homogenous, too thick and easily broken. This led to putting the use of these materials as a candidate for a transdermal delivery system on hold, and bio-polymers with more desirable properties being sought.

The creation of films made through cross-linking thiolated dextran with PEGDA was explored as a possible candidate. Cross-linking via Michael addition of the materials was successful, resulting in the formulation of a film. However, the resulting properties of the film also didn't meet the desired criteria either as the film was too hard and brittle to be considered for use as a transdermal delivery system. This led to these materials also being put on hold in favour of sodium alginate films as they yielded more promising results.

The use of sodium alginate with either calcium chloride or chitosan, using the LbL technique, resulted in films that met the desired criteria for films to be used as a candidate for a transdermal delivery system. These films were soft, flexible, homogenous, thin, and were not easily broken. When soaked in water, these films were able to swell, with the sodium alginate/chitosan films swelling and absorbing water to 7000-9000% of their original weights.

As sodium alginate and chitosan consisting films swelled by a substantial amount more than the sodium alginate and calcium chloride consisting films, these materials were deemed to be the best candidate for creating a film capable of loading and releasing a drug.

Sodium alginate and chitosan layered films are a promising candidate for use as a bio-based transdermal delivery system and will be explored for their ability to load and release selected drugs in future chapters.

References

1. R.K. Subedi, S.Y. Oh, M.K. Chun, H.K. Choi, *Archives of Pharmacal Research,* 2010, **33**, 339-351
2. C. M. Schoellhammer, D. Blankschtein, R. Langer, *Expert Opinion on Drug Delivery*, 2014, **11**, 393-407
3. R. P Babu, K. O'Connor, R. Seeram, *Progress in Biomaterials*, 2013, **2**, 1-16
4. A. F. Stallings, M. P. Lupo, *The Journal of Clinical and Aesthetic Dermatology*, 2009, **2**, 36-40
5. B. K. Ahn, S. Kraft, D. Wang, X. S. Sun, *Biomacromolecules*, 2011, **12**, 1839-1843
6. R. Omer, J. R. Hama, R. Rashid, H. Tai, *Advances in Polymer Technology.*, 2017, **36**, 1-8
7. D. P. Nair, M. Podgórski, S. Chatani, T. Gong, W. Xi, C. R. Fenoli, C. N. Bowman, *Chemistry of Materials*, 2014, **26**, 724-744
8. D. L. Hern, J. A. Hubbell, *Incorporation of Adhesion Peptides*, 1998, **39**, 266-276
9. I. Liakos, L. Rizzello, D. J. Scurr, P. P. Pompa, I. S. Bayer, A. Athanassiou, *International Journal of Pharmaceutics*, 2014, **463**, 137-145
10. R. C. Nagarwal, R. Kumar, J. K. Pandit, *European Journal of Pharmaceutical Sciences*, 2012, **47**, 678-685
11. R.Choi, J. Yang, J. Choi, E.K. Lim, E. Kim, J. S. Suh, Y. M. Huh, S. Haam. *Langmuir*, 2010, **22**, 17520–17527
12. D. Silva, L. F. V. Pinto, D. Bozukova, L. F. Santos, A. P. Serro, B. Saramago, *Colloids and Surfaces B: Biointerfaces*, 2016, **147**, 81-89
13. J. M. Silva, J. R. Garcí**a**, R. L. Reis, A. J. Garcí**a**, João F. Mano, *Acta Biomaterial*, 2017, **51,** 279-293
14. J. L. Whittingham, D. J. Scott, K. Chance, A. Wilson, J. Finch, J. Brange, G. G. Dodson, *Journal of Molecular Biology*, 2002, **318**, 479-490.
15. S. Shahbaz, C. Katti, M. M. Khan, K. Pawar, *International Journal of Current Research and Review*, 2017, **9**, 1-3
16. H. Pelletier, N. Balgacem, A. Gandini, *Journal of Applied Polymer Science*, 2006, **99**, 3218-3221

17. K. Peng, I. Tomatsu, B. van den Broek, C. Cui, A. V. Korobko, J. van Noort, A. H. Meijer, A. Kros, *Soft Matter*, 2011, 7, 4881-4887
18. Y. Qiu, C. Winterton, J. M. Lally, Y. Matsuzawa, *United States Patent*, 2005, **6896929**, 1-12
19. C. V. Liew, L. W. Chan, A. L. Ching, P. W. S. Heng, *International Journal of Pharmaceutics*, 2006, **309**, 25-37
20. J. J. Richardson, M. Björnmalm, F. Caruso, *Science*, 2015, **348**, 411- 422

Chapter 3 – Determination of Galantamine as a Contender for Drug Release from Bio-Based Polymer Films and the Alteration of Film Composition for Optimal Drug Release

3.1 Overview

Alkaloids have been used for their multiple medicinal properties for centuries. The alkaloids galantamine and haemanthamine can be extracted from plants such as Galanthus Nivalis, and Narcissus (commonly known as daffodils). Galantamine has been commonly used in the treatment of Alzheimer's disease, and haemanthamine is used as an anti-cancer agent. In this chapter, it is explored if galantamine can be extracted from daffodil bulb liquid extract and used as a candidate for drug loading and transdermal drug release from bio-based polymer films comprised of sodium alginate and chitosan. Extracted galantamine and haemanthamine was characterised by nuclear magnetic resonance (NMR). Purified galantamine HBr was loaded into sodium alginate and chitosan solutions, and films were created using the layer-by-layer technique (LbL). Drug loading was confirmed using scanning electron microscopy (SEM) as a means to visually confirm the presence of galantamine within the bio-based polymer films and assess the porosity of the bio polymers. Resulting films were released in various of phosphate buffer solution's, with samples being withdrawn at set time intervals, to monitor the rate of release, and the overall release. Galantamine release from films was characterised using ultraviolet-visible spectroscopy (UV-VIS) as a means of determining the concentration of galantamine HBr present in the withdrawn samples. Film properties, including bio-based polymer concentration were altered to attempt to obtain an optimal bio-based polymer film candidate for drug release. Higher ratios of the guluronic acid sugar (G), as opposed to the mannuronic acid (M), found in alginate, was used to assess guluronic acids'

vertical orientation on the overall drug release, reducing the amount of horizontal orientation which is exhibited in mannuronic acid. The effect of the HBr salt in galantamine HBr on the drug release from bio-based polymer films was analysed by removing the HBr salt and formulation free base galantamine. Free base galantamine was characterized using NMR and Fourier-transform infrared spectroscopy (FTIR) techniques, and its effect on drug release was determined *via* further release studies.

3.2 Introduction

Alkaloids are basic organic compounds containing a minimum of one nitrogen atom [1-2], which are naturally occurring in nature[3-4]. The first uses of alkaloids as medicine dates back as far as 2000 BC[5] where people from continents across the globe would use alkaloid-containing plants as empirical medicines, and even as poisons in hunting[6]. By the early 19th century, the first alkaloids had been isolated and characterized[7]. The study of alkaloids had become increasingly popular, and began to advance at a rapid rate[8]. The first bioactive isoquinoline alkaloid was morphine, which was isolated from the opium plant[9], used as a pain suppressant[10]. Through scientific advancement, and the arrival of chromatographic and spectroscopic characterization methods, over 12000 alkaloids have been identified in plants up to the modern day[11].

Galantamine is a naturally occurring alkaloid from the Amaryllidaceae family[12]. Galantamine is commonly used in the treatment of Alzheimer's Disease[13] to help ease the rate of cognitive decline in patients[14]. Galantamine is an acetylcholinesterase inhibitor[15], and can promote the reduction of insoluble amyloid-β-peptide deposits present in brain parenchyma and in blood vessel walls[16]. It is a type 1 positive modulator of alpha-7-nicotinic acetylcholine which has been proven to inhibit enzymes from degrading acetylcholine in-turn preventing the breakdown of acetylcholine neurotransmitters[17-19]. This is achieved through galantamine's amine functional group allowing it to bind to the allosteric site of the nicotinic acetylcholine receptors[20]. By use of galantamine preventing acetylcholinesterase enzyme degradation of acetylcholine, it is possible for acetylcholine neuro transmitters to

remain active for longer[21]. Acetylcholine is a neurotransmitter present at multiple synapses and nerves[22]. The acetylcholine neurotransmitter supports the learning and memory process in the hippocampus[23]. Alzheimer's Disease causes the acetylcholine levels in the brain to decrease[24] causing the memory of those with Alzheimer's Disease to decline[25]. Through galantamine acting as an acetylcholinesterase inhibitor, it can slow down the effects of acetylcholine degradation caused by Alzheimer's Disease[26], when used on patients inflicted with mild to moderate levels of the disease.

Alzheimer's patients have been identified as target candidates for the use of transdermal drug delivery[27]. This is due to benefits including higher efficiency, and also prolonged drug release, when comparing transdermal drug delivery to alternatives such as oral drug consumption[28]. Transdermal drug delivery is also preferable as a matter of convenience for patients struggling with the effects of Alzheimer's Disease. It can be considered more of a convenience for patients to use prolonged drug delivery methods, as opposed to those which may require multiple daily oral doses[29]. This is convenient for those who have Alzheimer's Disease as they are less likely to forget to use prescribed medication if the amount of times per day they need to medicate is reduced[30]. The use of bio-based polymer transdermal methods could be even more desirable as they will biodegrade over time[31]. This can be beneficial for Alzheimer's patients as bio-based transdermal medication will eventually biodegrade if accidentally left on, without harming the patient[32].

Galantamine can be extracted from daffodil bulbs along with fellow alkaloid haemanthamine[33-34]. Haemanthamine has been explored for its use as an anti-cancer drug, due to its cytotoxic potential against cancer cell lines[35]. Both galantamine and haemanthamine are considered to be members of the amaryllidaceae alkaloid family[36]. Amaryllidaceae being plants consisting of perennial herbs. The stems are bulbs, enveloped by membranous leaf bases, known as the tunica[37]. Galantamine and haemanthamine are members of the amaryllidaceae as the daffodil meets the amaryllidaceae criteria[38]. Due to galantamine being found naturally in the daffodil plant [Figure 3- 1], it has the potential to be readily loaded into bio-based polymer materials and released in a suitable release media[39].

Figure 3- 1: Galantamine can be found in nature and extracted from daffodil bulbs[33].

Bio-based polymer transdermal films can be loaded with drugs *via* the layer by layer technique (LbL)[40]. Drug loading into the resulting bio-based polymer films can be confirmed visually by use of high magnification photography obtained through scanning electron microscopy (SEM)[41]. SEM uses an electron beam, on a material's surface, to produce images of high magnifications which can be clearly analysed[42]. Electrons interact with the materials' surface to generate signals which can give information about the topography, morphology, and sample composition[43]. Multiple signals can be generated, through the SEM electron beam, including secondary electrons, back-scattered electrons, transmitted electrons, absorbed current, X-rays and light[44].

It is possible to produce images with resolutions even below 1 nm[45]. This means it will be possible to use SEM to locate galantamine deposits, and analyse the pore size of the bio-polymers used to create the transdermal films[46]. Drug release can be quantified *via* ultraviolet visible spectroscopy (UV) analysis, where the absorption value from the peak correlating to galantamine can be used to determine the concentration in a sample[47]. Multiple films of varying properties were created using LbL, loaded with galantamine, and analysed for their ability to release the galantamine drug.

3.3 Experimental

3.3.1 Materials and Methods

Low viscosity sodium alginate (100%), chitosan (90%), sodium phosphate dibasic heptahydrate, sodium phosphate monobasic monohydrate, deuterated chloroform ($CDCl_3$) (99.8%) and deuterated water (D_2O) (99.9%) was purchased from Sigma Aldrich. Chloroform (98%), hydrochloric acid (HCl) (35.6%), industrial methylated spirits (95.0%), acetic acid (glacial) (99.5%) ethyl acetate (99%), magnesium sulphate ($MgSO_4$), sodium chloride (NaCl), and sodium hydroxide (NaOH) were purchased from Fisher Scientific. Higher guluronic acid (G) was purchased from Convatec. Daffodil bulb liquid extract in 2 M ammonium hydroxide (NH_4OH), and galantamine hydrobromide (HBr) (95%) were kindly donated Bioextraction Wales Ltd.

The pH levels of solutions were determined *via* use of an 'Orion Star A111 pH Meter'. Products were analysed by NMR, using $CDCl_3$ containing 1% (v/v) TMS as reference (0.00 ppm) and a Bruker Top Spin 400 MHz NMR machine [Figure 3- 2]. SEM was conducted using a Hitachi TM4000+ Tabletop SEM [Figure 3- 2].

***Figure 3- 2:* 'Hitachi TM4000+ Tabletop SEM' (left) and the 'Shimadzu UV-3600 UV-Vis Spectrometer' (right).**

3.3.2 Extraction of Galantamine Hydrobromide from Daffodil Bulb Liquid Extract

Galantamine and haemanthamine were extracted from a 2 L solution of post ion exchange daffodil bulb liquid extract using a 2 M ammonium hydroxide (NH_4OH) solution. The extraction was attempted using three methods. The daffodil bulb liquid extract was kindly donated by Bioextraction Wales.

3.3.2.1 Extraction Method A

Sodium chloride (30.00 g, 0.51 mol) was added to post ion exchange daffodil bulb liquid extract in NH_4OH (100 mL), to salt out the galantamine HBr. Laboratory reagent grade chloroform (100 mL) was added to the daffodil bulb liquid extract, in order to extract alkaloids from the daffodil extract solution. Extractions with chloroform (100 mL x 2) on the solution were conducted. A 1 M sodium hydroxide solution was prepared by adding 40 g of NaOH to 1 L of deionised water and stirred for 1 hour. The resulting 1 M NaOH was added dropwise to the now combined organic layer extracts until pH 13.0 was reached, in order to prevent the alkaloids from forming salts and remain soluble in the solution. The resulting solution was concentrated *in vacuo* to remove the chloroform. The resulting solid residue was dried under high vacuum for 16 hours to afford the desired products (0.81 g) as a crude white solid.

This experimental procedure was repeated with the use of analytical reagent grade ethyl acetate, instead of chloroform, to assess which solvent used in the extraction process produced a greater resulting yield. The resulting solid residue was dried under high vacuum for 16 hours to afford the desired products (0.22 g) as a crude white solid.

The ratio of galantamine and haemanthamine were compared using the integrations of the resonances in NMR spectra at 6.00 ppm and 5.87 ppm, corresponding to galantamine and haemanthamine respectively.

3.3.2.2 Extraction Method B

'Method B' included the same steps as 'Method A' with the absence of the salting out step. This was conducted in order to make a comparison on the effect on the extraction yield.

Laboratory reagent grade chloroform (100 mL) was added to the daffodil bulb liquid extract solution, in order to extract alkaloids from the solution. Extractions with chloroform (100 mL x 2) on the daffodil solution were conducted. A 1 M sodium hydroxide solution was prepared by adding 40 g of NaOH to 1 L of deionised water and stirred for 1 hour. The resulting 1 M NaOH was added dropwise to the now combined organic layer extracts until pH 13.0 was reached, in order to prevent the alkaloids from forming salts and remain soluble in the solution. The resulting solution was concentrated in vacuo to remove the chloroform. The resulting solid residue was dried under high vacuum for 16 hours to afford the desired products (0.28 g) as a crude white solid.

This experimental procedure was repeated with the use of analytical reagent grade ethyl acetate, instead of chloroform, to assess which solvent used in the extraction process produced a greater resulting yield. The resulting solid residue was dried under high vacuum for 16 hours to afford the desired products (0.02 g) as a crude white solid.

The ratio of galantamine and haemanthamine were compared using the integrations of the resonances in the NMR spectra at 6.00 ppm and 5.87 ppm, corresponding to galantamine and haemanthamine respectively.

3.3.2.3 Extraction Method C

A sample of the post ion exchange daffodil bulb liquid extract in NH_4OH (100 mL) was concentrated in vacuo at 60ºC. 0.85 g of a brown solid residue was recovered. Chloroform (50 mL) was added to the residue and the resulting stirred for 48 hours in order to triturate the material. The chloroform was decanted. Ethyl acetate

(50 mL) was added to the flask to further triturate the remaining brown solid residue, again being stirred for 48 hours. The chloroform and ethyl acetate solutions were placed into separate round bottom flasks and concentrated *in vacuo* at 40ºC to afford a white solid. The white solids were left under a high vacuum for 24 hours to afford the desired products as a crude white solid. The mass of the material obtained from the initial trituration with chloroform was 0.35 g, and the mass obtained from the second trituration with ethyl acetate was 0.06 g, resulting in a total of 0.41 g of crude desired products.

This experimental procedure was repeated with the use of analytical reagent grade diethyl ether, instead of chloroform and ethyl acetate, to assess if using this solvent in the extraction process produced a greater resulting yield. No desired products were afforded using this method.

3.3.3 Loading of Pure Galantamine Hydrobromide into Bio-Based Polymer Films Consisting of Sodium Alginate and Chitosan

Bio-based polymer films, consisting of sodium alginate and chitosan, were loaded with galantamine HBr (95%), which was donated by Bioextraction Wales Ltd, and release studies were conducted in phosphate buffer solutions. A calibration curve for galantamine was created for quantitative analysis. A stock solution was prepared by dissolving galantamine HBr (140.0 mg, 0.38 mmol) in deionised water (50 mL). The resulting solution was stirred at 300 rpm for one hour. 0.1 mM, 0.2 mM, 0.3 mM, 0.4 mM, 0.5 mM, 0.6 mM and 0.7 mM samples were prepared and characterised using a ‘Shimadzu UV-3600’ UV spectrometer. The max absorbance peak recorded for the samples was at 288 nm. The data obtained [Table 3- 1] was used to create the calibration curve [Figure 3- 3] allowing for the determination of the molar absorptivity from the gradient of the graph. Using the Beer-Lambert Law[48], knowing the absorbance (A), molar absorptivity (ε) and length of the light path (b = 1 cm), it is possible to determine the concentration (C) [eq 3- 1].

Table 3- 1: UV absorbance at concentrations of 0.1 mM-0.7 mM galantamine HBr.

Concentration (mM)	Absorption
0.1 mM	0.6405
0.2 mM	0.8920
0.3 mM	1.1446
0.4 mM	1.4002
0.5 mM	1.6594
0.6 mM	1.9192
0.7 mM	2.2545

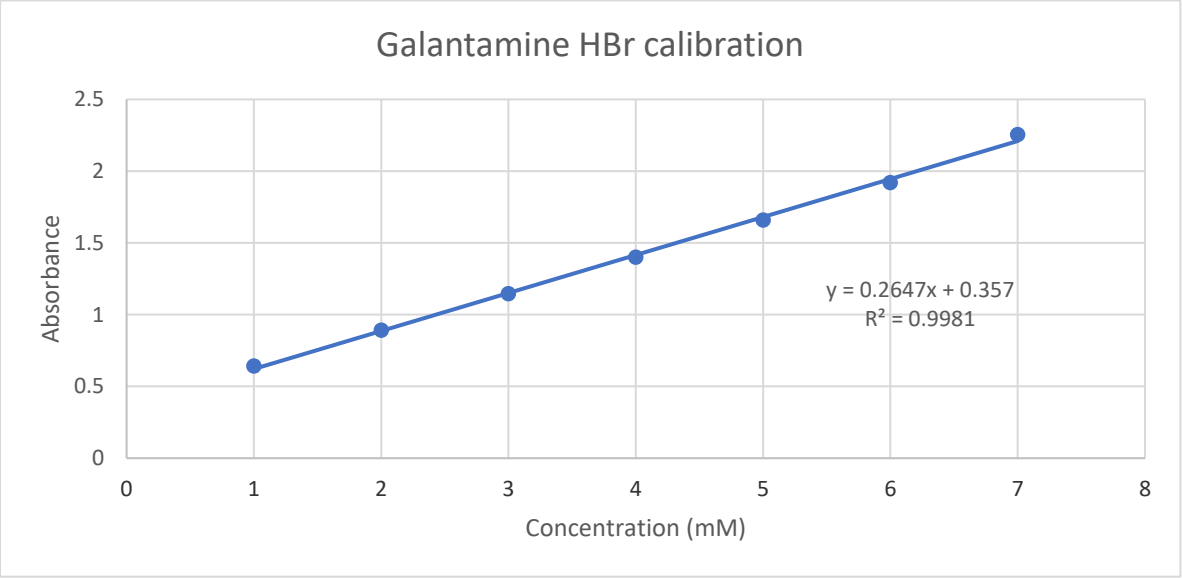

Figure 3- 3: The calibration curve for galantamine hydrobromide.

$R^2 = 0.99$ Max peak= 288 nm

Beer Lambert Law for absorbance at 0.1 mM:

$$A = \varepsilon.b.c \quad (eq\ 3\text{-}1)$$

A = 0.6405 mm ε = 0.2647 $mM^{-1}cm^{-1}$ b = 1 cm c = 2.42 mM

A sample of galantamine HBr (140.0 mg, 0.38 mmol) was dissolved in deionised water (50 mL), and then a second sample of galantamine HBr (140.0 mg, 0.38 mmol) was dissolved in pH 4 dilute glacial acetic acid (50 mL, 0.5 mM), which was prepared by adding concentrated 1 M glacial acetic acid dropwise to deionised water (1 L). Sodium alginate (1.5 g) was added to the solution containing only deionised water, and chitosan (1.5 g) was added to the acetic acid solution. The solutions were made up in a 50 mL volumetric flask and stirred at 300 rpm for 3 hours. This method was used to make galantamine HBr loaded 3% biopolymer solutions [Figure 3- 4]. The same method was used in biopolymer solutions of varying concentrations, where the amount of sodium alginate or chitosan was altered in accordance with the desired percentage concentration required, for example 2.5 g of the desired biopolymer for a solution of 5% biopolymer concentration.

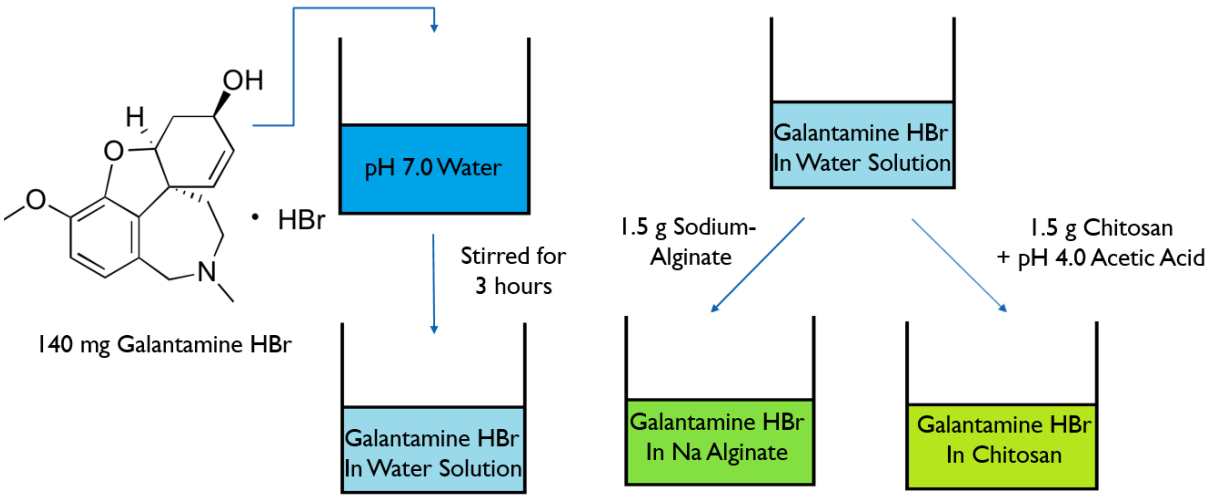

Figure 3- 4: Procedure for loading galantamine HBr into sodium alginate and chitosan solutions.

The layer by layer technique was used to create a galantamine loaded film consisting of sodium alginate and chitosan. A 7.5 cm x 2.5 cm PET slide was cut. The PET slide was cleaned using deionised water, then submerged in industrial methylated spirit for 1 hour to ensure the slide was clean. After drying, the PET slide was submerged vertically in a centrifuge tube containing galantamine HBr loaded 3% sodium alginate solution for 5 minutes. The galantamine HBr loaded sodium alginate covered slide was then dried for 12 hours. The slide was then transferred to the galantamine HBr loaded 3% chitosan solution for 5 minutes using the same method. The process was repeated once, and then dried in air for 12 hours. The result of this process was a galantamine HBr loaded biopolymer film [Figure 3- 5]. The film was thin, homogenous, flexible, transparent, strong and durable, and exhibited a plastic like texture, similar to that of previous films made without loading a drug into them.

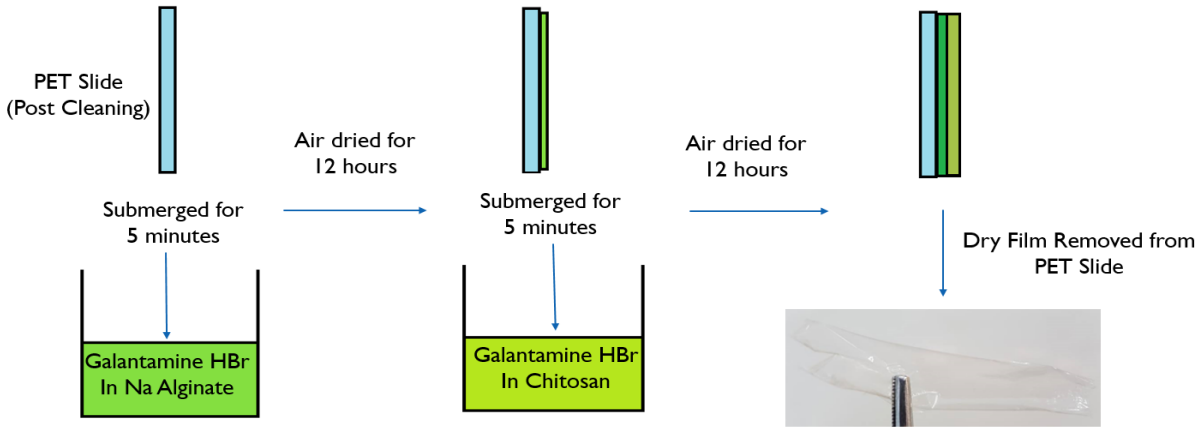

Figure 3- 5: Formation of galantamine HBr loaded sodium alginate and chitosan bio-based polymer films.

A pH 7.8 phosphate buffer solution (50 mL, 10 mg/mL) was prepared by dissolving sodium phosphate dibasic heptahydrate (417 mg, 1.56 mmol) and sodium phosphate monobasic monohydrate (83 mg, 0.6 mmol), in deionised water (50 mL). The resulting solution was made to the appropriate pH level *via* addition of either dilute sodium hydroxide solution (1.0 M), or a dilute hydrochloric acid solution (0.1 M), depending on what was required to reach the pH 7.8. The galantamine loaded sodium alginate and chitosan comprised films were submerged in the phosphate buffer solution for 3 hours. 2 mL samples were withdrawn from the solution after 10, 20, 30, 50, 70, 90, 120 and

180 minutes in which the solution had 2 mL of fresh phosphate buffer solution added after each sample withdrawal. Each withdrawn sample was characterised using through the 'Shimadzu UV-3600' UV-Vis spectrometer using 1 mL quartz cuvettes, cleaned using IMS followed by water, then dried between each sample being run. Phosphate buffer (10 mg/mL) of the appropriate pH was used as the blank. Each release study was completed in duplicate. The percentage release of galantamine was calculated using [eq 3- 2].

$$C_w = C_0 \,.\, C_r$$
$$W_r = W_s - W_o$$
$$V = W_r \,.\, \rho \qquad \textit{(eq 3- 2)}$$
$$n = V \,.\, C_w$$
$$M = n \,.\, M_r$$
$$\%M = 100(M_t / M)$$

Where C_w refers to the concentration of the drug in the film. C_o is the prepared concentration of the drug. C_r refers to the concentration of the drug in the initial sample withdrawn. W_o is the original film weight. W_s refers to the swollen film weight. W_r refers to the difference between the original film weight and the swollen film weight, i.e the amount of weight increase of the film post swelling. V refers to the swollen volume. ρ refers to the density. n refers to the number of moles of the drug. M refers to the mass of the drug. M_r refers to the drug's molar mass. %M refers to the overall percentage release of the drug. M_t refers to the weight of the drug released at a set time in the release.

3.3.4 SEM Analysis of Bio-Based Polymer Films

Samples of bio-based polymer films consisting of 3% sodium alginate and 3% chitosan, were mounted onto a circular metal stud which used an adhesive carbon disk which enhanced conductivity. The samples were cut using a razor in order to encompass the entire surface area of the stub[49]. The sample coated stubs were then placed inside a “Hitachi TM4000+ Tabletop SEM” [Figure 3- 2] and analysed. Three images were photographed of both sides of the bio-based polymer films. Images were acquired using a BSE detector, a 15 kV voltage, and the sample chamber under full vacuum. The three Images taken consisted of magnifications of x150, x1000 and x10000. SEM internal measurement scale used to measure points of interest, such as pore sizes.

The SEM images were photographed from the perspective of the surface of the sodium alginate layer. Four films were submitted for SEM analysis:

1. GLT 1 Blank – 3% sodium alginate/3% chitosan. No Galantamine HBr loaded.
2. GLT 1 Loaded - 3% sodium alginate/3% chitosan. Galantamine HBr loaded.
3. GLTG 1 Blank - 3% higher guluronic acid (G) sodium alginate/3% chitosan. No galantamine HBr loaded.
4. GLTG 1 - 3% higher guluronic acid (G) sodium alginate/3% chitosan. Galantamine HBr loaded.

3.3.5 Removal of the Hydrobromide Salt to Form Free Base Galantamine

A 4 M solution of sodium hydroxide was prepared by adding sodium hydroxide (56.0 g, 1.4 mol) to deionised water (200 mL) at room temperature. The resulting solution was stirred in a 500 mL volumetric flask at room temperature for 15 minutes, which was the time it took for the NaOH to fully dissolve. Further deionised water (150 mL) was added to the volumetric flask to bring the total volume to 350 mL, and the mixture was stirred for a further 1 hour.

Galantamine HBr (0.50 g) was dissolved in 4 M NaOH solution (10 mL). Chloroform (25 mL) was added to the solution and stirred at room temperature for 16 hours. The solution was separated. The aqueous layer was extracted with further chloroform (2 x 25 mL). The combined chloroform extracts were dried over magnesium sulphate, filtered and concentrated *in vacuo* to afford free based galantamine (0.35 g, 90%) as a pale white solid. NMR analysis confirmed the substance was free base galantamine [Figure 3- 6].

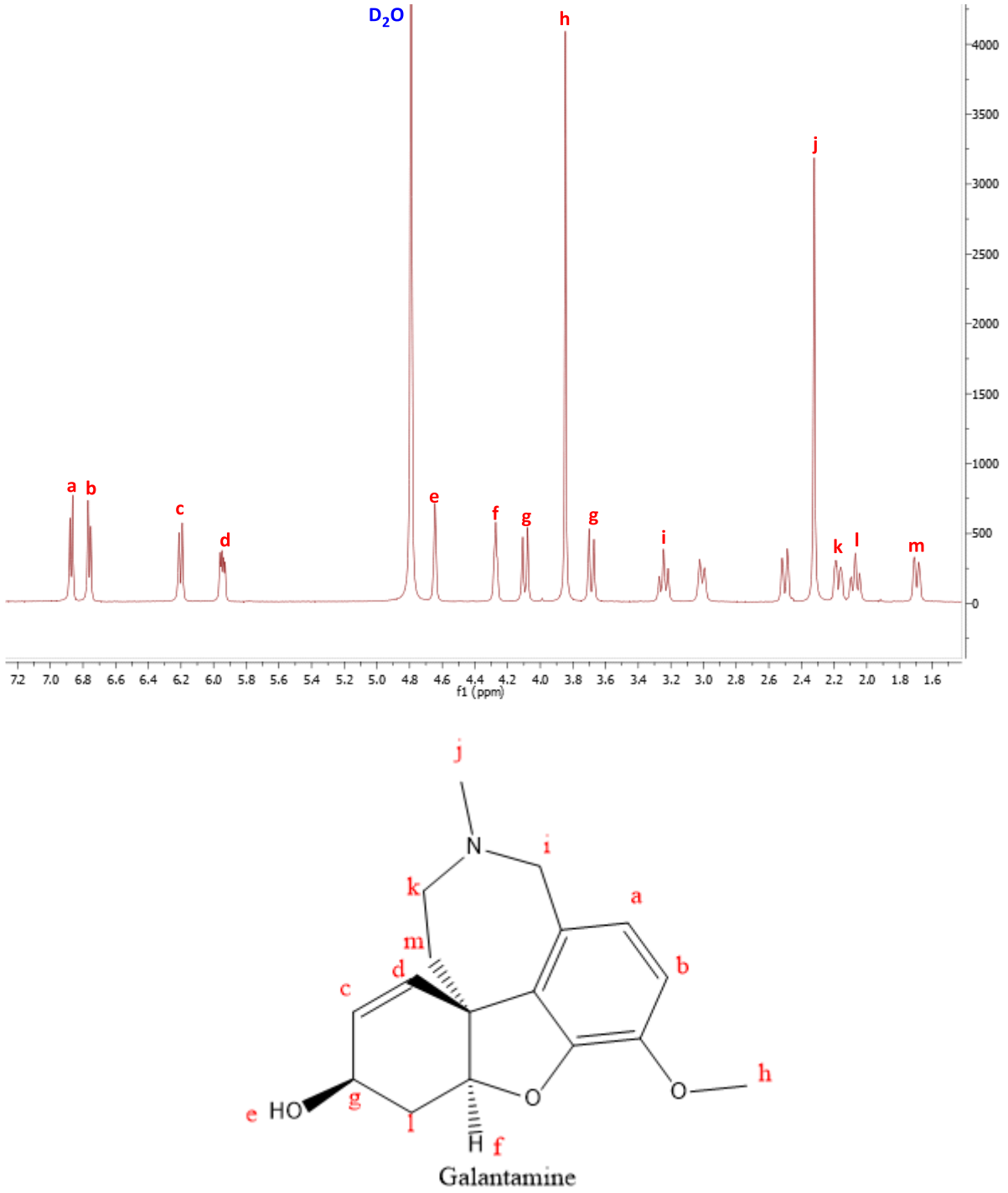

Figure 3- 6: ^{1}H NMR of free base galantamine in D_2O, and the compounds structure, showing which NMR peak correlates to its corresponding functional group.

The key difference in the NMR spectrum is the peak for the CH_3 attached to the tertiary amine, seen at 2.35 ppm in [Figure 3- 6] in the free base galantamine NMR, is shifted to 2.95 ppm in [Figure 3- 7] and the peak is broadened in the galantamine HBr NMR due to the presence of the HBr salt. This indicates that upon the removal of the HBr, there is no longer an N^+ charge present in the compound.

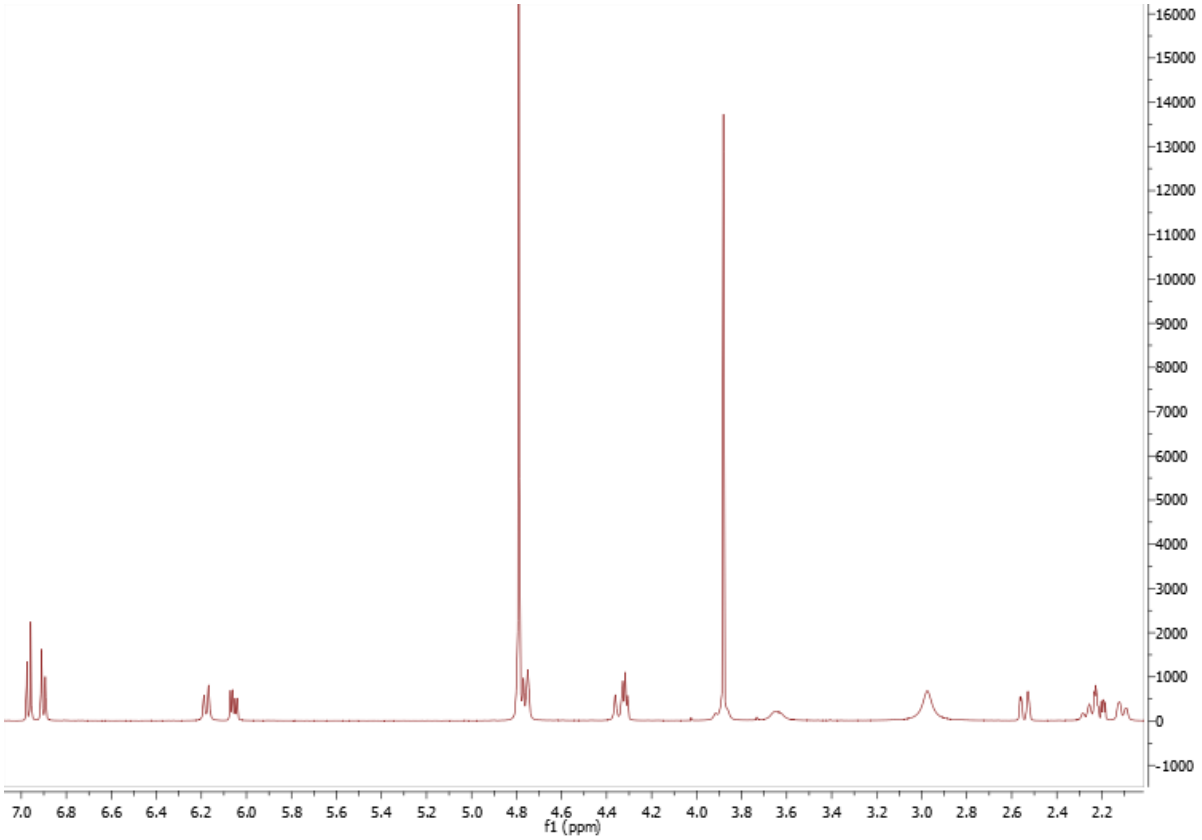

Figure 3- 7: ^{1}H NMR of galantamine HBr in D_2O, for comparison with the ^{1}H NMR of free base galantamine, emphasizing the lack of peak at 2.35 ppm. This reinforces the successful removal of the hydrobromide salt.

FTIR was conducted by placing a 5 mg sample onto a 'Bruker Alpha Platinum ATR FTIR machine'. The galantamine HBr samples were scanned 16 times per sample [Figure 3- 8, spectra A]. The scanning surface of the FTIR machine was then cleaned using IMS, and a sample of free base galantamine was studied using the same procedure [Figure 3- 8, spectra B].

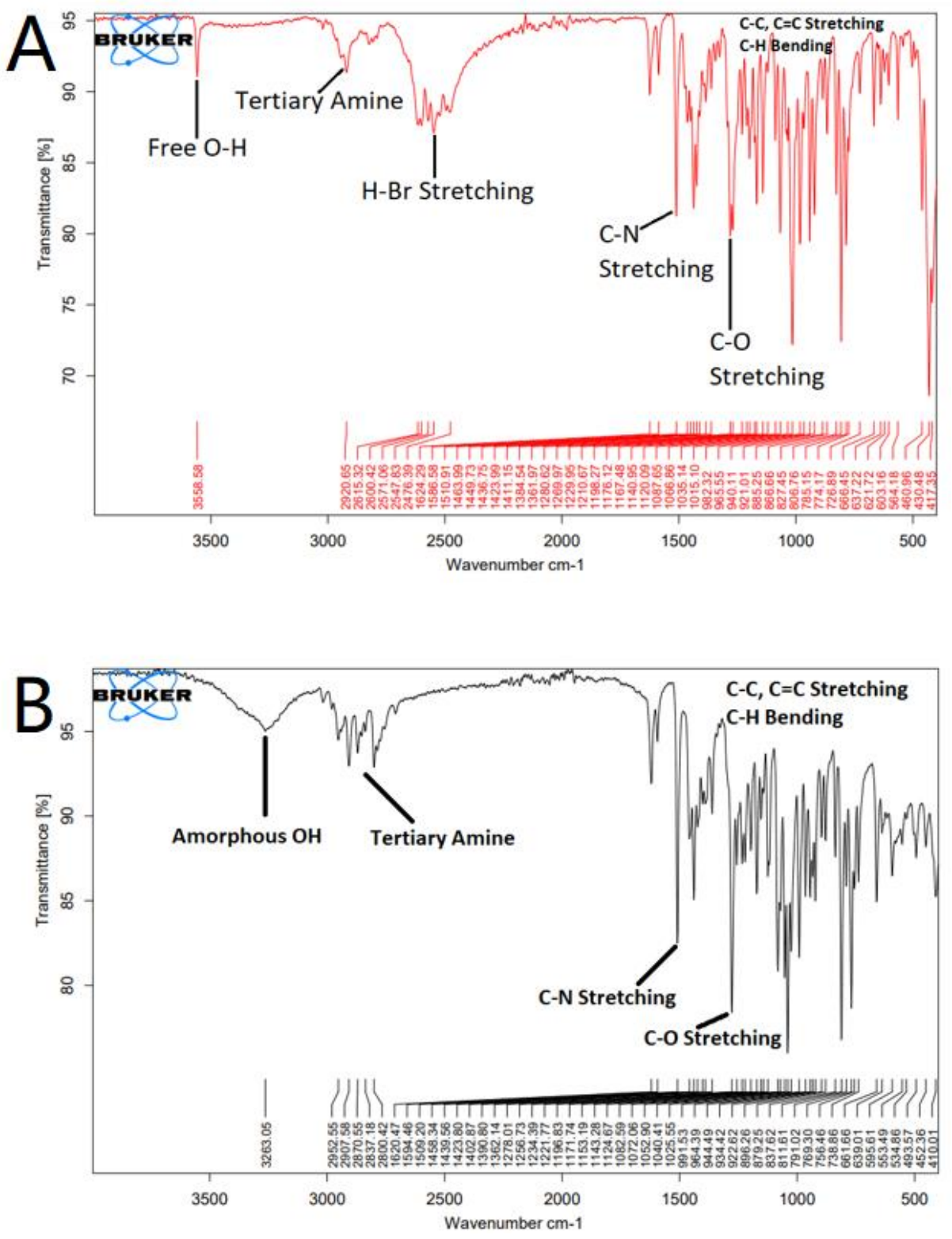

Figure 3- 8: FTIR spectra for galantamine HBr (spectrum A) and free base galantamine (spectrum B).

The key things to note when looking at the FTIR spectra of both the galantamine HBr, and the free base galantamine, is the fact that the peak that represents H-Br stretching at approximately 2500cm^{-1} in the galantamine HBr spectrum has massively regressed in the free base galantamine spectrum. The sharp O-H stretching at approximately 3550 cm^{-1} on the galantamine HBr spectra broadens in the free base galantamine FTIR spectrum. This indicates that a change from free bonding to intermolecular bonding at approximately 3250 cm^{-1} has occurred in the free base galantamine, which indicates a much-reduced interaction with the HBr salt. The rest of the spectra remains unchanged, indicating that none of the rest of the structure has been altered.

After NMR and FTIR analysis showed enough evidence that the HBr salt had been removed from galantamine, it was important to carry out a release study, using the free base galantamine to assess if removing the HBr salt has an effect on the release of galantamine from a bio-based polymer film.

A sample of free base galantamine (140 mg, 0.49 mmol) was dissolved in deionised water (50 mL). Another sample of free base galantamine (140 mg, 0.49 mmol) was dissolved in pH 4 dilute acetic acid solution (50 mL, 0.5 mM). Sodium alginate (1.5 g) was added to the solution containing only deionised water, and chitosan (1.5 g) was added to the solution containing acetic acid. The solutions were stirred for 5 hours until the samples had completely dissolved.

Using the layer by layer technique, a 7.5 cm x 2.5 cm cut and washed PET slide was submerged in the 3% sodium alginate solution for 5 minutes, removed and dried in air for 12 hours, and was then submerged in the 3% chitosan solution for 5 minutes. The resulting film was removed and left to dry in air for 12 hours.

A pH 7.8 phosphate buffer solution (50 mL, 10 mg/mL) was prepared by dissolving sodium phosphate dibasic heptahydrate (417 mg, 1.56 mmol) and sodium phosphate monobasic monohydrate (83 mg, 0.6 mmol), in deionised water (50 mL). The resulting solution was made to the appropriate pH level *via* addition of either dilute sodium hydroxide solution (1.0 M), or a dilute hydrochloric acid solution (0.1 M), depending on what was required to reach the pH 7.8. After the phosphate buffer solid had completely dissolved after 1 hour of stirring, the galantamine loaded 3% sodium alginate/3% chitosan film was submerged in the pH 7.8 phosphate buffer solution for

24 hours. 2 mL samples were removed after 10, 20, 30, 50, 70, 90, 120, 180, 240, 300, 360 and 1440 minutes in which the solution was topped up with 2 mL of fresh phosphate buffer solution. Each withdrawn sample solution was characterised through the 'Shimadzu UV-3600' UV spectrometer using 1 mL quartz cuvettes, cleaned using IMS followed by water, then dried between each sample being studied.

3.4 Results and Discussion

3.4.1 Analysis of Galantamine and Haemanthamine Extracted from Daffodil Bulb Liquid Extract

The results of extraction methods A, B and C were tabulated [Table 3- 2].

Table 3- 2: A comparison of results from post ion exchange daffodil bulb liquid extract in 2 M ammonium hydroxide extraction methods A, B and C. The total mass, and masses of the chloroform and ethyl acetate extracts, were recorded. The weight of the left-over insoluble residue, post extraction, was recorded. The ratios of haemanthemine to galantamine were recorded via NMR analysis.

Sample Number	Method	Total mass (g)	Mass of $CHCl_3$ Extraction (g)	Mass of EtOAc Extraction (g)	Mass of Insoluble Residue (g)	NMR Ratio H:G
2	A	1.78	0.81	0.22	0.75	2:1
3	B	1.15	0.28	0.02	0.85	2:1
1	C	1.31	0.35	0.06	0.90	2:1

Comparisons were made of the total masses obtained post extraction, and the ratios of galantamine and haemanthamine usage were compared *via* NMR analysis. The ratio of galantamine and haemanthamine were compared using the integrations of the resonances in the NMR spectra at 6.00 ppm and 5.87 ppm, corresponding to galantamine and haemanthamine respectively. The peak at 6.00 ppm corresponds to the CH proton at point ‘b’ on the structure of galantamine [Figure 3- 9]. This can be seen in the galantamine NMR ‘[Figure 3- 6]. The peak at 6.00 ppm corresponds to the CH proton at point ‘a’ on the structure of haemanthamine [Figure 3- 9].

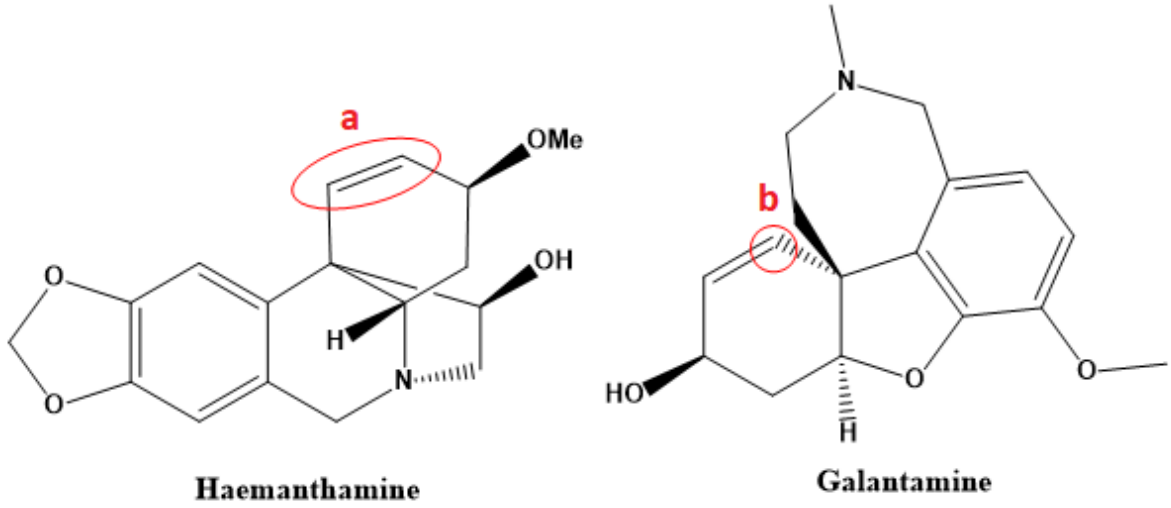

Figure 3- 9: The structures of haemanthamine (left) and galantamine (right), where a and b indicate the protons which correlate with the 5.87 ppm signal in the proton NMR for haemanthamine, and the 6.00 ppm signal in the proton NMR for galantamine respectively.

Extraction of galantamine and haemanthamine was possible using all methods. Using NMR, it was possible to identify peaks correlating to both galantamine and haemanthamine. However, the NMR showed that they were acquired along with other undefined insoluble plant materials. The trituration method used in ‘Method C’ resulted in much lower yields than that of the basification and extraction method used in ‘Method A’ and ‘Method B’. The results [Table 3- 2] show that ‘Method A’ is the most optimal for extracting galantamine and haemantamine.

In all three methods, it was possible to obtain larger extract masses when chloroform was used as the extraction solvent, which indicates alkaloids are more

easily extracted when using chloroform, with its slightly lower polarity than ethyl acetate.

Through NMR analysis, it was possible *via* integration of the peaks correlating to haemanthamine and galantamine, to determine the ratio of the two compounds that are present in the daffodil bulb liquid extract. In all 3 methods, the ratio of the integrations yielded a 2:1 ratio of haemanthamine to galantamine, leading to the overall conclusion that there is twice as much haemanthamine present than there is that of galantamine.

There were large amounts of brown insoluble residue in flasks post extraction with chloroform and ethyl acetate. It was not possible to extract any compounds from these solid residues.

3.4.2 Loading and Release of Galantamine from Bio-Based Polymer Films via UV and SEM Analysis

3.4.2.1 SEM Analysis

Galantamine HBr (95%), which was donated by Bioextraction Wales Ltd, was loaded into sodium alginate and chitosan solutions by dissolving galantamine HBr in water and pH 4 acetic acid (0.5 M). The appropriate amounts of chitosan and sodium alginate were added, and the mixture stirred until the bio-based polymers had dissolved in the solution. Using these solutions, galantamine HBr loaded sodium alginate and chitosan formulated bio-based polymer films were successfully made using the layer by layer technique. SEM analysis was used to determine if galantamine HBr loading was successful *via* visual confirmation of galantamine deposits within the bio-based polymer films. SEM was also used to determine the pore sizes of the sodium alginate and chitosan layers. As seen in [Image 3- 3] it was observed that the morphology of the film had changed with the formation of circular sites of varying sizes appearing on the surface of the film. These sites could be an indication of galantamine

deposits within the films; whether they are or not was not determined, however the morphology change is a direct result of galantamine loading.

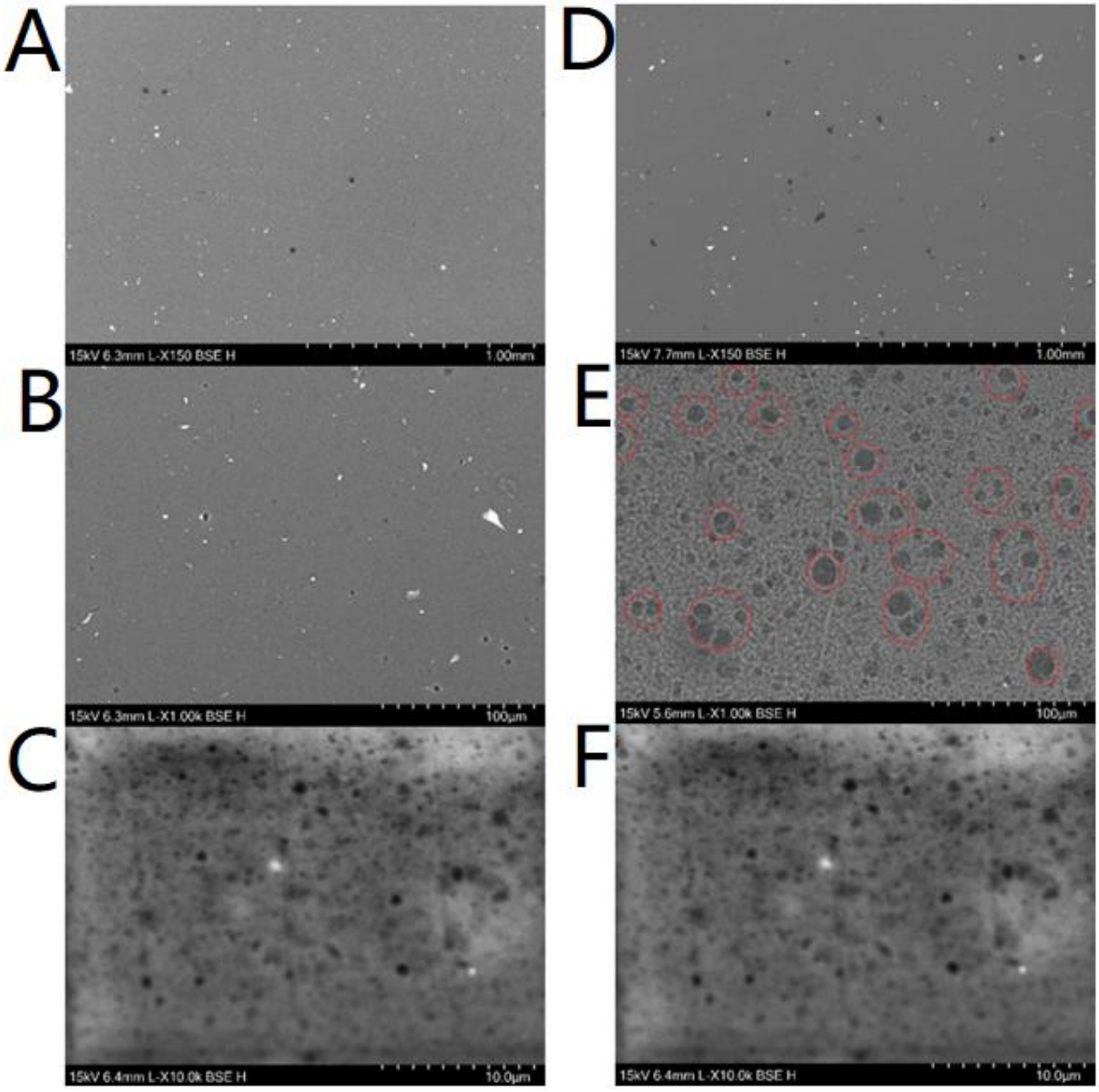

Figure 3- 10: SEM images of 3% sodium alginate/3% chitosan biopolymer films from the sodium alginate face. The images of the film on the left (A-C) are absent of the galantamine HBr. The galantamine HBr is present in the images of the film on the right (D-F). Image magnifications increase from x150 (A and D) to x1000 (B and E) to x10000 (C and F). Large galantamine HBr deposits are highlighted in red in the x1000 magnification image (E).

Comparing the SEM images at x1000 magnification, it was possible to determine that the morphology of the film had changed, thus visually indicating the changes in morphology post loading of galantamine into the sodium alginate and chitosan comprised bio-based polymer films. The size of the newly formed circular sites are between 5 µm and 200 µm in diameter which, if they are galantamine deposits, could result in different rates of release in different segments of the film. However, deposits were universally distributed across the surface of the film, meaning the overall impact on the galantamine release from films should be consistent in films formulated with the same properties and bio-polymer concentrations.

It was possible to determine the size of the pore diameters in both the sodium alginate and chitosan layers of the film with the sodium alginate layer exhibiting pore diameter size range of 1 µm - 10 µm, and the chitosan layer exhibiting 300 nm – 2 µm. The pore size of both the sodium alginate and chitosan layers meant that the loaded drugs will be able to release from the drug without a large amount of difficulty in pH 7.4 phosphate buffer solution.

3.4.2.2 Loading and Release of Galantamine HBr from Sodium Alginate and Chitosan Films

Several bio-based polymers consisting of varying polymer concentrations and numbers of layers were made [Figure 3- 11].

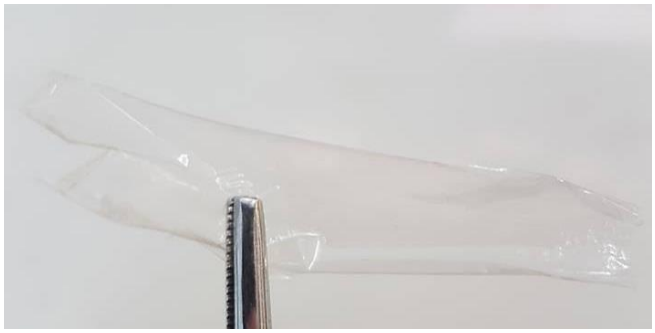

Figure 3- 11: A 3% sodium alginate/ 3% chitosan film, after removal from a 7.5 cm x 2.5 cm PET slide, loaded with galantamine hydrobromide.

In some instances, galantamine HBr was loaded into both the sodium alginate and chitosan layers, whereas in others, galantamine HBr was loaded into either the sodium alginate or chitosan layers. The films were submerged in phosphate buffer solution for 24 hours with 2 mL of the solution removed after 10, 20, 30, 50, 70, 90, 120, 180, 240, 300, 360, and 1440 minutes. A sample of 2 mL of phosphate buffer was added back to the solution after each withdrawal. The overall release of galantamine from each sample was determined *via* UV analysis and calculated using [eq 3- 1] and [eq 3- 2].

The first film to be selected as a candidate for drug release was 'GLT1', where the film's properties can be found in [Table 3- 3]. This film composition was selected as the first candidate due to the results of the swelling study, thickness study, and insulin release study conducted in Chapter 2 of this thesis, concluding that this was the likely optimal film composition. Five more films, whose properties can also be found in [Table 3- 3], were then compared with GLT1 to assess how the change in properties affected both the rate of galantamine HBr released in pH 7.8 phosphate buffer solution (10 mg/mL), and the overall final release of galantamine HBr after 24 hours.

Table 3- 3: A list of alternating alginate and chitosan layered bio-based polymer films, their composition, number of layers, pH of the alternating layers, the presence of galantamine HBr, and the percentage (%) release of galantamine HBr from each film.

Sample Name	Alginate Percentage	Chitosan Percentage	Number of Layers in Film	pH of Alginate Layer(s)	pH of Chitosan Layer(s)	Galantamine HBr in Alginate Layer(s)?	Galantamine HBr in Chitosan Layer(s)?
GLT1	3	3	2	7	4	✓	✓
GLT2	5	3	2	7	4	✓	✓
GLT3	3	5	2	7	4	✓	✓
GLT4	3	3	2	7	4	✓	*x*
GLT5	3	3	2	7	4	*x*	✓
GLT6	3	3	4	7	4	✓	✓

What we can see in [Figure 3- 12] and [Table 3- 4] is that over 50% of the galantamine is released in the first 10 minutes of submersion, with a total average release of approximately 75% released after 24 hours. The amount released between 14 hours and 24 hours is between 0.1% and 0.9% on average, which means that the GLT1 films are not optimal for 24 hours due to the rate of release being too slow.

Table 3- 4: The percentage release of galantamine HBr from GLT1 films, in pH 7.8 phosphate buffer solution, over 24 hours.

Time (mins)	Release 1 (%)	Release 2 (%)	Release Average (%)	Percentage Error (%)
10.00	53.8	51.0	51.3	2.4
20.00	54.2	52.4	53.0	1.0
30.00	55.5	53.5	54.4	1.0
50.00	57.2	55.7	56.6	0.8
70.00	57.8	57.4	58.3	1.1
90.00	59.8	59.3	60.1	1.0
120.00	61.7	60.8	61.8	1.1
180.00	63.5	61.8	63.3	1.4
240.00	64.9	64.2	65.0	0.8
300.00	65.7	65.7	66.3	0.9
360.00	67.4	67.8	67.9	0.6
1440.00	75.5	74.2	75.0	0.8

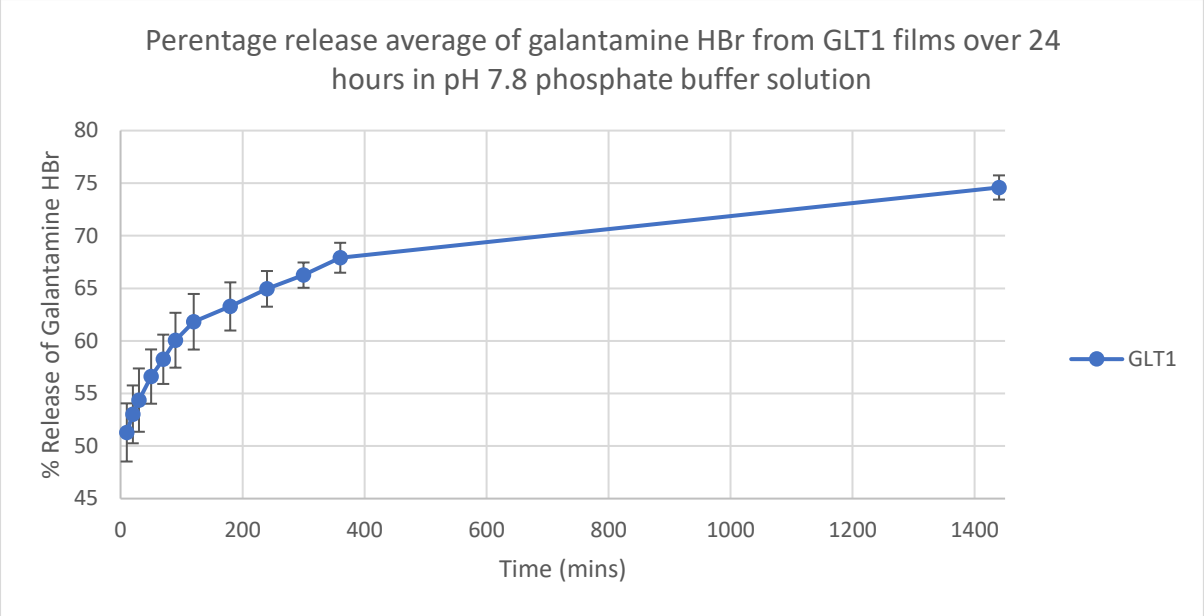

Figure 3- 12: The 24-hour average release profile of galantamine HBr from GLT1 films in pH 7.8 phosphate buffer solution.

The release profile tells us that over half of the galantamine HBr is released in the first 10 minutes. The film continues to release galantamine HBr over 15 hours before slowing down, and then slowing down further until the graph begins to plateau after 16 hours. 75% of the galantamine HBr had been released after 24 hours on average, though it is possible for higher amounts of release to occur. It also appears that not much more galantamine HBr would be able to be released past 16 hours from the GLT1 film. It can be determined that patients which have been recommended to use galantamine HBr could receive transdermal drug delivery from this film, and it can be used for 16 hours before needing to be discarded or replaced.

The benefit of the patch not needing to be replaced for 16 hours is that forgetting to regularly replace the patch, by either the patient or the carer, should not be an issue due to it only being required once or twice a day. One issue could be that patches may be discarded before all of the drug is released as a result of the patient having to sleep during the time the film stops releasing the drug. This means the patient will have to replace a patch before they sleep in order to ensure they are receiving their full dose whilst asleep, and the previous patch is partially wasted.

Films were made with different concentrations of sodium alginate and chitosan, and also an increased number of layers, to determine the effect on the release profile

and overall release. The first modification, when making ‘GLT2’, was to increase the concentration of sodium alginate to 5%, whilst keeping all the other film properties found in ‘GLT1’ the same. In the ‘GLT3’ film, the concentration of chitosan was increased to 5%, whilst returning the concentration of sodium alginate back to 3%. No further modifications were made to either ‘GLT2’ or ‘GLT3’. The data for the release of galantamine from the GLT2 film can be seen in [Table 3- 5] and [Figure 3- 13]. The data for the release of galantamine from the GLT2 film can be seen in [Table 3- 6] and [Figure 3- 14].

Table 3- 5: The percentage release of galantamine HBr from GLT2 films, in pH 7.8 phosphate buffer solution, over 24 hours.

Time (mins)	Release 1 (%)	Release 2 (%)	Release Average (%)	Percentage Error (%)
10.00	49.0	52.9	51.0	2.8
20.00	51.1	55.0	53.0	2.8
30.00	52.8	57.0	54.9	3.0
50.00	54.9	58.5	56.7	2.6
70.00	56.9	60.3	58.6	2.34
90.00	58.9	62.6	60.8	2.6
120.00	60.6	64.4	62.5	2.6
180.00	62.2	65.4	63.8	2.3
240.00	63.7	66.1	64.9	1.7
300.00	65.3	67.0	66.1	1.2
360.00	66.7	68.7	67.7	1.4
1440.00	67.5	69.2	68.3	1.2

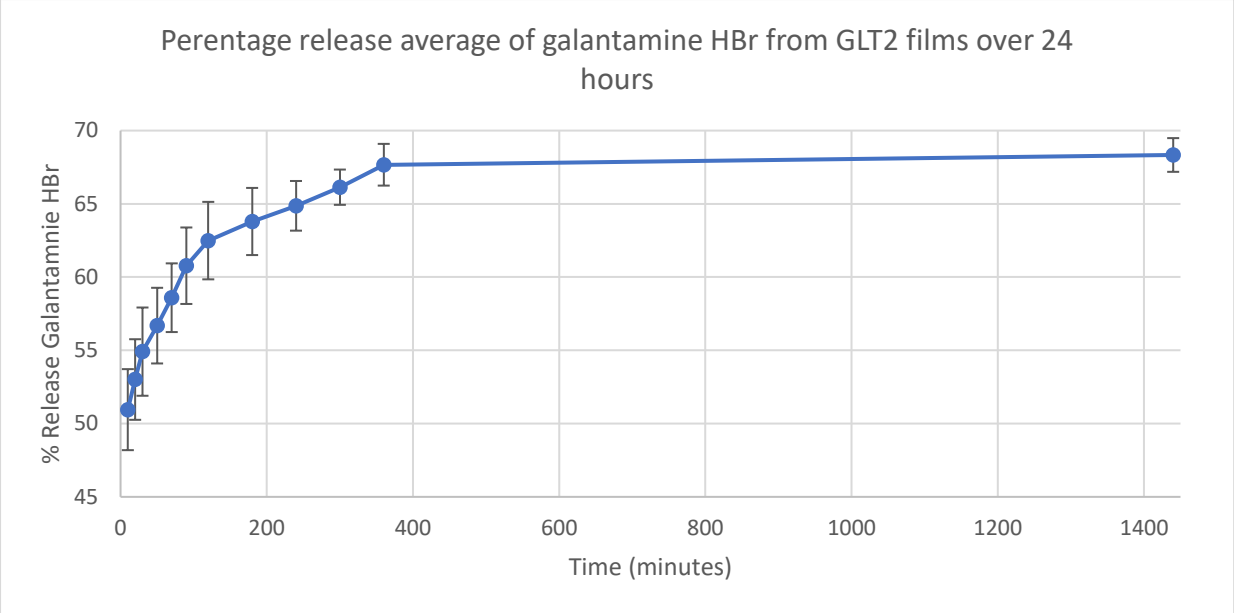

Figure 3- 13: The 24-hour average release profile of galantamine HBr from GLT2 films in pH 7.8 phosphate buffer solution.

Table 3- 6: The percentage release of galantamine HBr from GLT3 films, in pH 7.8 phosphate buffer solution, over 24 hours.

Time (mins)	Release 1 (%)	Release 2 (%)	Release Average (%)	Percentage Error (%)
10.00	53.8	54.9	55.8	1.4
20.00	57.0	56.4	58.7	3.3
30.00	60.2	58.6	60.9	3.2
50.00	62.8	60.8	63.3	3.5
70.00	65.4	62.7	65.6	4.0
90.00	69.3	64.3	67.8	5.0
120.00	70.5	66.0	69.3	4.6
180.00	71.1	67.2	70.6	4.9
240.00	71.9	68.5	72.7	5.9
300.00	72.8	69.4	73.6	6.0
360.00	73.2	70.2	74.2	5.7
1440.00	73.3	71.12	74.7	5.1

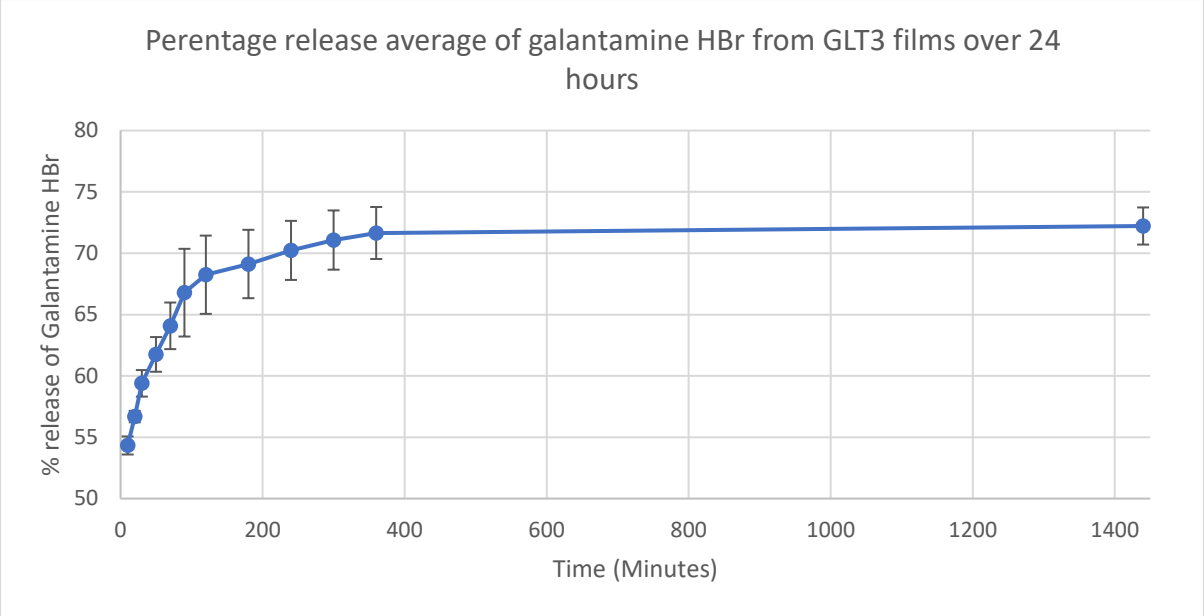

Figure 3- 14: The 24-hour average release profile of galantamine HBr from GLT3 films in pH 7.8 phosphate buffer solution.

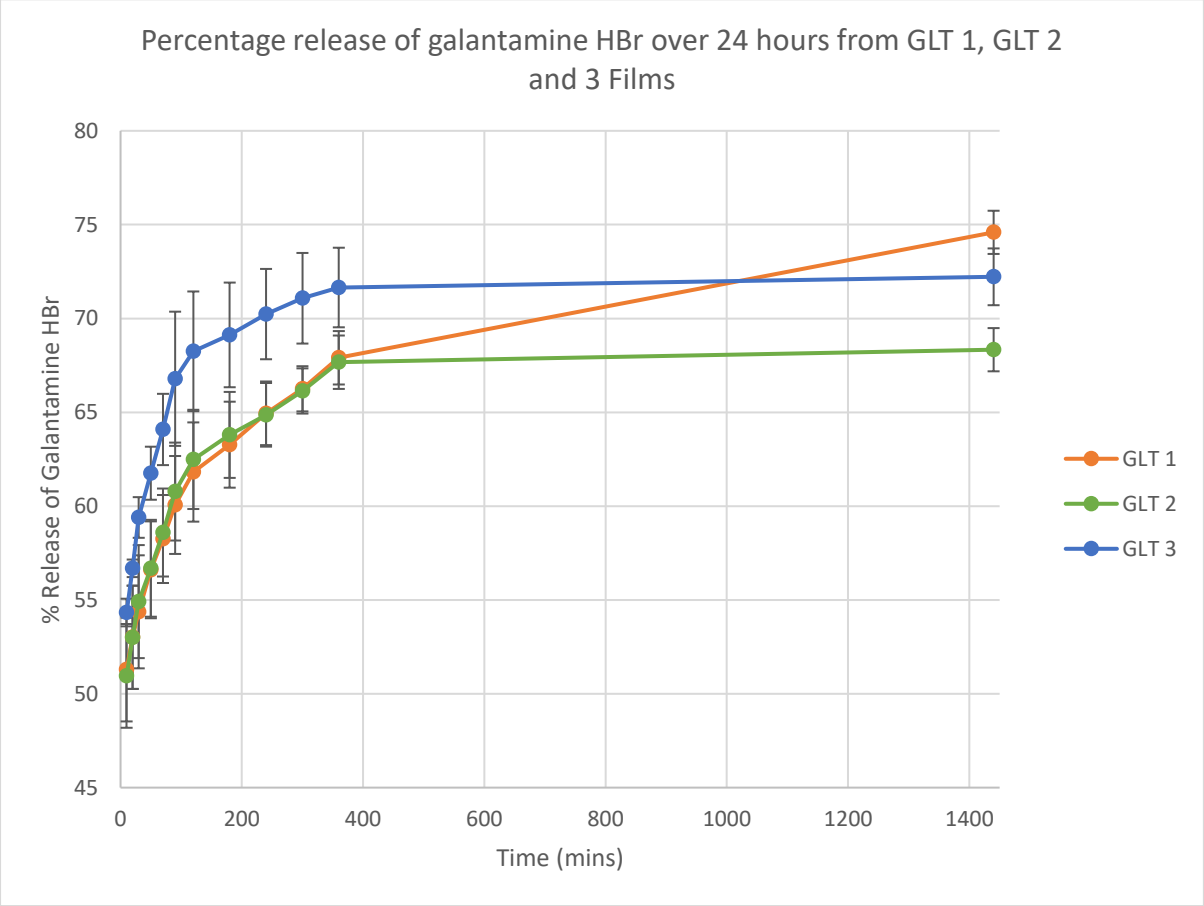

Figure 3- 15: The 24-hour release profile of galantamine HBr from GLT1, GLT2 and GLT3 films in pH 7.8 phosphate buffer solution.

It can be concluded from the data tabulated in [Table 3- 4], [Table 3- 5] and [Table 3- 6], which is plotted in [Figure 3- 15], that increasing the concentration of either biopolymer in a film will result in no change to the rate of release but decreases the amount of galantamine HBr released. This was far more apparent when increasing the concentration of sodium alginate than increasing the concentration of chitosan. The leading cause for the decrease in the amount of galantamine HBr being released can be attributed to the increased film thickness as a result of increasing the concentration. An increase in the film thickness, whilst not altering the galantamine concentration to compensate, will result in it being more difficult for galantamine to be released into solution as the size of the barrier the compound needs to pass through has become larger. As a result, the galantamine HBr loaded further from the film's surface is less likely to be released.

Comparing the data for GLT2 and GLT3 films' galantamine HBr release over 24 hours, it is apparent that increasing the concentration of alginate causes even less galantamine to be released than when you increase the concentration of chitosan. This can be attributed to two factors; the first of which being charge interaction. As chitosan and galantamine have complimentary charges, whereas alginate and galantamine are oppositely charged, which would suggest that galantamine is released slower and in smaller amounts from the sodium alginate layer than it would be from the chitosan layer. The second factor is the pores within the sodium alginate and chitosan layers. Using SEM analysis, it was possible to determine the size of the pore’s diameters in both the sodium alginate and chitosan layers of the film with the sodium alginate layer exhibiting a pore diameter size range of 1 µm - 10 µm, and the chitosan layer exhibiting 300 nm – 2 µm. The pore size of both the sodium alginate and chitosan layers meant that the galantamine HBr was able to be released from the drug without a large amount of difficulty in pH 7.4 phosphate buffer solution. Although the pore size in the sodium alginate is larger, it would appear in SEM image of a GLT1 film chitosan layer’s surface [Figure 3- 16] that there is a greater number of pores in the chitosan layer, meaning more pores for the galantamine HBr to be diffused through.

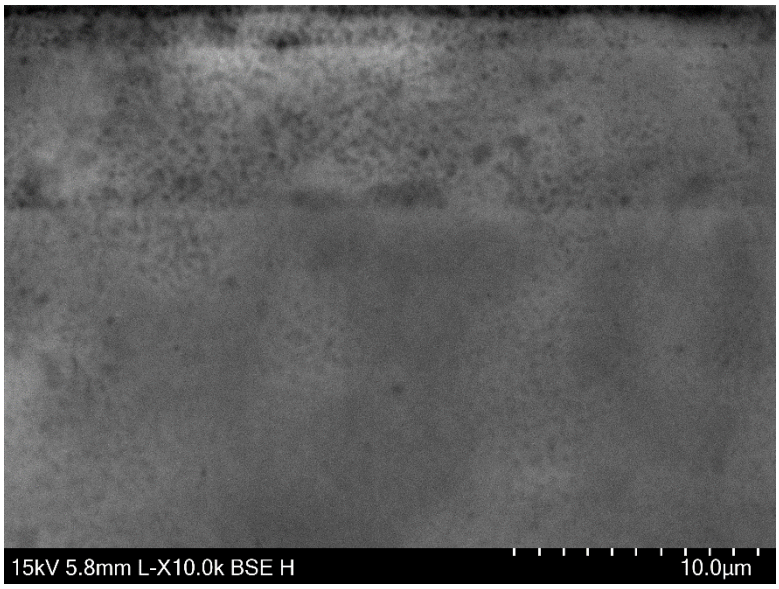

Figure 3- 16: SEM image of the 3% chitosan layer's surface in a GLT1 film at 10000x magnification.

These hypotheses were tested further by loading galantamine into the sodium alginate layer only, and then into the chitosan layer only in a separate film. These films were named 'GLT4' and 'GLT5', whose properties can be seen in [Table 3- 3]. All experimental parameters were kept the same as the previous release studies. The data for the release of galantamine from the GLT4 film can be seen in [Table 3- 7] and [Figure 3- 17]. The data for the release of galantamine from the GLT5 film can be seen in [Table 3- 8] and [Figure 3- 18].

Table 3- 7: The percentage release of galantamine HBr from GLT4 films, in pH 7.8 phosphate buffer solution, over 24 hours.

Time (mins)	Release 1 (%)	Release 2 (%)	Release Average (%)	Percentage Error (%)
10.00	28.8	38.1	33.5	6.6
20.00	29.4	39.4	34.4	7.1
30.00	30.0	40.6	35.3	7.5
50.00	32.1	42.2	37.2	7.1
70.00	33.0	43.2	38.1	7.2
90.00	35.1	43.5	39.3	5.9
120.00	36.7	45.0	40.9	5.8
180.00	38.7	45.2	42.0	4.6
240.00	40.4	45.3	42.9	3.5
300.00	41.9	46.3	44.1	3.2
360.00	42.7	47.2	44.9	3.2
1440.00	46.4	49.0	47.7	1.8

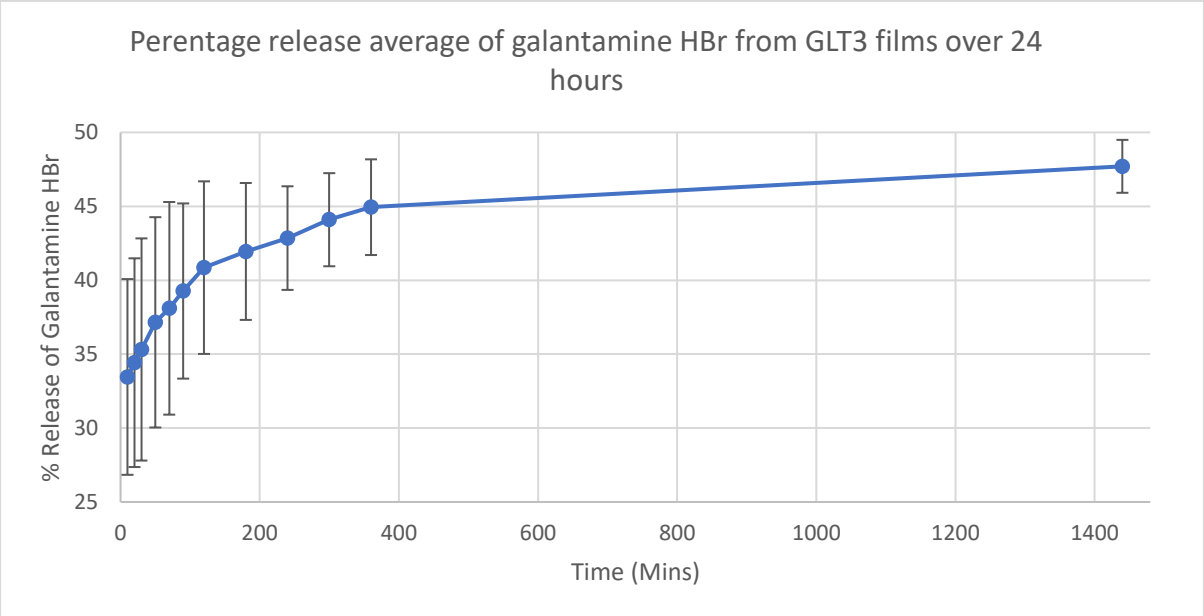

Figure 3 -17: The 24-hour release profile of galantamine HBr from GLT4 films in pH 7.8 phosphate buffer solution.

Table 3- 8: The percentage release of galantamine HBr from GLT5 films, in pH 7.8 phosphate buffer solution, over 24 hours.

Time (mins)	Release 1 (%)	Release 2 (%)	Release Average (%)	Percentage Error (%)
10.00	49.6	43.1	46.3	4.5
20.00	50.5	46.7	48.6	2.7
30.00	52.8	47.7	50.3	3.6
50.00	53.3	51.1	52.2	1.6
70.00	53.8	51.4	52.6	1.7
90.00	54.5	52.2	53.3	1.6
120.00	56.1	55.1	55.6	0.7
180.00	60.2	55.4	57.8	3.4
240.00	61.3	55.6	58.5	4.0
300.00	61.8	55.8	58.8	4.2
360.00	62.3	56.7	59.5	3.9
1440.00	63.0	59.3	61.2	2.6

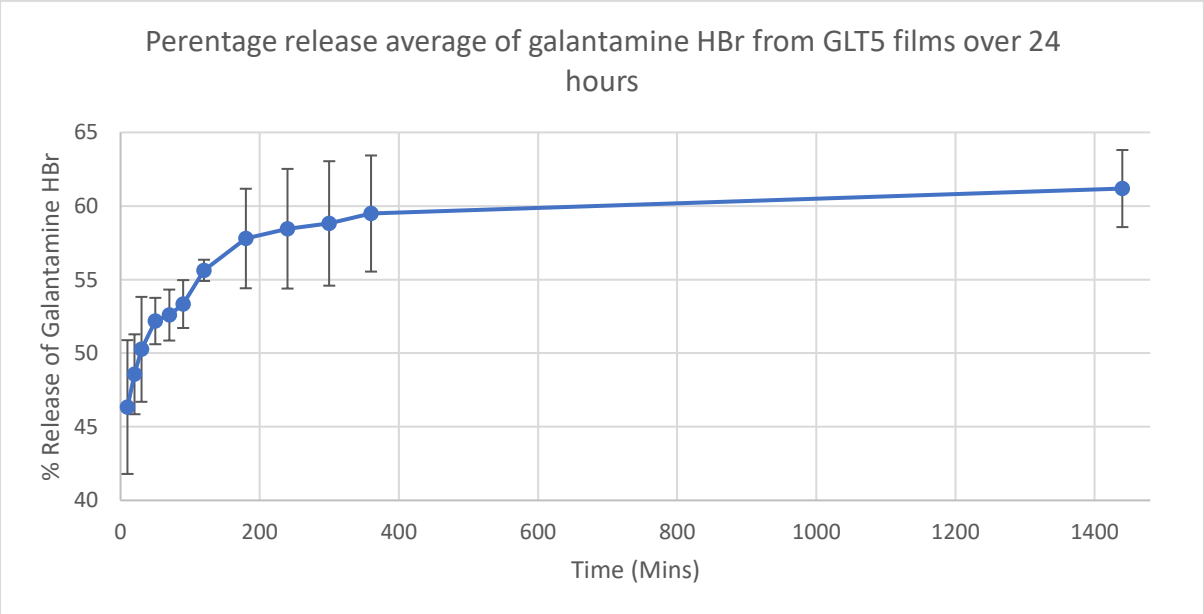

Figure 3- 18: The 24-hour release profile of galantamine HBr from GLT5 films in pH 7.8 phosphate buffer solution.

The release studies conducted on the GLT4 and GLT5 films, plotted in [Figure 3- 19] confirm that a larger amount of galantamine is released from the chitosan layer than the alginate layer, but less overall galantamine HBr is released than when galantamine HBr is present in both of the bio-based polymer layers. The release profile also plateaus faster in the GLT4 films due to the opposing charge between sodium alginate and galantamine, causing galantamine loaded deeper in the alginate layer to be withheld in the film *via* ionic interaction.

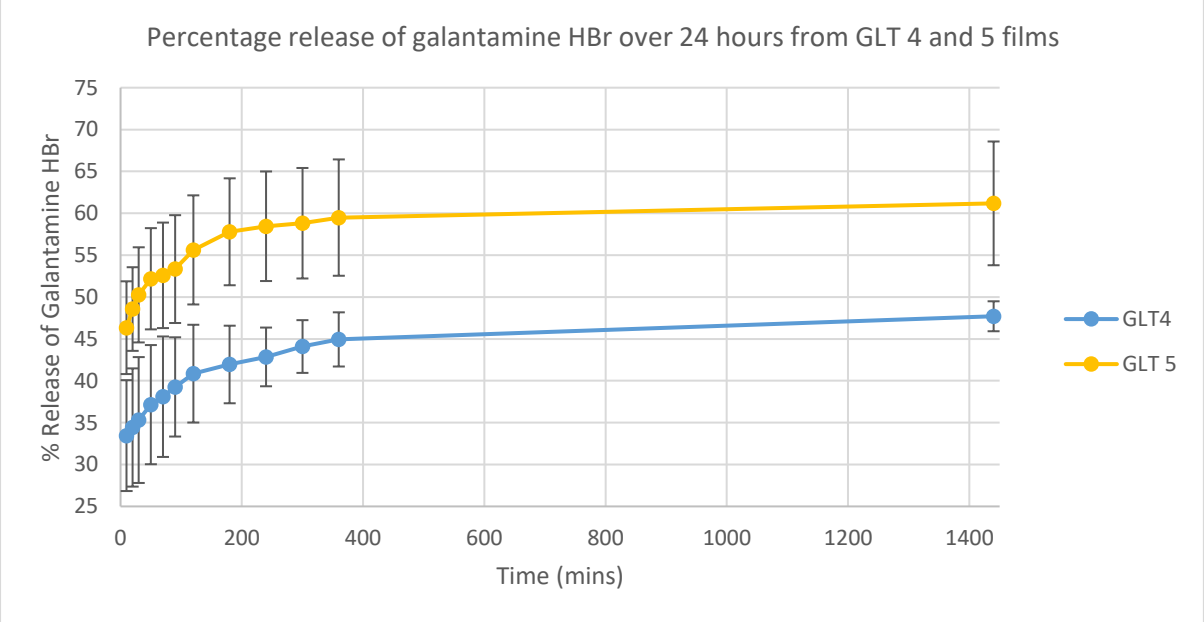

Figure 3- 19: The 24-hour release profile of galantamine HBr from GLT4 and GLT5 films in pH 7.8 phosphate buffer solution.

The increased release when galantamine is in both layers has to be attributed to there being more galantamine HBr closer to the film's surfaces, and the interaction between galantamine HBr and sodium alginate causing the galantamine HBr loaded deeper in the alginate portion of a film to release more slowly than that of the galantamine HBr in the chitosan portion of a film.

'GLT6' is a film consisting of 3% sodium alginate and 3% chitosan, as noted in [Table 3- 3]. This film has 4 layers as opposed to the 2 layers in 'GLT1'. In order to ensure a similar level of thickness, half of the time was spent in submersion when making the layers in GTL6 than those of GTL1. No other modifications were made to the experimental procedure for making the film, or to the procedure of the release

study. The data for the release of galantamine from the GLT6 film can be seen in [Table 3- 9] and [Figure 3- 20]. The percentage release of galantamine HBr from a GLT6 film was compared to that of a GLT1 film [Figure 3- 21].

Table 3-9: The percentage release of galantamine HBr from GLT6 films, in pH 7.8 phosphate buffer solution, over 24 hours.

Time (mins)	Release 1 (%)	Release 2 (%)	Release Average (%)	Percentage Error (%)
10.00	42.6	34.8	38.7	5.5
20.00	43.3	36.2	39.8	5.0
30.00	45.8	37.8	41.8	5.7
50.00	47.7	39.2	43.4	6.0
70.00	49.2	40.3	44.8	6.3
90.00	50.7	41.6	46.1	6.4
120.00	52.2	42.9	47.6	6.5
180.00	53.3	44.3	48.8	6.4
240.00	54.6	45.4	50.0	6.5
300.00	55.3	45.9	50.6	6.6
360.00	56.0	46.2	51.1	7.0
1440.00	57.3	46.8	52.0	7.4

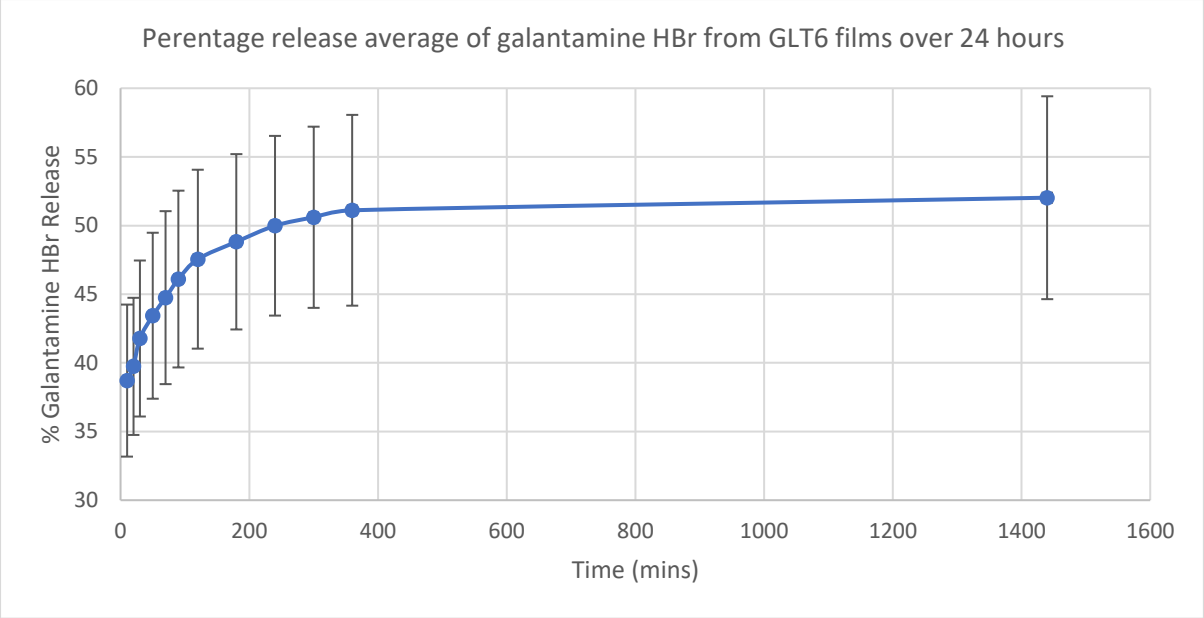

Figure 3- 20: The 24-hour release profile of galantamine HBr from GLT6 films in pH 7.8 phosphate buffer solution.

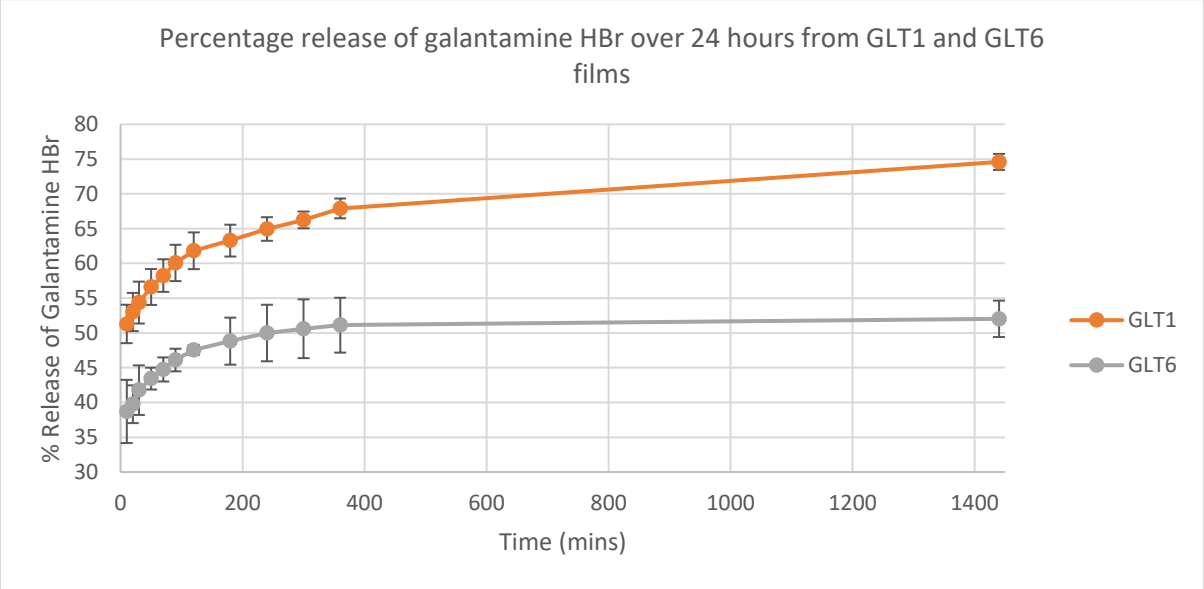

Figure 3- 21: The 24-hour release profile of galantamine HBr from GLT1, and GLT6 films in pH 7.8 phosphate buffer solution.

The conclusion we can take from the data plotted in [Figure 3- 20] and [Figure 3- 21] is that increasing the number of layers appears to increase the rate of release, but the overall release is less than that of a film of fewer layers. This must mean that the charge distribution, which changes in each layer of the film, creates larger barriers for galantamine HBr to pass through. The increased rate of release must be attributed

to the galantamine in the chitosan layers being released faster, until max release has been reached. As a result, using single layers of alginate and chitosan would be preferable due to fewer limiting factors on the overall release of galantamine HBr.

3.4.2.3 The Effect of Changing the pH of the Phosphate Buffer Solution on the Release of Galantamine from GLT1 Films

Release studies were conducted on GLT1 films in phosphate buffer solutions of different pH levels, to assess the effect of changing the pH of the release media on the release profile of galantamine HBr from sodium alginate and chitosan comprised bio-based polymer films. These studies were conducted in pH 4.0 [Table 3- 10] [Figure 3- 22], pH 9.2 [Table 3- 11] [Figure 3- 23] and compared to that of the pH 7.8 study data [Figure 3- 24].

Table 3- 10: The percentage release of galantamine HBr from GLT1 films, in pH 4.0 phosphate buffer solution, over 24 hours.

Time (mins)	Release 1 (%)	Release 2 (%)	Release Average (%)	Percentage Error (%)
10.00	57.7	66.4	62.1	6.1
20.00	62.0	72.0	67.0	7.1
30.00	64.6	73.0	68.8	6.0
50.00	66.7	74.5	70.6	5.5
70.00	68.9	76.1	72.5	5.1
90.00	70.7	78.7	74.7	5.6
120.00	73.1	81.1	77.1	5.7
180.00	74.4	81.4	77.9	5.0
240.00	75.3	82.4	78.8	5.1
300.00	76.1	84.6	80.3	6.0
360.00	77.9	84.7	81.3	4.8
1440.00	78.8	86.2	82.5	5.2

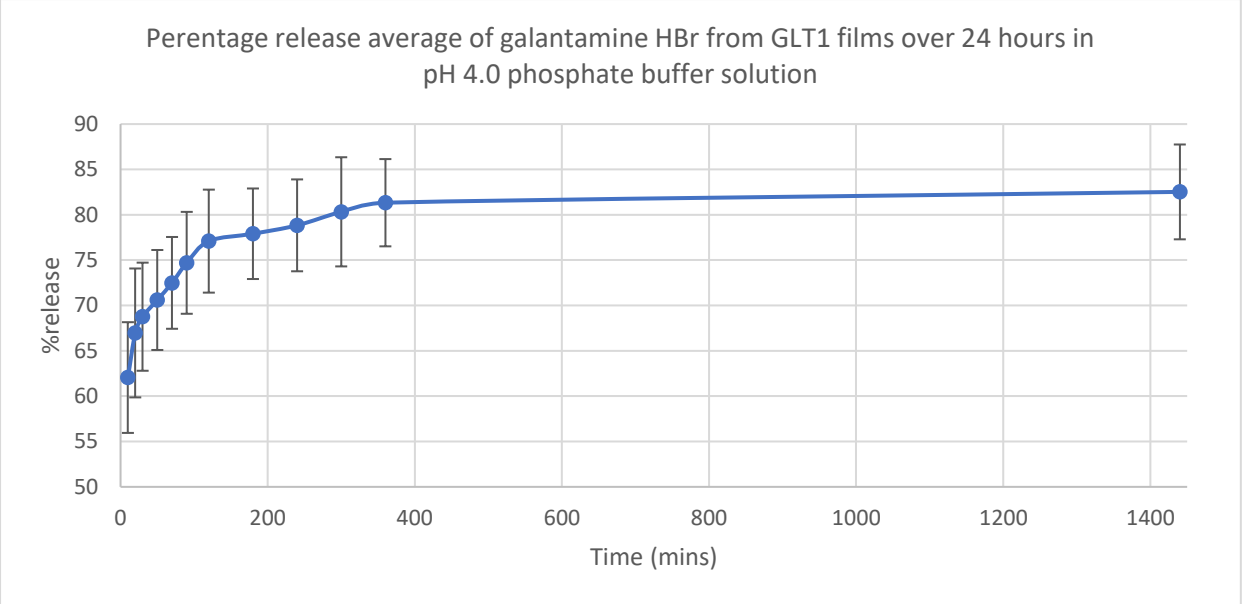

Figure 3- 22: The 24-hour release profile of galantamine HBr from GLT1 films in pH 4.0 phosphate buffer solution.

Table 3- 11: The percentage release of galantamine HBr from GLT1 films, in pH 9.2 phosphate buffer solution, over 24 hours.

Time (mins)	Release 1 (%)	Release 2 (%)	Release Average (%)	Percentage Error (%)
10.00	42.2	38.0	40.1	3.0
20.00	43.7	39.6	41.7	2.9
30.00	45.3	40.1	42.7	3.7
50.00	47.1	40.6	43.8	4.6
70.00	48.6	40.7	44.7	5.6
90.00	50.3	43.2	46.8	5.0
120.00	51.8	44.3	48.1	5.3
180.00	53.5	44.5	49.0	6.3
240.00	54.7	44.6	49.7	7.1
300.00	55.8	44.7	50.3	7.9
360.00	57.1	45.5	51.3	8.9
1440.00	58.1	51.4	54.8	4.7

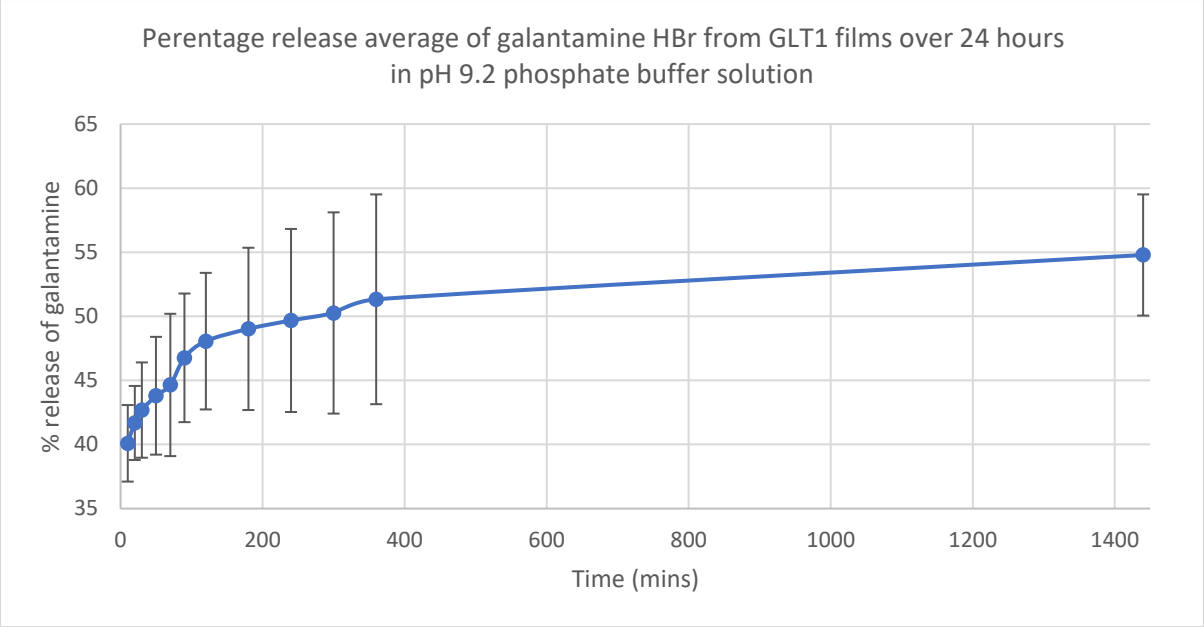

Figure 3- 23: The 24-hour release profile of galantamine HBr from GLT1 films in pH 9.2 phosphate buffer solution.

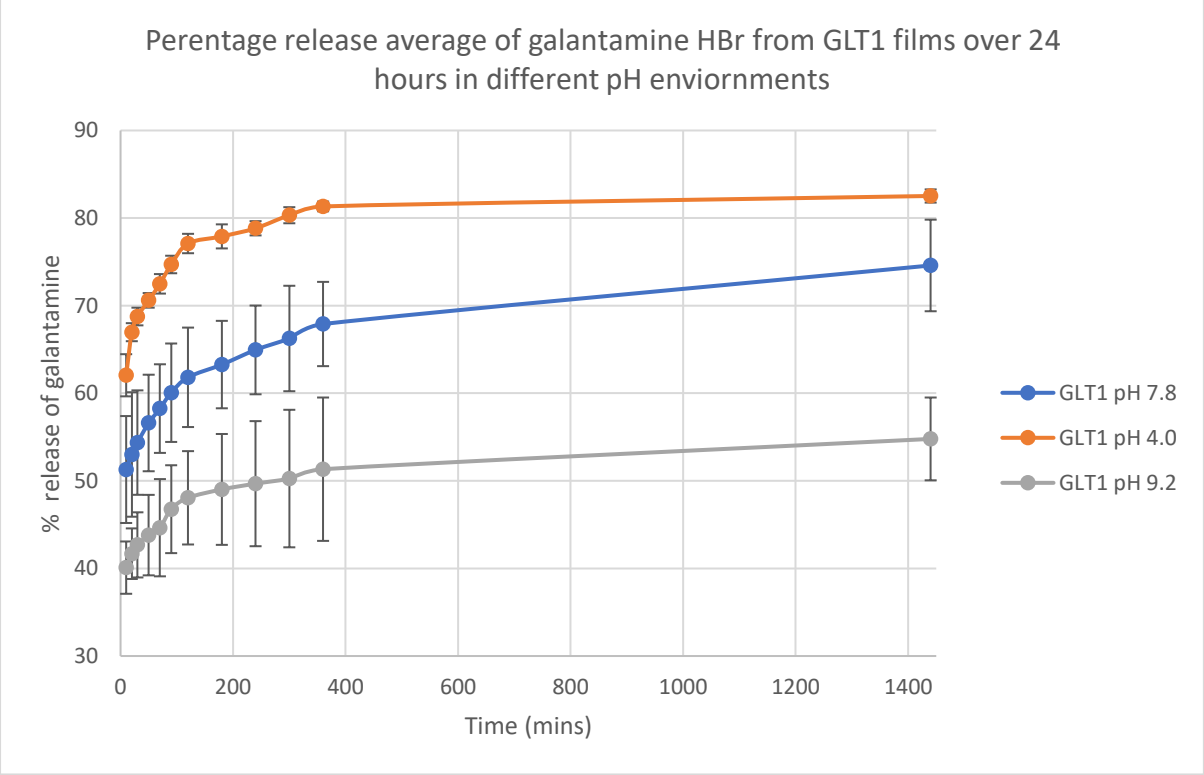

Figure 3- 24: The 24-hour release profile of galantamine HBr from GLT1 films in different pH 4.0, pH 7.8 and pH 9.2 phosphate buffer solutions.

From the data obtained and plotted in [Figure 3- 24], it can be concluded that decreasing the pH of the release media can result in a greater amount of release of

galantamine HBr from GLT1 films, and most likely all of the GLT films as a result. This is most likely a result of the bio-based sodium alginate and chitosan comprised films degrading at increased rates in lower pH environments. Of course, it would not be recommended to reduce the pH too much when applying this to patients' skin.

3.4.2.4 Analysing the Effect of Galantamine Release from Films Consisting of Alginate Comprised of Higher Amounts of Guluronic Acid

In order to determine the effect of formulating films which had an increased amount of guluronic alginate (High G) on the release of galantamine, the release studies for GLT1, GLT4 and GLT6 using 'high G', as opposed to 'low G' seen in the previous release studies.

The reason for exploring this is due to pore size. In low G sodium alginate, layers exhibited pore diameter sizes ranging between 1 µm - 10 µm. In high G sodium alginate, layers exhibited pore diameter sizes ranging between 1 µm - 30 µm. The overall increase in pore size will allow for more galantamine HBr to be released, though it will have no effect on the overall rate of release of galantamine from the GLT Films.

The data for the release of galantamine from the high G GLT1 film can be seen in [Table 3- 12] and [Figure 3- 25]. A release medium of pH 7.8 phosphate buffer solution was used in all of the repeated release studies. The data for the release of galantamine from the high G GLT4 film can be seen in [Table 3- 13] and [Figure 3- 26]. The data for the release of galantamine from the high G GLT6 film can be seen in [Table 3- 14] and [Figure 3- 27]. The data for the high G films is then compared with their low G film counterparts in [Figure 3- 28]

Table 3- 12: The percentage release of galantamine HBr from high G GLT1 films, in pH 7.8 phosphate buffer solution, over 24 hours.

Time (mins)	Release 1 (%)	Release 2 (%)	Release Average (%)	Percentage Error (%)
10.00	56.3	51.2	53.7	3.6
20.00	60.2	53.1	56.6	5.0
30.00	62.7	54.9	58.8	5.5
50.00	65.7	57.0	61.3	6.2
70.00	66.9	58.9	62.9	5.6
90.00	67.6	60.7	64.2	4.9
120.00	69.5	62.5	66.0	5.0
180.00	69.7	64.0	66.9	4.0
240.00	73.3	65.4	69.3	5.6
300.00	74.0	66.8	70.4	5.0
360.00	74.5	68.0	71.3	4.6
1440.00	77.7	73.1	75.4	3.2

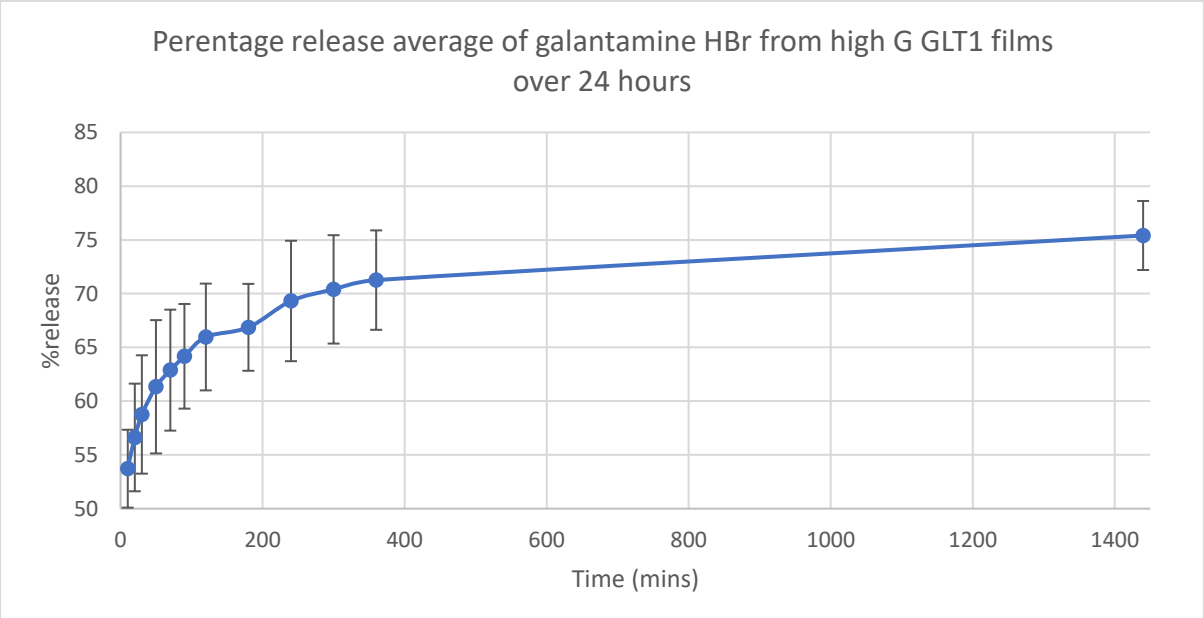

Figure 3- 25: The 24-hour release profile of galantamine HBr from high G GLT1 films in pH 7.8 phosphate buffer solution.

Table 3- 13: The percentage release of galantamine HBr from high G GLT4 films, in pH 7.8 phosphate buffer solution, over 24 hours.

Time (mins)	Release 1 (%)	Release 2 (%)	Release Average (%)	Percentage Error (%)
10.00	57.4	57.4	57.4	0.0
20.00	57.8	58.8	58.3	0.8
30.00	60.5	60.0	60.2	0.4
50.00	62.4	62.1	62.3	0.2
70.00	65.3	62.9	64.1	1.7
90.00	68.0	63.3	65.6	3.3
120.00	70.0	66.3	68.2	2.6
180.00	71.8	68.5	70.1	2.4
240.00	74.3	71.2	72.7	2.2
300.00	75.3	73.0	74.2	1.6
360.00	76.1	74.0	75.0	1.4
1440.00	77.6	75.6	76.6	1.4

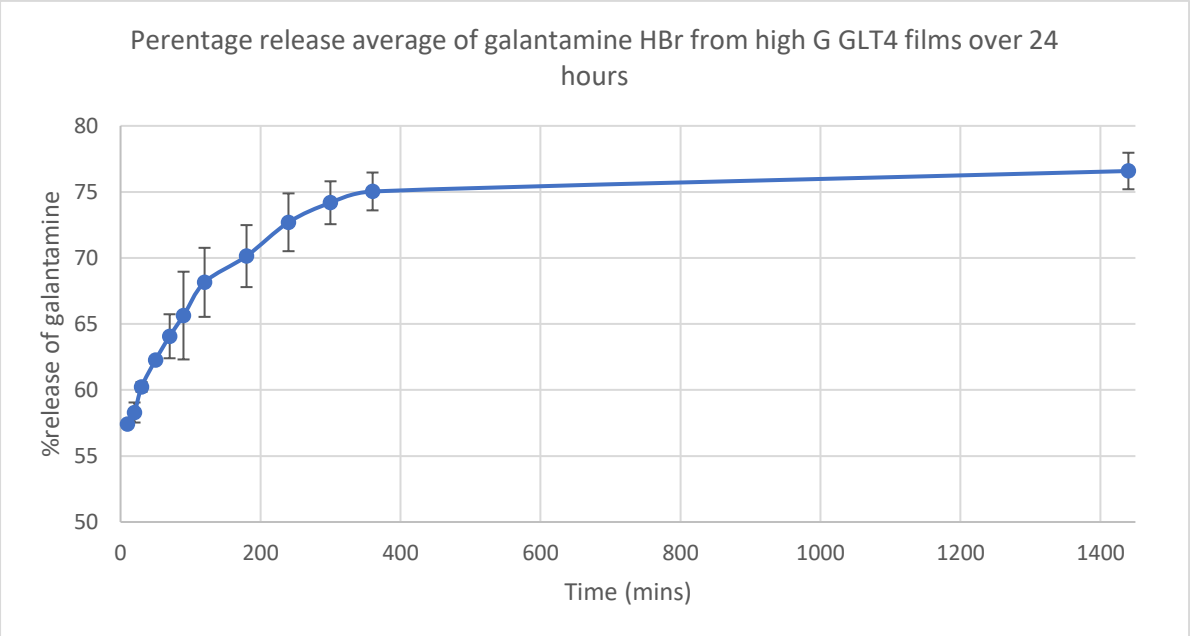

Figure 3- 26: The 24-hour release profile of galantamine HBr from high G GLT4 films in pH 7.8 phosphate buffer solution.

Table 3- 14: The percentage release of galantamine HBr from high G GLT6 films, in pH 7.8 phosphate buffer solution, over 24 hours.

Time (mins)	Release 1 (%)	Release 2 (%)	Release Average (%)	Percentage Error (%)
10.00	34.7	35.3	35.0	0.4
20.00	36.3	35.9	36.1	0.3
30.00	37.7	36.8	37.3	0.7
50.00	38.6	37.6	38.1	0.7
70.00	39.3	39.4	39.4	0.1
90.00	40.5	40.3	40.4	0.2
120.00	42.8	40.9	41.8	1.4
180.00	43.7	42.2	43.0	1.0
240.00	44.6	43.3	43.9	1.0
300.00	45.7	44.5	45.1	0.9
360.00	46.3	45.1	45.7	0.8
1440.00	46.4	45.5	46.0	0.6

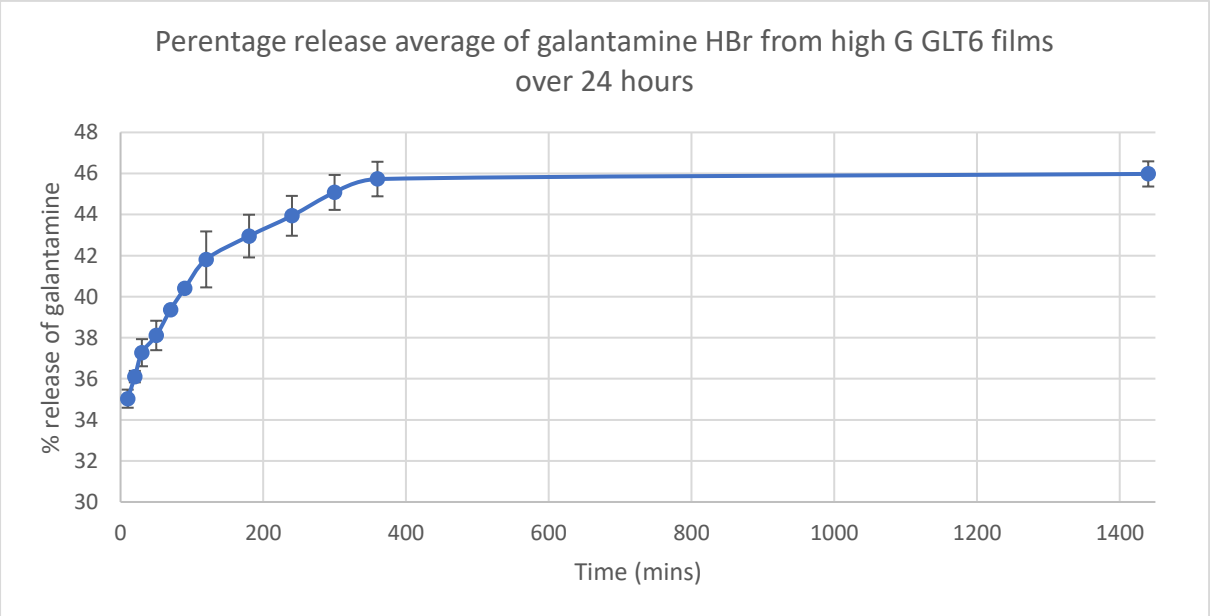

Figure 3- 27: The 24-hour release profile of galantamine HBr from high G GLT6 films in pH 7.8 phosphate buffer solution.

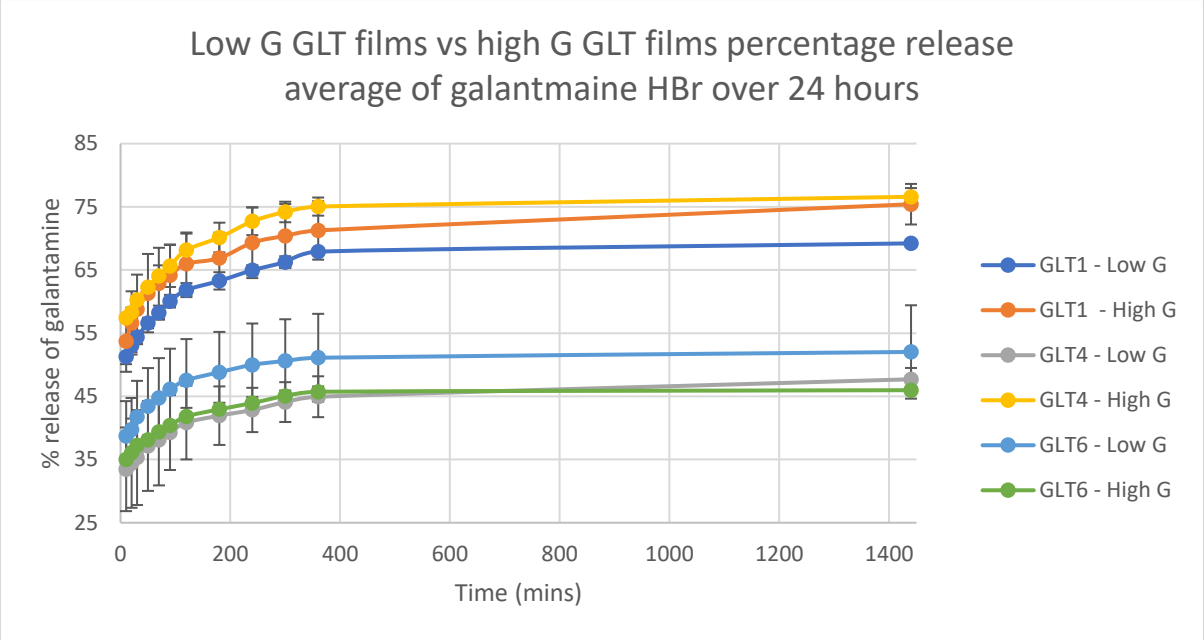

Figure 3- 28: The 24-hour release profile of galantamine HBr, comparing the release of low G and high G GLT films, in pH 7.8 phosphate buffer solution.

It is apparent, from the data plotted in [Figure 3- 28], that when high G alginate is used, there is a larger amount of release of galantamine than when low G is used – this is the case for all of the high G films compared to their low G counterparts. Interestingly, when using high G alginate, the release of galantamine in films where alginate is only in the alginate layer is substantially higher than when low G alginate is used. Increasing the number of layers still reduces overall release.

These results could be attributed to an increase in pore size when using high G alginate in the alginate layers of the alginate/chitosan films. SEM analysis was used to confirm this [Figure 3- 29] and to assess the ability for the high G films to load galantamine HBr [Figure 3- 31]. Higher pore size is expected due to the steric effects that guluronic acid has on the alginate polymer, as it adopts a vertical orientation unlike mannuronic acid (M) which has a horizontal orientation[50] [Figure 3- 30].

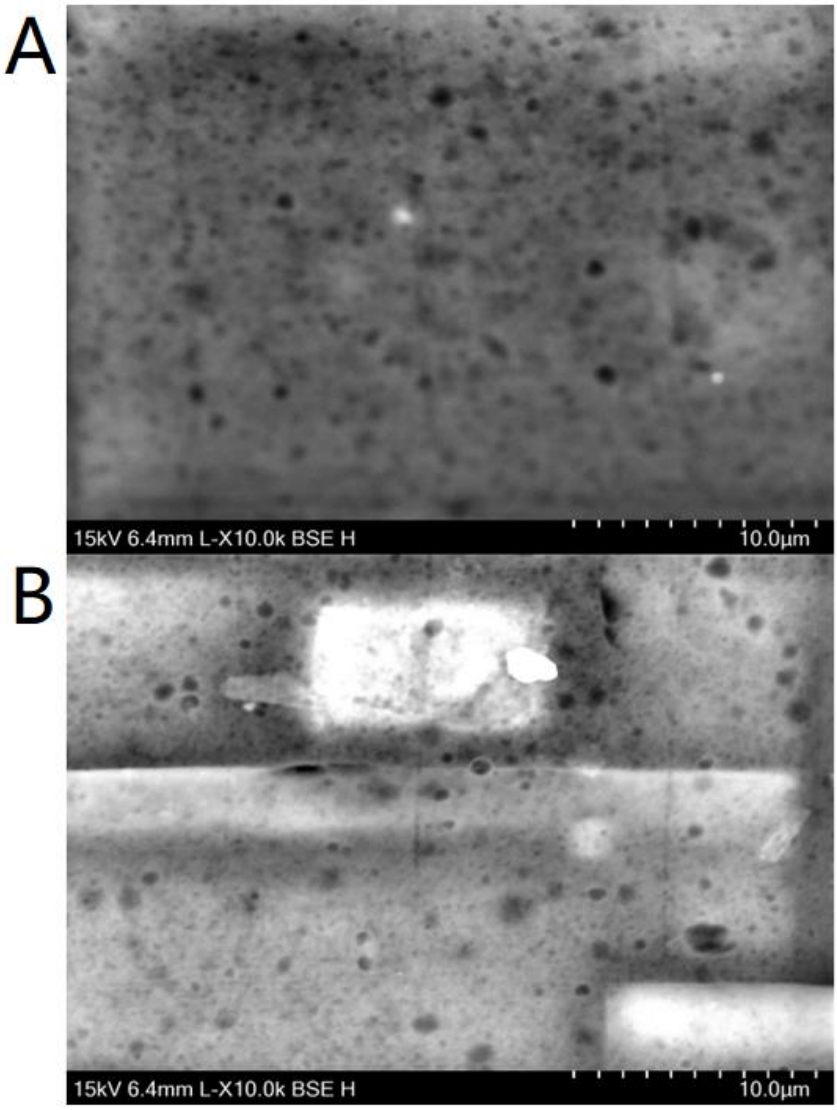

Figure 3- 29. SEM images of low G (A) and high G (B) unloaded GLT 1 films at 10000x to emphasize difference in pore size between the two types of alginates.

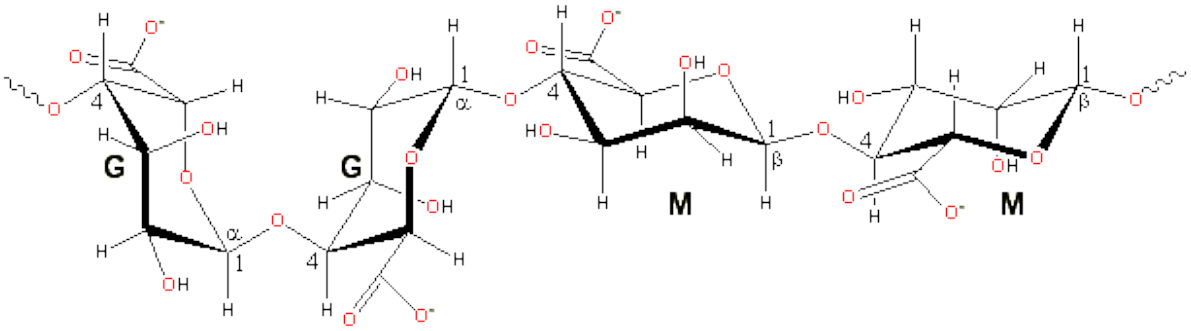

Figure 3- 30: β-(1->4)-Linked D-Mannuronic Acid (M) and α-(1->4)-Linked L Guluronic Acid (G) Orientations Represented in a Linear Alginate Polymer Chain[50].

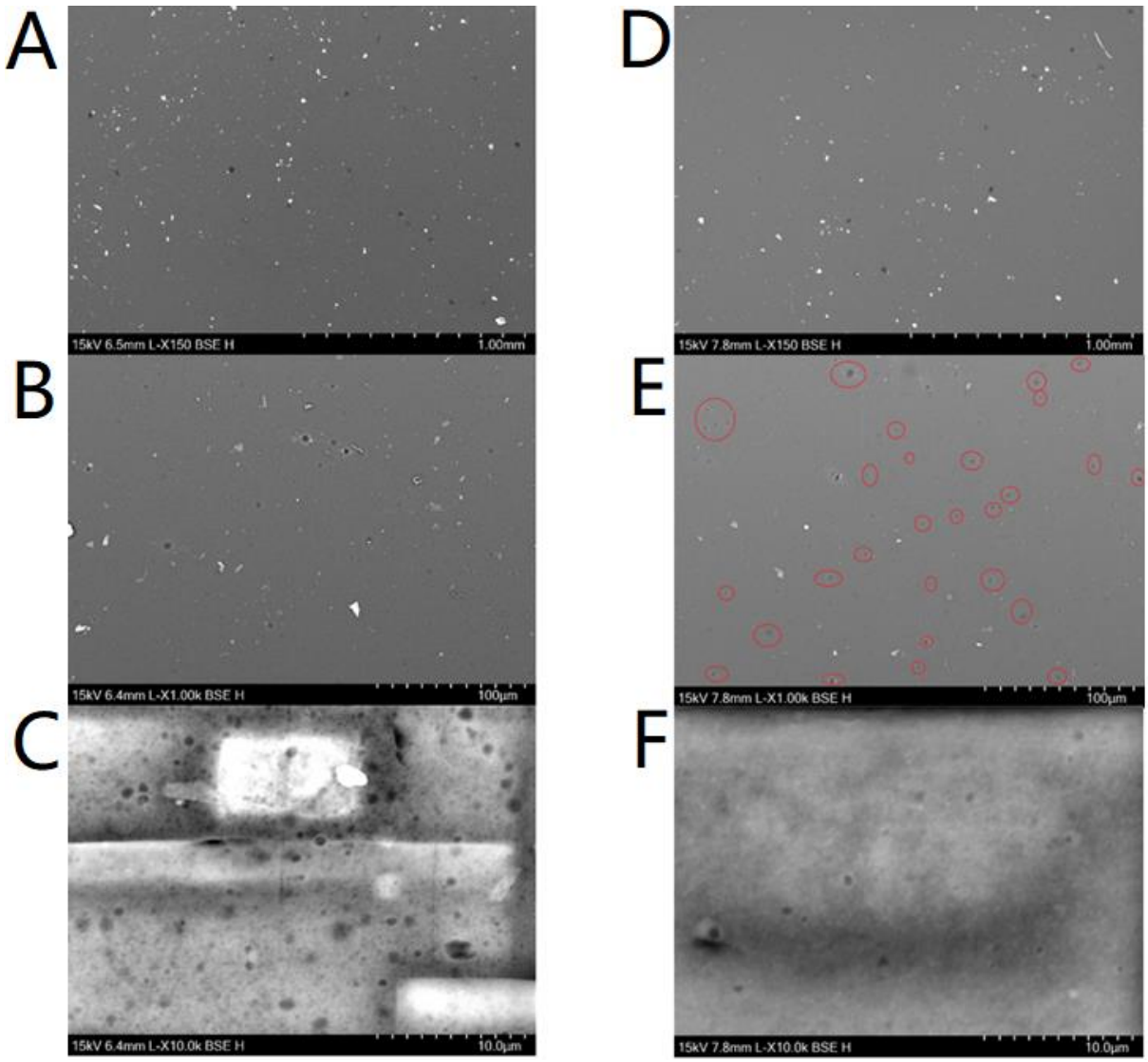

Figure 3- 31: SEM images of 3% High G sodium alginate/3% chitosan biopolymer films from the sodium alginate face. The images of the film on the left are absent of the galantamine HBr (A-C). The galantamine HBr is present in the images of the film on the right (D-F). Image magnifications increase from x150 (A and D) to x1000 (B and E) to x10000 (C and F). Large galantamine HBr deposits are highlighted in red in the x1000 magnification image (E).

3.4.2.5 Comparison of Galantamine Hydrobromide and Free Base Galantamine on Drug Release

Concerns were raised by “P&S Nano Limited” that the HBr salt in galantamine HBr may cause problems when trying to release galantamine through the epidermis and dermis layers of human skin[51]. Through the method described in the experimental section of this chapter, the HBr salt was removed from galantamine HBr to leave free base galantamine behind [Figure 3- 8 (Spectrum B)]. It was important to repeat a GLT1 film release study to analyse the effect of using free base galantamine, as opposed to galantamine HBr. A free base galantamine loaded GLT1 film was successfully made, and free base galantamine was released in pH 7.8 phosphate buffer solution. No further modifications were made to the release study.

When comparing the release study data for free base galantamine from GLT1 films, with galantamine HBr from GLT1 films, it was noted that free base galantamine had an increased burst release, but the average overall release difference was less than 2% [Table 3- 15] [Figure 3- 32] [Figure 3- 33].

Table 3- 15: The percentage release of free base galantamine from GLT1 films, in pH 7.8 phosphate buffer solution, over 24 hours.

Time (mins)	Release 1 (%)	Release 2 (%)	Release Average (%)	Percentage Error (%)
10.00	53.9	54.3	54.1	0.3
20.00	56.2	55.2	55.7	0.7
30.00	58.5	57.4	57.9	0.8
50.00	60.8	59.4	60.1	1.0
70.00	63.3	61.8	62.5	1.1
90.00	64.9	63.6	64.3	0.9
120.00	67.1	65.4	66.2	1.2
180.00	68.7	67.0	67.9	1.2
240.00	70.3	67.9	69.1	1.7
300.00	71.2	69.4	70.3	1.2
360.00	71.8	70.8	71.3	0.6
1440.00	73.3	72.0	72.6	0.9

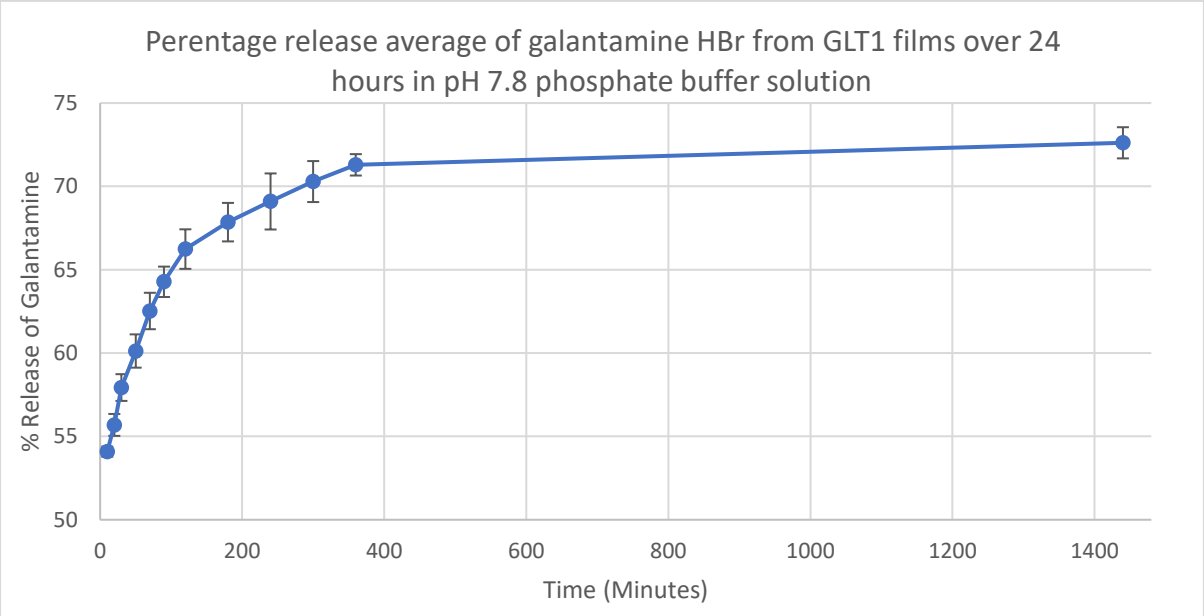

Figure 3- 32: The 24-hour average release profile of free base galantamine from GLT1 films in pH 7.8 phosphate buffer solution.

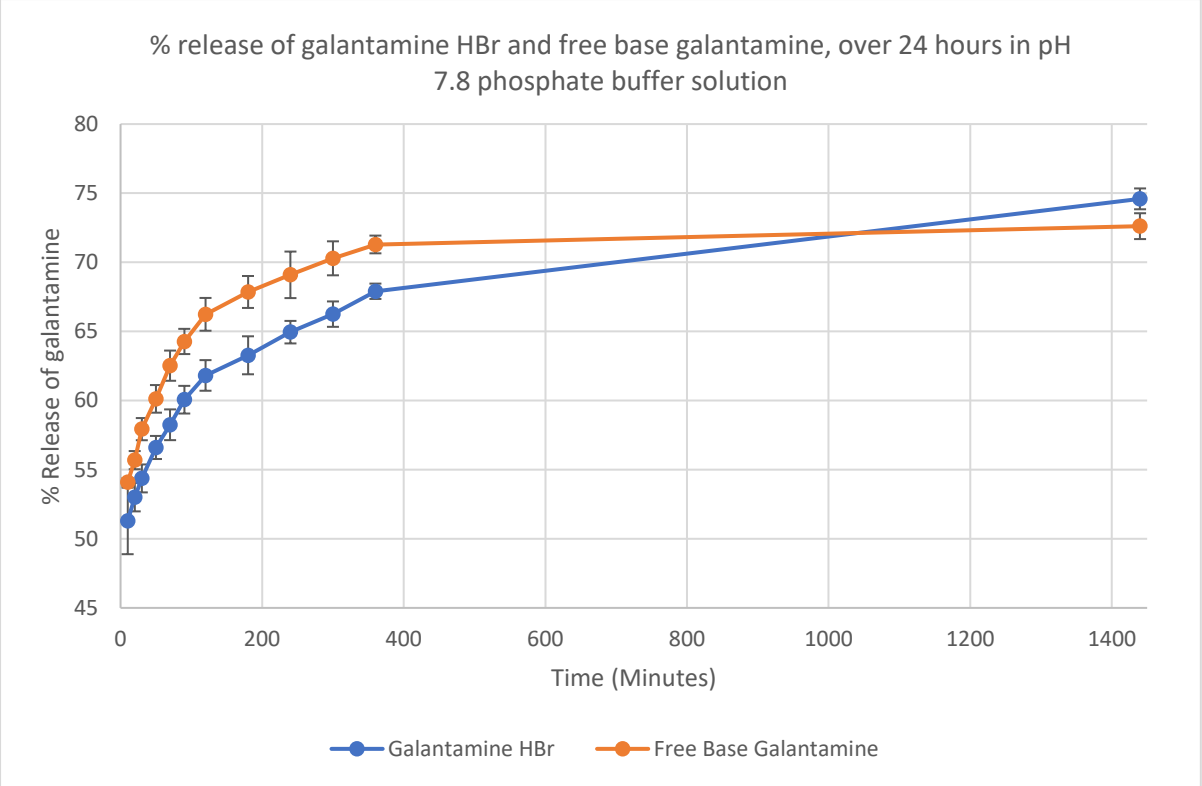

Figure 3- 33: The release of free base galantamine HBr compared with the release of galantamine HBr from GLT1 films in pH 7.8 phosphate buffer solution, over 24 hours.

The data in [Figure 3- 33] leads to the conclusion that the reduced size of free base galantamine allows for it to be released faster, but the deeper loaded galantamine still remains in the film after 24 hours. The free base galantamine films are still effective over a 16 hour period. There are no major issues noticed when using free base galantamine instead of galantamine HBr in GLT1 films, though no tests were carried out on human skin to see the effects of using either compound on a patient.

3.5 Conclusion

Alkaloid materials, galantamine and haemanthamine, were successfully extracted from post ion exchange daffodil bulb liquid extract. The extraction method yielding in the highest amount of alkaloid materials extracted was the method involving salting out the alkaloids[52], before extraction in chloroform *via* separation, in basic

conditions. Galantamine and haemanthamine were extracted, and the ratio of the two alkaloids was determined, *via* NMR analysis, to be 2:1 haemanthamine to galantamine.

Galantamine HBr was successfully loaded into sodium alginate and chitosan films using the Layer by Layer technique[53]. UV analysis confirmed that galantamine HBr could be loaded and released from the sodium alginate and chitosan bio-based polymer films. SEM analysis was used to determine the morphology of the biopolymer films - both pre and post drug loading. Films using as low a concentration of sodium alginate and chitosan, whilst not compromising the films structural integrity, make for better candidates for the use in drug release. It was determined that increasing the concentration of chitosan results in a negligibly lower release of galantamine HBr. However, increasing the concentration of sodium alginate greatly reduces the amount of release, due to iconic interaction between the bio-based polymer and galantamine. When loading galantamine into one bio-based polymer layer, the overall release is lower as a result of there being no galantamine on one of the film's surfaces. More galantamine was released from the chitosan layer, as a result of alginate and galantamine being oppositely charged, which results in galantamine being released slower and in smaller amounts from the sodium alginate layer than it is from the chitosan layer. An increased amount of galantamine release from the chitosan portion of the film can be attributed to what appears to be a larger number of pores in the chitosan layer. Increasing the acidity of the release media caused more galantamine to be released from the bio-based polymer films as a result of increased film degradation in acidic conditions.

Films were tested using sodium alginate with an increased amount of guluronic acid (G) to assess using a higher guluronic acid (G) to mannuronic acid (M) ratio's effect on the release of galantamine HBr. A larger amount of galantamine HBr release was observed from films with a higher G ratio. SEM analysis confirmed that the pore sizes of the alginate layer was larger when using a higher G ratio and could be attributed to the steric effects that guluronic acid exhibits. Using sodium alginate with a higher ratio of guluronic acid, allows for a greater amount of drug release due to its vertical orientation resulting in larger pores.

Free base galantamine was loaded into a sodium alginate and chitosan comprised bio-based polymer film, and successfully released in pH 7.8 phosphate buffer solution. UV analysis showed that using free base galantamine, as opposed to galantamine HBr, has a negligible effect on the overall release of galantamine, though it does have a faster burst release, due to a smaller size and a reduced amount of ionic interaction. It can be concluded that both galantamine HBr and free base galantamine can be released from bio-based polymer films with similar overall amounts of release whilst releasing effectively for approximately 16 hours. Free base galantamine allowing for a faster initial release but had no overall effect on the final amount of the drug release. Further studies on skin samples would be required to determine if removing the HBr salt does have an effect on galantamine permeating the skin. The similar levels of release for free base galantamine and galantamine HBr is likely due to the free base galantamine being protonated during either the loading or release process.

Drug release from sodium alginate and chitosan comprised bio-based polymer films is larger in lower pH's due to increased film degradation. Use of free base galantamine as opposed to galantamine HBr allowed for faster initial release but had no overall effect on the final amount of the drug release. The most effective release of galantamine HBr was obtained from films comprised of a single 3% sodium alginate layer, with a larger amount of guluronic acid content, and a single 3% chitosan layer. These statements should be considered if trials for the release of galantamine from bio polymer films onto skin were to take place.

References

1. A. Laskin, J. S. Smith, J. Laskin, *Environmental Science & Technology.* 2009, **43**, 3764–3771
2. Y. Wang, M. Hu P. Lin, Q. Guo, Z. Wu, M. Li, L. Zen, Y. Song, L. Zeng, Y. Wu, S. Guo, X. Huang, L. He, *Environmental Science & Technology.* 2017, **51**, 5951–5961
3. J. R. Hama, B. W. Strobel, *Environmental Science Europe.* 2020, **32**, 1-12

4. S. Rehman, H. Khan, *Advances in Antioxidant Potential of Natural Alkaloids*, Bentham Science Publishers, United Arab Emirates, 2017, **13**, 101-108
5. T. Aniszewski, *Alkaloids - Secrets of Life*, Elsevier Science, United Kingdom, 2007
6. V. Amirkia, M. Heinrich, *Phytochemistry Letters*, 2014, **10**, xlviii–liii
7. X. Shang, C. Yang, S. L. Morris-Natschke, J. C. Lai, X. Yin, Y. Liu, X. Guo, J. Peng, M. Goto, J. Y. Zhang, K. Leem, *Medicinal Research Reviews*, 2020, **40**, 2212-2289
8. J. L. Müller, *Clinical Toxicology*, 1998, **36**, 617-627
9. C. Krishnamurti, S. C. Rao, *Indian Journal of Anaesthesia*, 2016, **60**, 861-862
10. R. J. Huxtable, S. K. W. Schwarz, *Reflections*, 2001, **1**, 189-191
11. E. Dehghan, B. Hosseini, H. Naghdi Badi, F. Shahriari Ahmadi, *Journal of Medicinal Plants*, 2010, **9**, 33-50
12. G. S. Santos, S. B. P. Sinoti, F. T. C. de Almeida, D. Silveira, L. A. Simeoni, K. K. P. Gomes-Copeland, *Plant Cell, Tissue and Organ Culture (PCTOC)*, 2020, **143**, 13-29
13. M. M. Koola, *Psychiatry Research*, 2020, **293**, 1-8
14. Y. Liu, Y. Zhang, X. Zheng, T. Fang, X. Yang, X. Luo, A. Guo, K. A. Newell, X. Feng Huang, Y. Yu, *Journal of Neuroinflammation*, 2018, **15**, 1-15
15. T. Saito, S. Hisahara, N. Iwahara, M. C. Emoto, K. Yokokawa, H. Suzuki, T. Manabe, A. Mastsumura, S. Suzuki, T. Matsushita, J. Kawamata, H. Sato-Akaba, H. G. Fujii, S. Shimohama, *Free Radical Biology and Medicine*, 2019, **145**, 20-32
16. R. Weller, M. Subash, S. Preston, I. Mazanti, R. Carare, *Brain Pathology*, 2008, **18**, 253-266
17. M. M. Koola, S. W. Looney, H. Hong, A. Pillai, W. Hou, *Psychiatry Research*, 2020, **291**, 1-7
18. Y. T. Lin, M. Chou, S. Wu, Y. Yang, *Peer J*, 2019, **7**, 1-12
19. B. A. English, A. A. Webster, *Primer on the Autonomic Nervous System*, 2012, **3**, 631-633
20. F. A. Dajas-Bailado, K. Heimala, S. Wonnacott, *Molecular Pharmacology*, 2003, **64**, 1217-1226

21. G. Stavrakov, I. Philipova, D. Zheleve-Dimitrova, I. Valkova, E. Salamanova, S. Konstantinov, I. Doytchinova, *Chemical Biology & Drug Design*, 2017, **5**, 709-718
22. M. E. Hasselmo, *Current Opinion in Neurobiology*, 2006, **16**, 710-715
23. M. B. Parent, M. G. Baxter, *Learning & Memory*, 2004, **11**, 9-20
24. S. Lombardo, U. Maskos, *Neuropharmacology*, 2015, **96**, 255-262
25. S. Verma, A. Kumar, T. Tripathi, A. Kumar, *Pharmacy and Pharmacology*, 2018, **70**, 985-993
26. L. Fan, J. Wang, F. Meng, Y. Luo, X. Sui, B. Zhao, W. Li, D. Quan, J. Yang, Y. Wang, *Biomedical Nanotechnology*, 2018, **14**, 2066-2076
27. J. L. Molinuevo, F. J. Arranz, *Expert Review of Neurothrapeutics*, 2012, **12**, 31-37
28. I. P. Siafaka, Ö. E. Bülbül, G. Mutlu, E. Mehmet, D. Ioannis, Ü. Neslihan, *CNS & Neurological Disorders*, 2020, **19**, 360-373
29. B. Winblad, J. C. Machado, *Expert Opinion on Drug Delivery*, 2008, **5**, 1377-1386
30. J. T. Shelton, J. H. Lee, M. K. Scullin, N. S. Rose, P. G. Rendell, M. A. McDaniel, *American Geriatrics Society*, 2016, **64**, 1307-1312
31. V. Vijayan, K. R. Reddy, S. Sakthivel, C. Swetha, *Colloids and Surfaces B: Biointerfaces*, 2013, **111**, 150-155
32. P. Nnamanil, F. C. Kenechukwi, E. U. Dibua, C. C. Ogbonna, M. A. Momohl, J. D. N. Ogbona, D. C. Okechkwul, A. U. Olisemekel, A. A. Attamal, *Pharmacy and Pharmacology,* 2013, **7**, 1987-1993
33. S. Sharma, *Sustainable Agriculture Reviews*, 2020, **43**, 131-159
34. E. Remos-Morales, J Tibble-Howlings, L. Lyons, M. O. Ogbu, P. J. Murphy, R. Braganca, C. J. Newbold, *Scientific Reports*, 2019, **9**, 1-7
35. R. Havelek, M. Seifrotova, K. Kravolec, L. Bruckova, L. Cahlikova, M. Dalecka, J. Vavorva, M. Reacova, L. Opletal, Z. Bilkova, *Phytomedicine*, 2014, **21**, 479-490
36. E. Kohelova, R. Perinova, N. Maafi, J. Korabecny, D. Hulcova, J. Mankova, T. Kucera, L. M. Gonzalez, M. Hrabinova, K. Vocakova, L. Novakova, A. De Simone, R. Havelek, L. Cahilkova, *Molecules*, 2019, **24**, 1-18
37. S. Baerkov, J. Bastida, *The Alkaloids: Chemistry and Biology*, 2020, **83**, 113-185

38. J. Lopez-Tirado, *Phytotaxa*, 2019, **394**, 161-170
39. C. E. Salmas, A. E. Giannakas, M. Baikousi, A. Leontiou, Z. Siasou, M. A. Karakassides, *Processes,* 2021, **9**, 1-13
40. P. P. Campos, L. F. Fraceto, M. Ferreira, *Colloids and Surfaces B: Biointerfaces*, 2018, **162**, 69-75
41. P. Kanmani, J. Rhim, *Carbohydrate Polymers*, 2014, **106**, 190-199
42. W. C. Lenthe, J. C. Stinville, M. P. Echlin, Z. Chen, S. Daly, T. M. Pollock, *Ultramicoscopy*, 2018, **195**, 93-100
43. J. E. Castle, P. A. Zhdan, *Journal of Physics D: Applied Physics*, 1997, **30**, 722-740
44. Y. A. Novikov, *Journal of Surface Investigation*, 2019, **12**, 1224-1232
45. M. A. Sutton, N. Li, D. C. Joy, A. P. Reynolds, X. Li, *Experimental Mechanics*, 2007, **47**, 775-787
46. R. Ziel, A. Haus, A. Tulk, *Journal of Membrane Science*, 2008, **323**, 241-246
47. S. M. R. Wahba, A. S. Darwish, S. M. Kamal, *Medical Science and Engineering*, 2016, **65**, 151-163
48. S. O. Sommerer, J. Kovac, D. Calloway, *Journal of Chemical Education*, 1997, **74**, 744-761
49. A. K. Pathan, J. Bond, R. E. Gaskin, *Materials Today*, 2010, **12**, 2010, 32-43
50. J. L. Dávila, M .A. d'Ávila, *Carbohydrate Polymers*, 2017, **157**, 1-8
51. W. Rangsimawong, Y. Obata, P. Opanasopit, T. Ngawhirunpat, K. Takayama, *AAPS PharmSciTech.*, 2018, **19**, 1093-1104
52. H. Nasiri, M. Forouzandeh, M. J. Rasaee, F. Rahbarizadeh, *Journal of Clinical Laboratory Analysis*, 2005, **19**, 229-232
53. S. Afzal, M. Maswal, A. A. Dar, *Colloids and Surface*, 2018, **169**, 99-106

Chapter 4 – Synthesis of Reducible Hyperbranched Polymers with Stimuli Responsive Properties and Drug Modifications to Enhance and Control Drug Delivery

4.1 Overview

This chapter focuses on the synthesis of polymers and drug modifications to aid, enhance and control drug delivery of galantamine from bio-based polymer films. Stimuli responsive hyperbranched polymers have demonstrated promising advantages for use as nanosized drug carriers in Targeted Drug Delivery (TDD) applications because of their unique 3D structure and ability to respond to external stimuli, such as fluctuations in pH and temperature. In this chapter, three reducible and dual responsive (pH and temperature) hyperbranched polymers were synthesized *via* Reversable Addition-Fragmentation Chain Transfer (RAFT) copolymerization of 2-(dimethylamino)ethyl methacrylate (DMAEMA) and disulfanediylbis(ethane-2,1-diyl) diacrylate (DSDA) using varying ratios; subsequently polymer chain extension using N-isopropylacrylamide (NIPAM) was conducted to afford the temperature responsive properties to the polymers. These polymers were characterised *via* Nuclear Magnetic Resonance (NMR), Gel Permeation Chromatography (GPC), and Ultraviolet-Visible Spectroscopy (UV-VIS). Responsive and reducible properties of the hyperbranched polymers were demonstrated by studying their solubility in acidic and basic solutions at different temperatures. The results demonstrated that the synthesis of reducible dual-stimuli responsive hyperbranched polymers that have the potential to load drug molecules and act as nanocarriers for drug delivery. These dual-stimuli responsive polymers can respond to changes in pH and temperature. Galantamine hydrobromide was encapsulated within a selected hyperbranched polymer, which was loaded into a sodium alginate – chitosan transdermal film and used to assess its effect on the release of galantamine hydrobromide against a film where the polymer is absent.

Drug modification of galantamine is explored in an attempt to improve drug release and drug efficacy. (4a*S*,*6R*,8a*S*)-3-methoxy-11-methyl-4a,5,9,10,11,12-hexahydro-6H-benzo[2,3]benzofuro[4,3-cd]azepin-6-yl, commonly known as 'memogain' is a galantamine derived compound made through esterification of galantamine with benzoyl chloride. The resulting compound, memogain, has an increased lipophilicity as a result, which is assumed to give it an improved release from bio-based polymer films into the skin, and also to improve its bioavailability in the brain. Memogain was loaded into sodium alginate and chitosan bio-based polymer films *via* the Layer by Layer technique (LbL), which relies on the ionic interaction between alginate and chitosan to form films. Resulting films were released in pH 7.8 phosphate buffer solutions, with samples being withdrawn at set time intervals, to monitor the rate of release, and the overall release. Memogain release from films was characterised using UV-VIS as a means of determining the concentration of galantamine HBr present in the withdrawn samples. These studies were conducted in order to better understand which of using stimuli responsive polymers, or using galantamine pro drugs, can better improve drug release and rate of release from bio-polymer films.

4.2 Introduction

The use of stimuli responsive polymers in drug delivery is still seen as a recent scientific development. A common technique for synthesising stimuli responsive polymers is *via* the use of the RAFT polymerisation technique which allows for the tailoring of the functionality of stimuli responsive polymers depending on the functionality of the monomers, and the RAFT agent used[1]. Their unique functionalities have attracted attention as they can be used in what is commonly referred to as targeted drug delivery[2]. The functionality of the polymers allows them to respond to changes in microenvironments in the body which can be caused by various ailments[3].

These compounds have been seen to respond to small changes in the microenvironment caused by the unique physiology[4]. Diseases which cause environmental changes within the human body have resulted in research focused on the possibility of using pH and thermo-responsive polymers for use in targeted drug

delivery, with the advantage of avoiding adverse side-effects[5]. As a result of promising research, it may be possible to use stimuli responsive polymers to aid and enhance drug delivery from transdermal films to patients.

Whilst polymers have been revolutionary in drug delivery, improved methods of drug delivery are constantly being reviewed. One such method of improvement is the introduction of hyperbranched polymers. Hyperbranched polymers are also three-dimensional macromolecules, though they are highly branched structures capable of incorporating a vast number of functional groups[6]. Hyperbranched polymers have a wide variety of applications including use in light-emitting materials, biomaterials, coatings, adhesion and supramolecular chemistry[7]. Their increased solubility is advantageous in improving the rate of drug delivery. The first use of hyperbranched polymers was noted to be in 1990 in a description of the synthesis of poly(phenylene)[8]. Hyperbranched polymers have been exploited for their unique characteristics which have made them preferable to linear and dendritic polymers[9]. Hyperbranched polymers exhibit a three-dimensional structure and are mostly polydisperse with a globular shape, as opposed to a two-dimensional linear polymers[10]. The persistent level of synthesis required to formulate hyperbranched polymers is no more time consuming than that of its linear counterparts. As the name would indicate, hyperbranched polymers consist of a large degree of branching throughout the polymer structure. Branching can be quantified *via* the ratio of the branched units and terminal units consisting in the polymer structure in comparison to the linear segments, and can be calculated using their molar fractions[10]. There are various different topologies which can be exhibited in different types of hyperbranched polymers including star, brush, dendritic, cyclic and more. These are classed as non-linear topologies [Figure 4- 1], where linear indicates continuous backbone structure with no significant side chains or branch points[11].

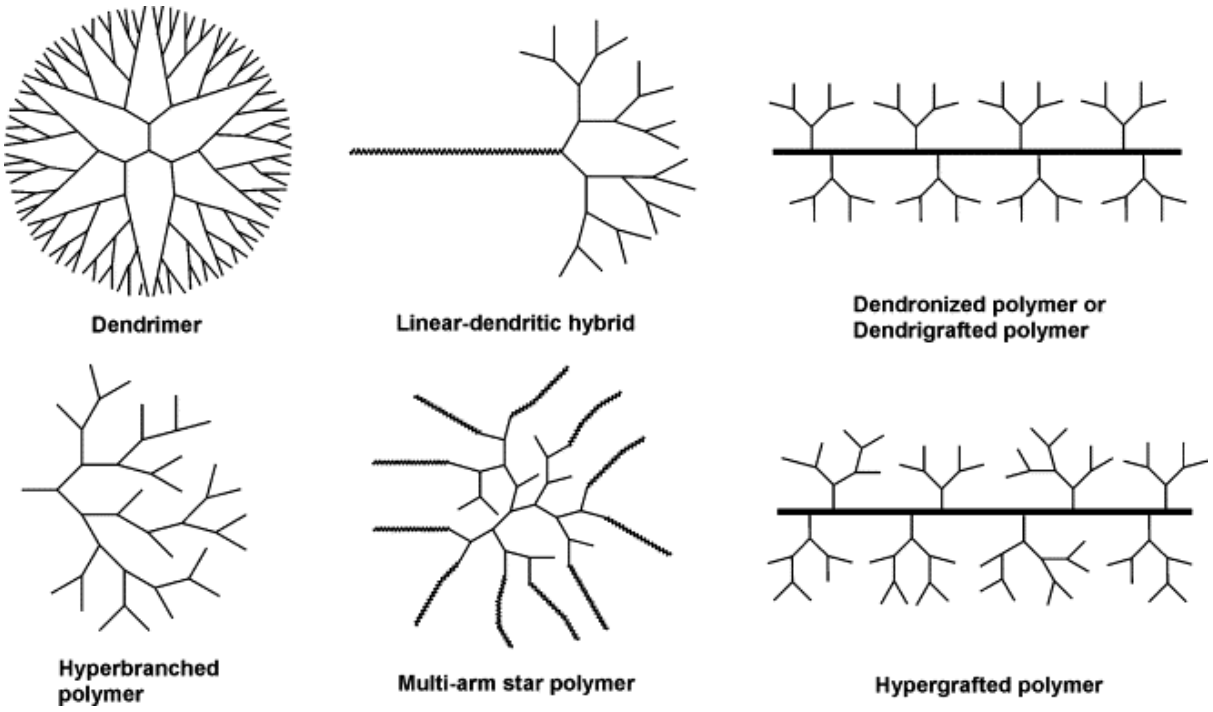

Figure 4- 1: Six examples of non-linear hyperbranched topologies which can be exhibited[11].

Hyperbranched polymers are three-dimensional macromolecules which consist of monomers that are able to exhibit a large amount of branching, which can be seen in Multi Vinyl Monomers (MVMs)[12]. Hyperbranched polymers also have a desirably high solubility whilst possessing a low viscosity[13]; all properties which have been seen as beneficial in the aspect of drug delivery. Hyperbranched polymers tailored to have pH and thermo-responsive functionality could have increased efficacy and a larger drug payload than their linear counterparts, for use as drug delivery nanocarriers. It is also advantageous that whilst exhibiting properties that make hyperbranched polymers highly soluble, they have a number of terminal groups capable of being easily modified[14]. Hyperbranched polymers have been seen to be more stable *in vivo* than in classic self-assembled micelle drug delivery systems[15].

When formulating hyperbranched polymers it is imperative that the molecular weight of the polymer is considered, along with its dispersity (Đ). Synthetic polymers have a distribution of chain lengths, each chain is denoted by a degree of polymerisation, which indicates how many monomers there are within a chain. If the degree of polymerisation is high, and the molecular weight of the monomers is high,

then the chain will have a high molecular weight. Low molecular weight monomers require a longer chain length to achieve a higher molecular weight. Polymer distribution makes it so the absolute molecular weight cannot be determined, but using analytical techniques, like GPC, the weight average molecular weight (Mw) and the number average molecular number (Mn) can be determined. Dispersity is the ratio of Mw to Mn where a dispersity value of close to 1 suggests the chains have a narrow distribution, and values greater than 1.5 indicate the chain distribution is broad. A high Đ can be expected in hyperbranched reactions[16]. The synthesis of a hyperbranched polymer can utilise controlled methods by slow monomer addition to the reaction, copolymerisation with core molecules, and purification methods where it is possible to limit the point of polymer precipitation to obtain a more desirable molecular weight[17].

When designing a stimuli responsive hyperbranched polymer for targeted drug delivery, there are many factors to consider. When synthesizing the designed polymer structure, it is important to factor in the purification and safety, while trying to make the polymer as cost effective as possible[18]. Polymers which contain disulfide bonds can provide an effective method for the design of biodegradable polymeric delivery systems. An example of this can be how disulfide linkages have been used to resist accumulation in serum, and to reduce cytotoxicity levels in polyethylene glycol (PEG) - poly(aspartamide) hyperbranched polymers[19].

Hyperbranching allows for a multitude of chemical modifications which in turn allows for a multitude of varying properties depending on the chosen modifications. For example, in the case of the N-isopropylacrylamide (NIPAM) monomer, the ability to respond to temperature due to its thermo-responsive capability makes NIPAM an attractive monomer for the use in chain extension of a pre-synthesised hyperbranched polymer, in order for these properties to be added to the polymer functionality. NIPAM has a lower critical solution temperature (LCST) of 32ºC[20] which is the temperature in which it is no longer fully soluble in aqueous media[21]. The LCST of poly(NIPAM) can be changed depending on what monomers it is copolymerized with, and the resulting impact on the level of hydrophobicity or hydrophilicity[22].

The synthesis of pH responsive polymers, using pH responsive monomers such as 2-(dimethylamino)ethyl methacrylate (DMAEMA), can be achieved using radical polymerisation techniques[23]. RAFT is a technique which enables the ability to pre-

plan the size, and the rate of reaction, of the resulting polymers. It is possible to use emulsion polymerization techniques for the synthesis of vinylic monomer polymerizations, though drug loading has been complicated when using this method[24].

RAFT was deemed an exciting technique due to there being a vast amount of suitable RAFT agents which are versatile and capable of being used with a large number of monomers and different solvent mixtures[25]. The RAFT technique was discovered by the Commonwealth Scientific and Industrial Research Organisation (CSIRO) in 1998. The CSIRO's work on RAFT attracted considerable amounts of attention, and RAFT quickly became viewed as a revolutionary next step in the advancement of polymer synthesis technology[26]. It was found that RAFT opened up the possibility to use new methods to create macromolecules where the desired molecular weight could be achieved with ease by using the technique. It was also found to be possible that the macromolecules architecture could be pre-planned *via* the use of RAFT, allowing for the creation of structural types such as star, graft, comb, block and various other structural types[27]. RAFT was found to be capable of being used in a range of experimental conditions, with a large number of monomers, in a multitude of solvents and even in the use of preparing water-soluble materials[28].

The RAFT technique is a conventional method of free radical polymerisation using a substituted monomer with a compatible RAFT agent tailored for a reversible chain-transfer experiment. Using the RAFT technique, it is possible to achieve polymer synthesis with a low dispersity yet also with a relatively high functionality [Figure 4- 2] [29-30].

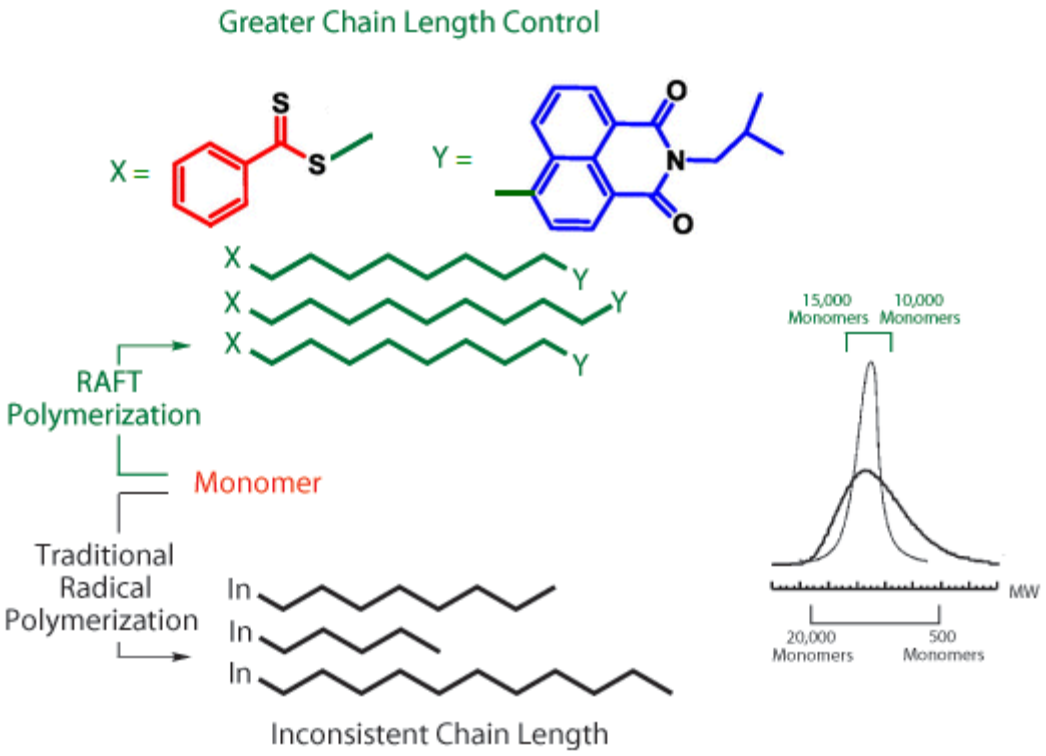

Figure 4- 2: A comparison of polymer chain lengths made via traditional free radical polymerisation technique against polymer chain lengths made using the RAFT polymerisation method with a dithiobenzoate raft agent[31].

The structure of a RAFT agent consists typically of a thiocarbonylthio group S=C-S with R and Z group substituents. R is a free radical leaving the group capable of reinitiating a polymerisation reaction, and Z has control over the reactivity of the C=S double bond and therefore impacts the rate of the radical additions and chain transfer [Figure 4- 3]. It is apparent that the R and Z substituents incorporated in the RAFT agents are integral to the prominence of the versatility when using the RAFT polymerisation technique[32].

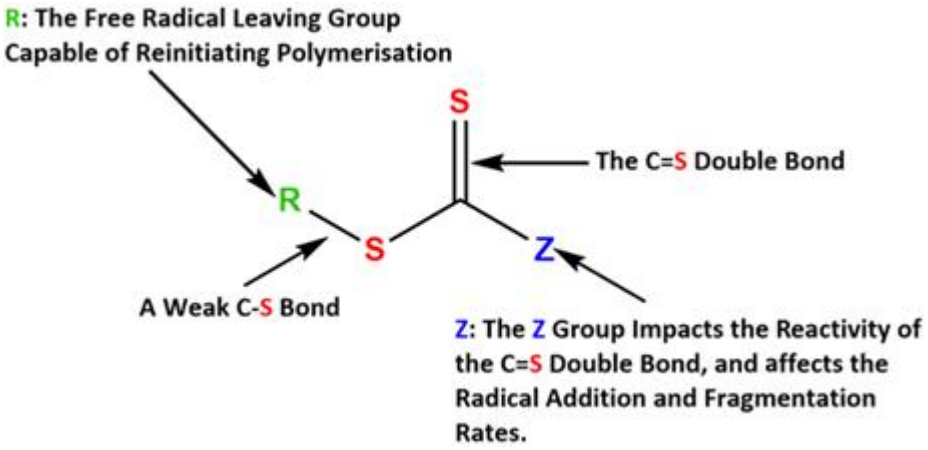

Figure 4- 3: The typical structure of a RAFT agent, and the associated characteristics of a RAFT agent caused by its bonding and substituents.

In terms of how the mechanism differs from its counterparts (e.g ATRP and FRP) in the area of controlled polymerisation techniques, the key difference is that the RAFT technique is dependent on degenerative chain transfer for the controllability of the reaction[33]. In RAFT polymerisation, the RAFT agent end groups become incorporated within the resulting synthesised polymer, which is advantageous as it can be used for bioconjugations[34]. The incorporation of the RAFT end groups can also cause polymers synthesised using this technique to obtain the colouration of its corresponding RAFT agent, which allows for studies including the resulting polymers redox sensitivity and susceptibility to heat degradation, possible to quantify *via* use of ultraviolet visible spectroscopy[35]. Like most polymerisation techniques, RAFT can be conducted as a one-pot synthesis.

It is also possible to determine the functional groups present in the RAFT end groups. The RAFT end groups exhibit properties which either class them as an α – end group or an ω – end group[36]. Regardless of being an α – end group or an ω – end group, it is possible to exploit these end groups to further modify polymers using methods including, but not limited to, radical induced reduction[37], thermolysis[38], nucleophilic attack[39], and even *via* use of a Diels-Alder reaction[40]. One potential drawback of polymer modification is the potential requirement to eliminate the sulfur present in the chain end resulting from the incorporation of the RAFT agent. When sulfur removal is required, it is important to plan accordingly as to not affect the polymer stability and functionality, and to avoid any potential toxicity[41].

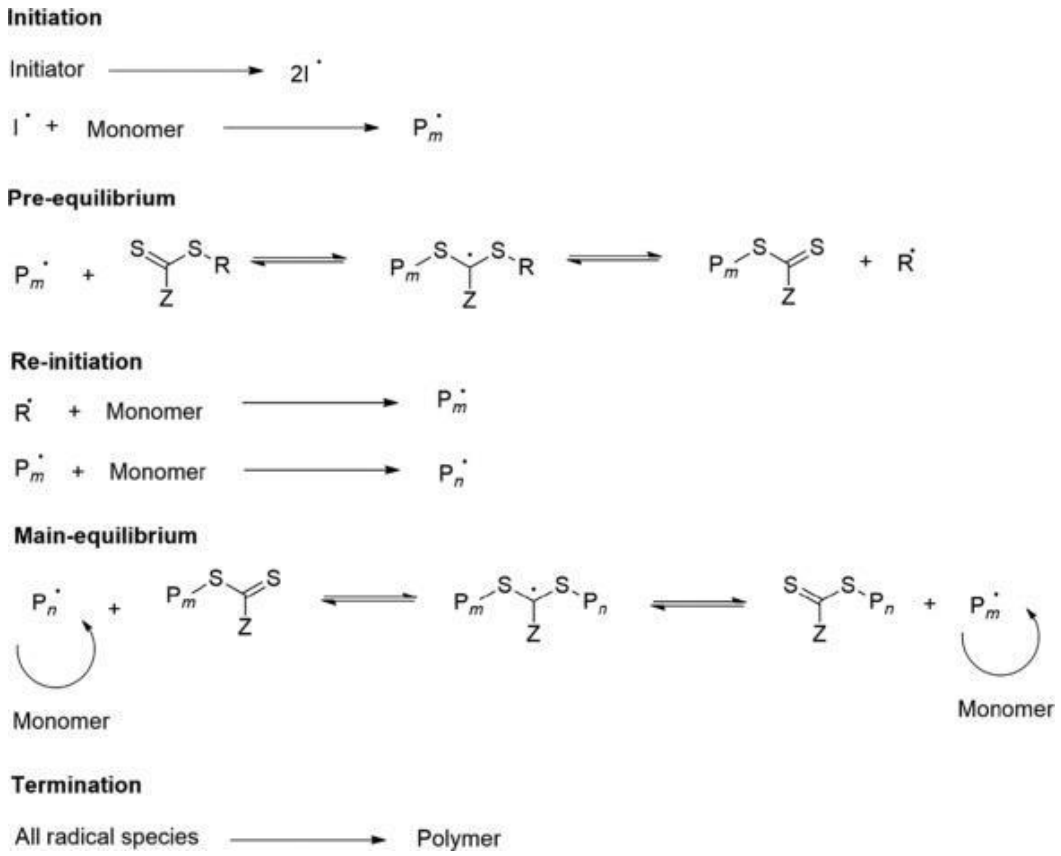

Scheme 4- 1: The RAFT polymerisation mechanism[42].

The benefits of using RAFT polymerisation in polymer synthesis, tailored towards drug delivery, have caused researchers to move away from traditional linear polymers, due to the advantages of using multi-functional hyperbranched polymers synthesised using RAFT polymerisation[43]. It is feasible for the RAFT polymerisation technique to be used to create hyperbranched polymers [Figure 4- 4] with stimuli-responsive properties, which can be used to encapsulate and release drugs in the human body when responding to environmental changes that trigger the polymer carrier to release the drug[44]. This is seen as a particularly interesting concept and is currently a very active area of research among those influencing the technological advancement of clinical drug delivery[45].

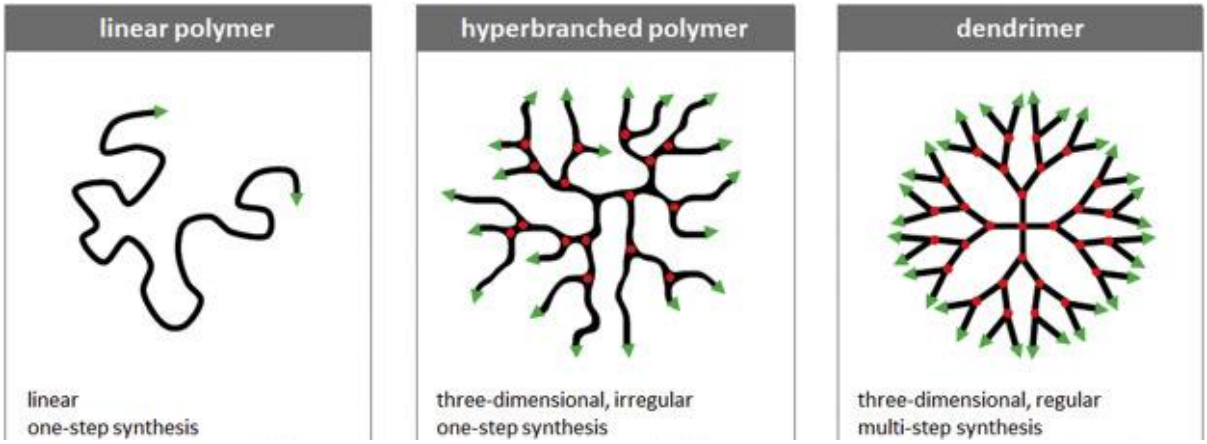

Figure 4- 4: Types of geometries for linear, hyperbranched and dendrimer polymers[46].

In this chapter, dual responsive hyperbranched polymers were designed by two steps: Step 1, RAFT polymerisation of DMAEMA with DSDA using 4-cyano-5-(((dodecylthio)carbonothioyl)thio)-4-methylpentanoic acid (CDTMA) and the initiator azobis(isobutyronitrile) (AIBN) resulting in the synthesis of the initial pH responsive hyperbranched polymer. Step 2 is the chain extension of the PDMAEMA-DSDA with NIPAM [Figure 4- 5], using the initiator 4,4'-azobis(4-cyanovaleric acid) (ACVA), adding the thermo-responsiveness to the hyperbranched polymer, cationic polymer poly(DMAEMA) (PDMAEMA) which contains a tertiary amine group.

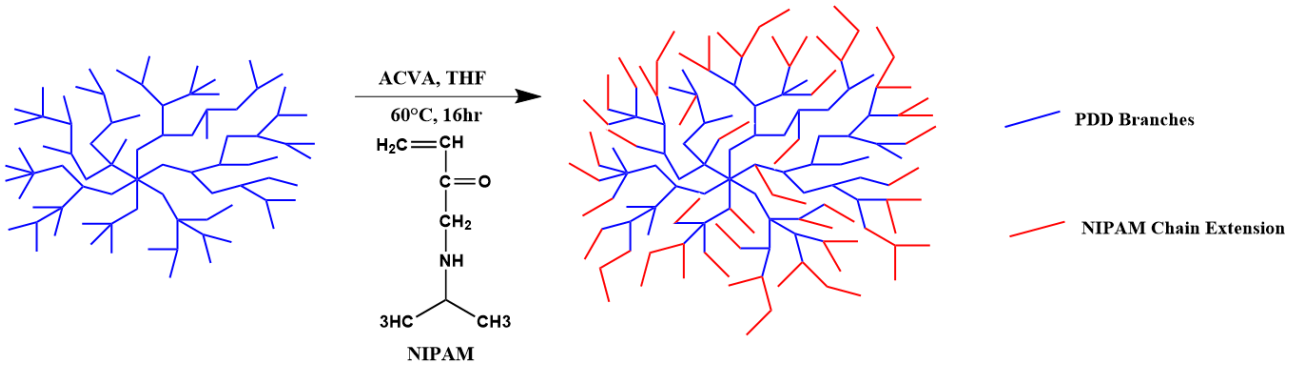

Figure 4- 5: NIPAM chain extension to form a PDMAEMA-DSDA-NIPAM hyperbranched polymer.

The polymers were characterised by NMR, GPC, and UV analysis. The polymer pH and thermo-responsiveness were tested by determining their solubility in acidic and basic conditions followed by analysing the polymers' LCST by heating the resulting dissolved polymers. The capability of being used as a drug carrier was

determined using the red dye carmoisine. Carmoisine was selected due to its ability to be loaded and released by the hyperbranched polymers and because it is easily detectable by UV-Vis. Carmoisine was loaded into the polymers and released upon the dissolving of the polymers – UV analysis was used to determine the extent of release.

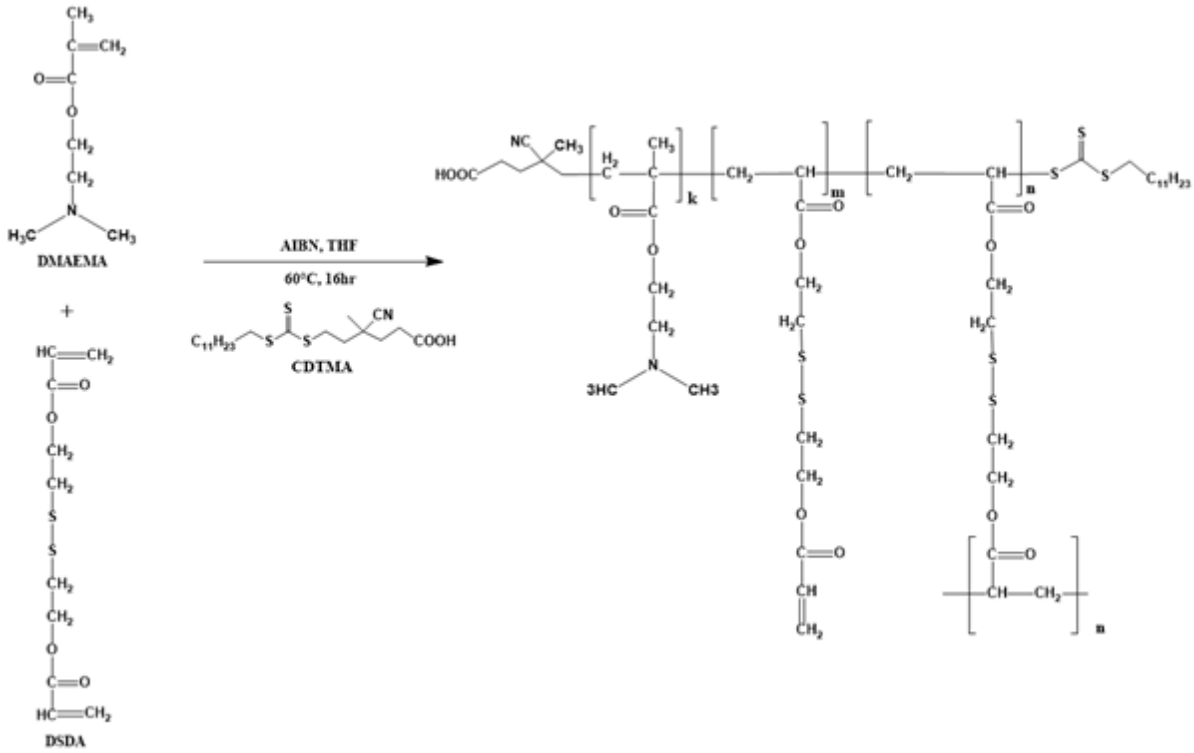

Scheme 4- 2: Synthetic route towards the product Poly(DMAEMA-DSDA).

After the carmoisine was successfully loaded and released by the hyperbranched polymers, the loading and release of galantamine hydrobromide (HBr) was explored. Galantamine hydrobromide (HBr) was loaded into a p(DMAEMA-DSDA) hyperbranched polymer consisting of a 99:1 ratio of DMAEMA to DSDA. The galantamine HBr infused p(DMAEMA-DSDA) was implanted into films comprised of alginate and chitosan – this was achieved *via* use of the Layer-by-Layer (LbL) technique[47]. These films were tested for their ability to release the drug by submerging the films in pH 7.4 and pH 4.0 phosphate buffer solutions to assess how the infusion of galantamine HBr in p(DMAEMA-DSDA) would affect the release of

galantamine HBr from the films. Samples were taken over a course of 24 hours, and then analysed *via* UV spectroscopy to determine the release of galantamine HBr.

As previously discussed, galantamine is a type 1 positive modulator of alpha-7 nicotinic acetylcholine which has been proven to inhibit enzymes from degrading acetylcholine in-turn preventing the breakdown of acetylcholine neurotransmitters[48-50]. Memogain is a pharmacologically inactive prodrug of galantamine[51]. The reaction of galantamine with benzyl chloride results in the formation of benzoic ester analogue of galantamine, given the name memogain[52]. This results in memogain having increased levels of lipophilicity and hydrophobicity, as opposed to its parent drug galantamine, allowing it to penetrate the blood-brain barrier more readily[53]. Memogain has proven to have greater than a 15-fold higher bioavailability when compared to galantamine as the same dose[54]. Once in the brain, memogain undergoes enzymatical cleavage, returning it to its precursor drug, galantamine[55]. Once memogain has been cleaved back to galantamine in the brain, its ability to act as an acetylcholinesterase inhibitor is returned, though higher levels of galantamine can be present in the brain as a result of the ability to use increased dosages of memogain[56]. The ability to increase the dosage, and the increased levels of lipophilicity and hydrophobicity, makes memogain an exciting prospect as an improved acetylcholinesterase inhibitor[57].

Memogain has also proven to reduce the number of side effects when used as an alternative to galantamine. When memogain was used in place of galantamine, reduced amyloid plaque density in the brain was observed[58-59]. It has also been determined that gastrointestinal side effects, which are common occurrences in patients with acetylcholinesterase inhibitors, have been seen to be significantly reduced when memogain is administered[60]. Animal testing has also indicated that memogain may improve cognition more effectively than galantamine[61].

4.3 Experimental

4.3.1 Materials and Methods

Triethylamine (99%), 2-hydroxyethyl disulphide, acryloyl chloride (97%), sodium bi-carbonate (Na_2HCO_3), $MgSO_4$, tetrahydrofuran (99%), $CDCl_3$ (99.8%), 2-dimethylamino)ethyl methacrylate, N-isopropylacrylamide (97%), azobis(isobutyronitrile) (98%), 4,4'-azobis(4-cyanovalericacid) (>75%), low viscosity sodium alginate (100%), chitosan (90%), acetic acid (99.5%), benzoyl chloride (99%), triethylamine (TEA) were purchased from Sigma Aldrich. Chloroform (98%), hexane (97%), HCl (36.6%), industrial methylated spirits (95.0%), ethyl acetate (99%), dichloromethane (DCM) (99.8%), dimethyl formamide (DMF) (99%), toluene (99.8%), diethyl ether (99.7%), magnesium sulphate ($MgSO_4$), sodium chloride (NaCl), sulfuric acid (H_2SO_4), (99.99%), sodium carbonate (Na_2CO_3), sodium bicarbonate ($NaHCO_3$) and sodium hydroxide (NaOH), formic acid (Optima LC-MS grade), methanol (Optima LC-MS grade) and acetonitrile (Optima LC-MS grade) purchased from Fisher Scientific. Galantamine hydrobromide was kindly donated by the Patrick Murphey Group at Bangor University. 4-cyano-5-(((dodecylthio)carbonothioyl)thio)-4-methylpentanoic acid was synthesized according to published method[62]. If not otherwise stated, products were analysed by ^1H NMR using $CDCl_3$, containing 1% (v/v) TMS as reference (0.00 ppm), using a Bruker top spin 400 MHz NMR spectrometer.

4.3.2 DSDA Synthesis

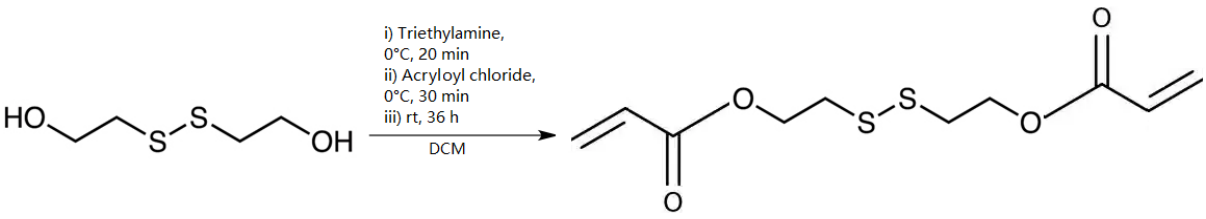

Scheme 4- 4: Synthesis of DSDA Monomer.

DSDA was synthesized according to the published method by Y. Huang et al[63]. Trimethylamine (22.25 mL, 0.16 mol), chloroform (100 mL), 2-hydroxyethyl disulphide (6.16 g, 0.04 mol) was placed in a 250 ml two neck round bottom flask (RBF). The solution was then purged with nitrogen and stirred at 0°C in an ice bath for 20 minutes. Acryloyl chloride (12.6 mL, 0.16 mol) was added dropwise at 0°C using a syringe, over a period of 30 minutes. The reaction mixture was allowed to warm to room temperature and left to stir for 36 hours under a nitrogen atmosphere. The formed salt by-product was removed by vacuum filtration. The remaining solution of the crude product was then washed sequentially with deionised water (2 x 75 mL), 0.1 M $NaHCO_3$ solution (2 x 75 mL) and an 0.1 M NaCl solution (2 x 75 mL). The organic layer was dried over $MgSO_4$, filtered and concentrated in vacuo. The material was purified by gravity chromatography (Aluminium oxide, elution with dichloromethane) to afford the desired product DSDA (8.45 g, 61% yield). TLC was performed in 100% dichloromethane, showing the product R_f equalled 0.32. DSDA was analysed by NMR using a 'Bruker top spin 400 mHz NMR spectrometer [Figure 4- 6].

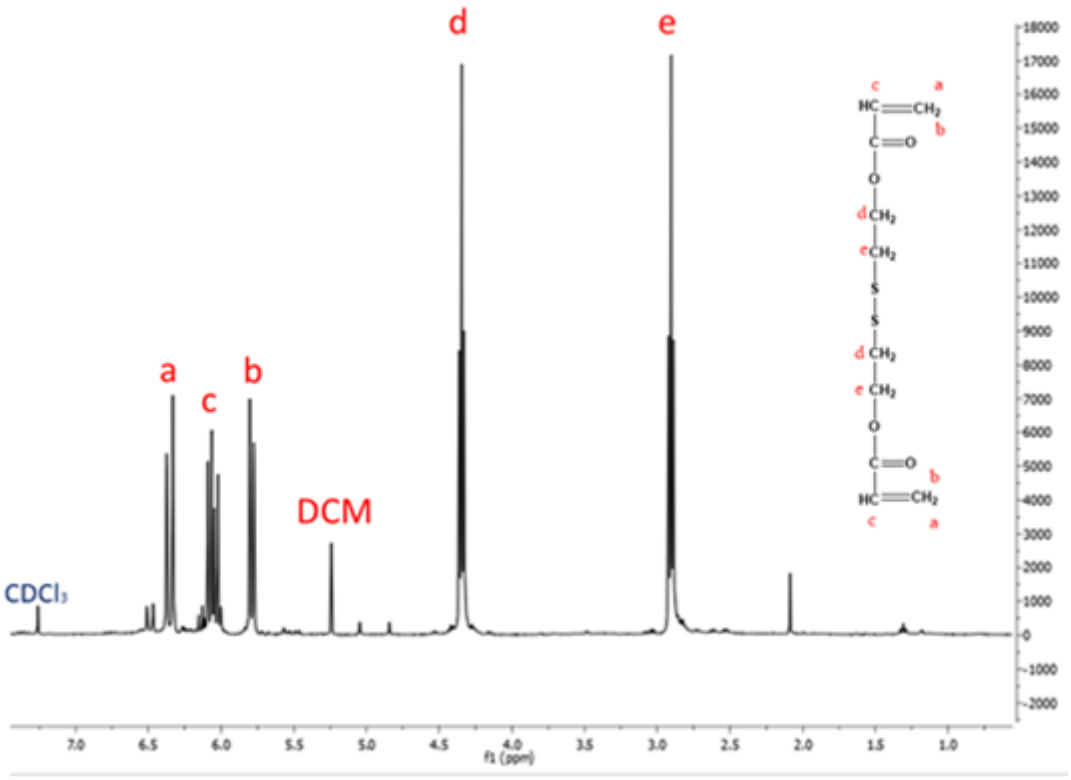

Figure 4- 6: ^{1}H NMR of DSDA in $CDCl_3$.

4.3.3 Synthesis of Hyperbranched Core DMAEMA-DSDA Copolymer

Using RAFT polymerization, three different ratios of PDMAEMA:DSDA copolymers were synthesized, 99:1, 95:5, 90:10, and given the names 'PDD1, PDD2 and PDD3' respectively. DMAEMA (5.4 mL, 35.2 mmol) was used in all three ratios, with varying amounts of DSDA. RAFT agent '4-cyano-5-(((dodecylthio)carbonothioyl)thio)-4-methylpentanoic acid' (CDCTMA), and -initiator 'azobis(isobutyronitrile)' (AIBN) [Table 4- 1].

Table 4- 1: The ratios used for the synthesis of the three P(DMAEMA-co-DSDA) copolymers synthesised via RAFT polymerisation.

Material	**Polymer Molar Ratio and Material Quantity**		
	PDD1	**PDD2**	**PDD3**
	99:1	**95:5**	**90:10**
DMAEMA	99	95	90
DSDA	1	5	10
CDCTMA	1	5	10
AIBN	1	5	10
Yield (% wt.)	**83%**	**78%**	**66%**

All the materials in the three different ratios were dissolved in tetrahydrofuran (5 mL). In all three processes, materials were placed in a 100 mL round bottom flask, purged with nitrogen for 15 minutes at room temperature, and then heated at 60°C and stirred for 16 hours. It was determined based on the viscosity increase of the liquid mixtures, as the stirrer bead that previously spun freely was no longer able to stir, that polymerization had occurred. Tetrahydrofuran (2 mL) was then added to dilute solutions and the reaction mixture was precipitated twice into a 7:1 hexane:diethyl ether solution 50 mL. The solutions were then decanted leaving a solid copolymer. Samples were dissolved in tetrahydrofuran (5 mL) and then precipitated into a 7:1 hexane:diethyl ether solution (80 mL) again to improve purity. The solution was decanted, and the resulting solid was dried *via* the use of a vacuum oven for 24 hours at 40°C with a pressure of 150 mbar. 2 mg samples of each of the polymers were analysed *via* NMR analysis [Figure 4- 7] and the polymer composition was able to be determined using the resonances of peaks d and f in the spectra [Table 4- 2].

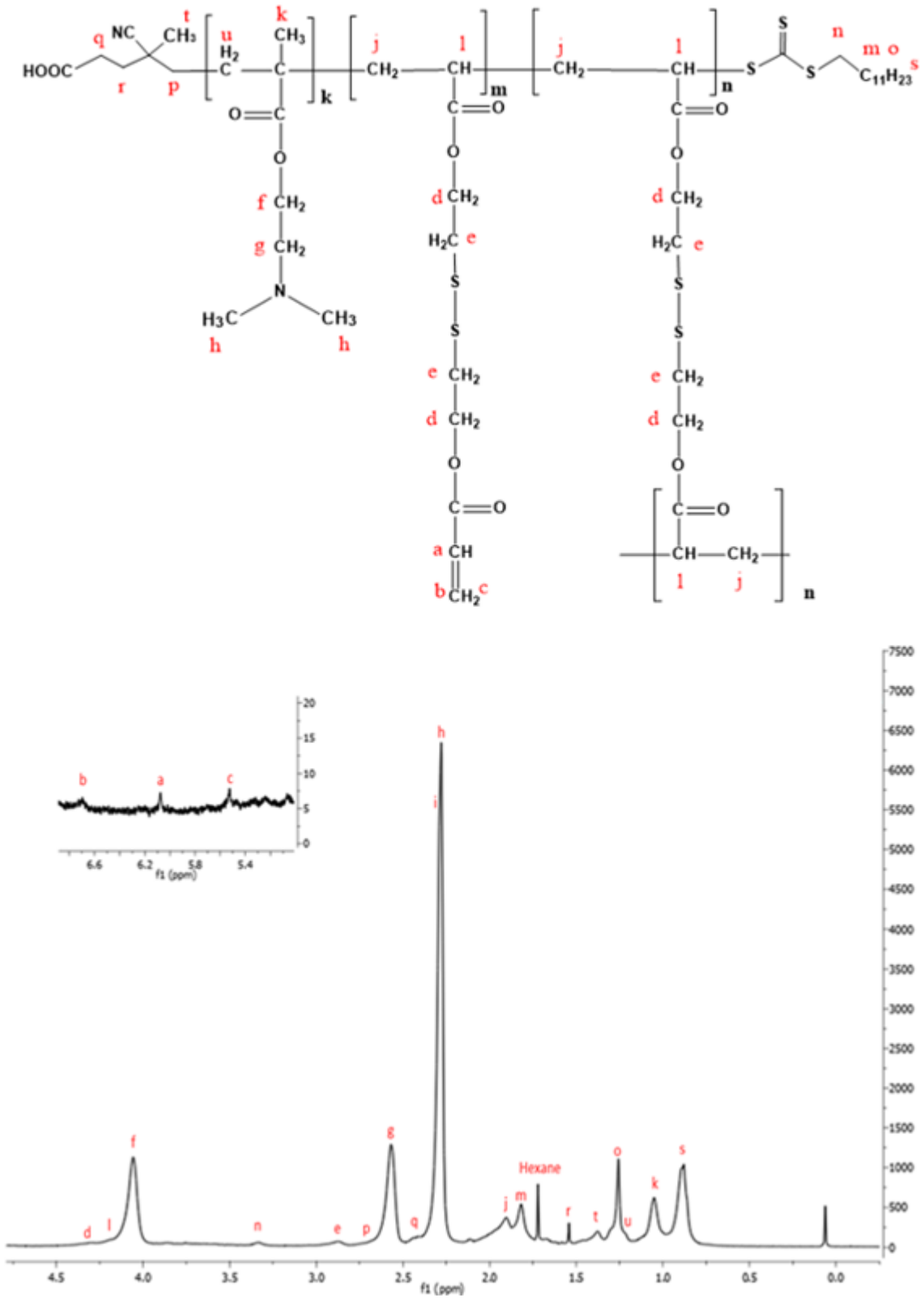

Figure 4- 7: Structure and ^{1}H NMR of P(DMAEMA-co-DSDA).

Table 4- 2: The actual ratios of PDMAEMA:DSDA samples obtained when attempting to synthesize the desired ratio. The feed ratio refers to the ratio of the monomers in the reaction. The polymer composition refers to the actual ratio of monomers comprised within the synthesized polymer. Polymer composition was obtained via NMR using (eq. 1).

Sample Name	Feed Ratio	Polymer Composition	Observation
PDD1	99.0 : 1.0	99.0 : 1.0	Malleable, clumpy pale yellow solid
PDD2	95.0 : 5.0	96.6 : 3.4	Varying sizes of Solid yellow flakes
PDD3	90.0 : 10.0	94.8 : 5.2	Very viscous deep yellow solid

Using sample PDD2 as an example calculation, the integration value per proton is calculated. This is performed using the sum of the integrations per repeat unit where A = DMAEMA and K = DSDA and the value is divided by the total number of hydrogens within the repeat unit. (eq. 4-1)

$$\int per\ H = \frac{\int A}{3x} = \frac{\int K}{6y} \qquad \text{(eq. 4-1)}$$

The next step is to calculate the ratio of the repeat units in the polymer. This is determined by using the ratio of A, K, and Q from eq. 4-1. (eq. 4-2).

$$\frac{4.115}{3} : \frac{0.290}{6} = 1.3717 : 0.0483 = 137.17 : 4.83 \qquad \text{(eq. 4-2)}$$

The sum of the ratio repeat units is then used to calculate the overall polymer composition as a percentage. (eq. 4-3)

$$\%\ Polymer\ Composition =: \frac{137.17}{142} ; \frac{4.83}{142} * 100\% = 96.6 : 3.4 \qquad \text{(eq. 4-3)}$$

4.3.4 Polymer Chain Extension with NIPAM

Chain extension with NIPAM was achieved by reacting each of the three P(DMAEMA-co-DSDA) polymers (2.00 g) individually with NIPAM (2.00 g, 14.0 mmol) and initiator 4,4'-azobis(4-cyanovaleric acid) (ACVA) (40 mg, 0.14 mmol) in tetrahydrofuran (25 mL) [Table 4- 3].

Table 4- 3: The actual ratios of P(DMAEMA-co-DSDA)-PNIPAM obtained when attempting to synthesize the desired ratio. Polymer composition obtained via NRM.

Sample Name	Feed Ratio	Polymer Composition	Yield (% wt.)	Observation
PDDN1	99.0 : 1.0 : 99.0	41.6 : 0.6 : 57.8	76%	Pale Yellow Flakes
PDDN2	95.0 : 5.0: 95.0	34.4 : 2.7 : 64.4	72%	Deep Yellow Flakes
PDDN3	90.0 : 1.0 : 90.0	47.5 : 4.9 : 47.6	70%	Very Viscous Deep Yellow Solid

In all three processes, materials were placed in a 100 mL round bottom flask, purged with nitrogen for 15 minutes at room temperature, before being stirred for 16 hours at 60°C. Polymerization was determined based on the viscosity increase of the liquid mixtures, as the stirrer bead that previously spun freely was no longer able to stir. Precipitation and purification was achieved using the same method as the PDD polymers.

The polymer composition of the P(DMAEMA-co-DSDA)-PNIPAM copolymers was determined in a similar manner to that of the P(DMAEMA-co-DSDA) copolymers (eq. 4- 1, eq. 4- 2 and eq. 4- 3) with the only change being accounting for the third repeating unit. An example of how to do this is shown in (eq. 4- 4) after which the step in (eq. 4- 2 and eq. 4- 3) are followed to determine the overall polymer composition. In (eq. 4- 4) A = DMAEMA and K = DSDA and Q = NIPAM.

$$\int per\ H = \frac{\int A}{3x} = \frac{\int K}{6y} = \frac{\int Q}{4z} \qquad \text{(eq. 4- 4)}$$

Three P(DMAEMA-DSDA)-PNIPAM (PDDN) polymers of the ratios 99:1:99, 95:5:95 and 90:10:90 were obtained and given the names 'PDDN1, PDDN2 and PDDN3' respectively. These samples were analysed by NMR. [Figure 4- 8].

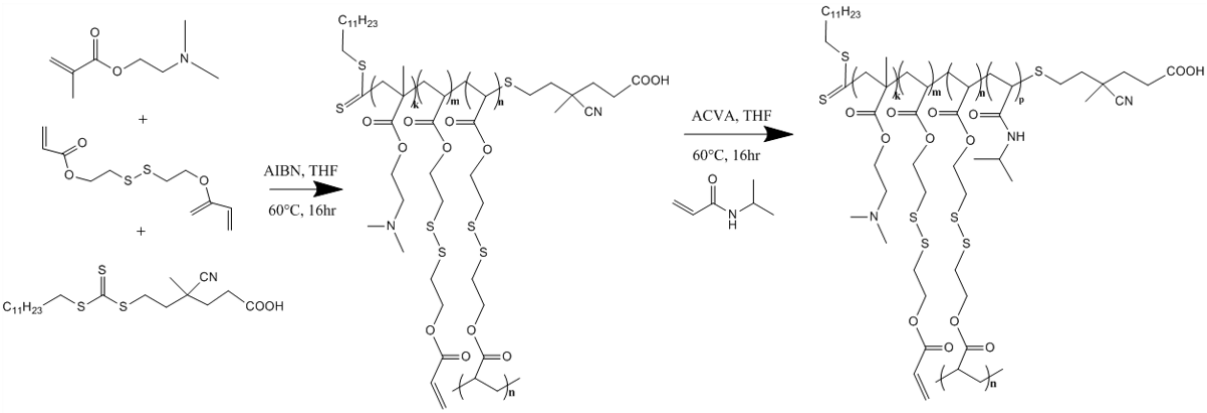

Scheme 4- 5: The synthesis of P(DMAEMA-co-DSDA) and P(DMAEMA-co-DSDA)-PNIPAM copolymers.

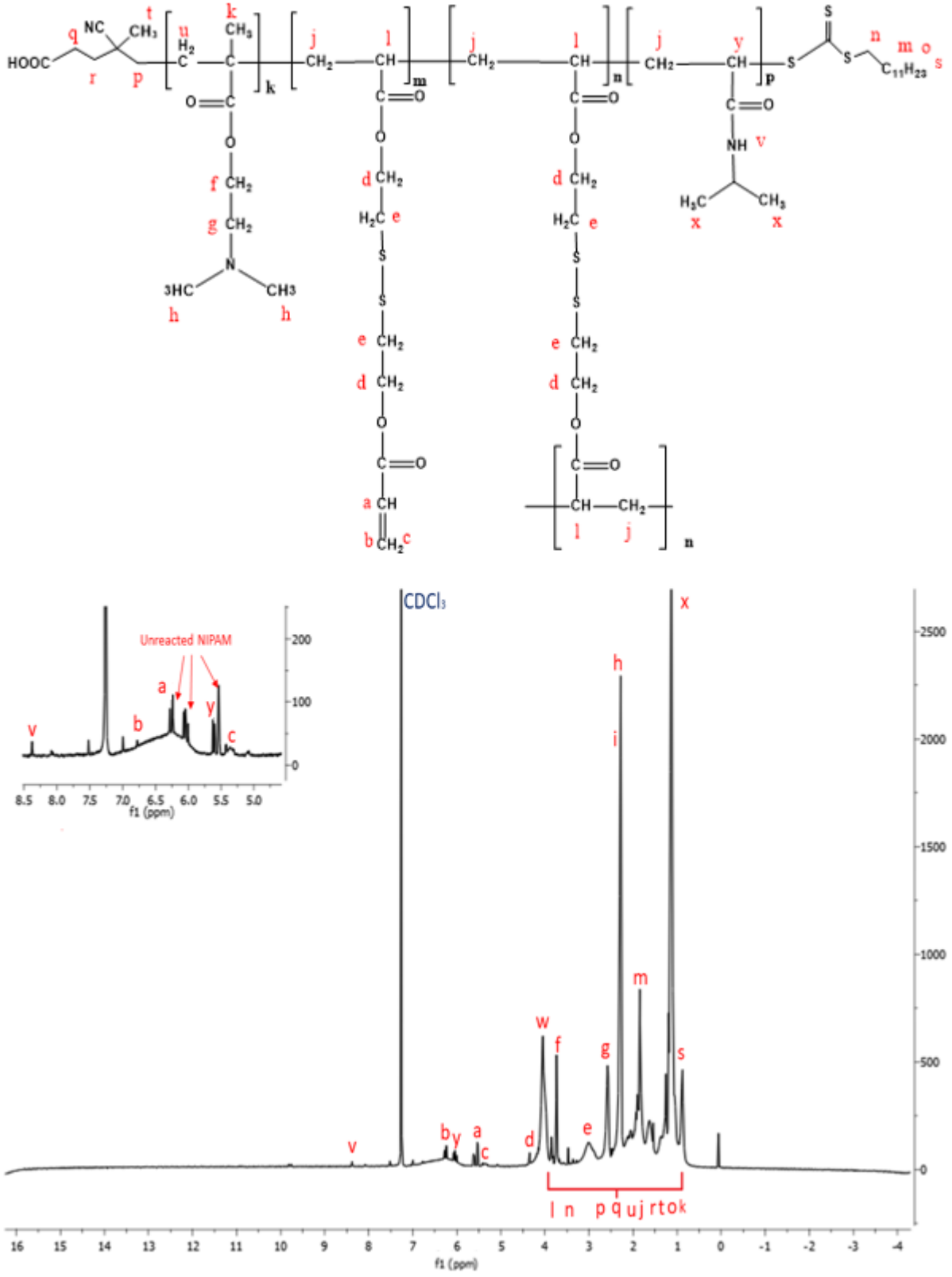

Figure 4- 8: Structure and ^{1}H NMR of P(DMAEMA-DSDA)-PNIPAM (PDDN) polymers.

4.3.5 Testing for pH and Thermo Sensitivity

10 mg samples of each of the P(DMAEMA-co-DSDA) polymers and the P(DMAEMA-co-DSDA)-PNIPAM polymers were subject to a solubility test by attempting to dissolve the polymers in media of varying pH values. Polymers were dissolved in pH values of 8.0, 7.4, 6.8, 6.0 at 25°C in order to determine the polymers' response to acidic and basic conditions, and the amount of dissolving which occurred at those pH levels. HCl and NaOH were used to adjust the pH values accordingly. The pH level of the solutions was determined *via* use of an 'Orion Star A111 pH Meter'. The results of this testing can be found in the results and discussion in section 4.4.3.

4.3.6 UV Testing

A carmoisine dye solution was prepared by adding carmoisine (3.5 mg, 0.01 mmol) to a pH 6.8 HCl solution (17.5 mL). 2.5 mL samples of the carmoisine solution were added to 7 separate sample vials; 6 for each polymer and one blank sample. Samples of 10 mg of each of the 3 PDMAEMA:DSDA, and the 3 PDMAEMA:DSDA:NIPAM polymers were prepared and individually added to a sample vial containing carmoisine solution. The samples were heated to 50°C until precipitation occurred, then left to stand for 1 hour to allow for the precipitate to settle. After the carmoisine loading was complete, 1 mL samples of the supernatant liquid solutions were analysed *via* UV spectrometry at 380-700 nm. This gave a measure of the absorption of carmoisine into the polymer to assess drug loading potential. Samples were analysed using a 'Shimadzu UV-3600' UV spectrometer. The results of this testing can be found in the results and discussion in section 4.4.4.

4.3.7 GPC Testing

5 mg samples of each polymer were dissolved using DMF + 0.1% LiBr (1 mL). Samples were analysed using a 'PL-GPC 50 Plus' fitted with a refractive index (RI) detector at 40ºC. Samples were eluted through a one column system, with a guard column, at 15 minutes per sample. The column's running temperature was 40ºC and the column type was PolarGel-M with a flow rate of 1 mL/minute and an injection

volume of 100 µL. Poly(methyl methacrylate) (PMMA) was used as the calibration standard ranging from 180 Mp – 642000 Mp. The results of this testing can be found in the results and discussion in section 4.4.2.

4.3.8 SEM Analysis

Samples of bio-based polymer films consisting of 3% sodium alginate and 3% chitosan, were mounted onto a circular metal stud which used an adhesive carbon disk which enhanced conductivity. The samples were cut using a razor in order to encompass the entire surface area of the stub. The sample coated stubs were then placed inside a “Hitachi TM4000+ Tabletop SEM” and analysed. Three images were photographed of both sides of the films. Images were acquired using a BSE detector, a 15 kV voltage, and the sample chamber under full vacuum. The three Images taken consisted of magnifications of x150, x1000 and x10000. Two sodium alginate and chitosan biopolymer films were analysed - one loaded with the PDD3 encapsulated galantamine HBr, and a blank film with no loaded sample. No additional coatings were required. The results of this testing can be found in the results and discussion in section 4.4.5.

4.3.9 Galantamine Release Study from Bio-Polymer Films

Two samples of galantamine HBr (140 mg, 0.38 mmol) were added to solutions of deionised water (50 mL) and pH 4 dilute acetic acid (0.5 mM, 50 mL) respectively. A 250 mg sample of a PDD1 polymer was added to the solutions. The solutions were stirred for 3 hours. The 3% sodium alginate solutions, containing the galantamine infused P(DMAEMA-co-DSDA), were prepared by adding low viscosity sodium alginate (1.5 g) to the galantamine infused P(DMAEMA-co-DSDA) in deionised water solution. The 3% chitosan solutions, containing the galantamine infused P(DMAEMA-co-DSDA), were prepared by adding chitosan (1.5 g) to the galantamine infused P(DMAEMA-co-DSDA) in dilute acetic acid (0.5 mM) solution. PET slides were cut into rectangular shapes with the dimensions of 7.5 cm x 2.5 cm. PET slides were washed with deionised water and industrial methylated spirits. LbL technique was used to obtain the films. The washed PET slide was placed into a solution of 3% sodium alginate for 5 minutes before being withdrawn, dried for 1 hour in air at room

temperature, and then placed into the 3% chitosan solution for 5 minutes. The contents of the PET slide were dried for 16 hours before the film was removed from the PET slide and weighed. 10 mg/mL phosphate buffer (50 mL) solution was prepared by dissolving phosphate buffer powder (500 mg) in deionised water (50 mL) and made to the appropriate pH level *via* addition of either dilute sodium hydroxide solution (1.0 M), or a dilute hydrochloric acid solution (0.1 M). After the film had been weighed, the film was submerged into a beaker containing phosphate buffer solution (50 mL, 10 mg/mL) for 24 hours with 2 mL samples being withdrawn at 10, 20,30, 50, 70, 90, 120, 180, 240, 300, 360, 1440 minutes. 2 mL of fresh phosphate buffer solution was added each time a sample was withdrawn. Film drug release was tested in pH 7.4 and pH 4.0. The swollen film was then weighed. 1 mL of each of the collected samples was taken for UV analysis, using a 'Shimadzu UV-3600', and ran between ranges of 270 nm – 300 nm using quartz cuvettes. The results of this testing can be found in the results and discussion in section 4.4.7.

4.3.10 Synthesis of Memogain via Esterification Reaction of Galantamine with Benzoyl Chloride

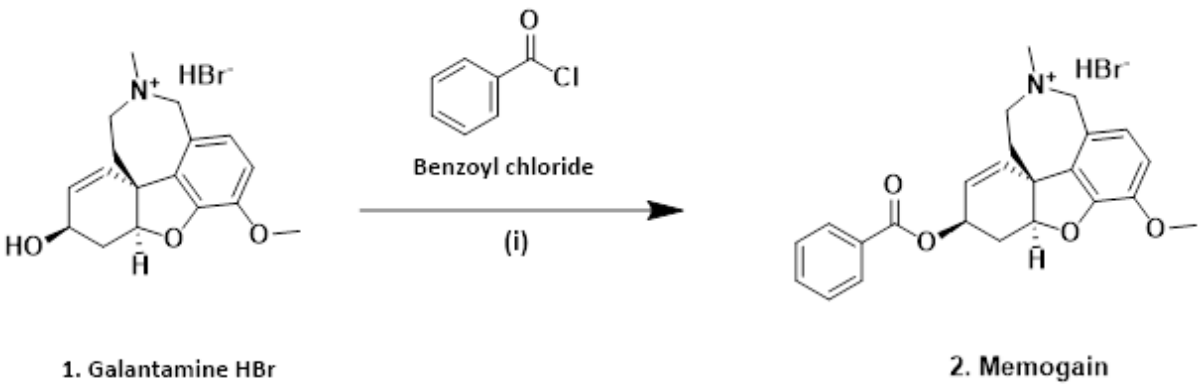

1. Galantamine HBr

2. Memogain

Scheme 4- 4: The synthesis of memogain using galantamine HBr and benzoyl chloride. (i) DMAP, triethylamine, Stirred at 300 rpm at room temperature for 20 hours.

Galantamine HBr (5.00 g, 13.58 mmol) was dissolved in dichloromethane (110 mL), and the solution was cooled to 0ºC. Triethylamine (4.0 mL, 28.66 mmol) was added to the solution and the mixture stirred for 20 minutes at 0°C. DMAP (0.83 g

0.50 mmol) was added followed by benzoyl chloride (2.2 mL, 1.20 mmol). The mixture was then allowed to warm to room temperature and stirred for 20 hours under nitrogen. TLC analysis in chloroform:methanol (9:1) indicated the reaction had gone to completion (Rf **1** = 0.45, Rf **2** = 0.53, spots were visualised in UV 254 nm [Figure 4-9]).

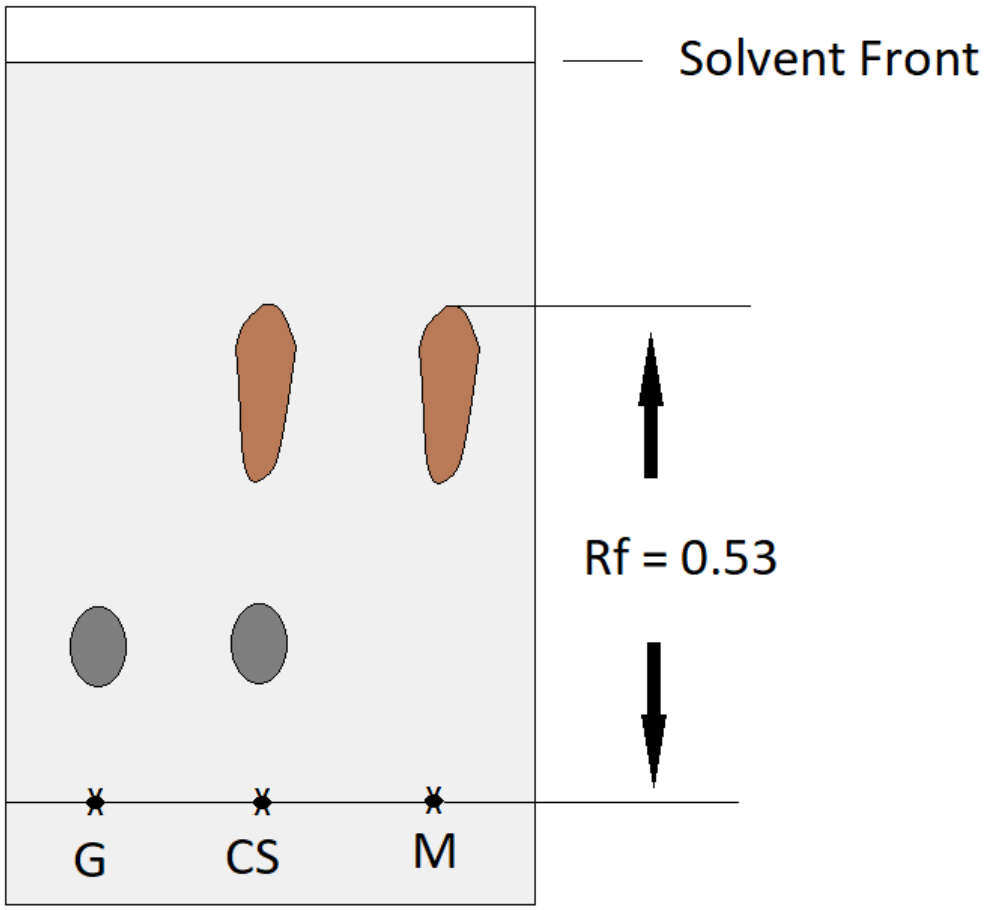

Figure 4- 9: TLC of galantamine (G), galantamine/memogain cross-spot (CS) and memogain (M) in 9:1 chloroform to methanol. Rf value for memogain was determined to be 0.53.

The reaction mixture was washed with 10% Sodium bicarbonate (3 x 150 mL), followed by brine (150 mL). The organic layer was dried over magnesium sulphate, filtered and concentrated in vacuo. The crude compound was analysed using NMR in $CDCl_3$, and then purified *via* column chromatography. The crude compound was

dissolved in dichloromethane (10 mL) and passed through a 100 g silica column, using a 9:1 solvent mixture of chloroform and methanol. The relevant fractions were concentrated *in vacuo* to give memogain (3.27 g, 65%) as a white solid. The purified product was then confirmed to be memogain *via* NMR spectroscopy in $CDCl_3$, and *via* mass spectroscopy analysis (MS) which gave an $[M+H]^+$ of 392.19 Daltons corresponding to the desired product. NMR spectroscopy further proved the synthesis of memogain was successful, detailed in [Figure 4- 10].

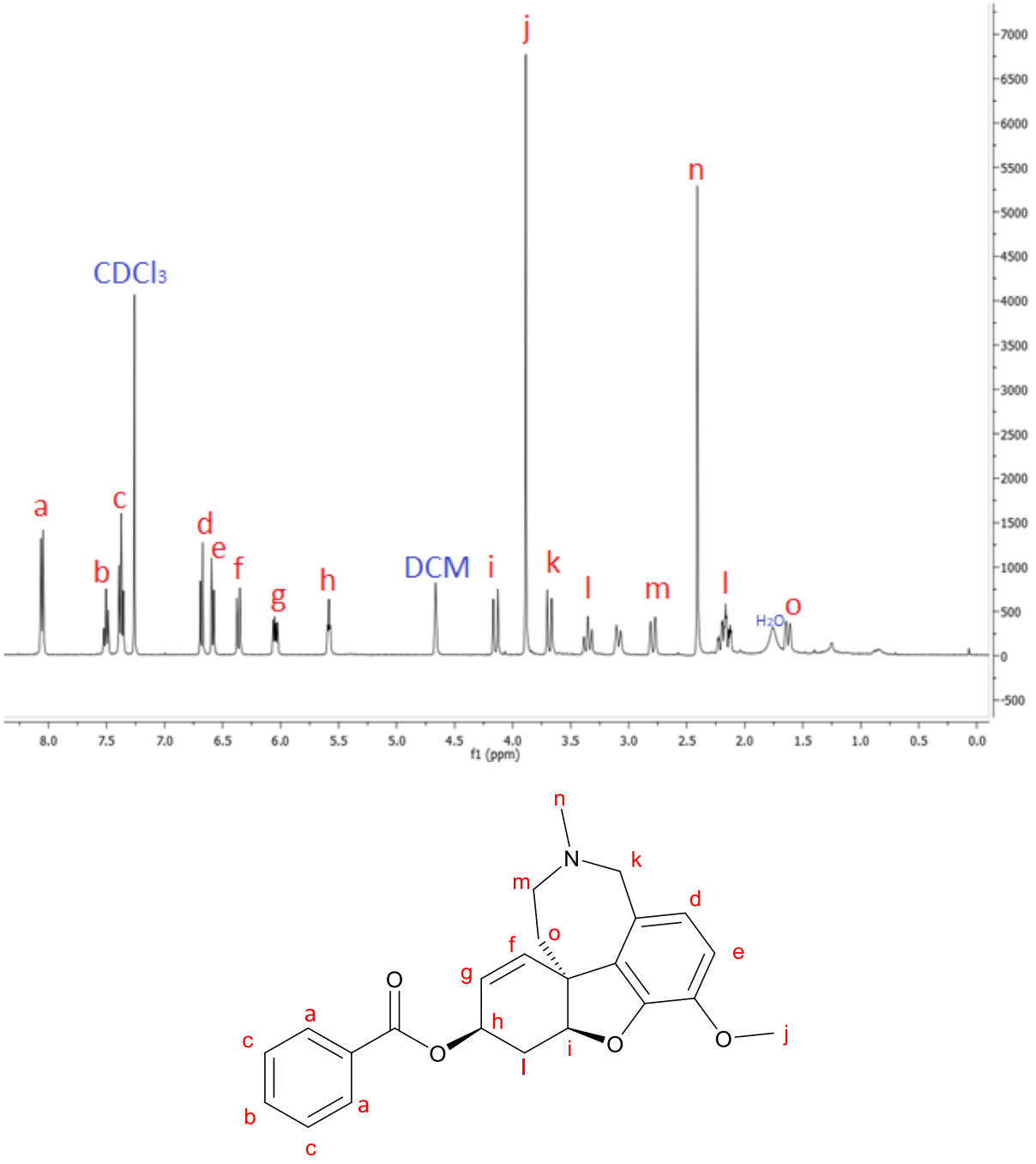

Figure 4- 10: The structure and ^{1}H NMR of memogain in $CDCl_3$.

4.3.11 Memogain Loading and Release from Sodium Alginate and Chitosan Bio-Based Polymer Films

A sample of Memogain (140 mg, 0.36 mmol) was dissolved in 9:1 deionised water to dimethylformamide (50 mL). A second sample of Memogain (140 mg, 0.36 mmol) was dissolved in pH 4 dilute glacial acetic acid (50 mL, 0.5 mM) prepared by adding concentrated glacial acetic acid (1 M) dropwise to 1 L of deionised water. Sodium alginate (1.5 g) was added to the solution of memogain in deionised water and dimethylformamide. Chitosan (1.5 g) was added to the solution of memogain dissolved in pH 4 dilute glacial acetic acid. Both solutions were made up in separate 50 mL volumetric flasks and stirred for 3 hours. This method was used to make memogain loaded 3% bio-polymer solutions.

Using the Layer by Layer technique (LbL), A 7.5 cm x 2.5 cm PET slide was cut. The slide was cleaned using deionised water, then submerged in industrial methylated spirit for 1 hour to ensure the slide was clean. After drying, the PET slide was submerged vertically in a centrifuge tube containing 3% sodium alginate solution for 5 minutes. The memogain loaded sodium alginate covered slide was then dried for 12 hours. The slide was then transferred to the galantamine loaded chitosan solution for 5 minutes using the same method. The process was repeated once, and then dried in air for 12 hours, resulting in the formation of a film. This process was repeated using sodium alginate consisting of higher amounts of α-1-glucuronic acid (G) as opposed to 1,4-β-d-mannuronic acid (M).

A phosphate buffer solution (50 mL, 10 mg/mL) was prepared by dissolving phosphate buffer (500 mg) in of deionised water (50 mL) and made to the appropriate pH level *via* addition of dilute sodium hydroxide solution (1.0 M), or a dilute hydrochloric acid solution (0.1 M) depending on the pH required. After the phosphate powder had completely dissolved after 1 hour of stirring, the memogain loaded sodium alginate and chitosan comprised films were submerged in the phosphate buffer solution for 3 hours. 2 mL samples were withdrawn from the solution after 10, 20, 30, 50, 70, 90, 120 and 180 minutes in which the solution had 2 mL of fresh phosphate buffer solution added after each sample withdrawal. Each withdrawn sample solution was analysed using a ‘Shimadzu UV-3600’ UV-Vis spectrometer using 1 mL quartz

cuvettes, cleaned using IMS followed by water, then dried between each sample being run. Phosphate buffer (10mg/mL) of the appropriate pH was used as the blank. Each release study was completed in duplicate. The percentage release of memogain was calculated using the Beer Lambert Law (eq. 4- 5). Release studies were completed in duplicate for each film of differing compositions. Maximum wavelength (λ_{max}) was equal to 283 nm.

$$A = \varepsilon.b.c \qquad \textit{(eq. 4- 5)}$$

The Beer-Lambert Law (eq. 4- 5) is used to determine the concentration, which can be used in (eq. 4- 6) to determine the percentage release.

$$\begin{aligned} C_w &= C_0 \,.\, C_r \\ W_r &= W_s - W_o \\ V &= W_r \,.\, \rho \\ n &= V \,.\, C_w \\ M &= n \,.\, M_r \\ \%M &= 100(M_t / M) \end{aligned} \qquad \textit{(eq. 4- 6)}$$

Knowing the absorbance (A), molar absorptivity (ε) and length of the light path (b = 1 cm), it is possible to determine the concentration (C) in (eq. 4- 5). This concentration can be used to determine the percentage release of memogain using (eq. 4- 6), where C_w refers to the concentration of the drug in the film. C_o is the prepared concentration of the drug. C_r refers to the concentration of the drug in the initial sample withdrawn. W_o is the original film weight. W_s refers to the swollen film weight. W_r refers to the difference between the original film weight and the swollen film weight, i.e the amount of weight increase of the film post swelling. V refers to the swollen volume. ρ refers to the density. n refers to the number of moles of the drug. M refers to the mass of the drug. M_r refers to the drug's molar mass. %M refers to the overall percentage release of the drug. M_t refers to the weight of the drug released at a set time in the release.

4.3.12 Exact Mass Determination of Memogain with LC-MS/MS

4.3.12.1 Sample Reconstitution and Preparation of Memogain

Dried samples were reconstituted and diluted as follows: memogain samples were reconstituted in acetonitrile, then diluted in 10% acetonitrile containing 0.1% formic acid. All samples were filtered through a 0.2micron PTFE filter.

4.3.12.2 Chromatographic Separation of Memogain

Reconstituted and diluted samples were kept at 15°C in the autosampler. The needle was washed with a solution of 10% methanol in water. The injection volume was 2 mL. Chromatographic separation was carried out on a Hypersil Gold C18 column (100 x 2.1 mm, 1.9 mm particle size, Thermo Scientific) which was kept at 40°C in the column oven. The flow rate was 0.4 mL/min throughout the experiment.

4.3.12.3 Mobile Phase and Gradients for Memogain

Memogain samples: mobile phase A consisted of 0.1% formic acid in water, mobile phase B consisted of 0.1% formic acid in acetonitrile. The gradient was: 0-3 min, 10%-95% B; 3-4 min, 100% B; 4-4.5 min, 100%-10% B, 4.5-7 min, 10% B.

4.3.12.4 Mass Spectrometry of Memogain

All LC-MS/MS experiments were performed on a Thermo Scientific Vanquish UHPLC system coupled to a Thermo Scientific Q Exactive Plus mass spectrometer, fitted with a heated electrospray ionisation (HESI-II) probe operated in positive ionization mode. The source parameters were: sheath gas flow rate, 45; auxiliary gas flow rate, 10; sweep gas flow rate, 2; spray voltage, 3.5 kV; capillary temperature, 300°C; S-lens RF level, 50; auxiliary gas heater temperature, 300°C. Full MS scans were carried out with the following parameters: in-source CID, 0 eV; microscans, 1; resolution, 140’000; AGC target, 1e6; maximum IT, 500 ms; scan ranges: 100-1200 m/z for memogain sample; spectrum data type, profile in appendices.

Figure 4- 11: The Q Exactive Plus (Thermo Fisher) mass spectrometer.

4.4 Results and Discussion

4.4.1 DMAEMA-DSDA Polymers and Extension with NIPAM

Upon synthesis of the three PDD polymers and the three PDDN polymers, the polymer compositions were determined *via* ^{1}H NMR analysis. With reference to [Table 4- 2] and [Table 4- 3], it is plausible that increasing the amount of DSDA results in a lower likelihood of achieving the desired polymer composition when left to stir for 16 hours at 60°C. The correlation would also appear to be exponential when looking at the actual values against the desired values for the PDD2 and PDD3 polymers, and PDDN2 and PDDN3 polymers. It is likely that as the amount of DSDA is increased, there is a larger amount of unreacted monovinyl monomers removed upon working up the reaction after 16 hours, resulting in the increasing contrast in feed ratio to polymer composition.

In the NIPAM chain extension step, there is a larger amount of NIPAM in the final polymer than DMAEMA, even though approximately equal weight amounts were used in the synthesis of the chain. This is believed to be due to the reactivity of NIPAM's vinyl group. It is only in the PDDN3 polymer sample that there is almost the correct ratio of DMAEMA to NIPAM. The NMR peaks were in the same positions on the spectra for PDD1, 2 and 3, and for PDDN1, 2 and 3. The difference for each polymer is the intensity changes depending on the differing amounts of DSDA and NIPAM [Figure 4- 6 and Figure 4- 7]. For the three PDD samples, it was evident that the tertiary amine group from the DMAEMA monomer was present due to the appearance of a doublet peak at ~2.28 ppm indicative of the two CH_3 groups in the tertiary amine group. The triplet peak at ~4.30 ppm-4.40 ppm is apparent due to the CH_2 adjacent to the acrylate group from the DSDA monomer. In the PNIPAM chain extension NMR spectra, a new peak at ~1.09 ppm-1.16 ppm can be observed. This is due to CH_3 groups adjacent to a CH in the chain, which is evidence of the amide group from the NIPAM monomer present in the polymer chain. Polymer composition was determined using the ratios of the integration values after normalization – This was obtained by dividing the integrations of the peaks indicative of each monomer by the total of the integration values.

4.4.2 GPC Analysis

With reference to the data tabulated in [Table 4- 4], it can be determined that due to the size increase of the polymers after chain extension with NIPAM, it represents successful chain extension. As the amount of DSDA in the polymer make-up increases, the molecular weight decreases. The largest polymers were made using the 99:1 ratios, while the smallest were made using the 95:5 ratios.

Table 4- 4: Table contains GPC data for the six synthesized polymers in dimethylformamide.

*A**: Polymer feed mol ratio (DMAEMA : DSDA for entries 1-3 and DMAEMA : DSDA : NIPAM for entries 4-6).***

*B**: Reaction time.** C**: Number average molecular weight.** D**: Weight average molecular weight.** E**: Dispersity.***

Entry	Polymer Sampler	F[A]	RT[B] (hours)	Yield (wt %)	Mn[C] (g mol^{-1})	Mw[D] (g mol^{-1})	Đ[E]
1	PDD1	99.0 : 1.0	16	83%	14.7	36.9	2.52
2	PDD2	95.0 : 5.0	16	78%	1.1	3.6	3.45
3	PDD3	90.0 : 10.0	16	67%	1.1	7.5	7.11
4	PDDN1	99.0 : 1.0 : 99.0	16	76%	23.4	253.7	10.82
5	PDDN2	99.0 : 5.0: 95.0	16	72%	9.5	23.1	2.43
6	PDDN3	90.0 : 1.0 : 90.0	16	70%	7.1	31.5	4.44

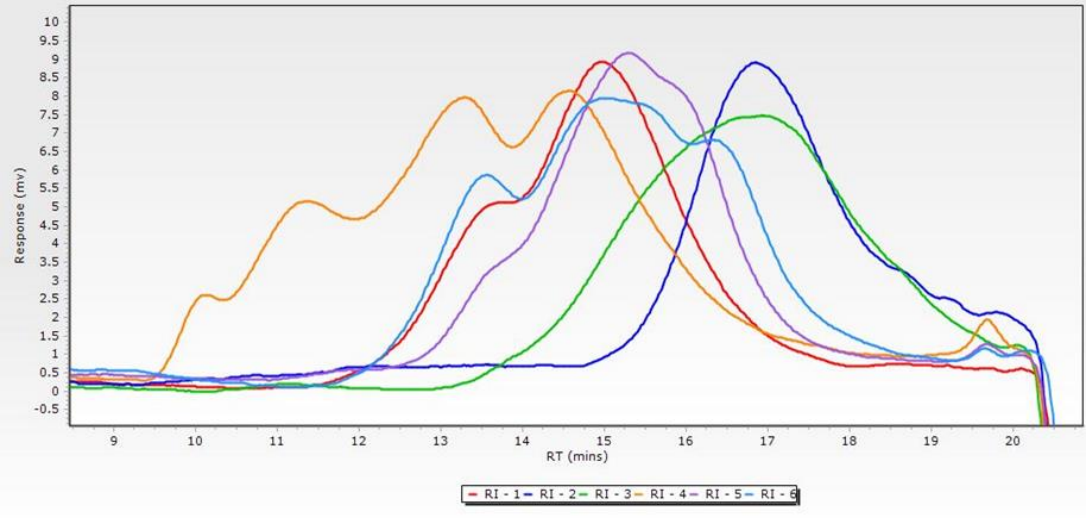

Figure 4- 12: SEC chromatogram for the PDD and PDDN polymer samples. RI - 1 to RI - 6 is representative of entries 1 to 6 in [Table 4 – 4].

4.4.3 pH Sensitive and Thermosensitive Properties Analysed

The PDD and PDDN polymer samples of different ratios were tested for their pH sensitive and thermo-sensitive capabilities. The data obtained [Table 4- 5] demonstrates that the polymer is pH sensitive as it dissolves in acidic solutions below pH 6.9. DMAEMA contains a tertiary nitrogen group which means it is a cationic monomer. This allows for proton acceptance upon being subjected to acidic conditions. Adding amide containing NIPAM to the polymer chain further increases the polymer hydrophilicity[64].

Table 4- 5: 10 mg samples of the three P(DMAEMA-co-DSDA) polymers and the Three P(DMAEMA-co-DSDA)-PNIPAM polymers of varying ratios tested for their solubility in four different pH's; 8.0, 7.4, 6.8, 6.0.

pH	Polymer Sample					
	PDD1	**PDD2**	**PDD3**	**PDDN1**	**PDDN2**	**PDDN3**
8.0	X	X	X	X	X	X
7.4	/	/	/	X	X	X
6.8	✓	✓	✓	✓	✓	✓
6.0	✓	✓	✓	✓	✓	✓

'✓' symbol represents 'soluble','/' symbol represents 'partially soluble',' X' symbol represents 'insoluble'.

The DMAEMA monomer has a pKb of 8.3 at 25°C[65]. The results of the pH testing of the 6 polymers are in agreement with the proposed hypothesis that they would dissolve in acidic conditions due to its cationic nature. PDD polymers partially dissolved at pH 7.4, but fully dissolved in pH 6.8 and 6.0, while no dissolution at pH 8.0 was observed. PDDN polymers also followed this trend apart from not partially dissolving at pH 7.4 unlike its PDD counterparts which is a result of a lesser content of DMAEMA in the polymer composition. The dissolved polymers were subjected to temperature increase to assess thermo-responsive capability. Above certain temperatures, and depending on pH, the PDD and PDDN polymers are water-insoluble[66]. In double hydrophilic copolymers such as PDD and PDDN, changes to pH and temperature can cause parts of the polymer chain to become hydrophobic, as a result of coiling[67], while leaving other segments hydrophilic. This allows for the polymer to still be water soluble, but the solution will precipitate back out at higher temperatures[68].

Upon reaching a temperature at which a polymer in solution goes from a clear homogeneous solution to precipitating and becoming visibly 'cloudy' as it has reached its cloud point (CP), otherwise known as Lower Critical Solution Temperature (LCST), and therefore the polymer LCST has been reached. LCST is the critical temperature at which the polymer in solution is completely miscible, whereas when the temperature of a solution is above the LCST, partial liquid miscibility is observed[69]. It is important to understand that the mixing of the phases is immediate when the temperature of the solution is below the LCST, but not above. The Gibbs free energy change in relation to the mixing of the phases is positive when above the LCST, and negative when below it[69]. The dissolved PDD and PDDN polymers, in pHs 6.0 and 6.8, were heated to 50°C to determine LCST values [Table 4- 6]. [Figure 4- 13] shows the change in properties of a PDD1 sample, in a pH 6.8 solution, when heated to its LCST of 32.7°C. The partially dissolved polymers observed very little clouding when heated and were omitted as a result [Figure 4- 13].

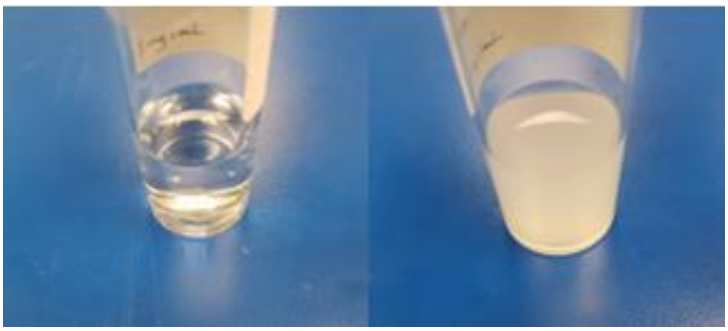

Figure 4- 13: PDD1 sample dissolved in pH 6.8 solution before (left) and after (right) heating to its LCST of 32.7°C. The solution appears to be 'cloudy' as it has reached CP.

Table 4- 6: The observed LCST values for the PDD, and PDDN polymers in acidic solutions.

Polymer Solution	**LCST (°C)**	
Sample	**pH 6.0**	**pH 6.8**
PDD1	35.5	32.7
PDD2	37.6	36.4
PDD3	43.7	41.3
PDDN1	39.4	33.1
PDDN2	43.1	36.7
PDDN3	45.0	38.9

LCST gives a strong indication of what temperature the polymer chain will collapse. As a result, the carried drug would be released when the polymers LCST is reached[70]. The data shows that increasing the amount of DSDA in the chain and adding NIPAM to the polymer chain decreases the solubility of the polymer. Usually

increasing the polymer chain length causes solubility to decrease. When a polymer becomes less linear, and more hyperbranched, it becomes less entangled. The surface area increases, but gaps form in between the branches of varying sizes. This allows water molecules to be able to enter and interact with the hydrophilic groups of the polymer.

When the LCST is reached, the hydrophobic isopropyl group collapses causing a configuration change. DMAEMA also exhibits a change resulting in the polymer chain coiling and no longer being able to interact with water[71]. At this point precipitation is observed. The data also shows that decreasing the pH to more acidic conditions increases the LCST. The lower the pH, the more protonated the DMAEMA chains are so they are more hydrophilic. Higher temperatures are required to reach the LCST of a more hydrophilic chain[72].

4.4.4 Carmoisine Loading

To determine each of the PDD and PDDN's ability to act as a nanocarrier in drug delivery, polymer samples were loaded with carmoisine (also known as Azorubine)[73]. Carmoisine [Figure 4- 14] is a red food colouring, which more importantly carries a negative charge. This allows for it to coordinate to the cationic positively charged tertiary amine group in DMAEMA.

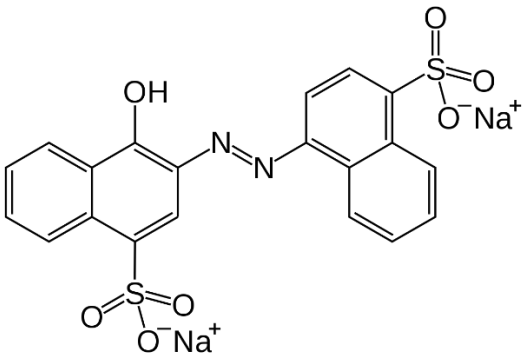

Figure 4- 14: The structure of carmoisine.

10 mg samples of each polymer were dissolved in pH 6.8 carmoisine solution (2.5 mL). With the polymers still in solution, samples were placed into quartz cuvettes and taken for UV analysis[74]. Carmoisine absorption was determined using the

indicative peak at 576 nm. Carmoisine loading into a polymer sample is indicative of the absorption of carmoisine left in the solution. When the polymer is introduced to the carmoisine solution, it is expected that the polymer will load an amount of carmoisine. The more carmoisine loaded into the polymer, the lower the absorption are there is now less carmoisine remaining in the solution. The results show that PDDN1 holds the most carmoisine, as the absorption of carmoisine in solution is the lowest for this sample [Figure 4- 15 and Table 4- 7] which suggests it has the highest drug loading potential.

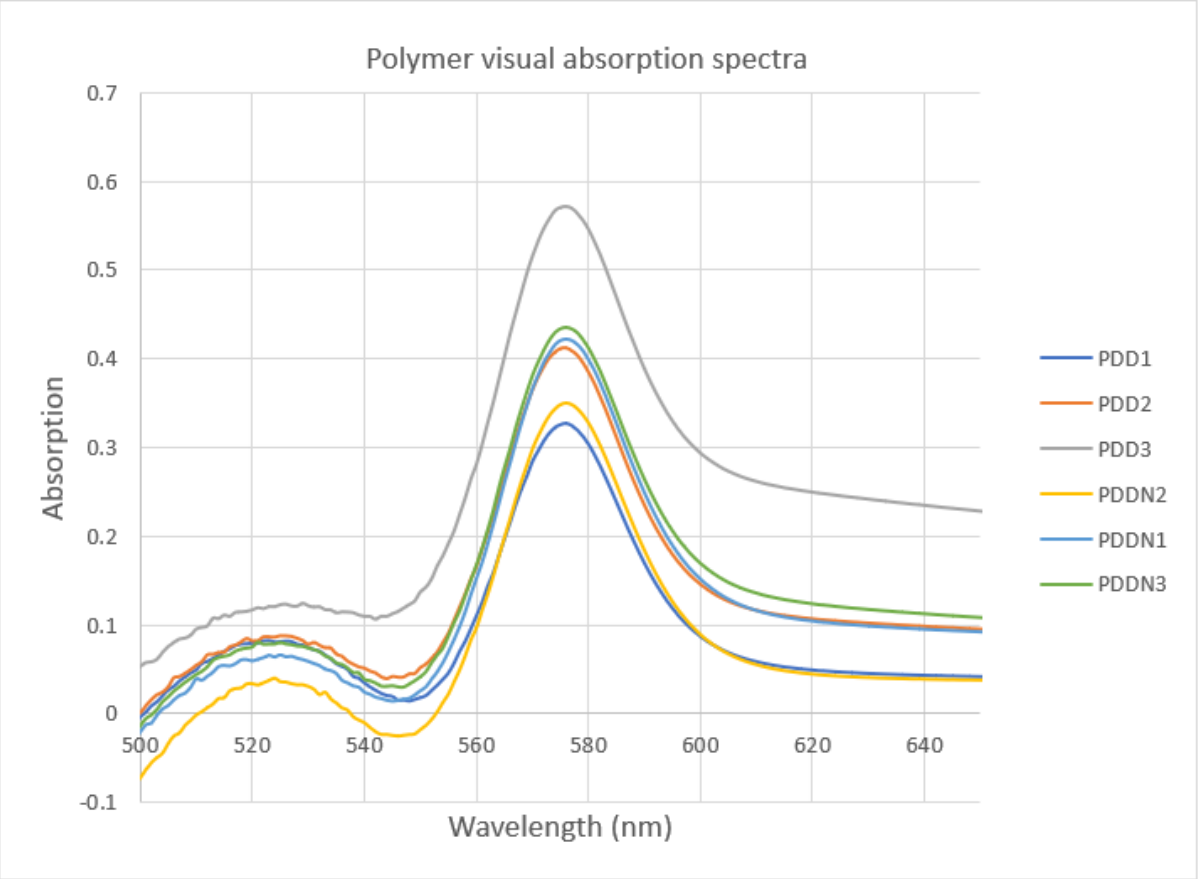

Figure 4- 15: Polymer sample absorption after being loaded with carmoisine.

Table 4- 7: PDD and PDDN polymer samples absorption amounts at wavelength λ_{max} (nm).

Sample	λ_{max} (nm)	Absorption
PDD1	576	0.423
PDD2	576	0.413
PDD3	576	0.572
PDDN1	575	0.328
PDDN2	576	0.351
PDDN3	576	0.436

The data also shows that the NIPAM chain extended polymers can hold more of the carmoisine, which is potentially due to the polymers' increased amount of hyperbranching. The areas of space within the polymer, created through hyperbranching, are able to hold more of the carmoisine, and therefore, more hyperbranching means more drug loading ability.

Loading carmoisine into the polymers demonstrated that they have the potential to be used as carriers in drug delivery, and has given an indication on which polymer composition is preferable for drug loading. Knowing this, it would be expected that it is possible to do the same with galantamine HBr, using the PDD1 polymer as the primary candidate to ensure optimal drug loading and release. PDDN1 was not selected due to its lower solubility.

4.4.5 SEM Analysis

SEM images were taken to determine if the PDD1 polymer, encapsulated with galantamine HBr, had been successfully loaded into a 3% sodium alginate 3% chitosan biopolymer film. A film loaded with galantamine HBr encapsulated within the polymer was compared against that of a film with nothing loaded into it.

Images were taken of both sides of the film to ensure both the sodium alginate and chitosan layer faces were analysed, to determine if loading had occurred, and to determine the size of the biopolymer films' pores. It is apparent from the SEM images taken from the sodium alginate faces of the two films that loading the galantamine encapsulated PDD1 polymer may have occurred due to the perceived change in the films' morphology [Figure 4- 16].

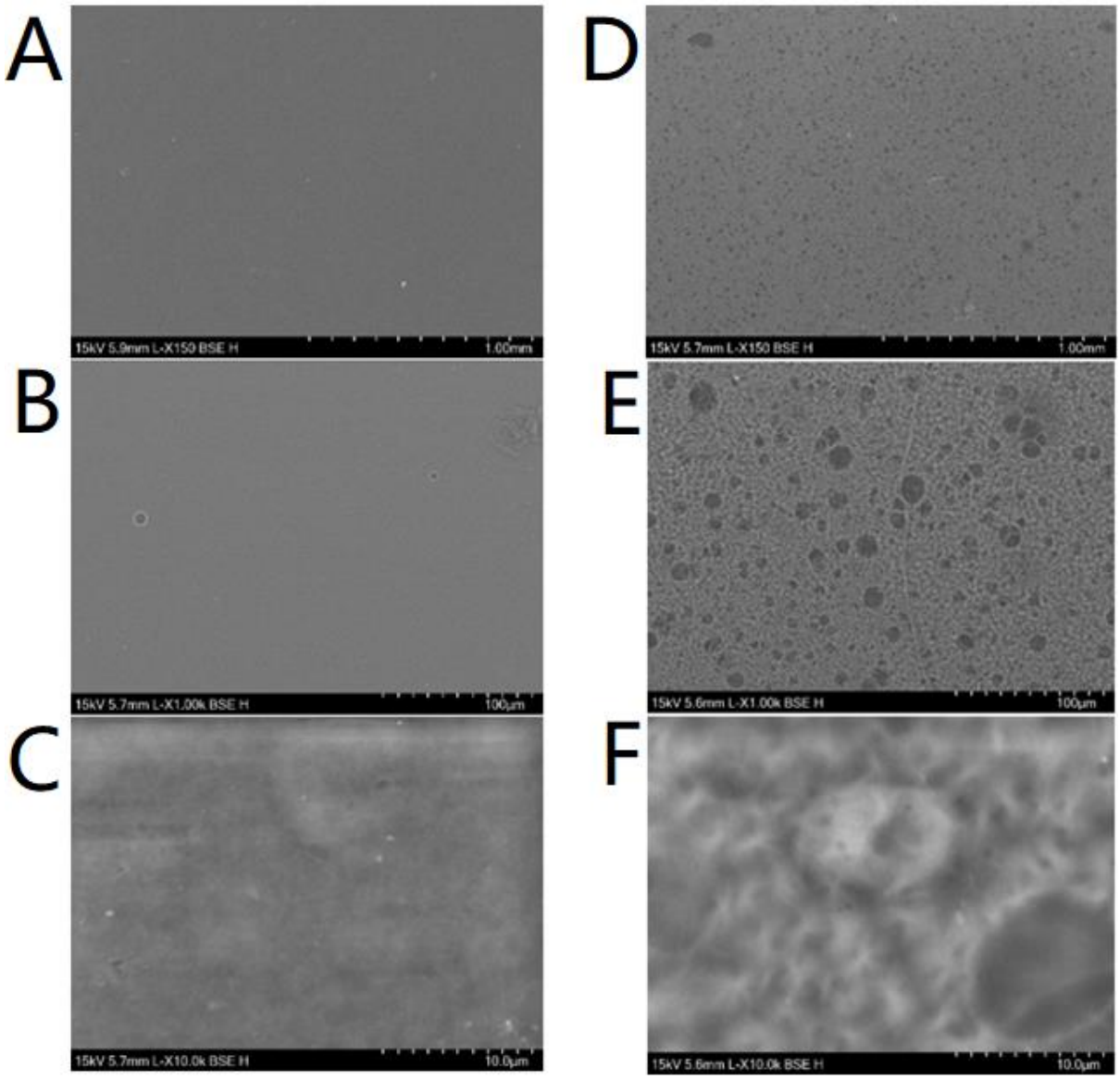

Figure 4- 16: SEM images of 3% sodium alginate 3% chitosan bio-polymer films from the sodium alginate faces. The features in the film on the left (A-C) are absent of the galantamine HBr encapsulated PDD1 polymer. The polymer is present in the images of the film on the right (D-F). Image magnifications increase from x150 (A and D) to x1000 (B and E) to x10000 (C and F).

In the x150 and x1000 magnification images from the sodium alginate faces, it is clear in the polymer loaded films that there are multiple circular sites which are not present in the polymer absent film, indicating that the sites could be phase separated PDD-rich zones. This was less apparent in the chitosan face images, however circular

sites can still be seen, although less clearly than in the images of the sodium alginate face counterpart [Figure 4- 17].

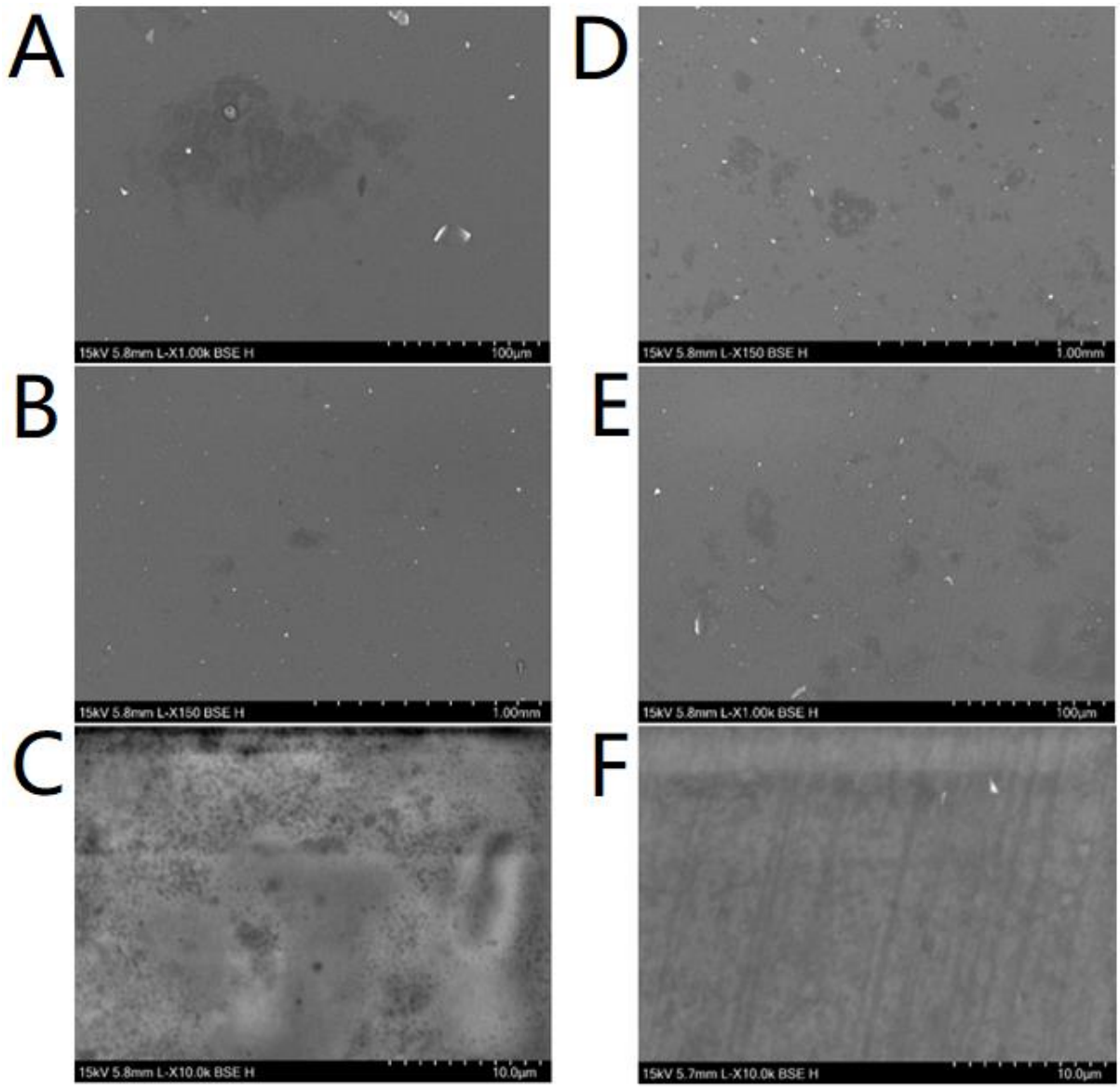

Figure 4- 17: SEM Images of 3% sodium alginate 3% chitosan bio-polymer films from the chitosan faces. The features in the film on the left are absent of the galantamine HBr encapsulated PDD1 polymer (A-C). The polymer is present in the images of the film on the Right (D-F). Image magnifications Increase from x150 (A and D) to x1000 (B and E) to x10000 (C and F).

It was possible to determine the size of the pore diameters in both the sodium alginate and chitosan layers of the film with the sodium alginate layer exhibiting pore diameter size range of 1 µm - 10 µm, and the chitosan layer exhibiting 300 nm – 2 µm.

The pore size of both the sodium alginate and chitosan layers could indicate that the loaded drugs will be able to release from the drug without a large amount of difficulty in pH 7.4 phosphate buffer solution.

4.4.6 Galantamine Release from Polymers in Transdermal Films

Transdermal films consisting of 3% sodium alginate and 3% chitosan were made, and loaded with galantamine HBr, encapsulated within the PDD1 polymer. Galantamine HBr was successfully released from transdermal films in pH 7.4 and pH 4.0 phosphate buffer solutions. Films where galantamine HBr was encapsulated within the PDD1 polymer were assessed for its effect on the release of galantamine HBr against films where the PDD polymer was absent. Each release study, from films where properties varied, was repeated in duplicate. From the data presented in [Figure 4- 18] it can be determined that encapsulating galantamine HBr in the PDD1 polymer increases the amount of galantamine released whilst also increasing the rate of release.

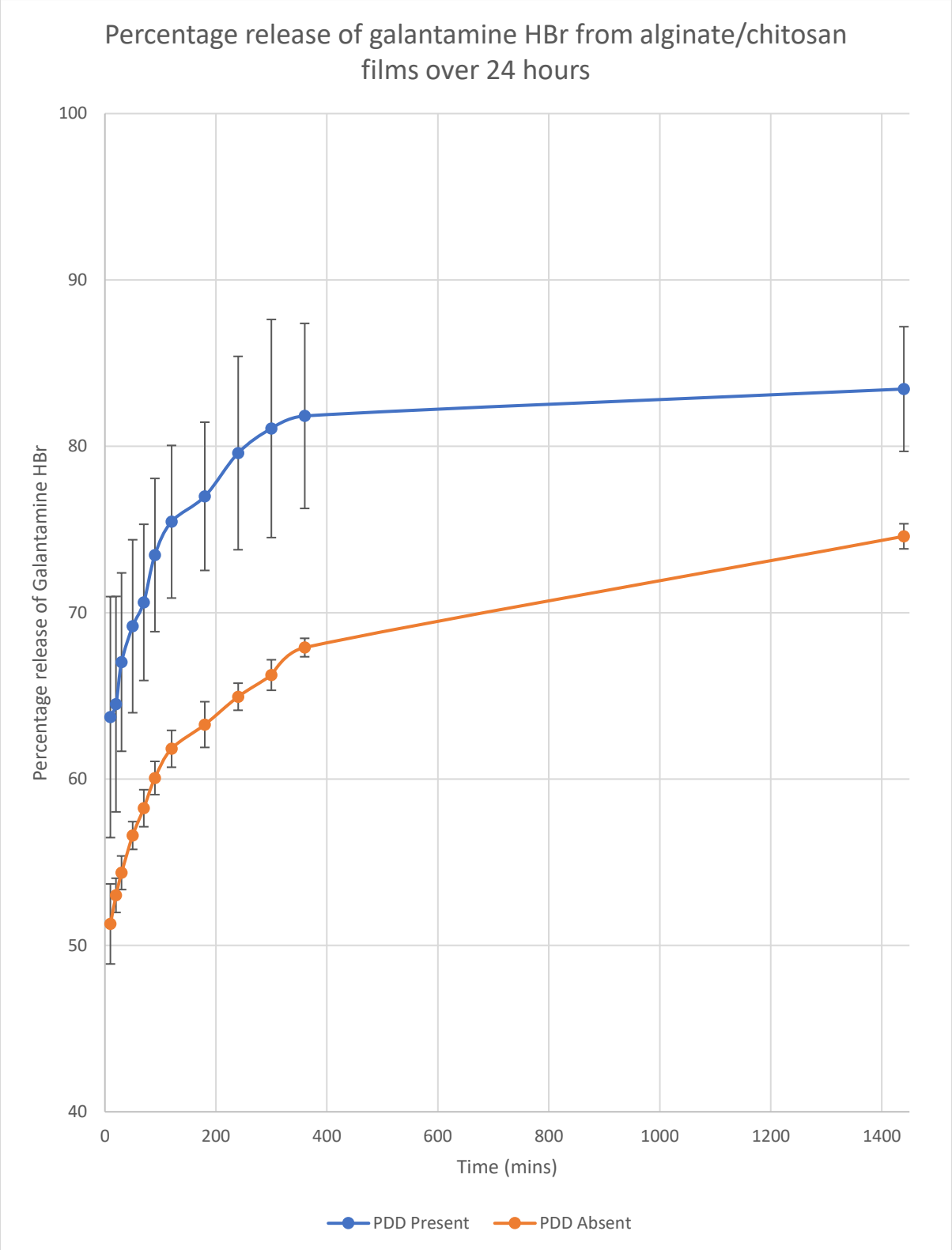

Figure 4- 18: The percentage release of galantamine HBr from 3% alginate and 3% chitosan bio-based polymer films, where galantamine is present in all film layers. Comparing the presence and absence of PDD1 on the release, over a 24-hour period in pH 4.0 phosphate buffer solution.

The film's drug release time is relatively consistent for up to 7 hours before the rate of release begins to slow. It can be assumed that the overall acidic nature of the film, as a result of chitosan being dissolved in pH 4, contributes to the increased release of galantamine HBr in film containing PDD1 when introduced to the pH 7.8 phosphate buffer solution, as seen in [Figure 4- 18]. This is due to the PDD1 polymer responding to the acidic pH caused by the pH4 acetic acid used to form the chitosan layer.

Through analysing the data in [Table 4- 8] and the results in [Figure 4- 19] comparisons are made between 3% sodium alginate/3% chitosan films where PDD1 is either present or absent to determine the best composition of film for the release of galantamine HBr, and to assess how the use of galantamine HBr infused PDD1 affects the release form the more promising film compositions. The reasons for the selection of these film compositions are due to the findings in chapters 2 and 3 of this thesis.

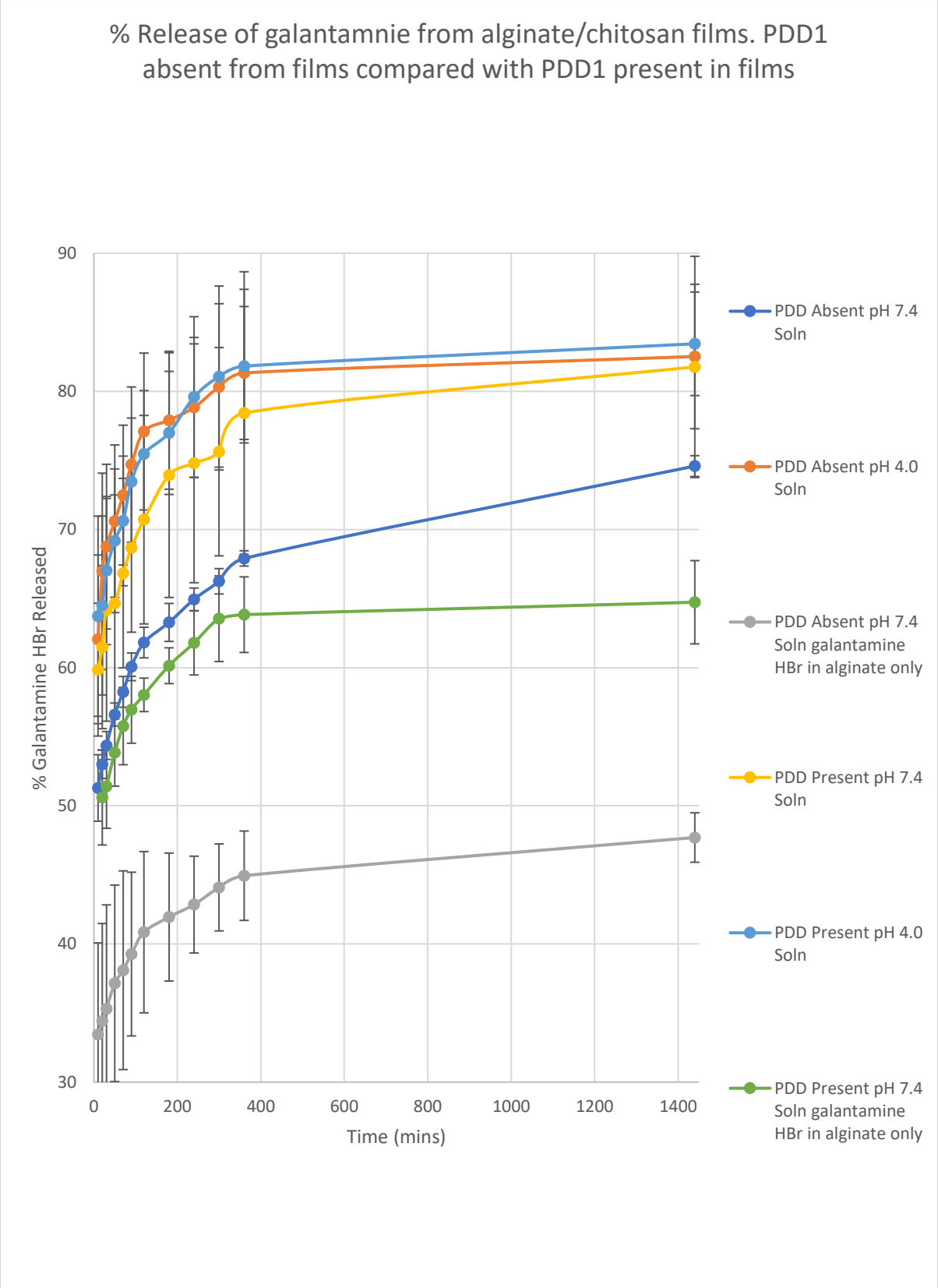

Figure 4- 19: ***The percentage release of galantamine HBr from alginate and chitosan films, comparing the presence and absence of PDD1, and altering the pH, over a 24-hour period in phosphate buffer solutions.***

Table 4- 8: A list of alternating alginate and chitosan layered bio-based polymer films, their composition, number of layers, pH of the alternating layers, the presence of galantamine HBr and PDD1, and the percentage (%) release of galantamine HBr from each film.

Sample Name	Alginate Percentage	Chitosan Percentage	Number of Layers in Film	pH of Alginate Layer(s)	Galantamine HBr in Alginate Layer(s)?	Galantamine HBr in Chitosan Layer(s)?	Galantamine HBr in Encapsulated in PDD?	Percentage Release After 10 Mins	Percentage Release After 1440 Mins
GLT1	3	3	2	7	✓	✓	x	51.3%	74.6%
GLT2	5	3	2	7	✓	✓	x	51.0%	68.3%
GLT3	3	5	2	7	✓	✓	x	55.8%	74.7%
GLT4	3	3	4	7	✓	✓	x	38.7%	52.0%
GLT5	3	3	2	4	✓	✓	x	62.1%	82.5%
GLT6	3	3	2	7	✓	x	x	33.5%	47.7%
GLT7	3	3	2	7	x	✓	x	46.3%	61.2%
GLT8	3	3	2	4	✓	✓	✓	63.7%	83.4%
GLT9	3	3	2	7	✓	✓	✓	50.6%	66.3%
GLT10	3	3	2	7	✓	x	✓	59.9%	81.8%

Every film not containing the PDD1 polymer was made using sodium alginate and chitosan solutions with 140 mg of galantamine dissolved in them. Every film containing the PDD1 polymer was made in the same way as that without it, with 250 mg of PDD1 added to each of the solutions. The data suggests that films containing PDD1 release a larger amount of galantamine HBr, and this can be attributed to acidic pH of the bio-based polymer films. When decreasing the pH of the solution to pH 4.0, the release of galantamine HBr from the bio-polymer films appears to increase, but by a negligible amount, and can be attributed to increased film degradation due to the acidic conditions. As seen in the previous chapter, films where drugs have been loaded into only the alginate layer have a lower release, which can be attributed to a

mixture galantamine and sodium alginate having complimentary charges, and there being no galantamine present on the surface of the chitosan face of the film.

It can be concluded that the pH responsiveness of the PDD1 polymers responds to the acidic conditions present when the film enters the phosphate buffer solution and releases the encapsulated galantamine HBr. The films without PDD1 present do not respond to the pH change, and as a result the PDD1 absent films release, on average, almost 9% less galantamine HBr than their PDD1 present counterparts.

The release of PDD1 encapsulated galantamine HBr from bio-based polymer films was finally compared to a film of the same 3% sodium alginate/3% chitosan composition in [Figure 4- 20]. It was concluded that the release of free base galantamine was comparable to that of galantamine HBr, likely as a result of free base galantamine becoming protonated during the LbL process, and therefore PDD1 encapsulation of galantamine resulted in the largest amount of release.

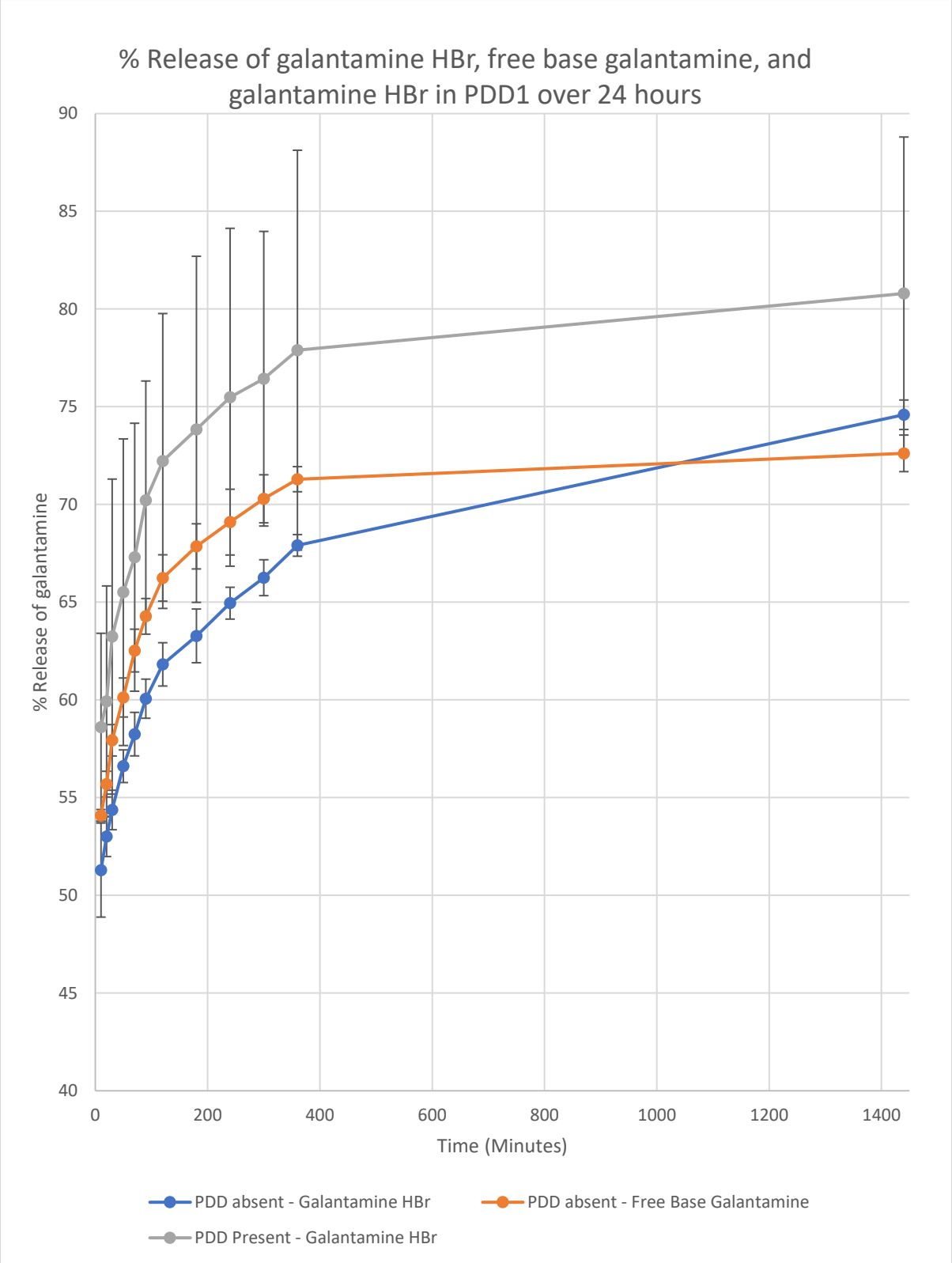

Figure 4- 20: Percentage release of galantamine comparison between films releasing galantamine HBr, PDD1 encapsulated galantamine HBr, and free base galantamine from 3% sodium alginate/3% chitosan bio-based polymer films, where galantamine is present in all film layers.

4.4.7 Memogain Synthesis and use in Bio-Based Polymer Films for Transdermal Drug Release

Using the method outlined in section 4.3.12, memogain was successfully loaded into bio-based polymer films[75]. As determined in Chapter Three, A larger amount of galantamine HBr release was observed from films with a higher guluronic acid (G) to mannuronic acid (M) ratio as a result of increase pore size in films comprised with alginate where the ratio of G is larger. Knowing this, the use of high G alginate in films loaded with memogain was desired in order to compare it to that of its galantamine loaded counterparts. Films were prepared consisting of 3% low G sodium alginate and 3% chitosan, and 3% high G sodium alginate and 3% chitosan. Release studies in pH 7.8 phosphate buffer solutions were conducted and compared with the results of galantamine HBr released from films of the same compositions obtained in Chapter Three.

The data collected in [Table 4- 9 and Figure 4- 21] shows the release of memogain from sodium alginate and chitosan films.

Table 4- 9: The percentage release of memogain from 3% low G sodium alginate and 3% chitosan films, in pH 7.8 phosphate buffer solution, over 24 hours.

Time (mins)	Release 1 (%)	Release 2 (%)	Release Average (%)	Percentage Error (%)
10	35.5	32.8	34.1	1.9
20	36.9	33.8	35.3	2.2
30	38.6	35.1	36.8	2.5
50	40.3	37.4	38.9	2.0
70	41.9	38.4	40.1	2.5
90	43.5	39.6	41.6	2.8
120	44.6	40.7	42.6	2.8
180	45.2	41.5	43.3	2.7
240	46.0	42.1	44.0	2.8
300	46.3	43.2	44.7	2.2
360	47.6	43.9	45.8	2.6
1440	48.4	45.6	47.0	2.0

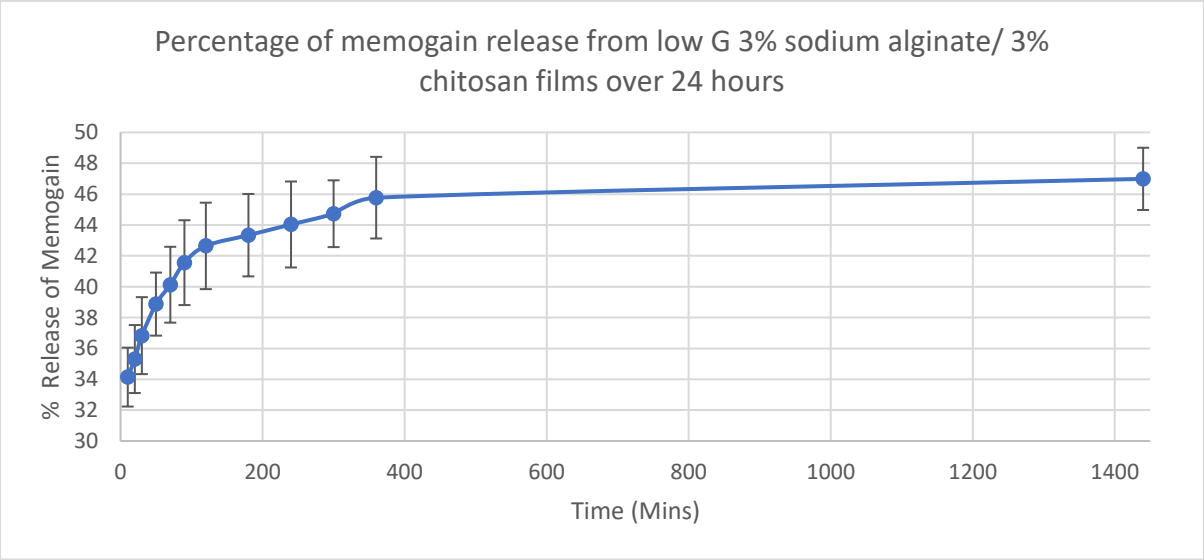

Figure 4- 21: The 24-hour average release profile of memogain from low G 3% sodium alginate/ 3% chitosan films in pH 7.8 phosphate buffer solution.

The data collected in [Table 4- 10 and Figure 4- 23] shows the release of galantamine HBr from sodium alginate and chitosan films, where the same amount of either memogain or galantamine was present in each film. This allows for comparison between the release of galantamine HBr and memogain from the bio-based polymer films.

Table 4- 10: The percentage release of memogain from 3% high G sodium alginate and 3% chitosan films, in pH 7.8 phosphate buffer solution, over 24 hours.

Time (mins)	Release 1 (%)	Release 2 (%)	Release Average (%)	Percentage Error (%)
10.00	66.7	69.8	68.3	2.2
20.00	74.4	72.3	73.4	1.5
30.00	76.0	74.5	75.2	1.1
50.00	79.4	75.0	77.2	3.1
70.00	81.8	77.8	79.8	2.9
90.00	84.3	81.1	82.7	2.3
120.00	86.5	83.2	84.9	2.3
180.00	88.5	85.5	87.0	2.1
240.00	90.4	87.7	89.1	1.9
300.00	91.6	89.9	90.7	1.2
360.00	91.8	91.8	91.8	0.0
1440.00	93.3	93.8	93.6	0.4

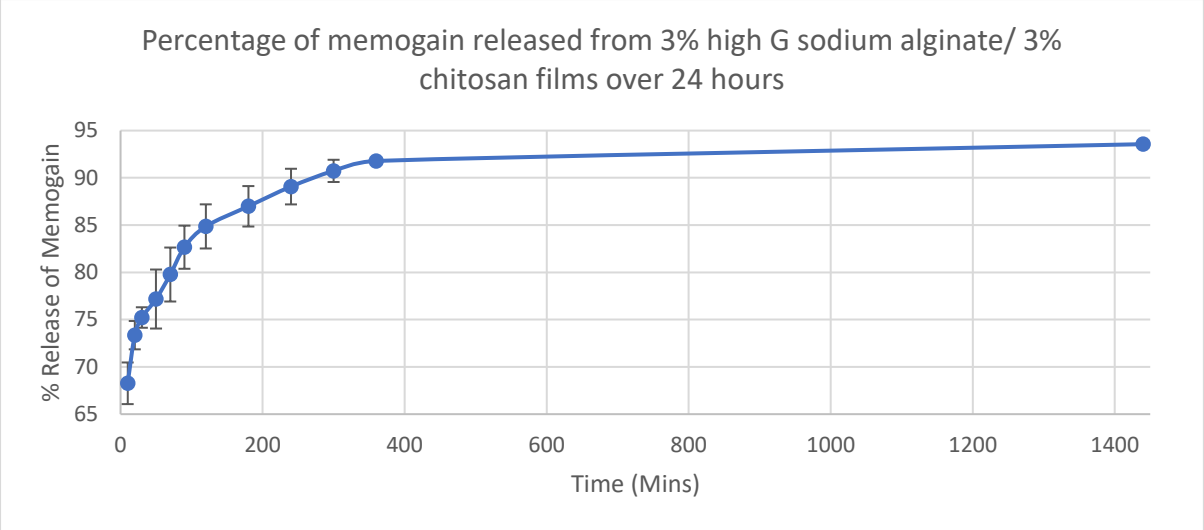

Figure 4- 23: The 24-hour average release profile of memogain from high G 3% sodium alginate/ 3% chitosan films in pH 7.8 phosphate buffer solution.

It can be concluded that the hydrophobic nature of memogain results in a lower release than galantamine HBr when released from films consisting of low G alginate, but a higher release when released from high G films. The reason for a much lower release in low G films is largely due to the pore size (measured in Chapter Three) in the low G alginate films[76]. However, when the vertically oriented chair structured glucuronic acid concentration is increased, the result is a larger pore size - large enough for memogain to permeate[77]. Over 93% release of memogain was observed in the high G sodium alginate and chitosan films, which is the highest amount of release achieved in this research, and close to a full release of a drug from a bio-based polymer film [Figure 4- 24].

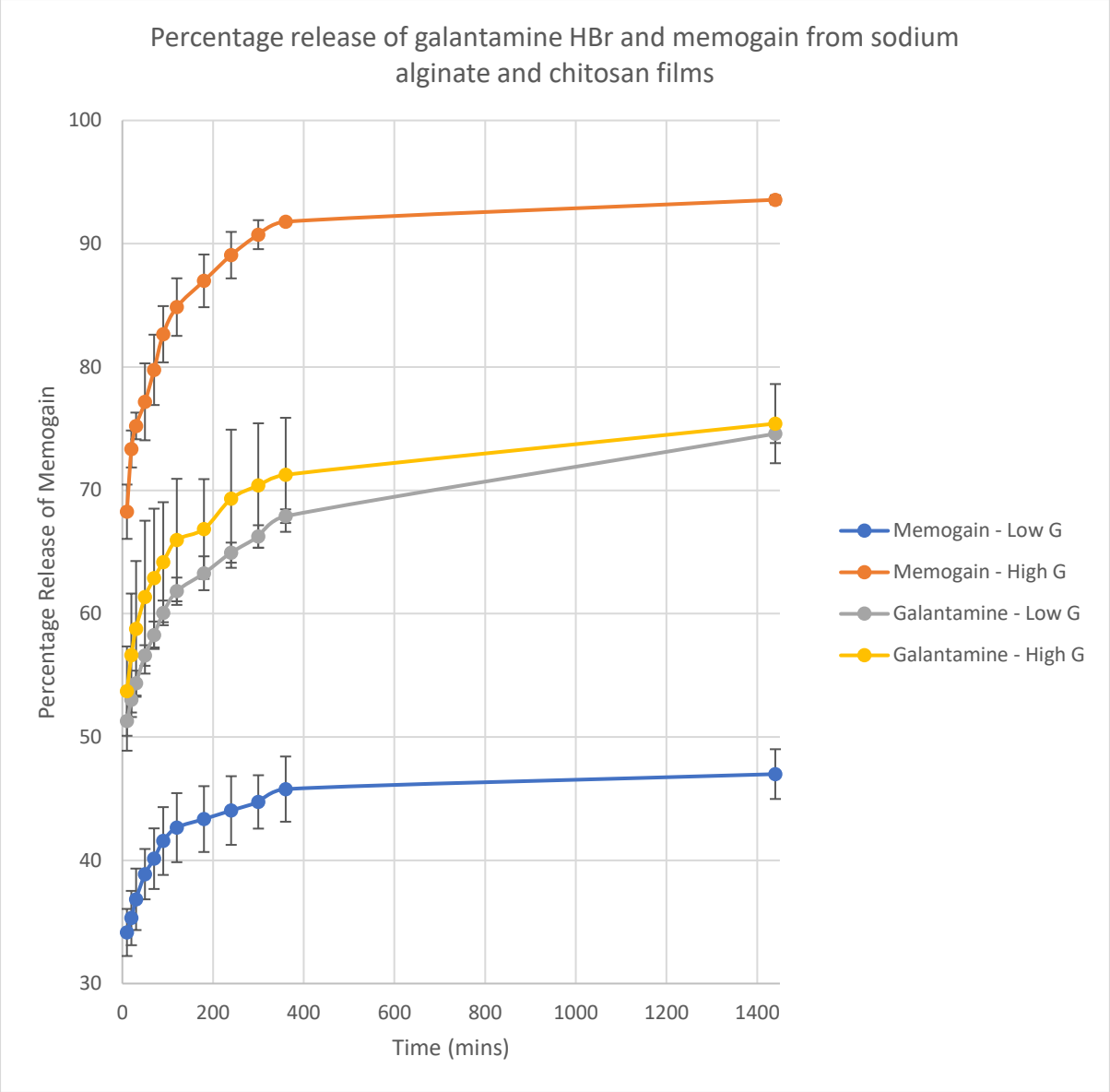

Figure 4- 24: The release of galantamine HBr and memogain released from films consisting of either low G or high G sodium alginate and chitosan, over 24 hours. Released in in pH 7.8 phosphate buffer solution.

This level of release can be attributed to the addition of the benzoic ester causing an increased amount of lipophilicity allowing it to permeate the film and release into a solution more easily due to memogain being less polar. Memogain's higher lipophilicity, whilst also reducing the level of side effects caused by galantamine, and its apparent larger release from bio-based polymer films, makes it an ideal candidate for drug release from bio-based polymer films *via* transdermal drug delivery for people suffering with Alzheimer's disease.

4.5 Conclusions

Three dual responsive hyperbranched polymers were successfully prepared using Reversible Addition–Fragmentation chain Transfer (RAFT) copolymerization of a monovinyl monomer DMAEMA with a divinyl monomer in DSDA following chain extension with NIPAM[78]. DSDA was copolymerized with DMAEMA *via* RAFT polymerisation process to generate a hyperbranched PDMAEMA-DSDA (PDD) copolymer. Three fee ratios of PDMAEMA:DSDA were used (99:1, 95:5, 90:10) in the synthesis of hyperbranched PDMAEMA-DSDA. Research was conducted to determine how the change in ratio affects the molecular weight, pH sensitivity and the lower critical solution temperature (LCST).

These new types of hyperbranched polymers have demonstrated pH-responsive properties due to the tertiary amine group in DMAEMA. The polymer's ability to act as a nanocarrier was assessed by loading the polymer with carmoisine dye and using qualitative UV spectrometry to analyse the amount of absorption for each polymer.

After excessive pH solubility testing, thermo-responsive testing, qualitative UV spectrometry analysis, and GPC analysis, it can be determined that the polymers respond to changing pH, temperature change. Polymer ‘PDDN1’ was deemed to be the best candidate due to its impressive responses and ability to load the highest amount of carmoisine. However, due to its lower solubility, it was not used in the trials for assessing the effect of using a stimuli responsive polymer in a galantamine loaded bio-based polymer film.

Galantamine was encapsulated inside PDD1 polymers. The polymer was assessed for its effect on galantamine release from films comprised of alginate and chitosan by monitoring the amount of galantamine released from films with and without PDD1 over a 24-hour period. The films are acidic in nature as a result of chitosan requiring a pH level of 4 to dissolve it. As the bio-polymer films are created using acetic acid, it is likely that the acidic properties of the films meant that the introduction of PDD1 cause an increased amount of galantamine to be released from films, as

opposed to films that did not contain PDD1, as PDD1 will respond to the acidic conditions. This is a direct result of the pH responsive DMAEMA groups in the hyperbranched polymer prompting an increased release of galantamine HBr due to the acidic conditions causing the PDD1 polymers to release the encapsulated galantamine. The films without PDD1 released less galantamine due to the pH having no effect on the release, meaning there was no prompt for the galantamine to be released as optimally as its PDD1 containing counterparts.

Research was conducted to determine ideal modifications which can improve the efficacy and release of galantamine. Memogain was selected for its increased lipophilicity, and its ability to better permeate the blood-brain barrier. Memogain was successfully synthesized by the addition of a benzyl ester to the galantamine compound. Release studies were conducted to compare the effect of release from bio-based polymer films between galantamine and memogain. It was found that in bio-based polymer films containing low G alginate and chitosan, that the release of memogain was lower than that of galantamine, due to the hydrophobic nature of memogain. However, when using high G alginate instead of low G alginate, the release of memogain is substantially increased, and even resulted in percentage release levels of above 93% of the loaded compound. High G alginate resulted in a higher release due to glucuronic acid's vertical orientation, as opposed to mannuronic acids horizontal orientation, resulting in a larger pore size which allows for the easier release of memogain. The increased level of release can be attributed to the addition of the benzoic ester causing an increased amount of lipophilicity which allows it to permeate the film and release into a solution more easily than galantamine. In conclusion, memogain is an exciting candidate for use in transdermal drug release due to its increased lipophilicity and percentage release from bio-based polymer films, along with its ability to permeate the blood brain barrier more effectively whilst reducing side effects which can be caused by galantamine.

In conclusion, galantamine was encapsulated inside PDD1 polymers which were loaded and released from bio-polymer films, with larger amounts of galantamine being released when PDD1 polymers were present than when they were absent, as well as faster rate of release. This showed promise for the use of infusing stimuli responsive polymers with galantamine to better improved drug release. However,

when exploring the effect of using galantamine prodrugs on overall drug release and the rate of release, it was found that when releasing memogain from a bio-polymer film the highest overall drug release and rate of release was observed. Memogain exhibits enhanced properties which allow for more efficient drug release or efficacy. Memogain can be released from sodium alginate and chitosan bio-based polymer films, with the release from films consisting of high G alginate observing large and desirable levels of drug release. This leads to the understanding that exploring the use of galantamine prodrugs to improve drug release, and the rate of release, appears to be preferred to the use of stimuli responsive polymers.

Further research is required to assess the release of galantamine, when infused in PDD1, from films comprised of high G alginate. This is in order to form a direct comparison between the release of galantamine from these films with the release of memogain from high G sodium alginate films. Whilst using memogain appeared to show the most promise in terms of improving the overall release, we cannot rule out the use of PDD1 until this data is obtained. It would also be sensible to attempt to infuse PDD1 with memogain and assess the release of the drug from the sodium alginate and chitosan comprised bio-polymer films.

It would be of interest to explore the use of different stimuli responsive polymers for candidates in aiding drug release to see how they compare to that of the PDD and PDDN polymers. Further work should include the synthesis of various galantamine prodrugs for the assessment of their ability to be loaded and released from bio-polymer films, as well as their overall drug release and rate of release. Whilst a higher overall release of galantamine (or a galantamine prodrug) is preferred, one factor of this research which has not yet been properly explored is what exactly is the optimal rate of release of galantamine, and potentially galantamine prodrugs. If this work is continued, it will be important to determine the optimal rate of release, and which conditions will allow for that rate of release to be obtained.

References

1. F. Liu, M. W. Urban, *Progress in Polymer Science*, 2010, **35**, 3-23
2. P. Bawa, V. Pillay, Y. E. Choonara, L. C. du Toit, *Biomedical Materials,* 2009, **4**, 22001
3. Q. Wang, L. Liu, Y. Wang, P. Liu, H. Jiang, Z. Xu, Z. Ma, S. Oren, E. K. C. Chow, M. Lu, L. Dong, *Scientific Reports*, 2015, **5**, 1-8
4. B. Taghizadeh, S. Taranejoo, S. Ali Monemian, Z. S. Moghaddam, l. Daliri, H. Derakhshankhah, Z. Derakhshani, *Drug Delivery*, 2015, **22**, 145-155.
5. S. Bhatnagar, V. V. K. Venuganti, *Journal of Nanoscience and Nanotechnology*, **15**, 1925-1945
6. S. I. Bhat, Y. Ahmadi, S. Ahmad, *Industrial & Engineering Chemistry Research*, 2018, **57**, 10754-10785
7. C. Lin, K. Anseth, *Pharmaceutical Research*, 2009, **26**, 631-643
8. Y. H. Kim, O. W. Webster, *Journal of the American Chemical Society*, 1990, **112**, 4592-4593
9. C. Porsch, Y. Zhang, C. Ducani, F. Vilaplana, L. Nordstierna, A. M. Nyström, E. Malmström, *Biomacromolecules*, 2014, **15**, 2235-2245
10. A. B. Cook, R. Barbey, J. A. Burns, S. Perrier, *Macromolecules*, 2016, **49**, 1296-1304
11. C. Gao, D. Yan, *Progress in Polymer Science*, 2004, **29**, 183-275
12. T. Zhao, Y. Zheng, J. Poly, W. Wang, *Nature Communications*, 2013, **4**, 1-8
13. B. I. Voit, *Comptes Rendus Chimie*, 2003, **6**, 821-832
14. M. Smet, Y. Fu, X. Zhang, E. H. Schacht, W. Dehaen, *Macromolecular Rapid Communications*, 2005, **26**, 1458-1463
15. D. Wang, T. Zhao, X. Zhu, D. Yan, W. Wang, *Chemical Society Reviews*, 2015, **44**, 4023-4071
16. A. H. E. Müller, D. Yan, M. Wulkow, *Macromolecules*, 1997, **30**, 7015-7023
17. P. Bharathi, J. S. Moore, *Macromolecules*, 2000, **33**, 3212-3218
18. F. Du, Y. Wang, R. Zhang, Z. Li, *Soft Matter*, 2010, **6**, 835-848
19. Y. Huang, X. Ding, Y. Qi, B. Yu, F. Xu, *Biomaterials*, 2016, **106**, 134-143.
20. Z. Li, Y. H. Kim, H. S. Min, C. K. Han, K. M. Huh, *Macromolecular Research*, 2010, **18**, 618-621.

21. M. Najafi, E. Hebels, W. E. Hennink, T. Vermoden, *Temperature-responsive Polymers, Properties, and Applications*, John Wiley & Sons Ltd, New Jersey, First Edition, Chapter 1, 2018.
22. H. H. Tønnesen, J. Karlsen, *Drug Development and Industrial Pharmacy*, 2002, **28**, 621-630.
23. L. García-Fernández, A. Mora-Boza, F. Reyes-Ortega, *Smart Polymers and their Applications*, 2019, **1**, 45-86
24. S. Dai, P. Ravi, K. C. Tam, *Soft Matter*, 2008, **4**, 435-449
25. A. K. Pearce, A. Travanut, B. Couturaud, V. Taresco, S. M. Howdle, M. R. Alexander, C. Alexander, *ACS Macro Letters*, 2017, **6,** 781-785
26. J. Chiefari, Y. K. Chong, F. Ercole, J. Krstina, J. Jeffry, T. P. T. Le, R. T. A. Mayadunne, G. F. Meijs, E. Rizzardo, S. H. Thang, *Macromolecules*, 1998, **31**, 5559-5562
27. G. Moad, E. Rizzardo, S. H. Thang, *Australian Journal of Chemistry*, 2005, **58**, 379-410
28. C. L. McCormick, A. B. Lowe, *Accounts of Chemical Research*, 2004, **37**, 312-325
29. A. Postma, T. P. Davis, R. A. Evans, G. Li, G. Moad, M. S. O'She, *Macromolecules*, 2006, **39**, 5293-5306
30. *RAFT: Choosing the Right Agent to Achieve Controlled Polymerization*, https://www.sigmaaldrich.com/GB/en/technical-documents/protocol/materials-science-and-engineering/polymer-synthesis/concepts-and-tools-for-raft-polymerization , (accessed January 2023)
31. D. J. Keddiem, G. Moad, E. Rizzardo, S. H. Thang, *Macromolecules*, 2012, **45**, 5321-5342
32. P. Derboven, P. H. M. Van Steenberge, M. Reyniers, C. Barner-Kowollik, D. R. D'hooge, G. B. Marin, *Macromolecular Theory and Simulations*, 2016, **25,** 104-115
33. H. Willcock, R. K. O'Reilly, *Polymer Chemistry*, 2010, **1**, 149-157
34. L. Yao, Y. C. Yuan, M. Z. Rong, M. Q. Zhang, *Polymer*, 2011, **52**, 3137-3145
35. J. Vandenbergh, T. Junkers, *Macromolecules*, 2014, **47**, 5051-5059
36. Y. K. Chong, G. Moad, E. Rizzardo, S. H. Thang, *Macromolecules*, 2007, **40**, 4446-4455

37. A. Postma, T. P. Davis, G. Moad, M. S. O'Shea, *Macromolecules*, 2005, **38**, 5371-5374
38. R. W. Lewis, R. A. Evans, N. Malic, K. Saito, N. R. Cameron, *Polymer Chemistry*, 2017, **8**, 3702-3711
39. A. J. Inglis, S. Sinnwell, T. P. Davis, C. Barner-Kowollik, M. H. Stenzel, *Macromolecules*, 2008, **41**, 4120-4126
40. J. Xu, J. He, D. Fan, W. Tang, Y. Yang, *Macromolecules*, 2006, **39**, 3753-3759
41. S. H. Kim, T. H. Nguyen, H. D. Maynard, *Comprehensive Biomaterials*, 2011, **4**, 377-388
42. J. A. Alfurhood, P. R. Bachler, B. S. Sumerlin, *Polymer Chemistry*, 2016, **7**, 3361-3369
43. A. Makwana, K. Sameja, H. Parekh, Y. Pandya, *Journal of Drug Delivery and Therapeutics*, 2012, **2**, 12-21
44. A. York, S. Kirkland, C. McCormick, *Advanced Drug Delivery Reviews*, 2008, **60**, 1018-1036
45. A. S. Hoffman, *Advanced Drug Delivery Reviews*, 2013, **65**, 10-16
46. A. Kavand, N. Anton, T. Vandamme, C. A. Serra, D. Chan-Seng, *Journal of Controlled Release*, 2020, **321**, 285-311
47. Z. Bilici, B. Keskinler, N. A. Perendeci, *Journal of Membrane Science and Research*, 2019, **6**, 211-217.
48. M. M. Koola, S. W. Looney, H. Hong, A. Pillai, W. Hou, *Psychiatry Research*, 2020, **291**, 1-7
49. Y. T. Lin, M. Chou, S. Wu, Y. Yang, *PeerJ Life and Enviornment*, 2019, **7**, 1-12
50. B. A. English, A. A. Webster, *Primer on the Autonomic Nervous System*, 2012, **3**, 631-633
51. A. C. Baakman, E. Hart, D. G. Kay. J. Stevens, E. S. Klaassen, A. Maelicke, G. J. Groeneveld, *Alzheimer's & Dementia: Translational Research & Clinical Interventions*, 2016, **2**, 13-22
52. H. O. Gulcan, I. E. Orhan, B. Sener, *Current Pharmaceutical Biotechnology*, 2015, **16**, 252-258
53. C. Bakker, J. van der Aart, E. P. Hart, E. S. Klassen, K. R. Bergmann, M. J. van Esdonk, D. G. Kay, G. J. Groeneveld, *Translational Reearch & Clinical Interventions*, 2020, **6**, 1-10

54. A. Maelicke, A. Hoeffle-Maas, J. Ludwig, A. Maus, M. Samochocki, U. Jordics, A. K. E. Kopke, *Journal of Molecular Neuroscience*, 2010, **40**, 135-137
55. N. Clayton, M. Ormeus, J. E. Tarride, P. Raina, *Alzheimer's and Dementian*, 2009, **5**, 326-227
56. S. Bhattacharya, D. Montag, *Neural Regeneration Research*, 2015, **1**, 43-45
57. S. Bhattacharya, A. Maelicke, D. Montag, *Journal of Alzheimer's Disease*, 2015, **46**, 123-136
58. S. Bhattacharya, C. Haertel, A. Maelicke, D. Montag, *PLOS ONE*, 2014, **9**, 1-12
59. R. Hardeland, *Clinical Medicine Insights*, 2011, **3**, 459-476
60. Z. Liu, A. Zhang, H.Sun, Y. Han, L. Kong, X. Wang, *RSC Advances.*, 2017, **7**, 6046-6058
61. D. S. Pisal, M. P. Kosloski, S. V. Balu-Iyer, *Journal of Pharmaceutical Sciences*, 2010, **99**, 2557-2575
62. Y. Zhao, Z. H. Housto, J. D. Simpson, L. Chen, N. L. Fletcher, A. V. Fuchs, I. Blakey, K. K. Thurecht, *Molecular Pharmaceutics*, 2017, **14**, 3539-3549
63. L. Zha, J. Hu, C. Wang, S.Fu, A. Elaissari, Y. Zhang, *Colloid and Polymer Science,* 2002, **280**, 1-6.
64. Y. Zhao, T. Bai, Q. Shao, S. Jiang, A. Q. Shen, *Polymer Chemistry,* 2015, **6**, 1066-1077.
65. L. Zha, J. Hu, C. Wang, S.Fu, M. Luos, *Colloid Polymer Chemistry,* 2002, **280**, 1116-1121.
66. L. Li, K. Raghupathi, C. Song, P. Prasad, S. Thayumanavan, *Chemical Communications*, 2014, **50**, 13417-13432.
67. F. A. Plamper, C. V. Synatschke, A. P. Majewski, A. Schmalz, H. Schmalz. A. H. E. Müller, *Polimery,* 2014, **59**, 66-73.
68. C. Wu, A. Ying, S. Ren, J. Xu, *Asian Journal of Chemistry*, 2013, **25**, 3806-3810.
69. M. A. Ward, T. K. Georgiou, *Polymers*, 2011, **3**, 1215-1242.
70. A. Hatefi, B. Amsden, *Journal of Controlled Release*, 2002, **80**, 9-28.
71. S. Ahn, E. C. Monge, S. C. Song, *Langmuir*, 2009, **25**, 2407-2418.
72. W. H. Koppenol, P. L. Bounds, C. V. Dang, *Nature Reviews Cancer*, 2011, **11**, 325-357.

73. G. Dehghan, M. Arvin, M. Hoeinpourfeizi, *International Conference on Medical, Biological and Pharmaceutical Sciences 2011,* 2011*,* **1**, 499-501.
74. O. Schiavon, G. Pasut, S. Moro, P. Orsolini, A. Guiotto, F. M. Veronese, *European Journal of Medical Chemistry,* 2004, **39**, 123-133.
75. F. Lv. L. Xu, Y. Zhang, Z. Meng, *ACS Applied Materials & Interfaces*, 2016, **7**, 19104-19111
76. I. Sanka, E. A. Suyono, P. Alam, *Carbohydrate Research*, 2017, **448**, 35-42
77. E. B. Cagmat, J. Szczepanski, W L. Pearson, D. H. Powell, J. R. Eyler, N. C. Polfer, *Physical Chemistry Chemical Physics*, 2010, **12**, 3474-3479
78. I. Bannister, N. C. Billingham, S. P. Armes, *Soft Matter*, 2009, **5**, 3495-3504

Chapter 5 – Concluding Remarks and Future Work

5.1 Introduction

The aim of the research conducted in this thesis was to develop a method for formulating a bio-based polymer transdermal drug delivery system capable of loading and releasing drugs which will be beneficial for use in the treatment of patients suffering with Alzheimer's Disease. The chapters in this PhD focused on the areas of bio-based polymer film formulation for transdermal drug release, stimuli responsive hyperbranched polymers, and drug modification tailored towards modifying drug release and improving drug efficacy. This concluding chapter focuses on the findings of the research which have been conducted over this project, and a general conclusion with regards to the outcomes determined by the results of this project. This chapter also includes a general discussion of how future research, in this project area, could be directed.

5.2 General Conclusion and Future Work

Bio-based polymers were used to create gels and films as candidates to be used as transdermal drug delivery systems. Soybean oil epoxidized acrylate (AESO) cross-linked with pentaerythritol tetrakis(3-mercaptopropionate) (QT) yielded gels that were soft, malleable and flexible, but did not meet the full criteria desired as the gels were not homogenous, too thick and easily broken. This led to putting the use of these materials as a candidate for a transdermal delivery system on hold, and instead bio-polymers with more desirable properties were sought.

Thiolated dextran cross-linked with PEG diacrylate (PEGDA) was explored as a possible candidate. Michael addition of the materials was successful, and a film was

created. However, the resulting properties of the film also didn't meet the desired criteria as the film was too hard and brittle to be considered for use as a transdermal delivery system. This led to the exploration of sodium alginate films.

Sodium alginate with either calcium chloride or chitosan, using the layer by layer technique (LbL), resulted in films that met the desired criteria for films to be used as a candidate for a transdermal delivery system. These films were soft, flexible, homogenous, thin, and were not easily broken. Chitosan was selected due to the resulting films being thinner and more durable. When soaked in water, these films were able to swell, with the sodium alginate/chitosan films swelling to 7000-9000% of their original weights.

As sodium alginate and chitosan comprised bio polymer films swelled by a substantial amount, more than the sodium alginate and calcium chloride comprised bio polymer films, these materials were explored for their ability to load and release galantamine. Galantamine HBr was successfully loaded into the bio polymer films, by using the Layer by Layer technique[1] highlighted in chapter 3 section 3.3.3. SEM and UV analysis confirmed that galantamine HBr could be loaded and released from the sodium alginate and chitosan bio-based polymer films. The release of galantamine from the films was made possible as a result of the bio polymers absorbing the phosphate buffer solution, allowing for the galantamine HBr to diffuse. The galantamine HBr present on the surface, and close to the surface, of the films is able to diffuse quickly which causes the large burst releases. The galantamine HBr embedded deeper within the films takes longer to diffuse as the barrier for them to cross is larger, and in the case of the galantamine loaded in the sodium alginate layer, is even slower to be released due to the charge interaction. Both galantamine and chitosan are positively charged, whereas sodium alginate is negatively charged. The films do not fully dissolve in solution which means the galantamine release must be attributed to the galantamine diffusing within the hydrated film structure [Figure 5- 1].

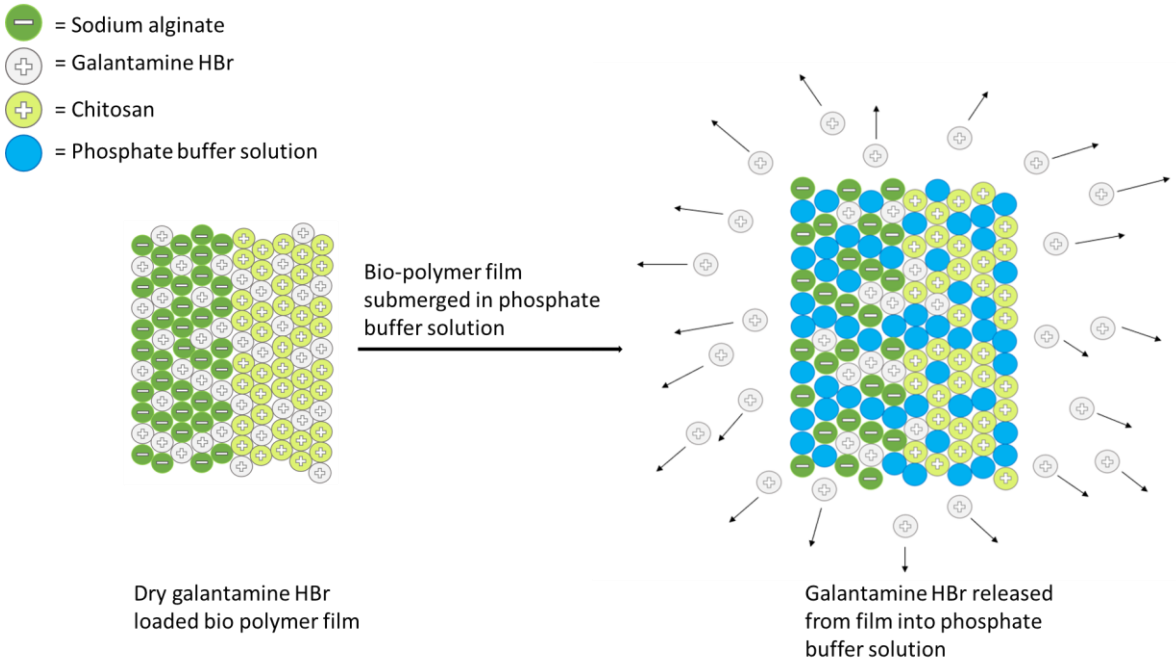

Figure 5- 1: The release of galantamine HBr from a sodium alginate and chitosan comprised polymer film when submerged in phosphate buffer solution.

Release studies were conducted to determine the optimal film composition, and the effect of altering the pH of the release media on the release. It was determined that increasing the concentration of chitosan results in a negligibly lower release of galantamine HBr. However, increasing the concentration of sodium alginate greatly reduces the amount of release, due to iconic interaction between the bio-based polymer and galantamine.

Films were tested using sodium alginate with an increased amount of guluronic acid (G) to assess the effect of using a higher ratio of guluronic acid (G) to mannuronic acid (M) and whether this affected the release of galantamine HBr. A larger amount of galantamine HBr release was observed from films with a higher G ratio. SEM analysis confirmed that the pore sizes of the alginate layer was larger when using a higher G ratio and could be attributed to the steric effects that guluronic acid has on the alginate polymer change, as it adopts a vertical orientation unlike mannuronic acid (M) which has a horizontal orientation.

Films using as low a concentration of sodium alginate and chitosan, whilst not compromising the films structural integrity, make for better candidates for drug

release. Using sodium alginate with a higher ratio of guluronic acid, allows for a greater amount of drug release due to its vertical orientation resulting in larger pores. A higher drug release from sodium alginate and chitosan comprised bio-based polymer films is observed in the presence of lower pHs due to increased film degradation. If films are formulated taking into account the statements made in this paragraph, whilst releasing at lower pH values the result will be upwards of a 70% release of galantamine over 16 hours, with the majority of that released within the first 6 hours.

There are concerns with regards to galantamine HBr being able to permeate the epidermis and dermis layers of the skin, due to the HBr salt having the capability to prevent absorption through the skin due to interactions with oils in the skin. The HBr salt was successfully removed from galantamine HBr to form free base galantamine. Free base galantamine was loaded into a sodium alginate and chitosan comprised bio-based polymer film, and successfully released in pH 7.8 phosphate buffer solution. However, there was negligible difference in the overall release of the free base galantamine when compared to that of galantamine HBr whilst releasing effectively for approximately 16 hours. This would suggest that the free base galantamine becomes protonated at some stage during the loading and release process, meaning that the same restrictions, caused by ionic interaction, are seen. Further studies on skin samples would be required to determine if removing the HBr salt does have an effect on galantamine permeating the skin.

Three dual responsive hyperbranched polymers were successfully prepared using Reversible Addition–Fragmentation chain Transfer (RAFT) copolymerization of a monovinyl monomer DMAEM with a divinyl monomer in DSDA following chain extension with NIPAM[2]. These new types of hyperbranched polymers have demonstrated pH-responsive properties due to the tertiary amine group in DMAEMA. The work conducted in chapter 4 section 4.4 showed that a film comprised of a 99:1 ratio of DMAEMA to DSDA showed the largest potential to be used as a drug delivery vehicle. Galantamine was encapsulated inside 99:1 PDMAEMA:DSDA (PDD1) formulated polymers [Figure 5- 2].

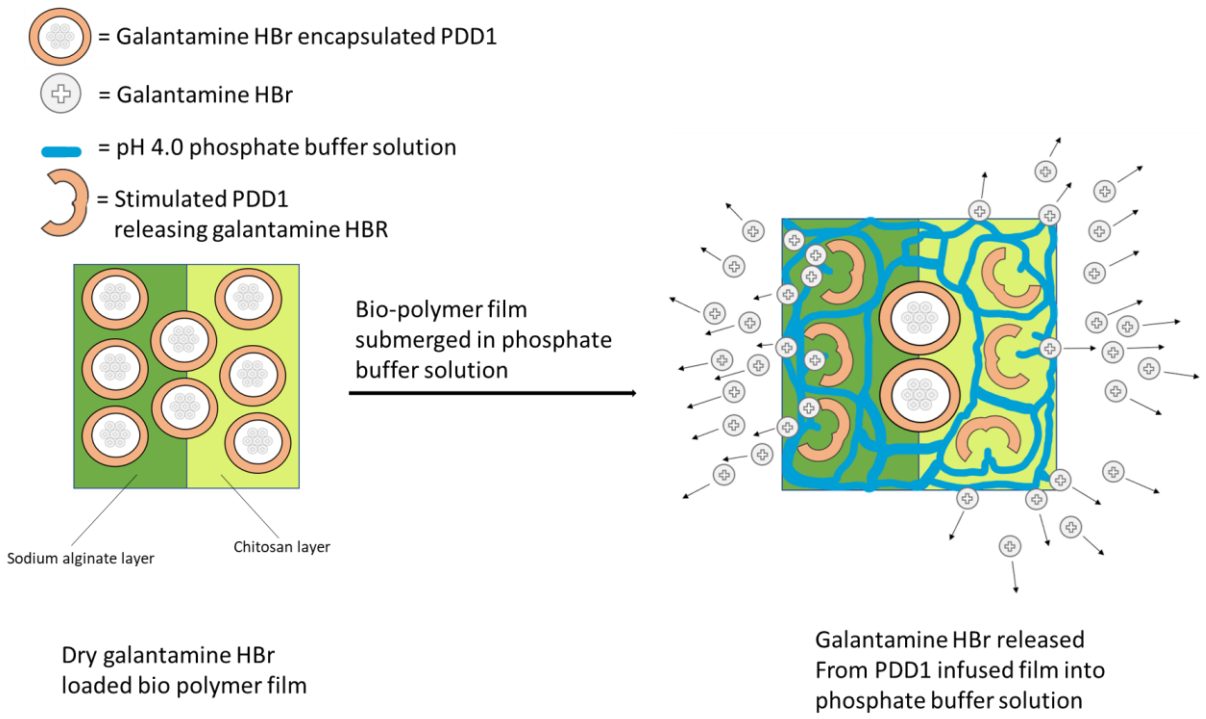

Figure 5- 2: PDD1 being stimulated to release galantamine HBr from a sodium alginate and chitosan comprised polymer film when submerged in a pH 4.0 phosphate buffer solution.

PDD1 encapsulates galantamine HBr within pockets of the bio-polymer film. As PDD1 is pH sensitive, when the pH 4 phosphate buffer solution is absorbed by the film, and comes into contact with PDD1, galantamine HBr is released by the polymer, and makes its way through the film and into the solution. It is likely that the PDD1 which is loaded deep within the film may not release the galantamine due to lack of stimuli. The galantamine released in the sodium alginate layer will face the same difficulties in terms of ionic interaction as discussed previously, resulting in a slower release from that portion of the film. It was observed in chapter 4 section 4.4.6 that larger amounts of galantamine being released when PDD1 polymers were present than when they were absent, as well as faster rate of release. Over 83% of the galantamine loaded within the sodium alginate and chitosan comprised film was released when PDD1 was present, and the film was submerged in a pH 4.0 phosphate buffer solution. 81% of the galantamine was released in the first 6 hours.

Stimuli responsive polymers showed promise for improving the control of the rate of release and improving the overall. Research was conducted to see how the release of galantamine prodrugs compares to that of galantamine both when PDD1 was present and absent. The galantamine prodrug ‘memogain’ was selected for its increased lipophilicity, and its ability to better permeate the blood-brain barrier. As seen in chapter 5 section 4.4.7, the release of memogain from a bio-polymer film comprised of high G sodium alginate and chitosan was the highest of all of the release studies, being the first release study to show over a 93% release of a drug from a bio-based polymer film, with 91% released in the first 6 hours.

Memogain has the ability enter the blood stream and permeate the blood brain barrier more effectively, whilst reducing side effects which can be caused by galantamine. Memogain’s higher lipophilicity, being more hydrophobic than galantamine, and its apparent larger release from bio-based polymer films, makes it an ideal candidate for drug release from bio-based polymer films *via* transdermal drug delivery for people suffering with Alzheimer’s disease.

Future work should include the exploration of alternative bio-based polymers for use in transdermal drug delivery, including a revisitation of soybean oil and dextran as candidates. Methods for delivery of drugs from bio-based polymer transdermal films into patients needs to be determined, with an emphasis on how the films will be administered to patients’ skin, and how release from films will be invoked.

Further release studies into determining how adding a calcium chloride layer, on the outside of a galantamine loaded sodium alginate and chitosan comprised film, should be explored. This would be in order to ensure that there would not be any galantamine on the surface of the film, and that the rate of release can be determined without assuming some galantamine may have been washed off of the film's surface on contact with the buffer solution. It is also important for future work to determine the desired rate of release of galantamine, and galantamine prodrugs, from bio-based polymer films.

Tests on drug release from bio-based films on skin are required to determine the effectiveness of the film's drug release through skin barriers, and to assess how the films interact with skin. It may also be prudent to seek an adhesive material to be

used as a sufficient cover for the films, and as a backing cover to the film, to ensure it is not exposed when applied to skin. It may be of interest to explore further drug modification, or use of different stimuli responsive polymers, which can improve the rate of overall release of drugs from transdermal films.

In the time that this thesis was being written, results were published of a study in which lecanemab, a monoclonal antibody with the ability to bind to amyloid-beta, was found to reduce the size of amyloid-beta build-ups in the brain[3]. This could be a historic breakthrough in the field and could lead to more efficient therapies. One downside is that lecanemab is administered as a two-weekly infusion[4]. The future of lecanemab may involve trying to source a more convenient form of delivering the therapy so that patients are not required to go to hospital as frequently and to allow for carers to assist in delivering the medicine. One such method could be to deliver lecanemab transdermally through a film, patch, or SC injection.

References

1. S. Afzal, M. Maswal, A. A. Dar, *Colloids and Surface*, 2018, **169**, 99-106
2. I. Bannister, N. C. Billingham, S. P. Armes, *Soft Matter*, 2009, **5**, 3495-3504
3. H. van Dyck, C. J. Swanson, P. Aisen. R. J. Bateman, C. Chen, M. Gee. M. Kanekiyo, D. Li, L. Reyderman, S. Cohen, L. Froelich, S. Katayama, M. Sabbagh, B. Vellas, D. Watson, S. Dhadda, M. Irizarry, L. D. Kramer, T. Iwatsubo, *The New England Journal of Medicine*, 2023, **388**, 9-21
4. E. Mahase, *The British Medical Journal*, 2023, **380**, 73-86

Chapter 6 – Appendices

6.1 Centrifuging

All the centrifuging conducted in this project was achieved using a 'Thermo Heraeus Megafuge 16r Centrifuge'.

Figure 6- 1: A Thermo Heraeus Megafuge 16r centrifuge.

6.2 Film Thickness

All film thickness measurements were obtained via the use of a ‘Z169048-1EA Micrometer’ (±0.01 mm) 0 mm -21 mm.

Figure 6- 2: The Z169048-1EA micrometer (±0.01 mm), length of 0 mm -25 mm, used to determine film thickness.

6.3 Nuclear Magnetic Resonance (NMR)

All NMR’s were obtained via use of a ‘Brucker 400 MHz Nuclear Magnetic Resonance spectrometer’.

Figure 6- 3: The Brucker Ultrashield Plus 400 MHz NMR machine.

6.4 Fourier-transform infrared spectroscopy (FTIR)

All IR-Spectra were obtained via use of a ‘Bruker Alpha Platinum ATR Machine’.

Figure 6- 4: A Bruker Alpha Platinum ATR machine used for FTIR.

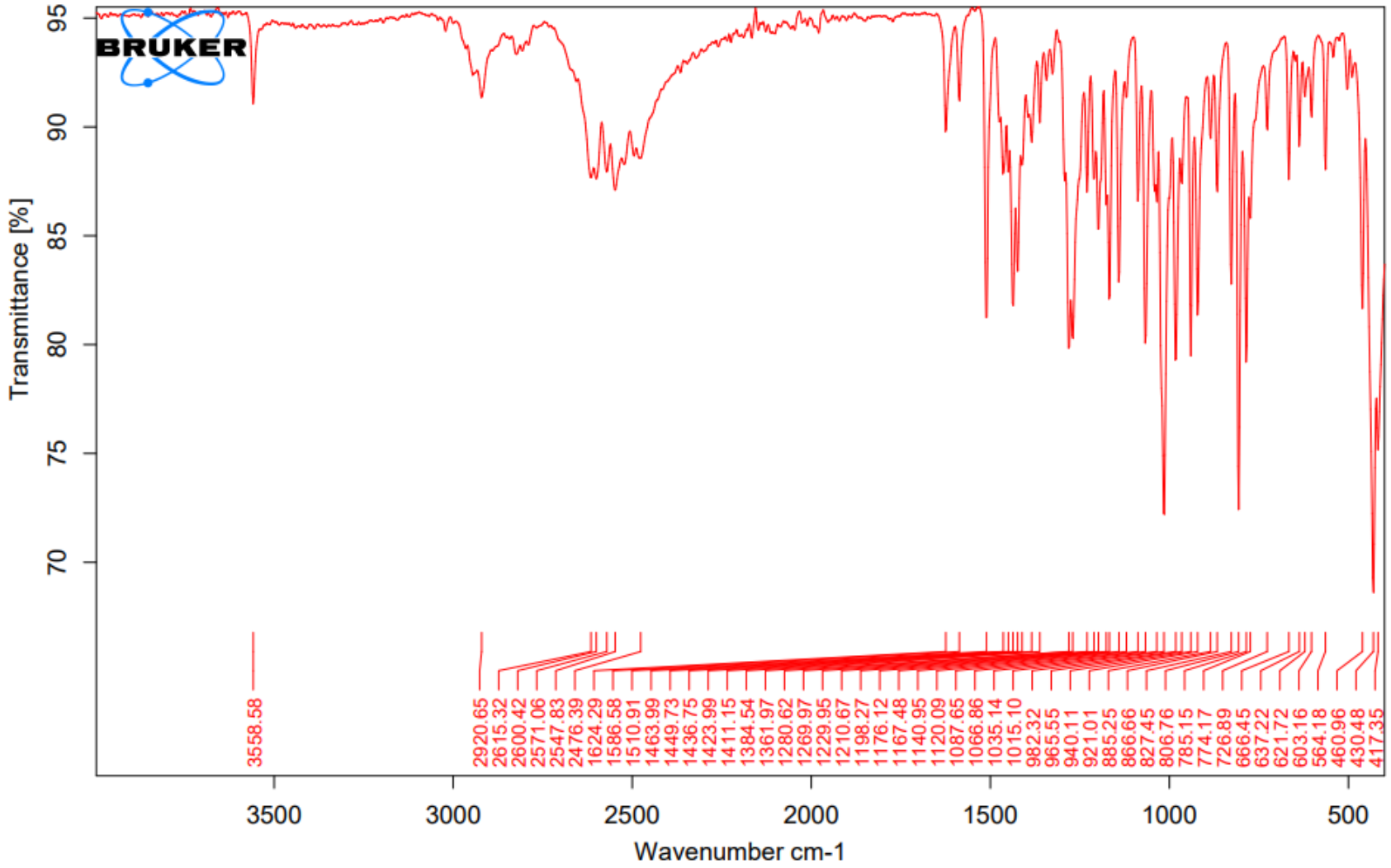

Figure 6- 5: IR spectra for galantamine hydrobromide.

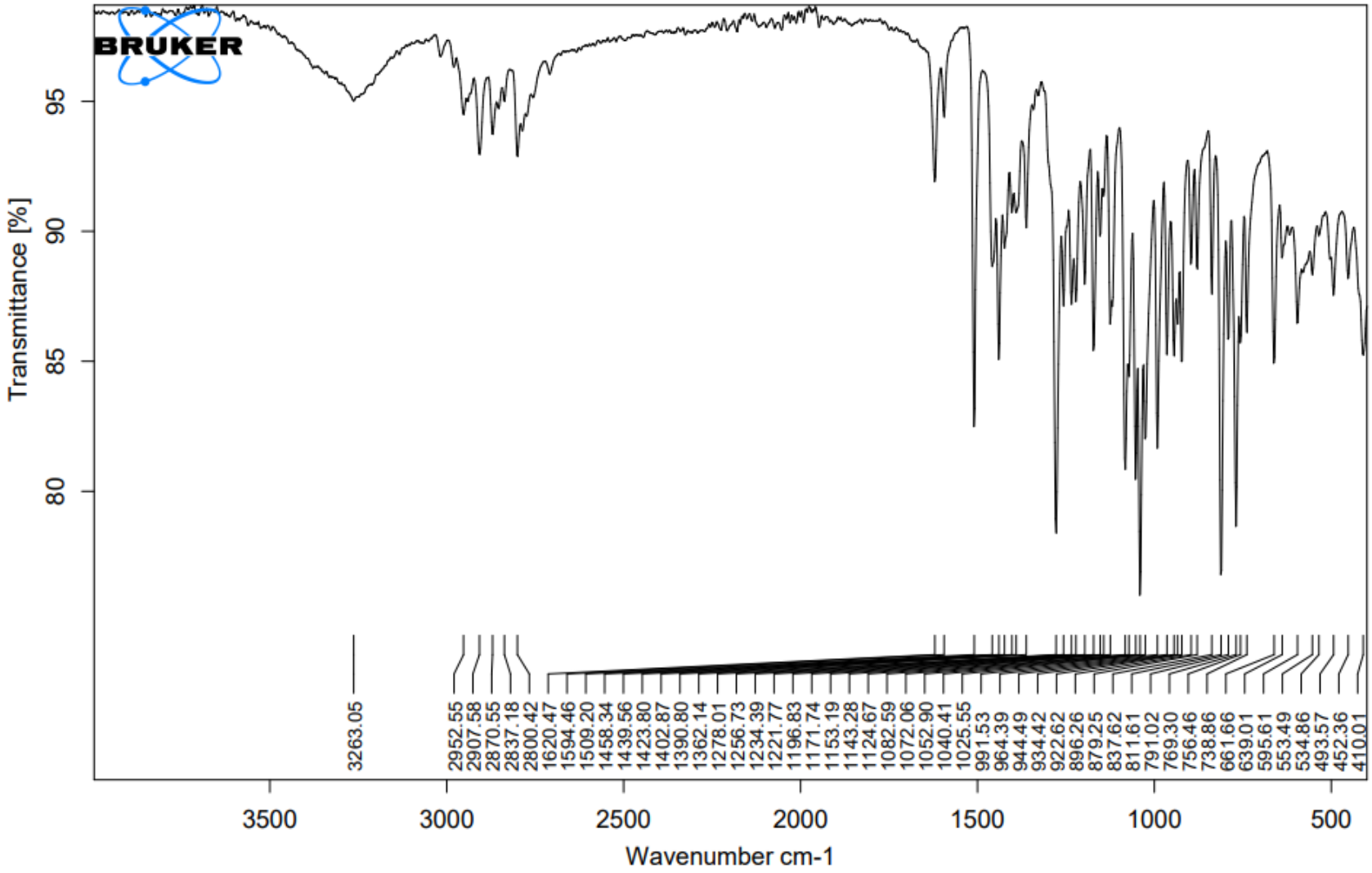

Figure 6- 6: IR spectra for free base galantamine.

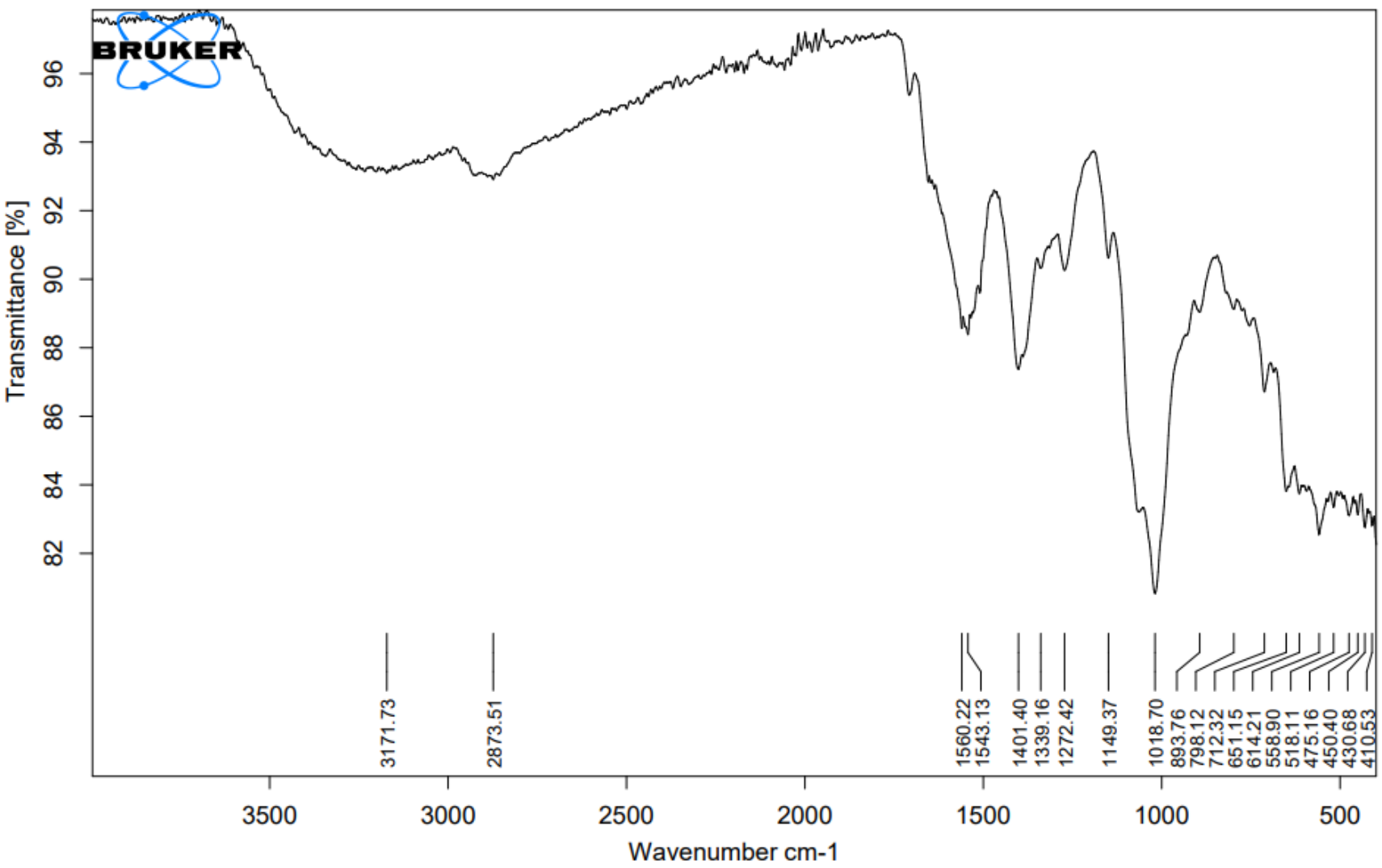

Figure 6- 7: IR spectra for memogain.

6.5 Thiolated Dextran 24 Hour Experiment NMR

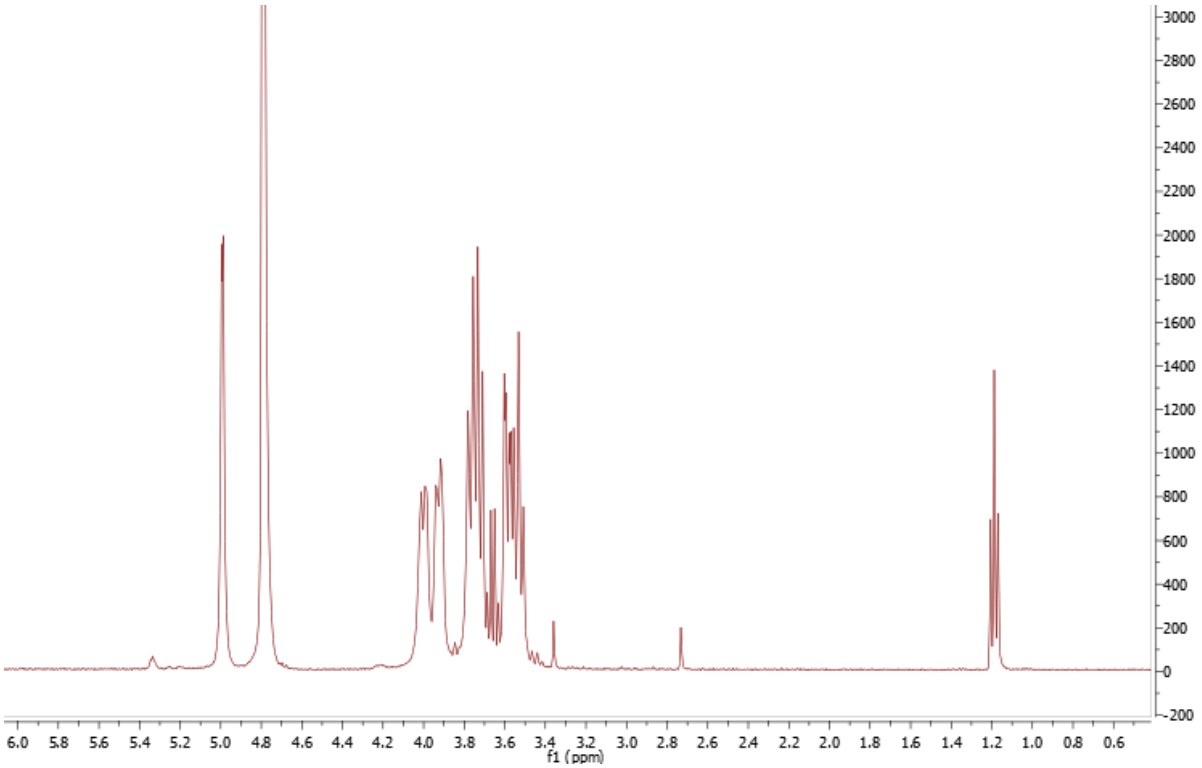

Figure 6- 8: The NMR for the 48-hour reaction of thiolated dextran.

6.6 NMR of Materials Extracted from Daffodil Bulb Liquid Extract

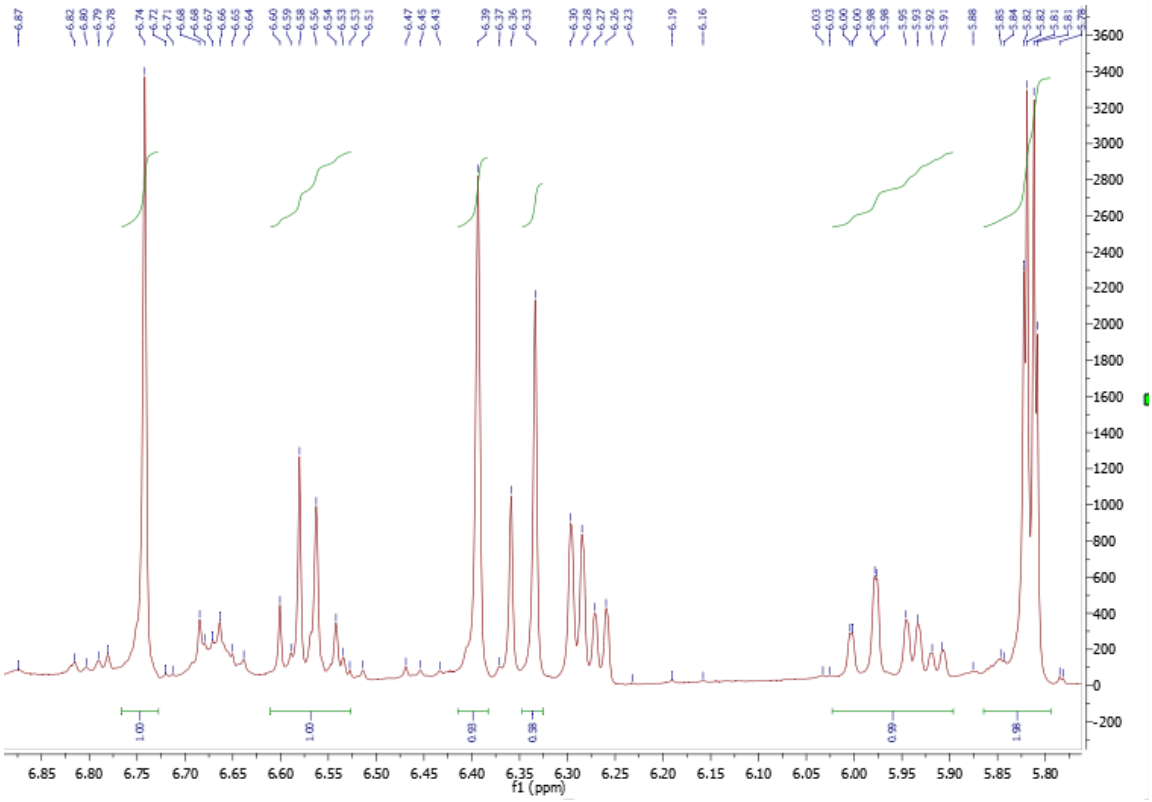

Figure 6- 9: Extraction from daffodil bulb liquid extract Method A NMR.

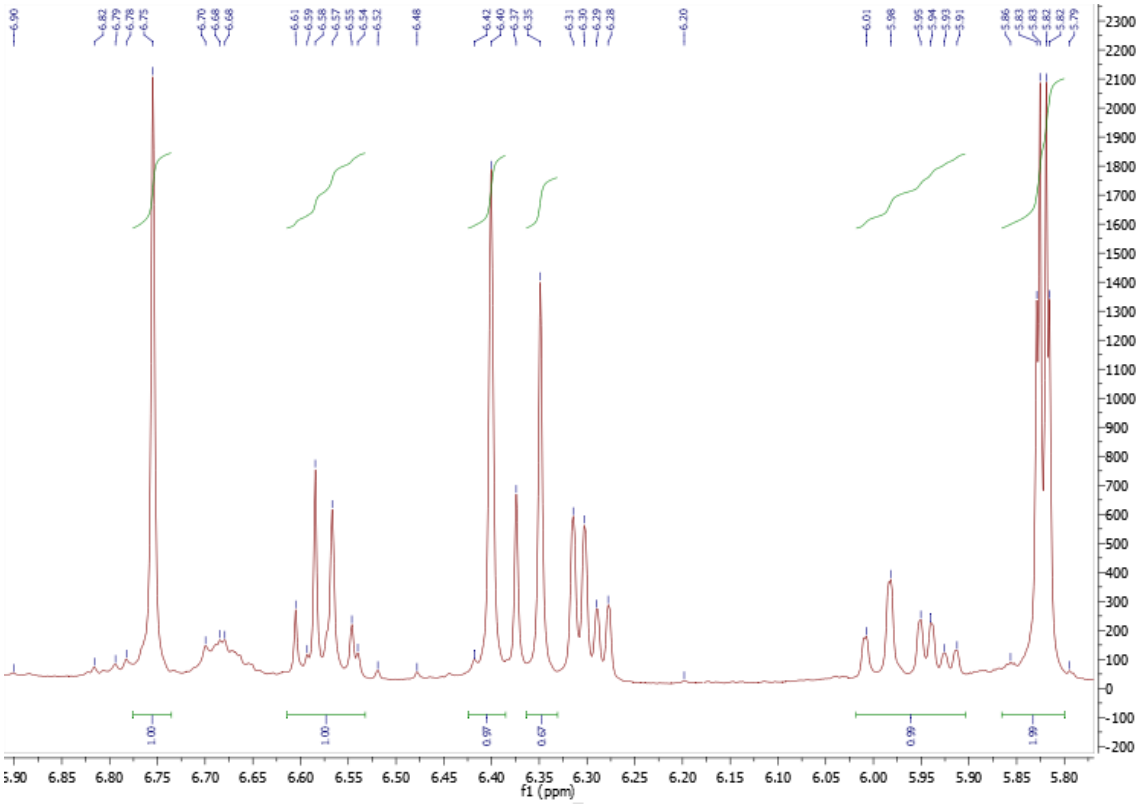

Figure 6- 10: Extraction from daffodil bulb liquid extract Method B NMR.

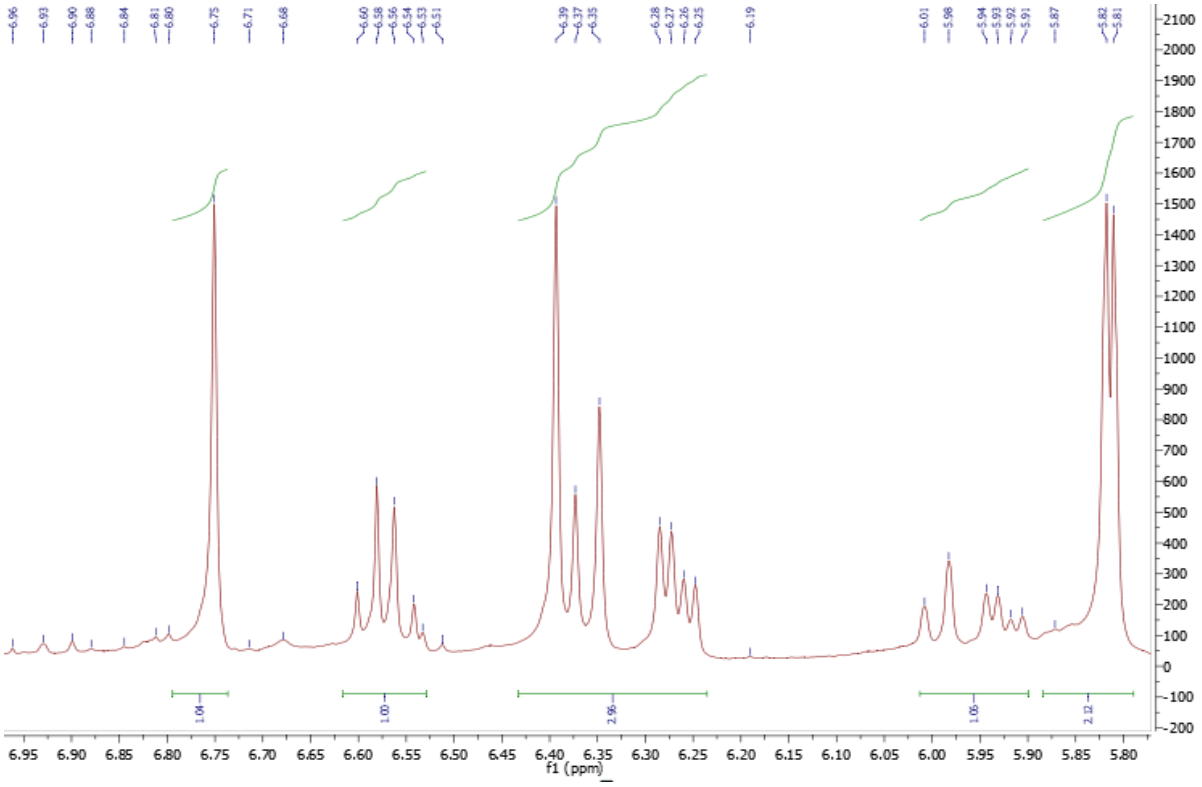

Figure 6- 11: Extraction from daffodil bulb liquid extract Method C NMR.

Table 6- 1: A list of alternating alginate and chitosan layered bio-based polymer films, their composition, number of layers, pH of the alternating layers, the presence of galantamine HBr and PDD, and the percentage (%) release of galantamine HBr from each film.

Sample Name	Alginate Percentage	Chitosan Percentage	Number of Layers in Film	pH of Alginate Layer(s)	pH of Chitosan Layer(s)	Galantamine HBr in Alginate Layer(s)?	Galantamine HBr in Chitosan Layer(s)?	Galantamine HBr in Encapsulated in PDD?
GLT1	3	3	2	7	4	✓	✓	x
GLT2	5	3	2	7	4	✓	✓	x
GLT3	3	5	2	7	4	✓	✓	x
GLT4	3	3	2	7	4	✓	x	x
GLT5	3	3	2	7	4	x	✓	x
GLT6	3	3	4	7	4	✓	✓	x
GLT7	3	3	2	4	4	✓	✓	✓
GLT8	3	3	2	7	4	✓	✓	✓
GLT9	3	3	2	7	4	✓	x	✓

6.7 UV-Vis spectra for galantamine released in phosphate buffer solutions and film weights

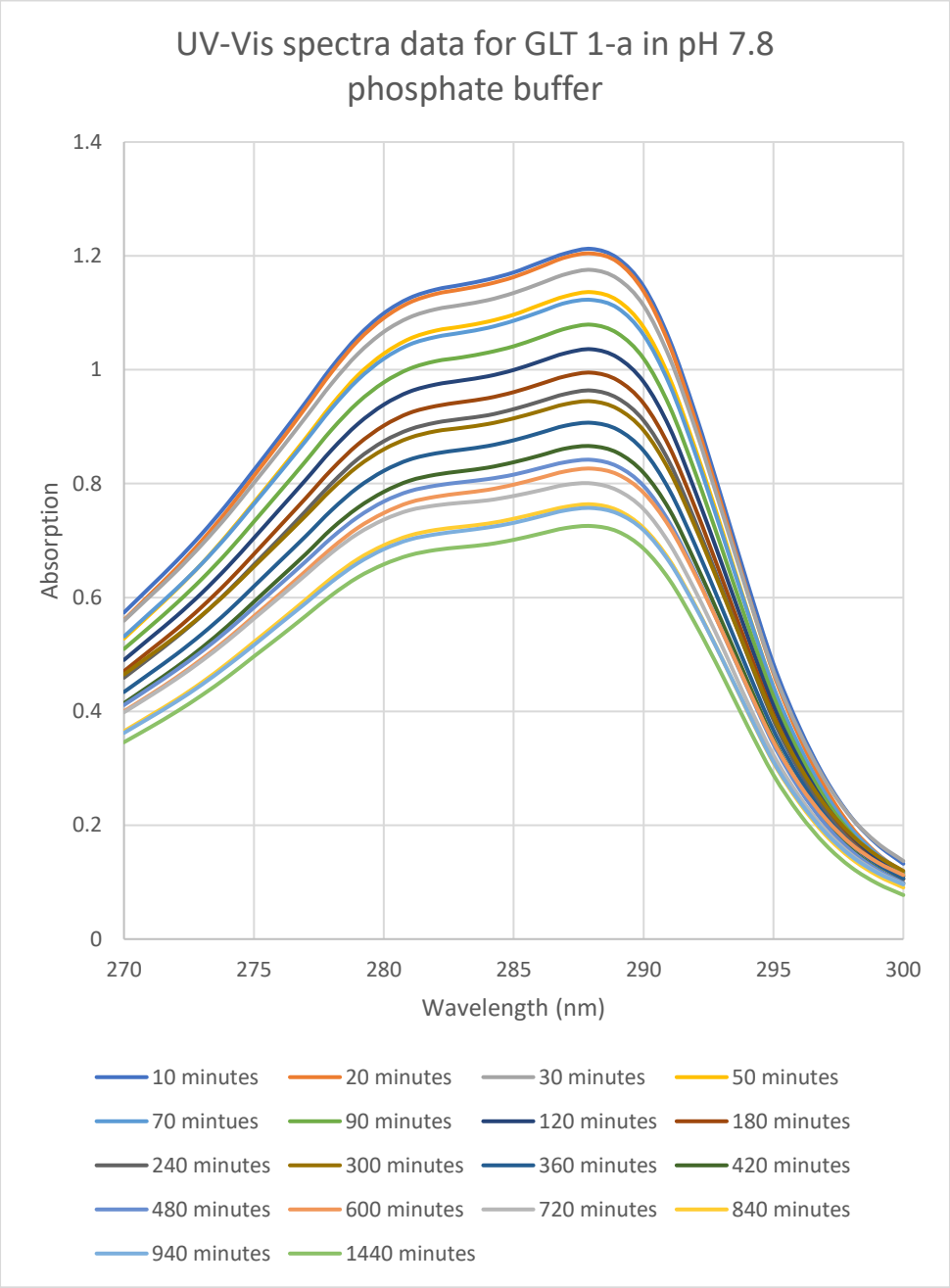

Figure 6- 12: UV-Vis spectra data for the first release of galantamine HBr over 24 hours, in pH 7.8 phosphate buffer solution, from a GLT 1 film.

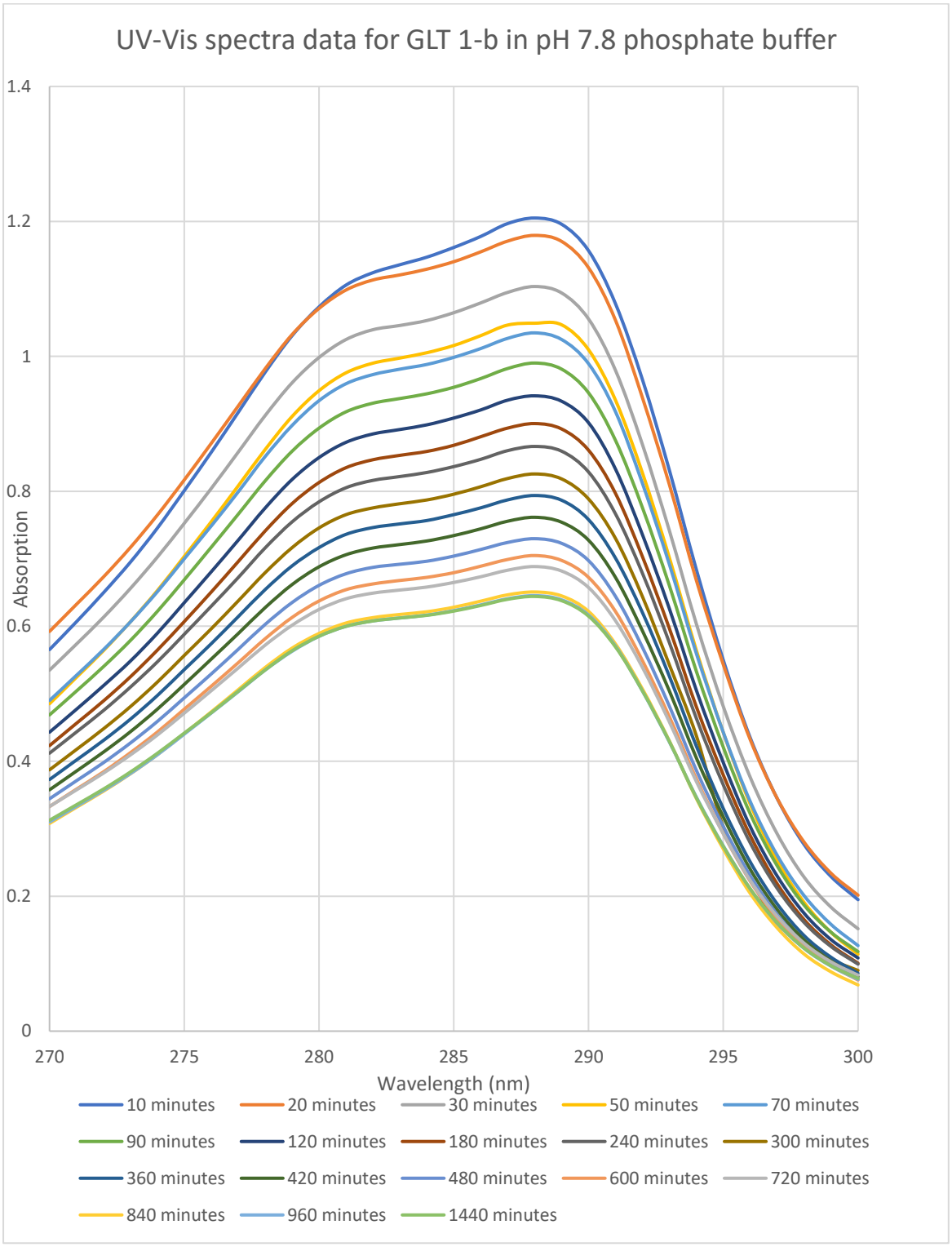

Figure 6- 13: UV-Vis spectra data for the second release of galantamine HBr over 24 hours, in pH 7.8 phosphate buffer solution, from a GLT 1 film.

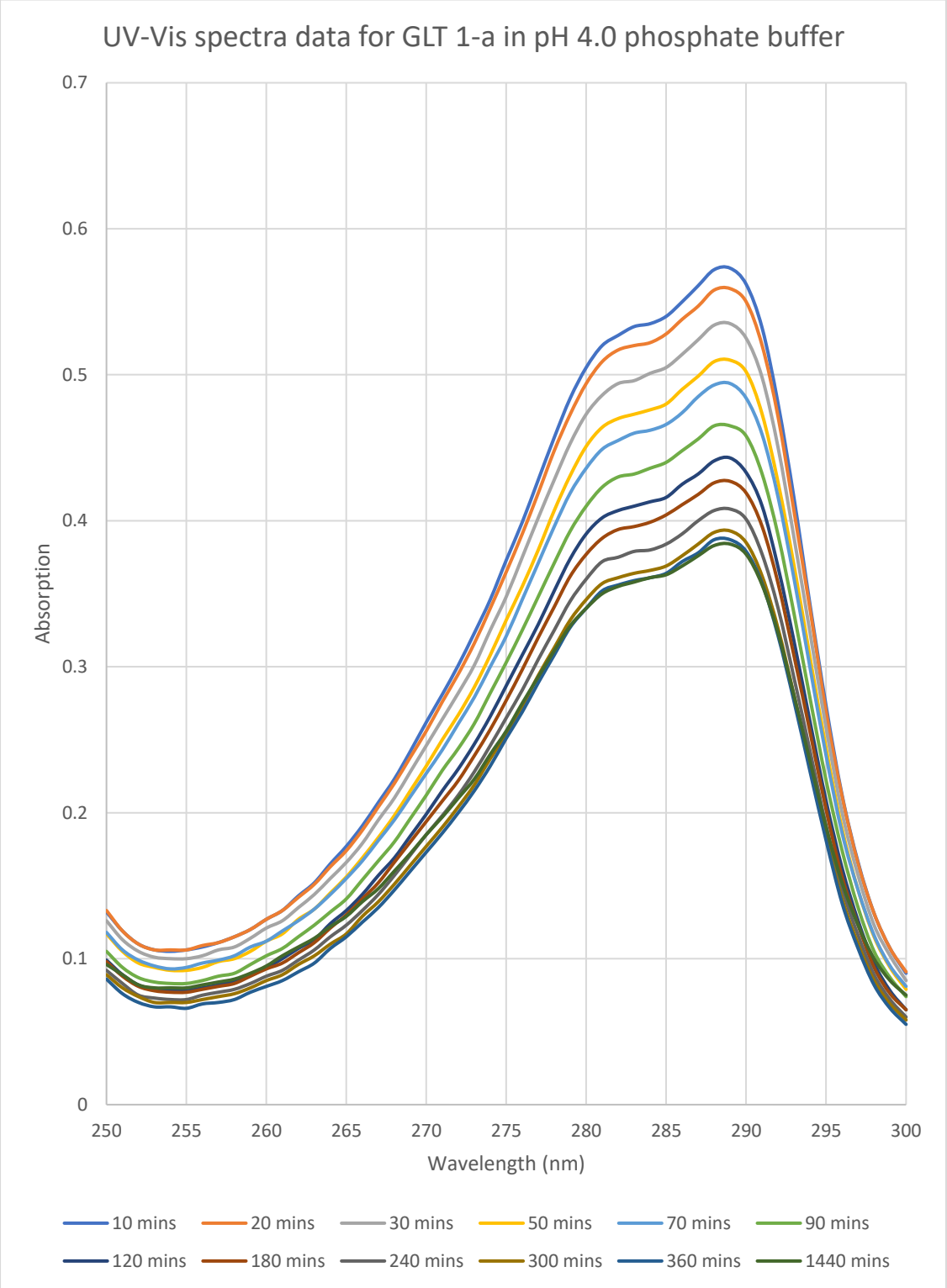

Figure 6- 14: UV-Vis spectra data for the first release of galantamine HBr over 24 hours, in pH 4.0 phosphate buffer solution, from a GLT 1 film.

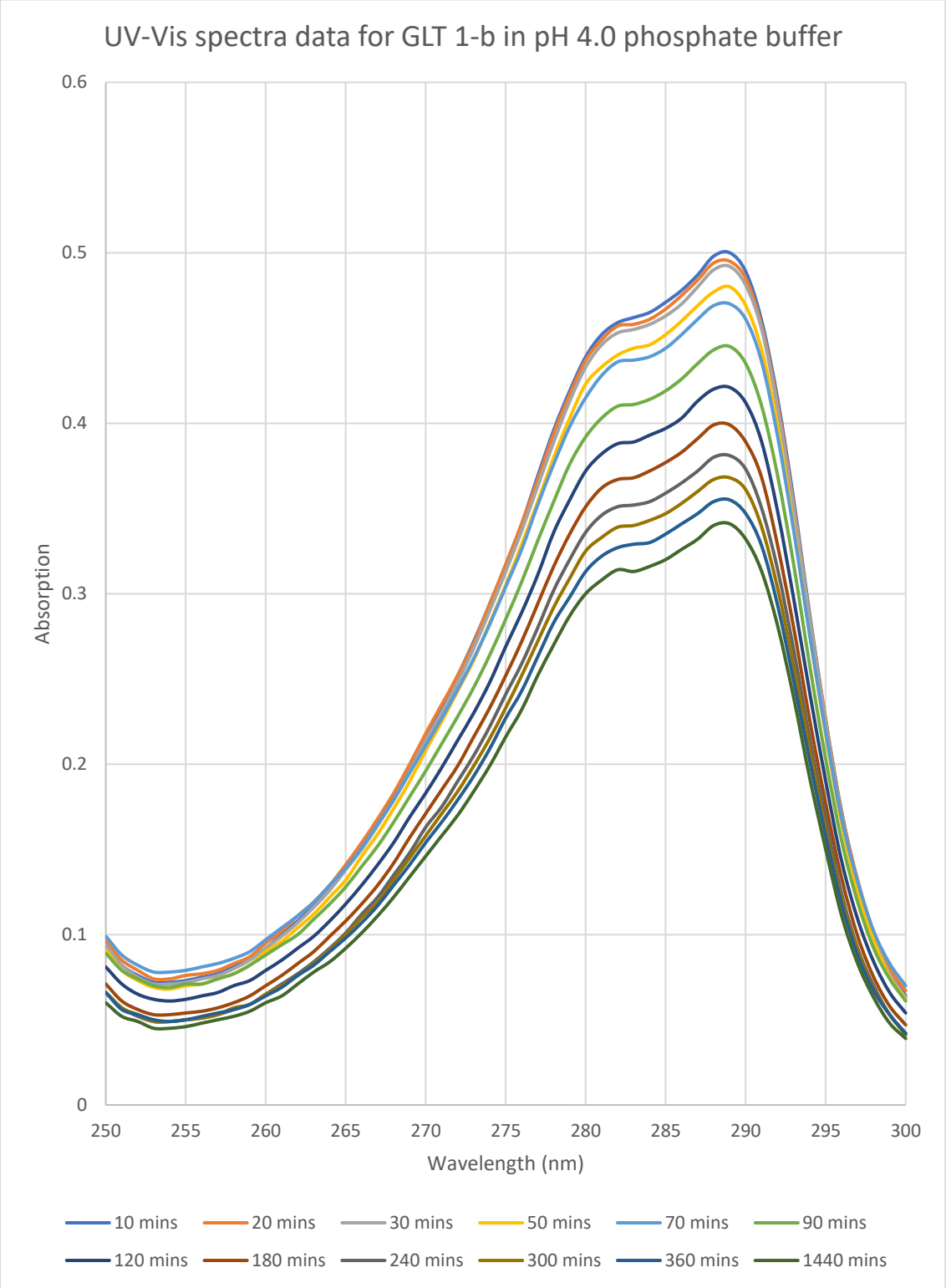

Figure 6- 15: UV-Vis spectra data for the second release of galantamine HBr over 24 hours, in pH 4.0 phosphate buffer solution, from a GLT 1 film.

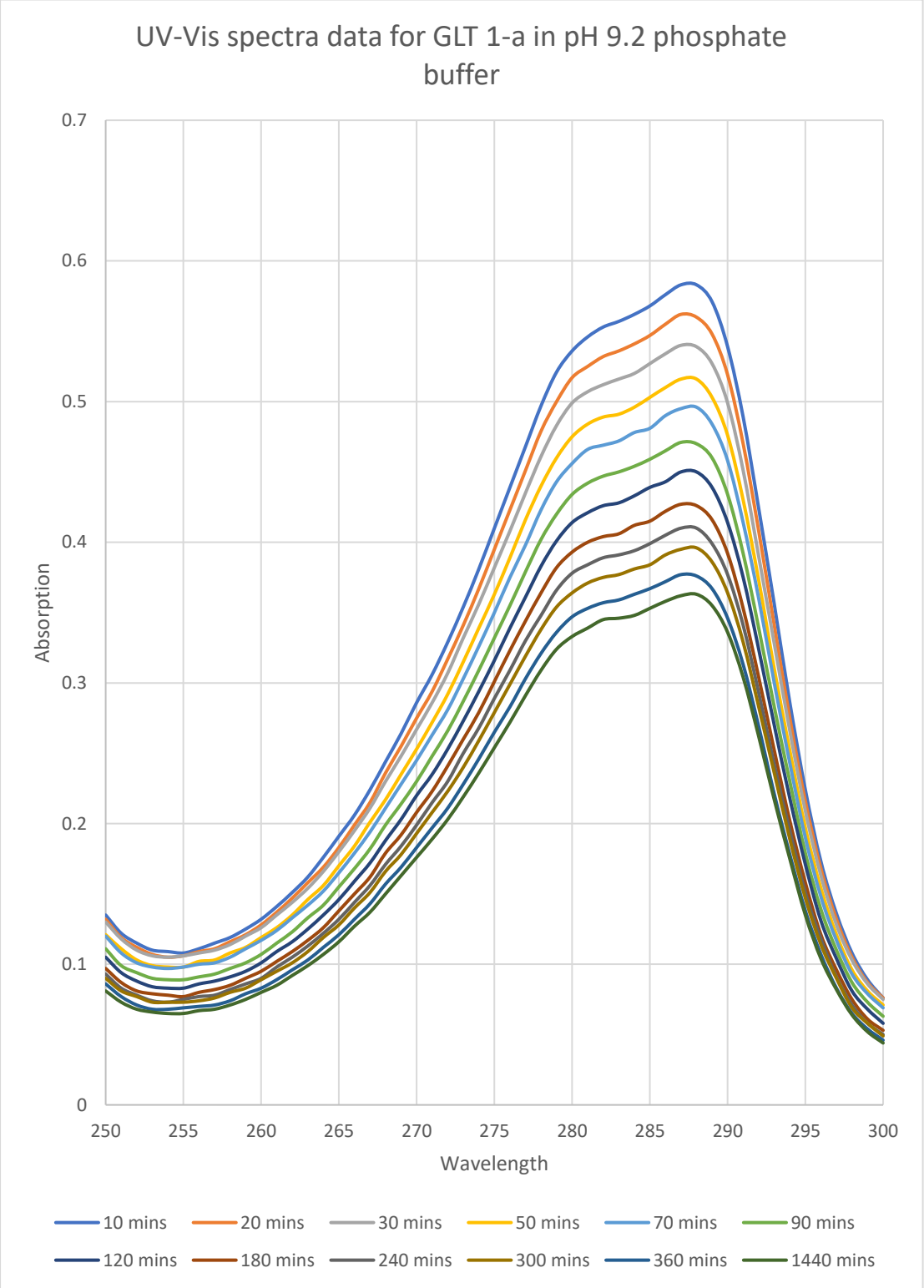

Figure 6- 16: UV-Vis spectra data for the first release of galantamine HBr over 24 hours, in pH 9.2 phosphate buffer solution, from a GLT 1 film.

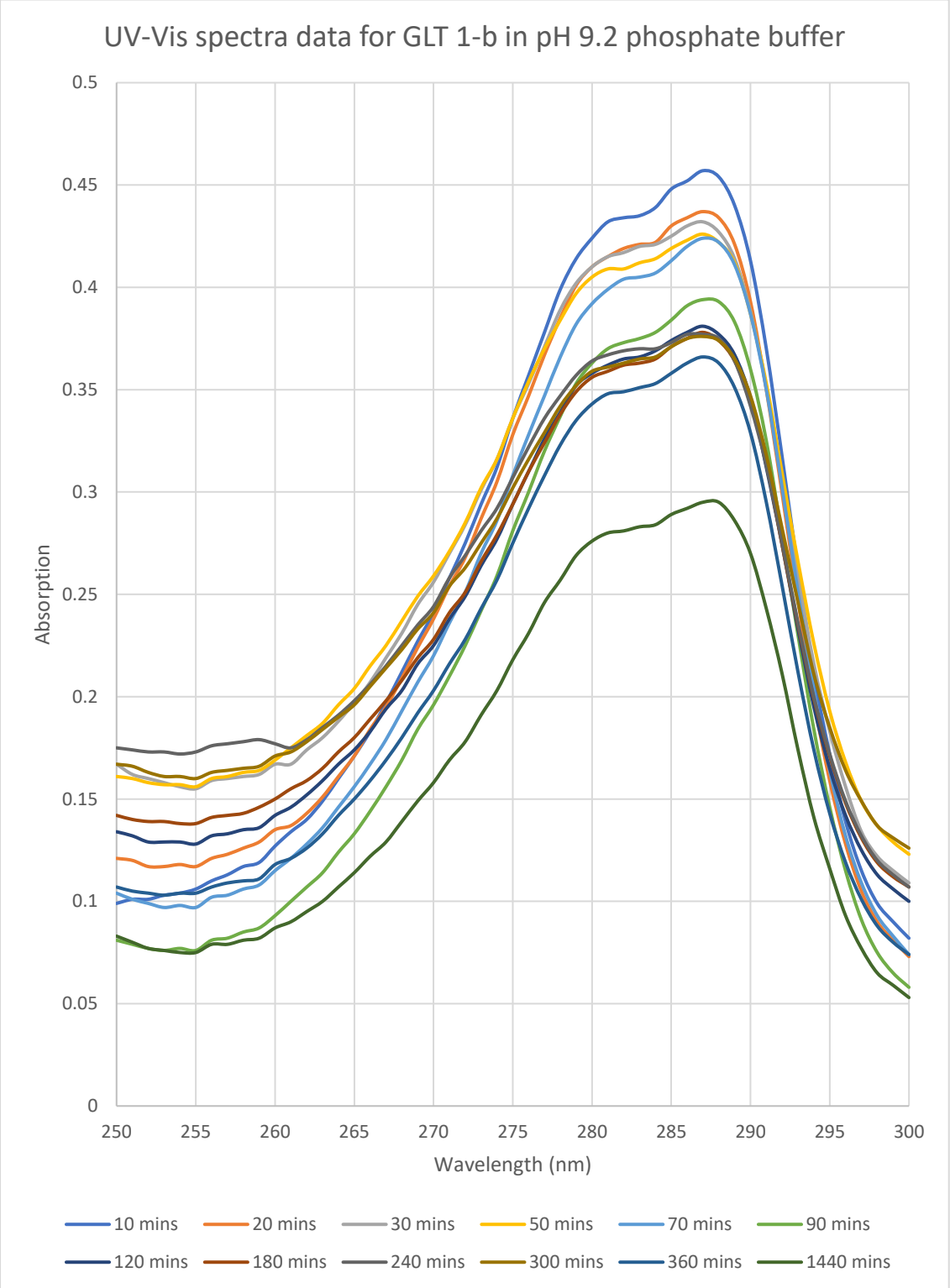

Figure 6- 17: UV-Vis spectra data for the second release of galantamine HBr over 24 hours, in pH 9.2 phosphate buffer solution, from a GLT 1 film.

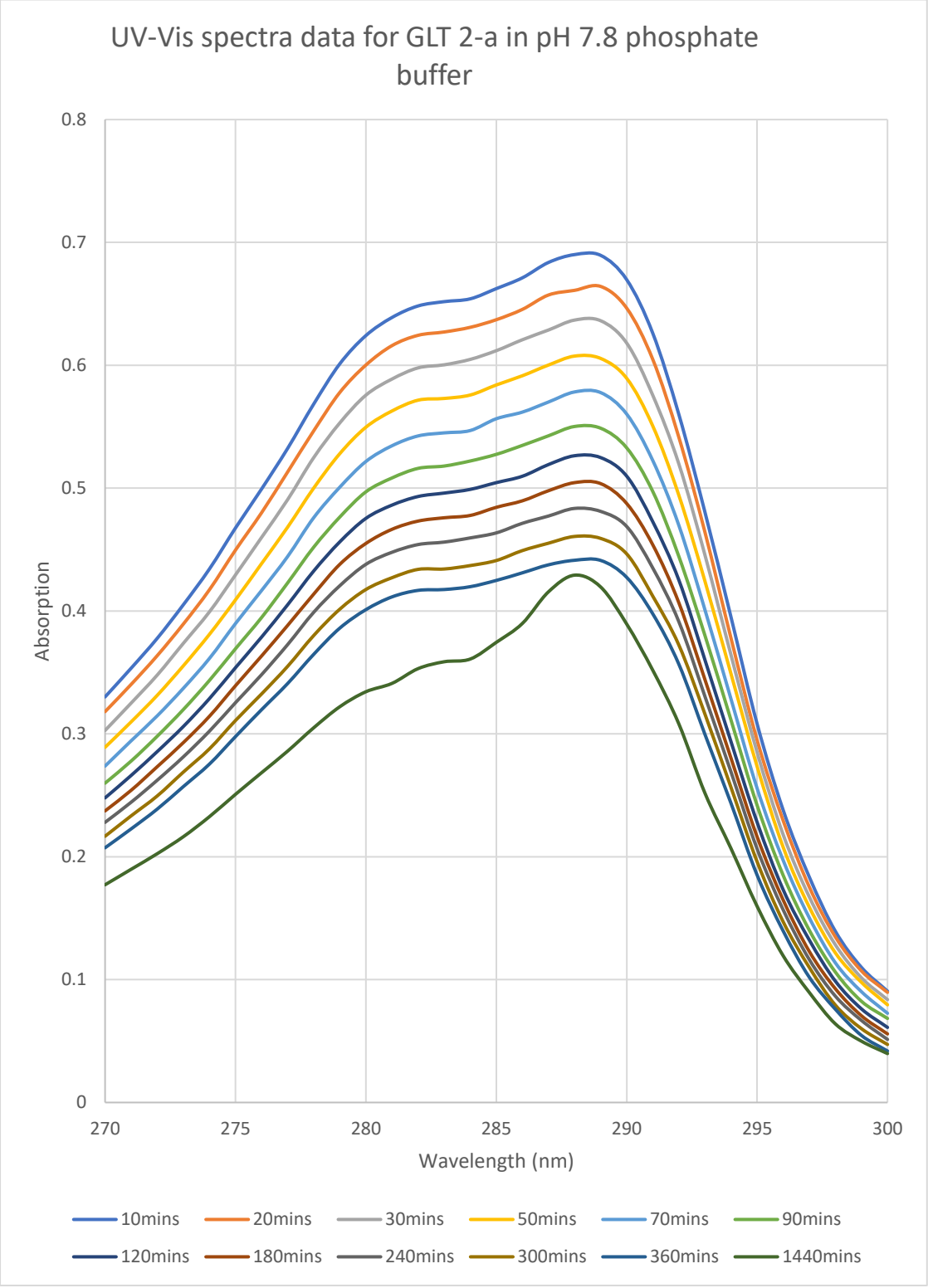

Figure 6- 18: UV-Vis spectra data for the first release of galantamine HBr over 24 hours, in pH 7.8 phosphate buffer solution, from a GLT 2 Film.

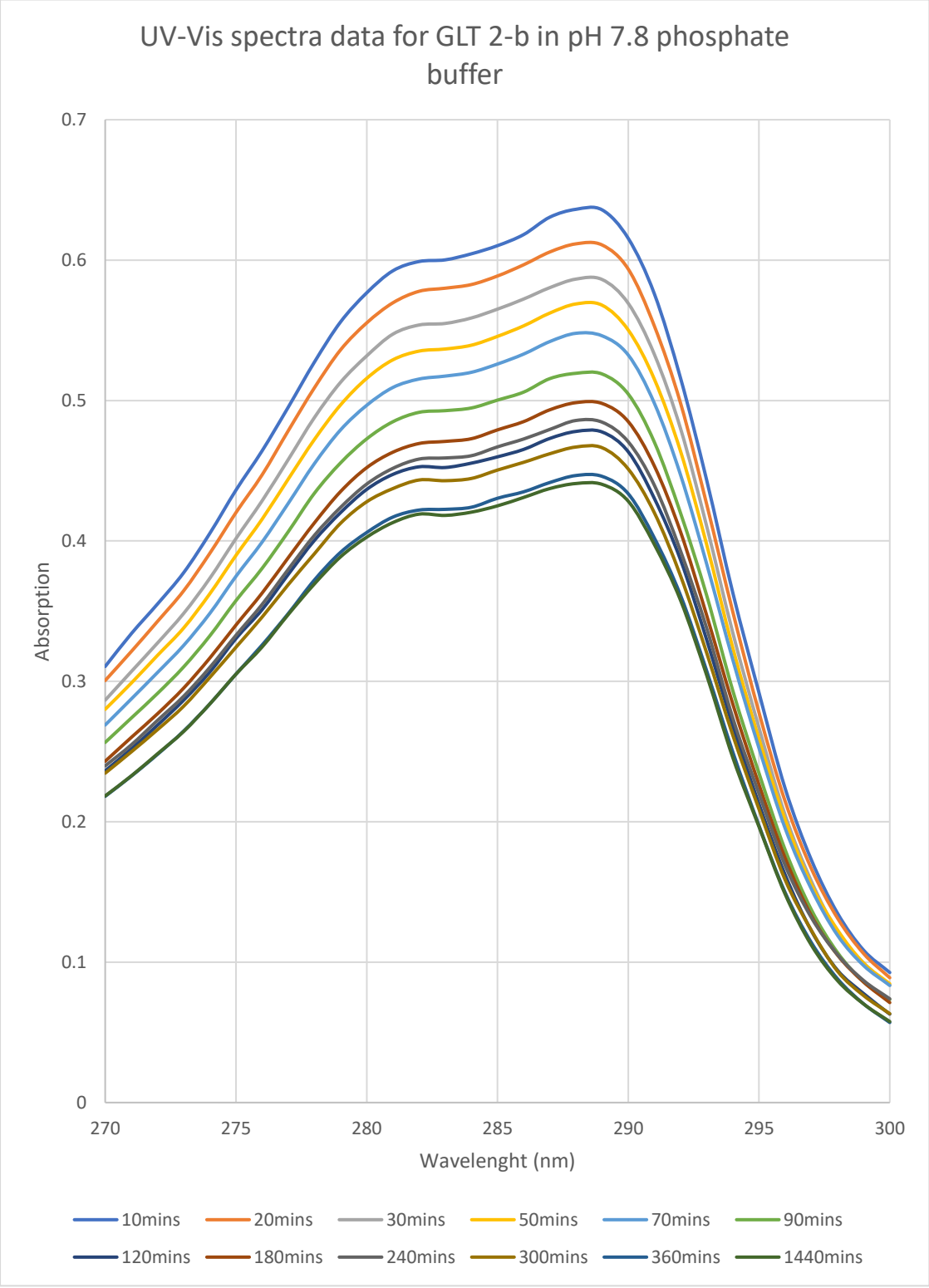

Figure 6- 19: UV-Vis spectra data for the second release of galantamine HBr over 24 hours, in pH 7.8 phosphate buffer solution, from a GLT 2 film.

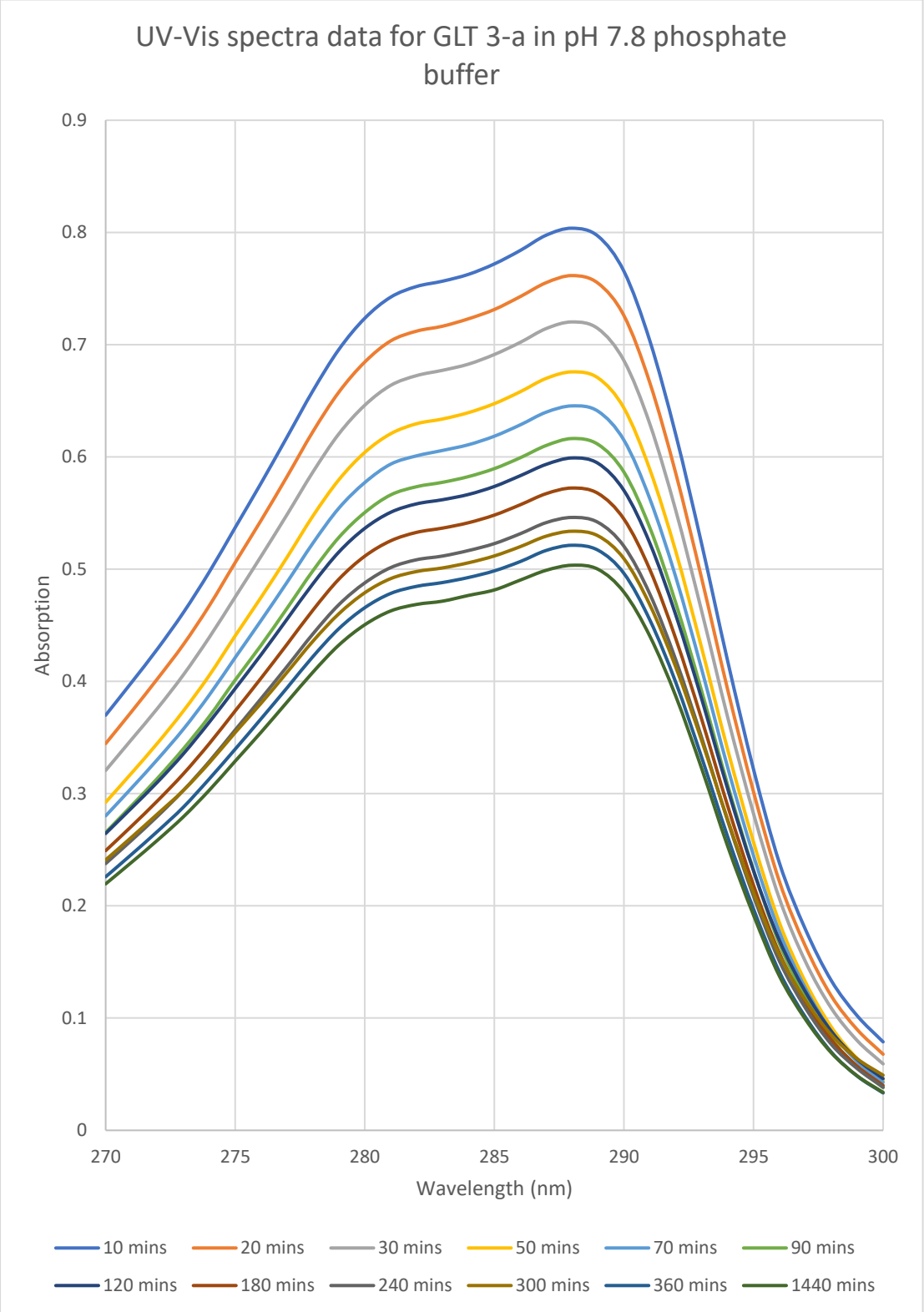

Figure 6- 20: UV-Vis spectra data for the first release of galantamine HBr over 24 hours, in pH 7.8 phosphate buffer solution, from a GLT 3 film.

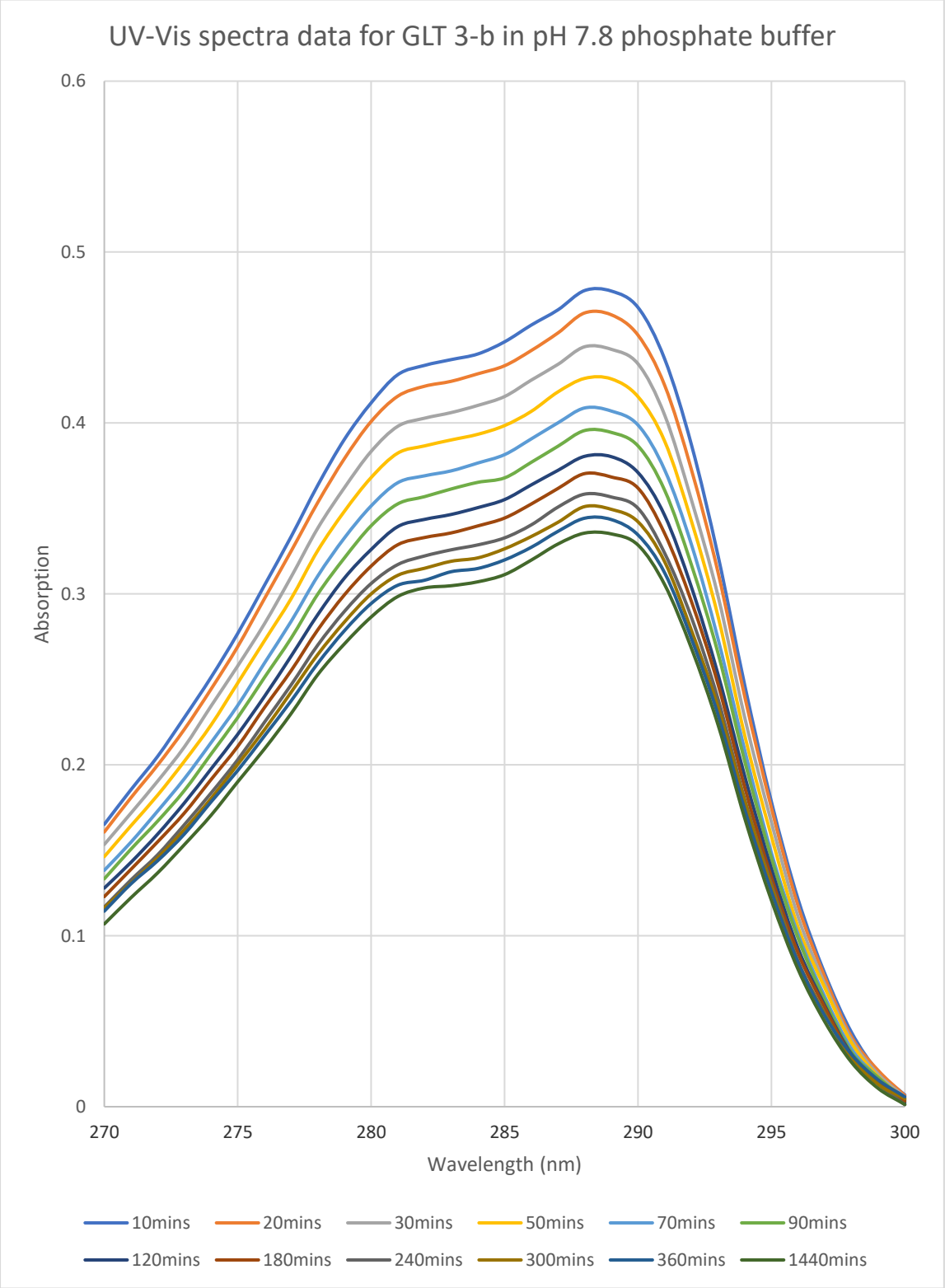

Figure 6- 21: UV-Vis spectra data for the second release of galantamine HBr over 24 hours, in pH 7.8 phosphate buffer solution, from a GLT 3 film.

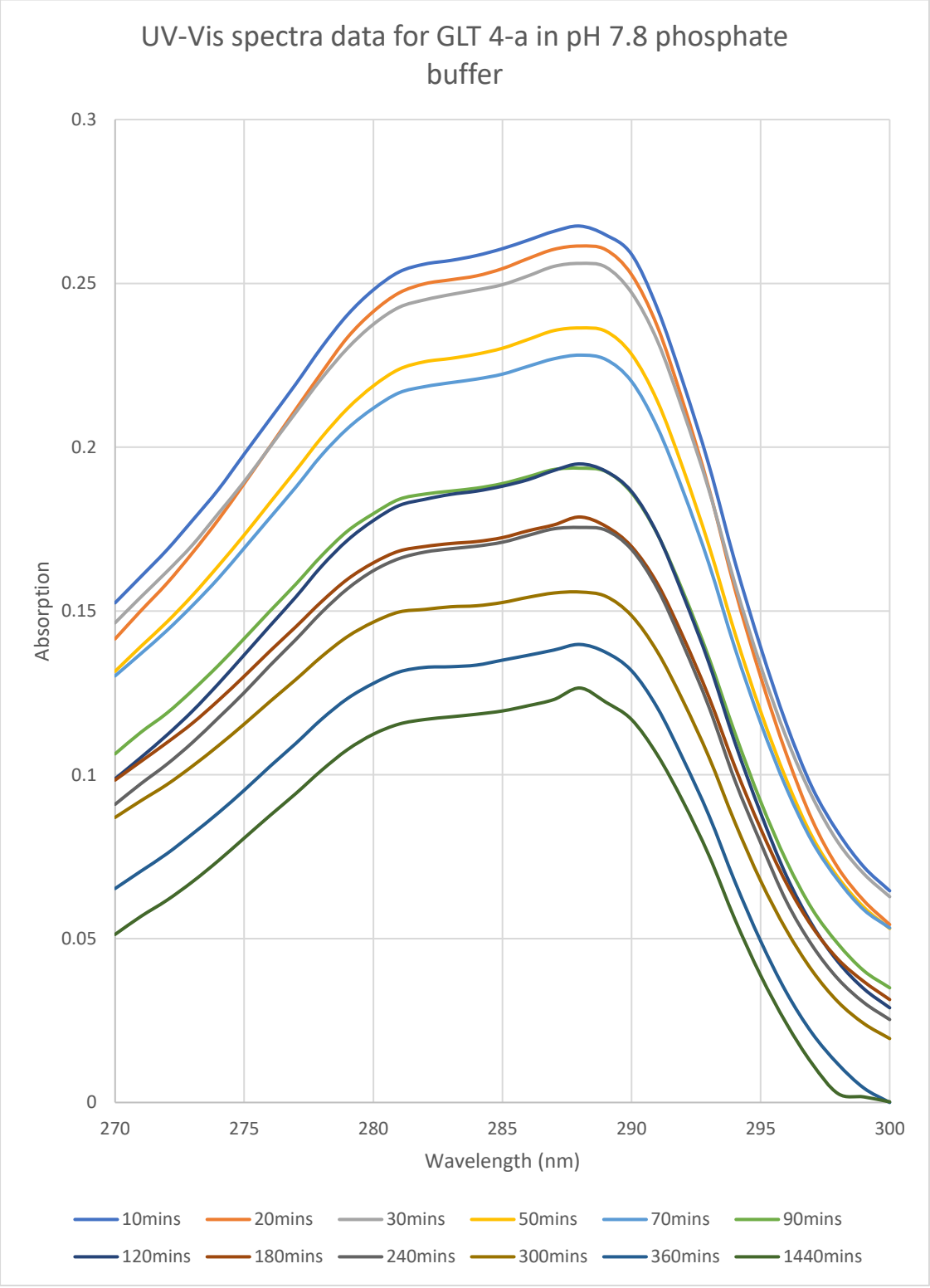

Figure 6- 22: UV-Vis spectra data for the first release of galantamine HBr over 24 hours, in pH 7.8 phosphate buffer solution, from a GLT 4 film.

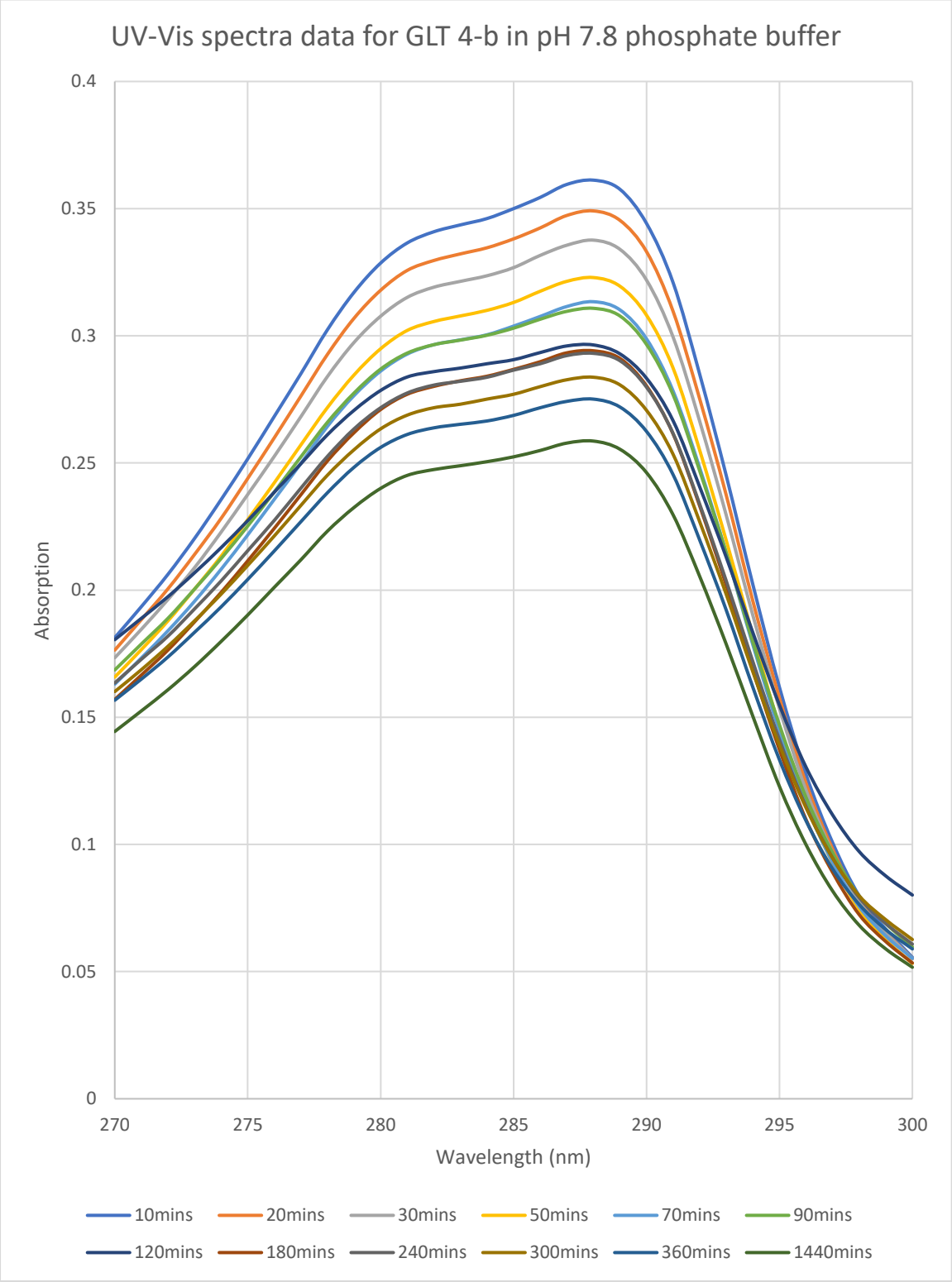

Figure 6- 23: UV-Vis spectra data for the second release of galantamine HBr over 24 hours, in pH 7.8 phosphate buffer solution, from a GLT 4 film.

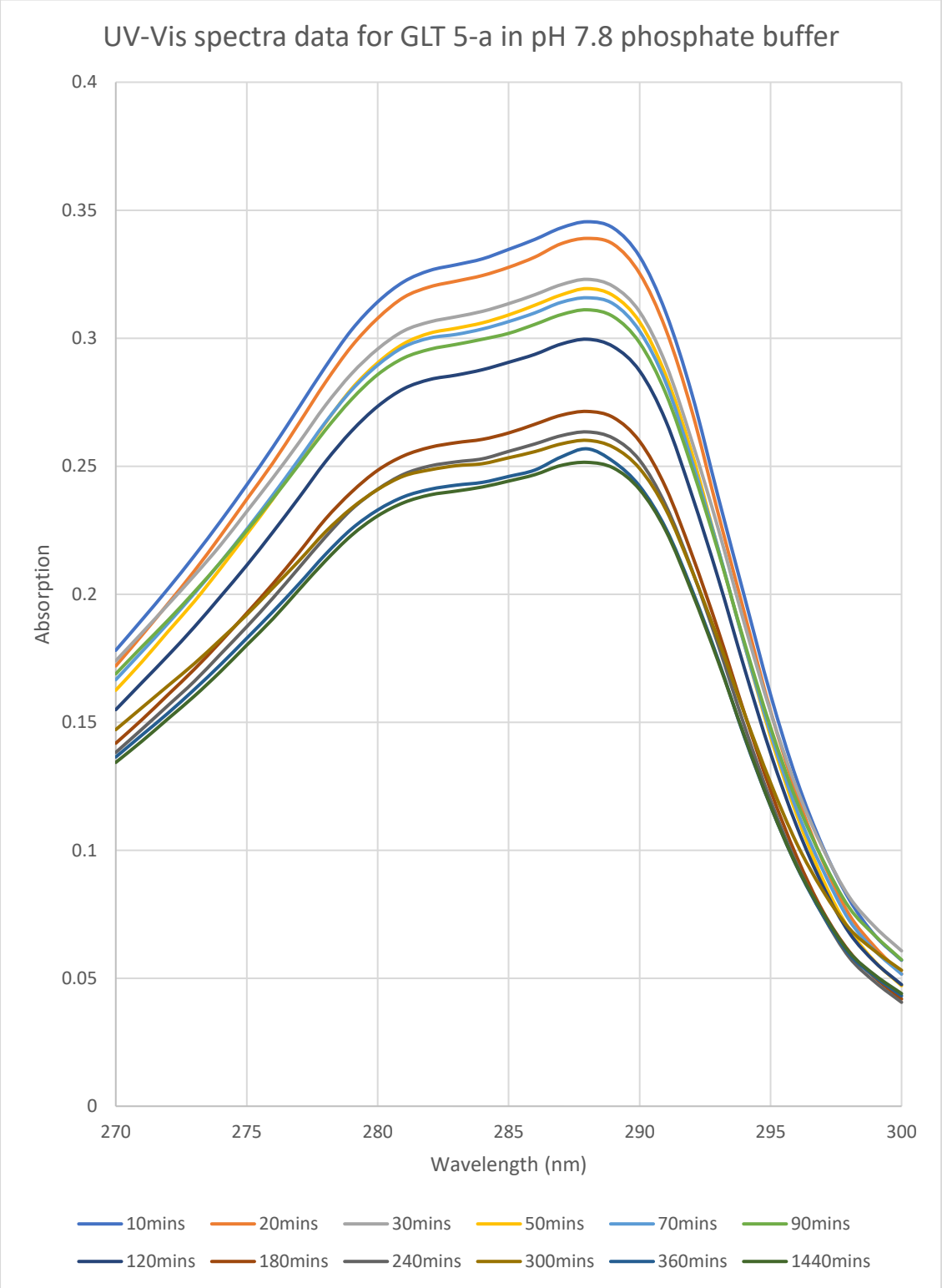

Figure 6- 24: UV-Vis spectra data for the first release of galantamine HBr over 24 hours, in pH 7.8 phosphate buffer solution, from a GLT 5 film.

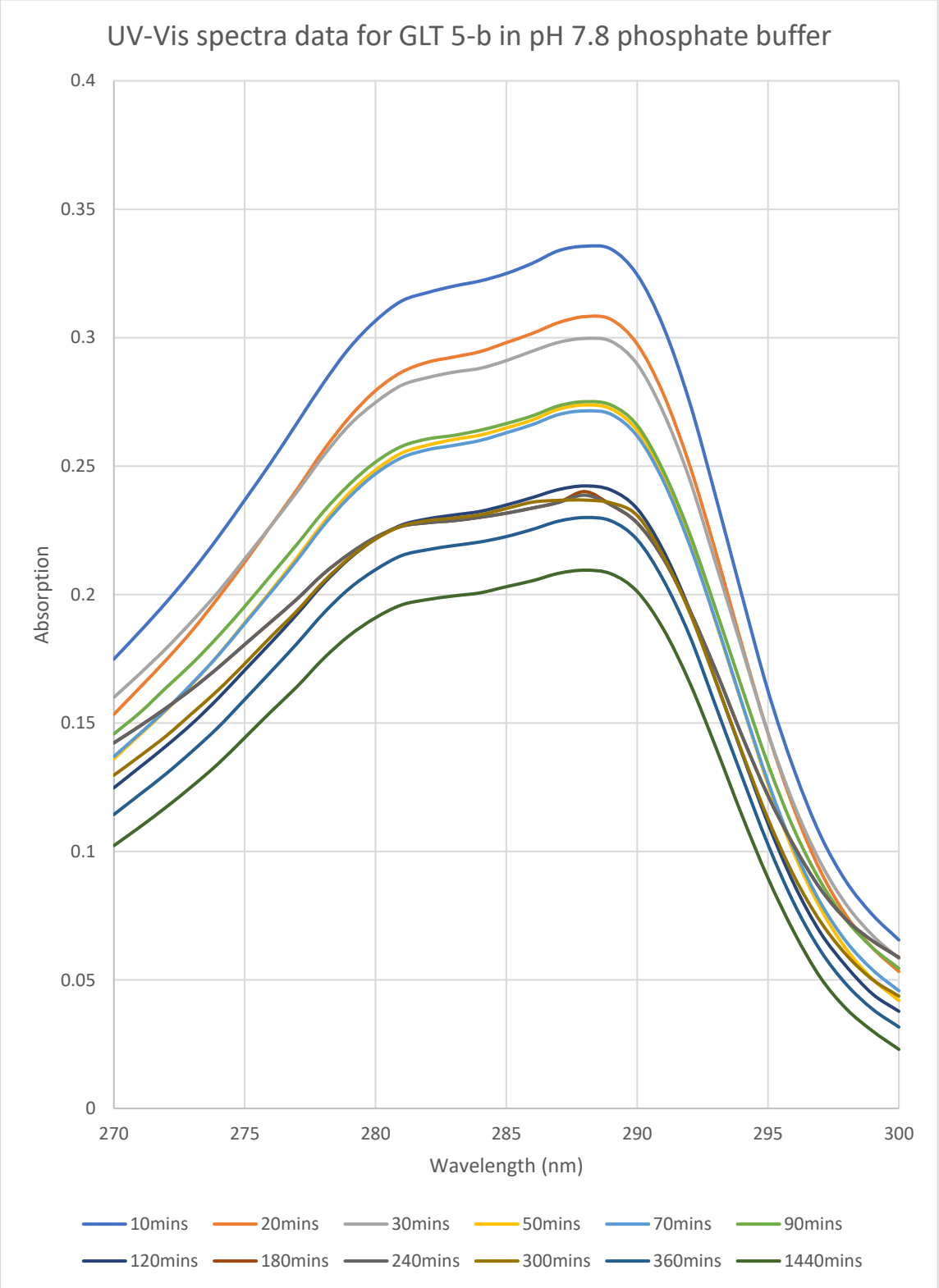

Figure 6- 25: UV-Vis spectra data for the first release of galantamine HBr over 24 hours, in pH 7.8 phosphate buffer solution, from a GLT 5 film.

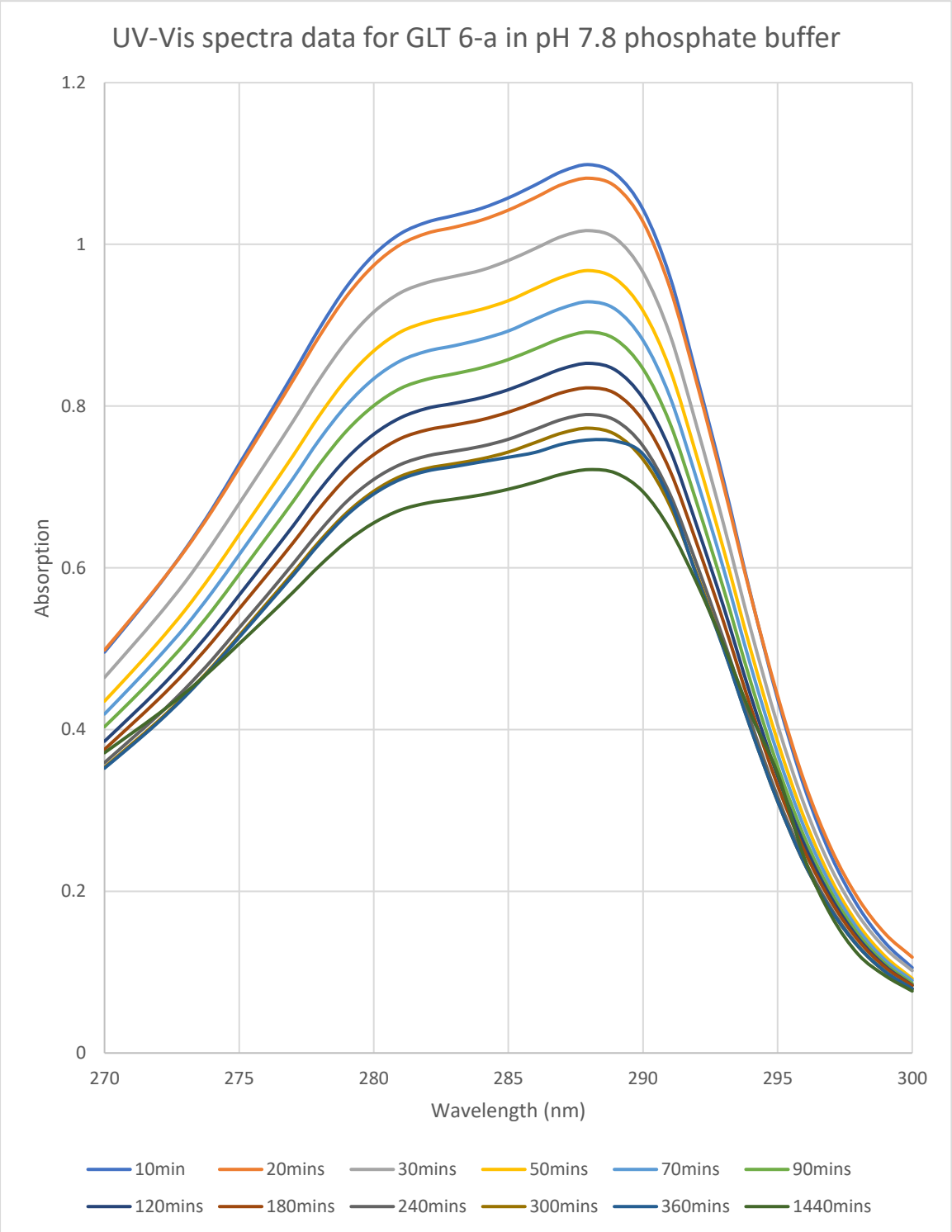

Figure 6- 26: UV-Vis spectra data for the first release of galantamine HBr over 24 hours, in pH 7.8 phosphate buffer solution, from a GLT 6 film.

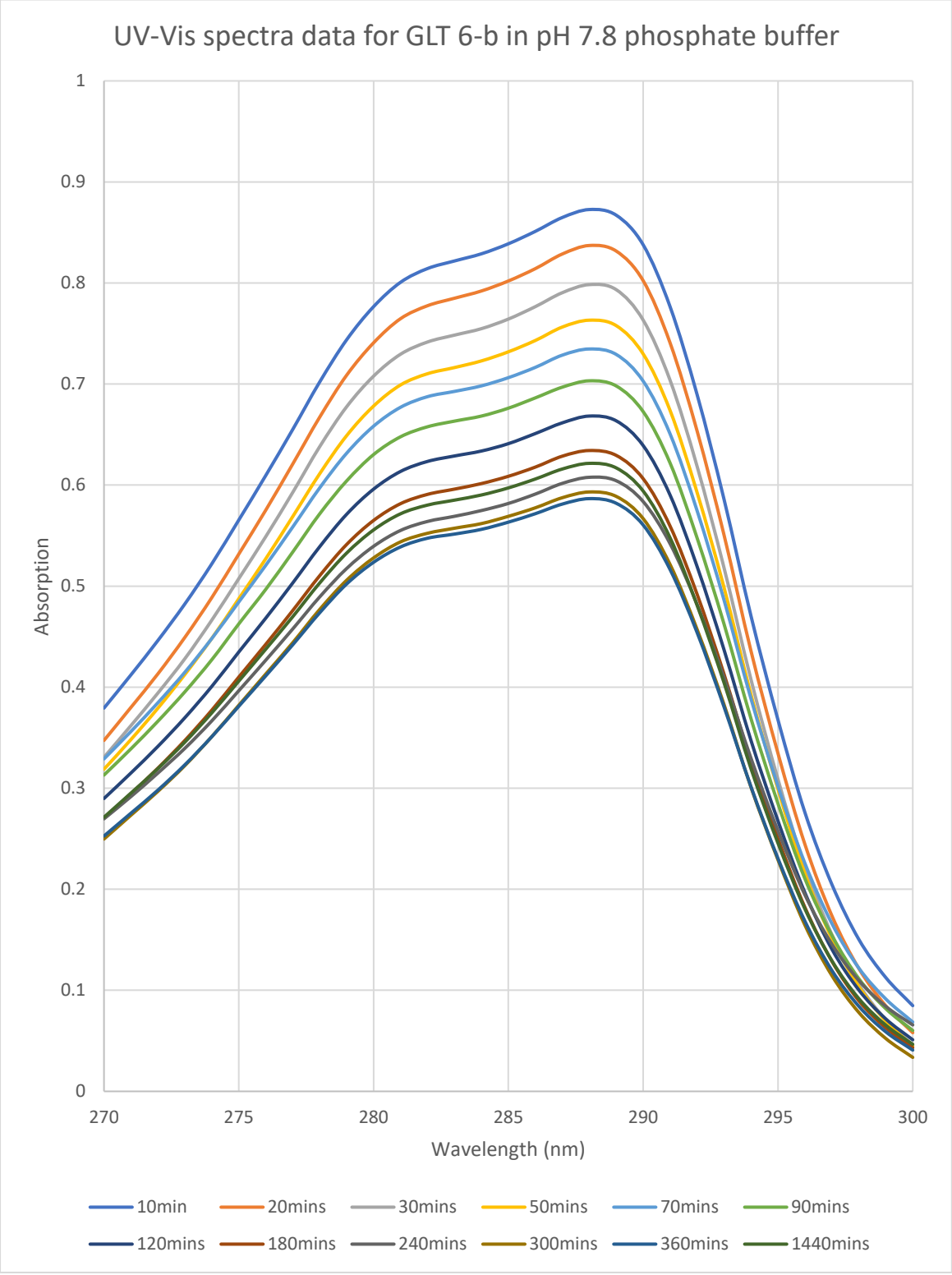

Figure 6- 27: UV-Vis spectra data for the second release of galantamine HBr over 24 hours, in pH 7.8 phosphate buffer solution, from a GLT 6 film.

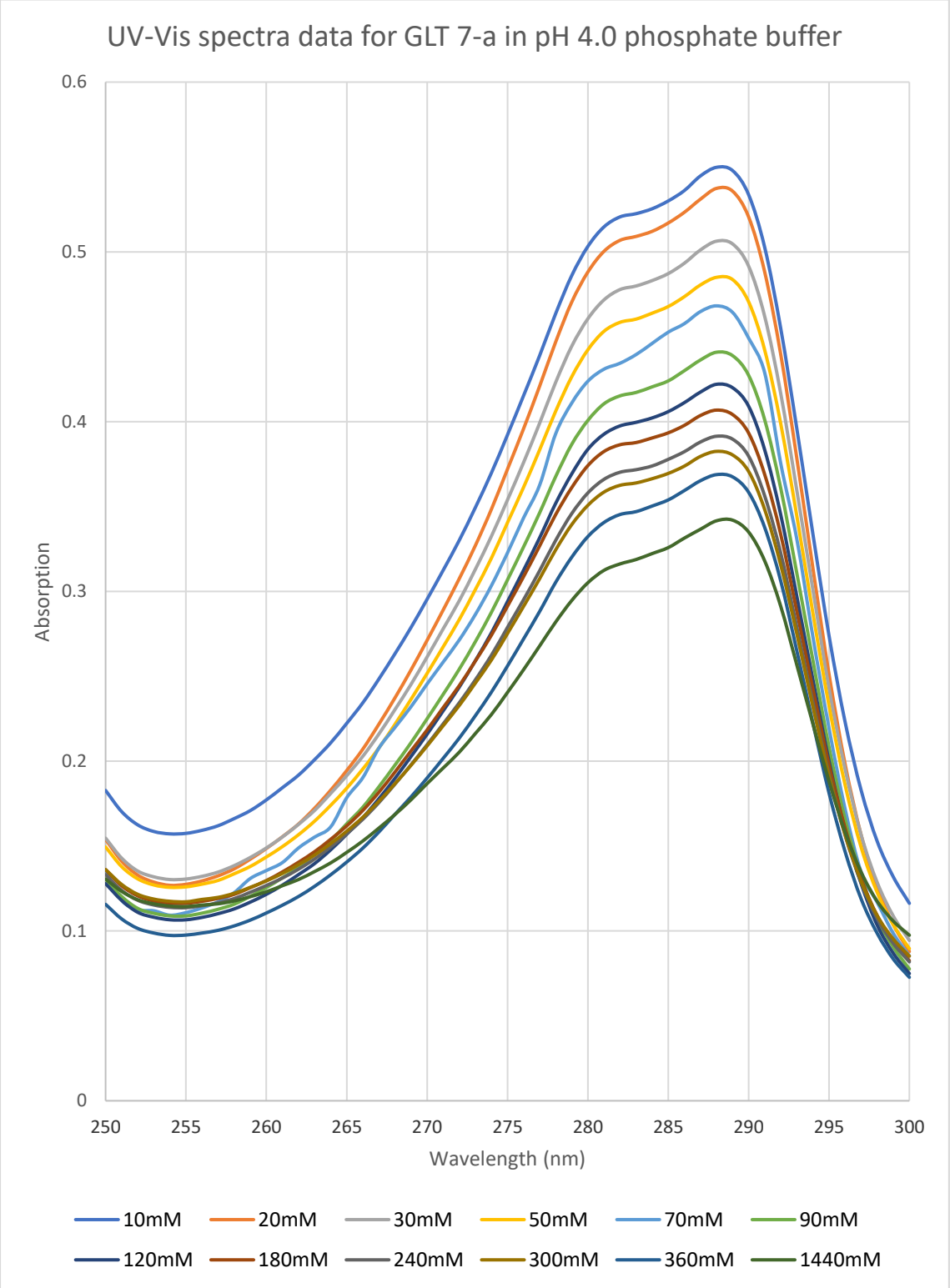

Figure 6- 28: UV-Vis spectra data for the first release of galantamine HBr over 24 hours, in pH 4.0 phosphate buffer solution, from a GLT 7 film.

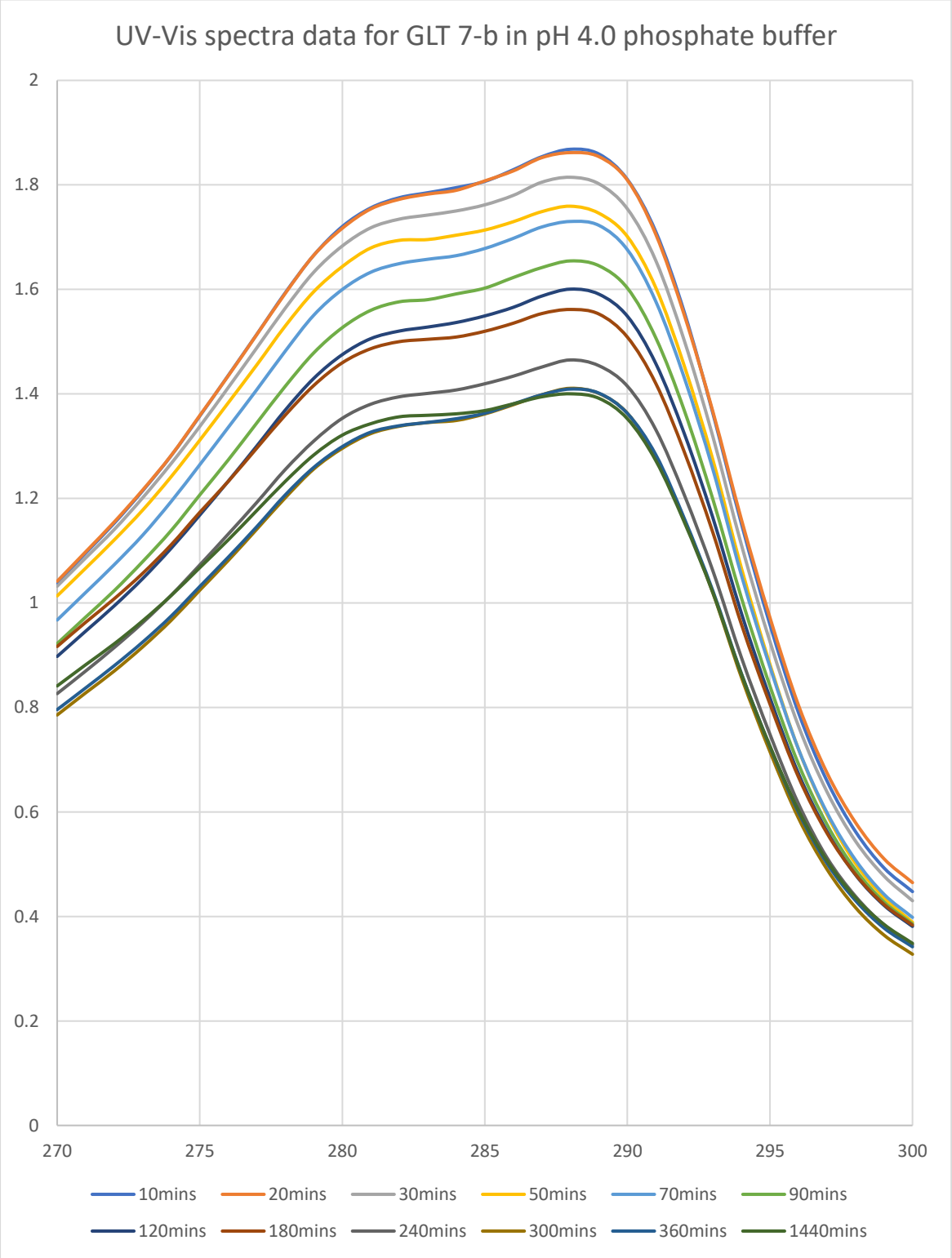

Figure 6- 29: UV-Vis spectra data for the second release of galantamine HBr over 24 hours, in pH 4.0 phosphate buffer solution, from a GLT 7 film.

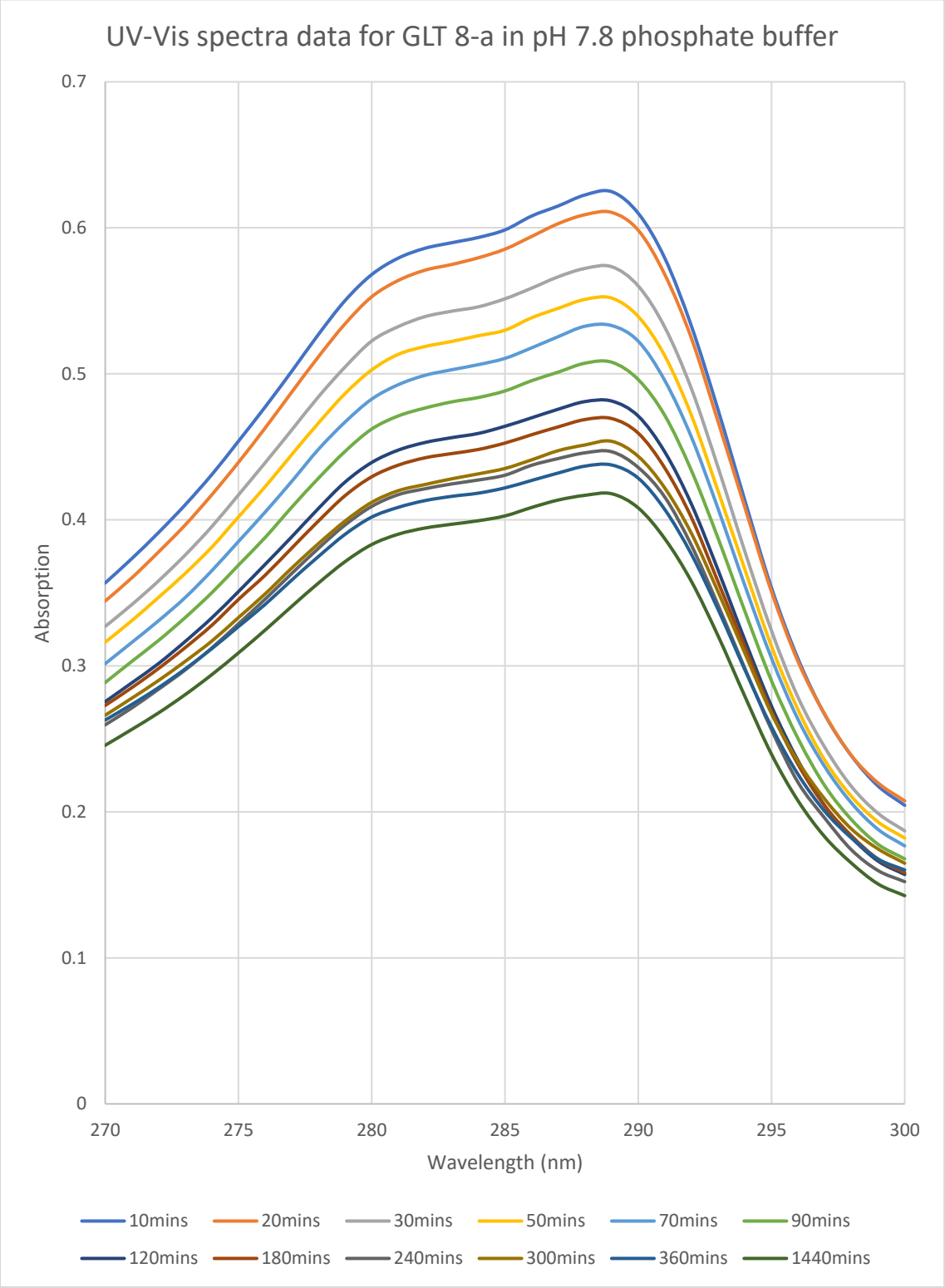

Figure 6- 30: UV-Vis spectra data for the first release of galantamine HBr over 24 hours, in pH 7.8 phosphate buffer solution, from a GLT 8 film.

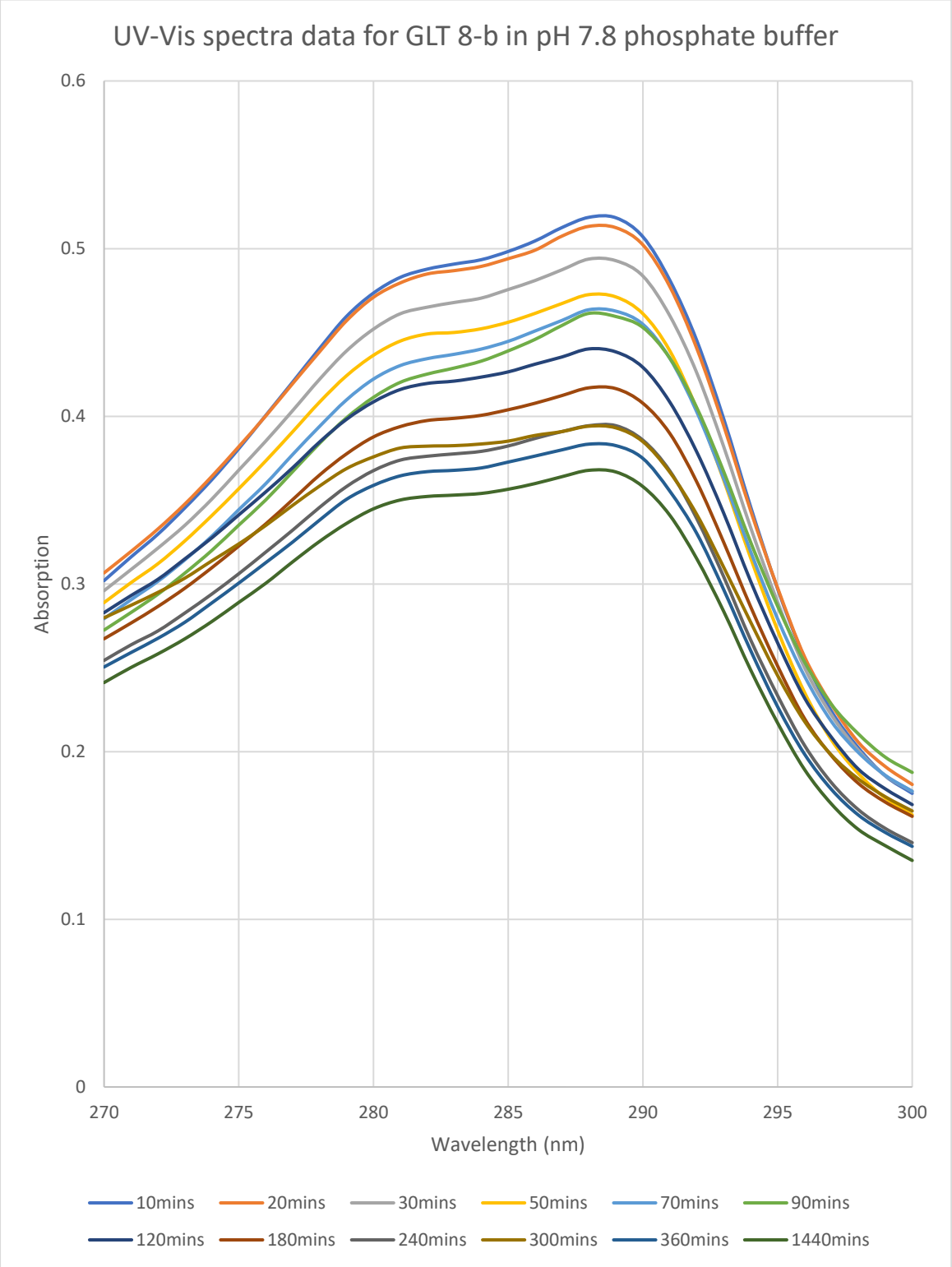

Figure 6- 31: UV-Vis spectra data for the second release of galantamine HBr over 24 hours, in pH 7.8 phosphate buffer solution, from a GLT 8 film.

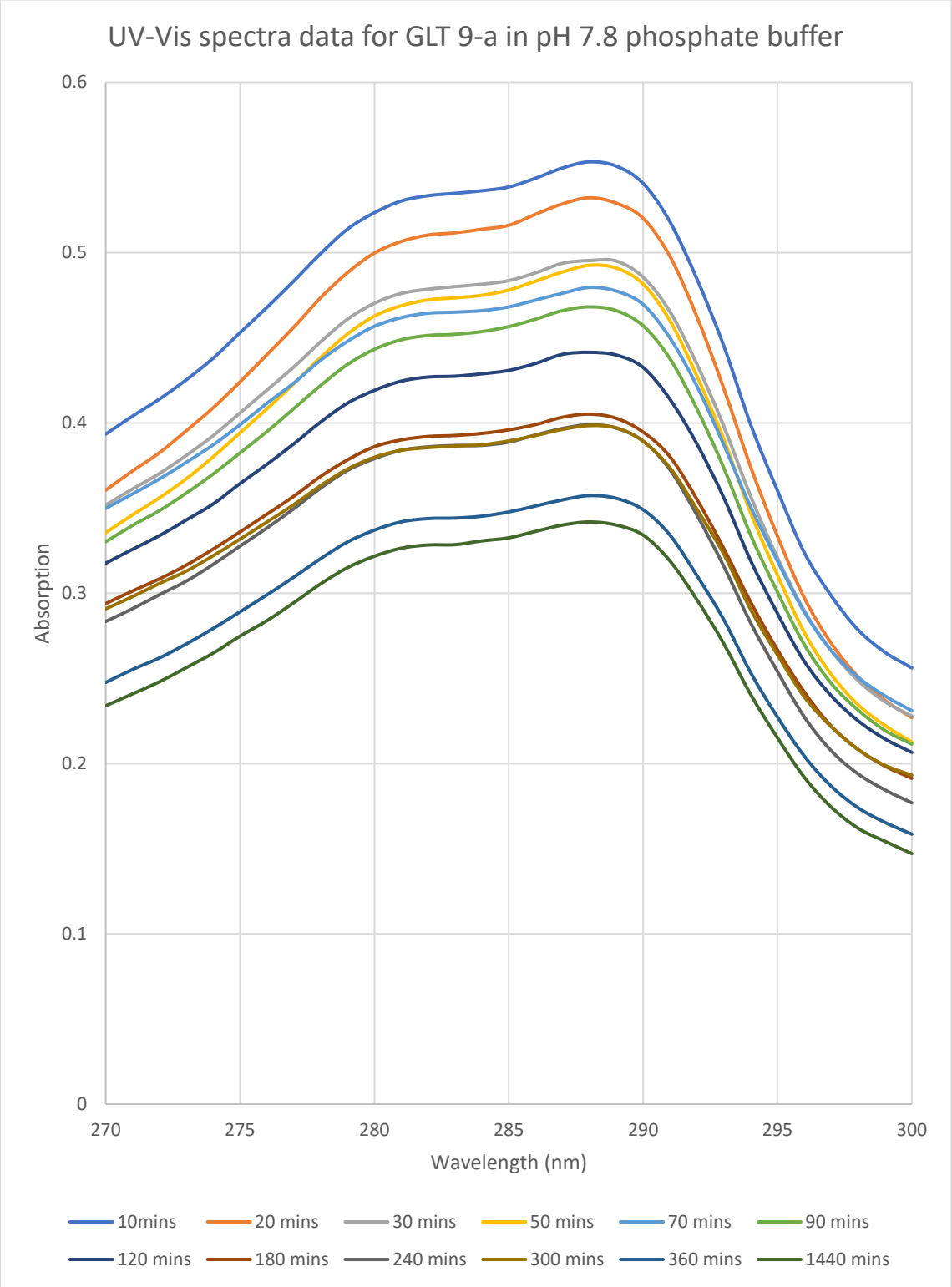

Figure 6- 32: UV-Vis spectra data for the first release of galantamine HBr over 24 hours, in pH 7.8 phosphate buffer solution, from a GLT 9 film.

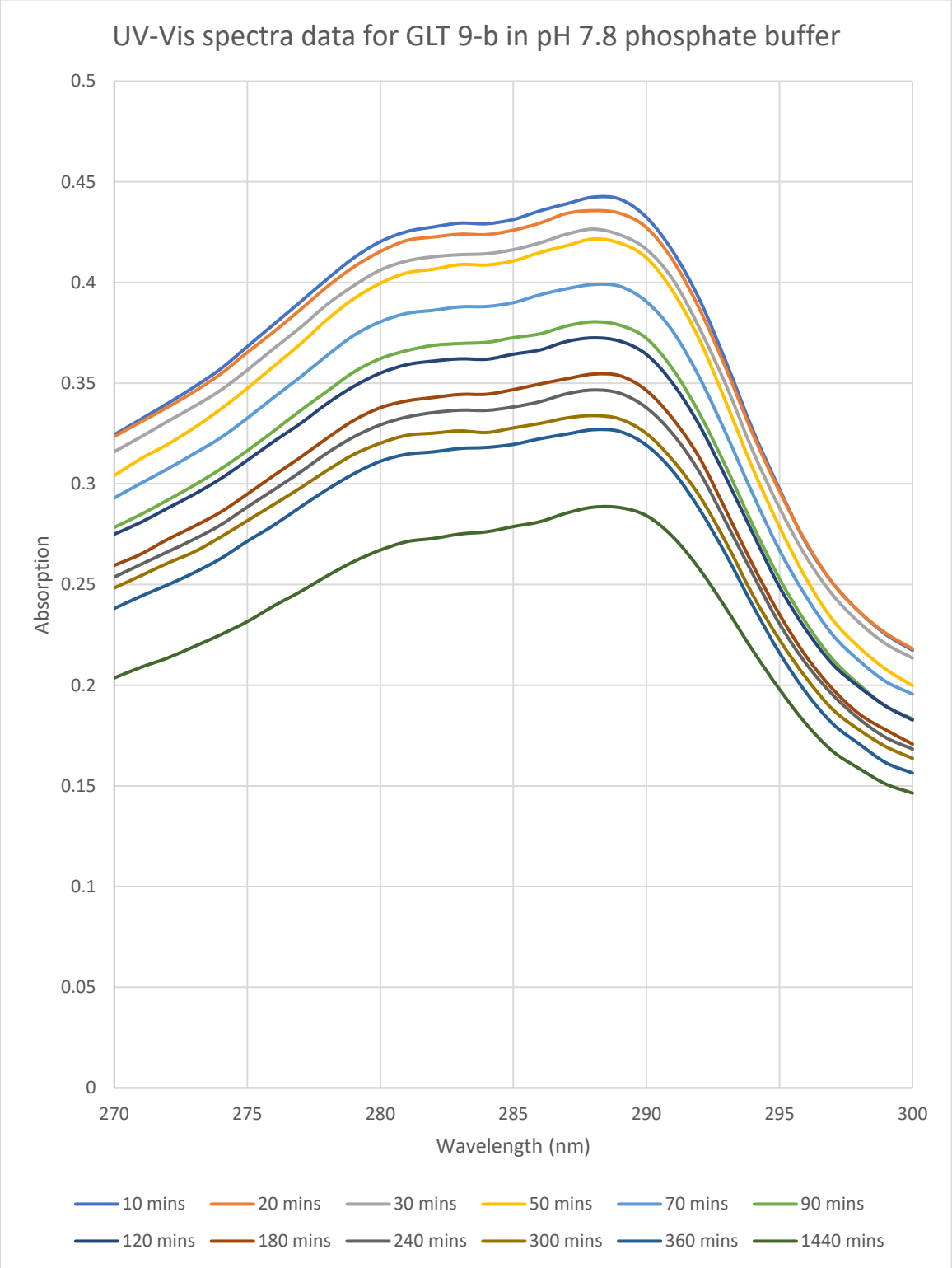

Figure 6- 33: UV-Vis spectra data for the second release of galantamine HBr over 24 hours, in pH 7.8 phosphate buffer solution, from a GLT 9 film.

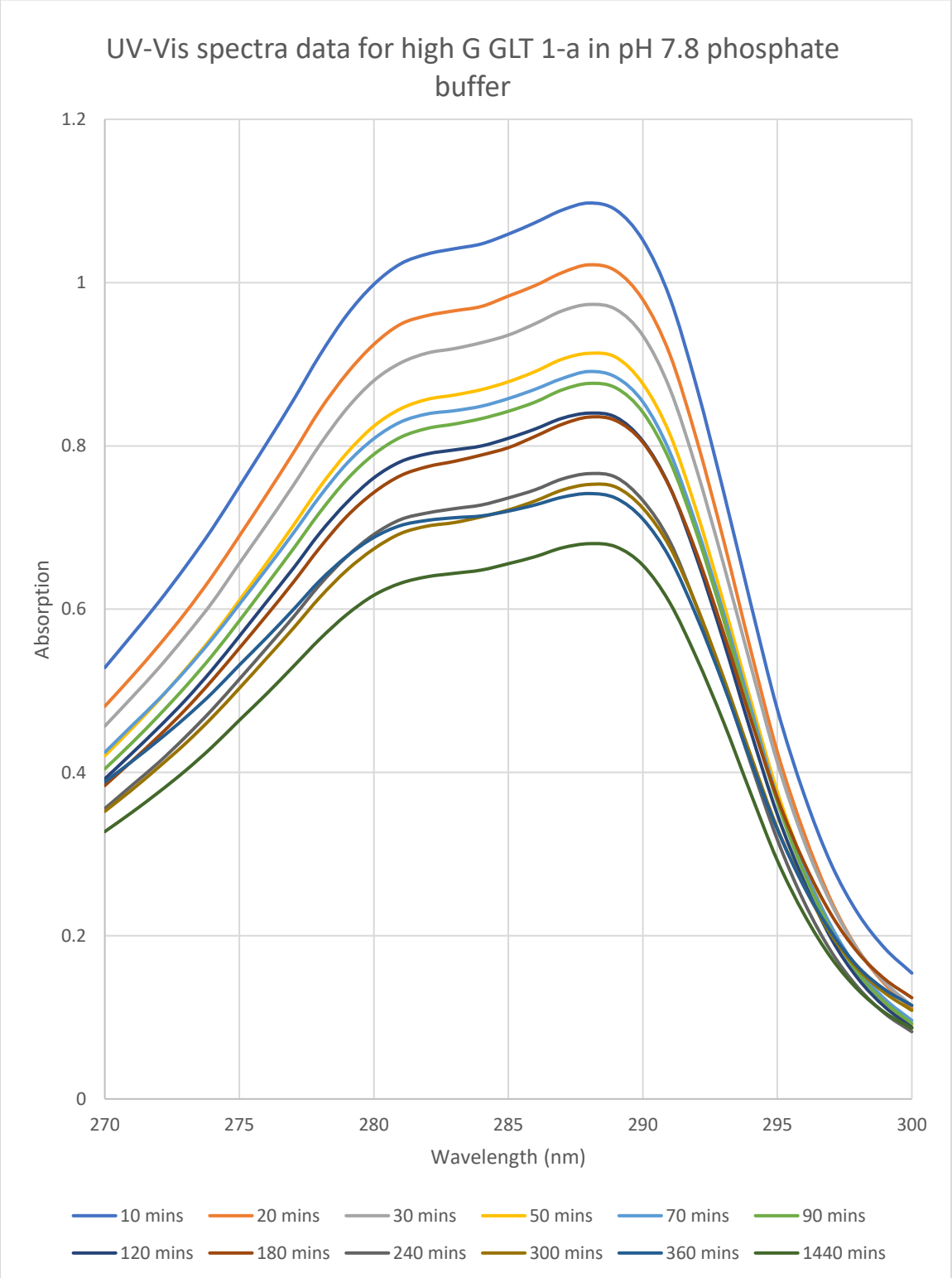

Figure 6- 34: UV-Vis spectra data for the first release of galantamine HBr over 24 hours, in pH 7.8 phosphate buffer solution, from a high G GLT 1 film.

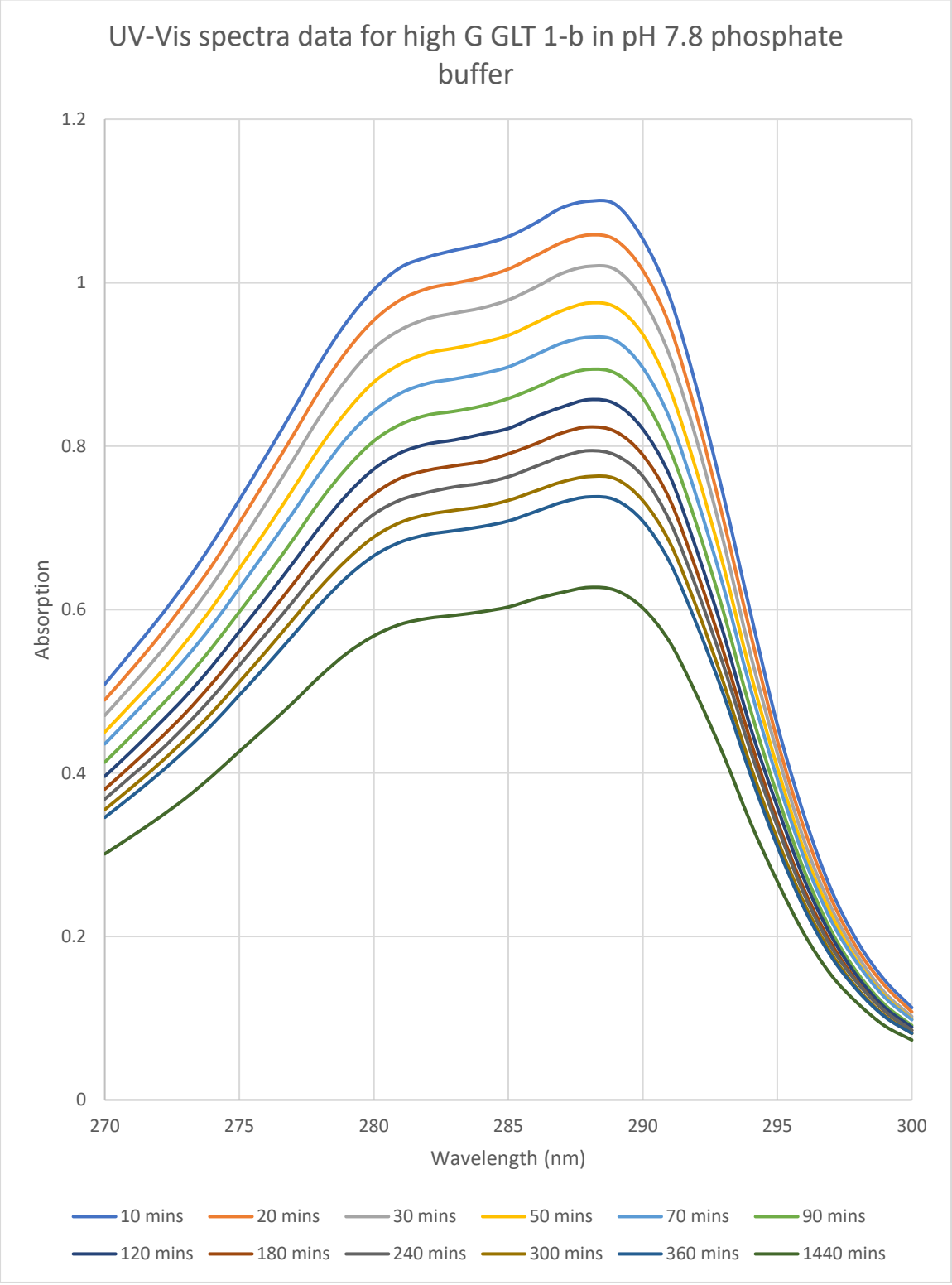

Figure 6- 35: UV-Vis spectra data for the second release of galantamine HBr over 24 hours, in pH 7.8 phosphate buffer solution, from a high G GLT 1 film.

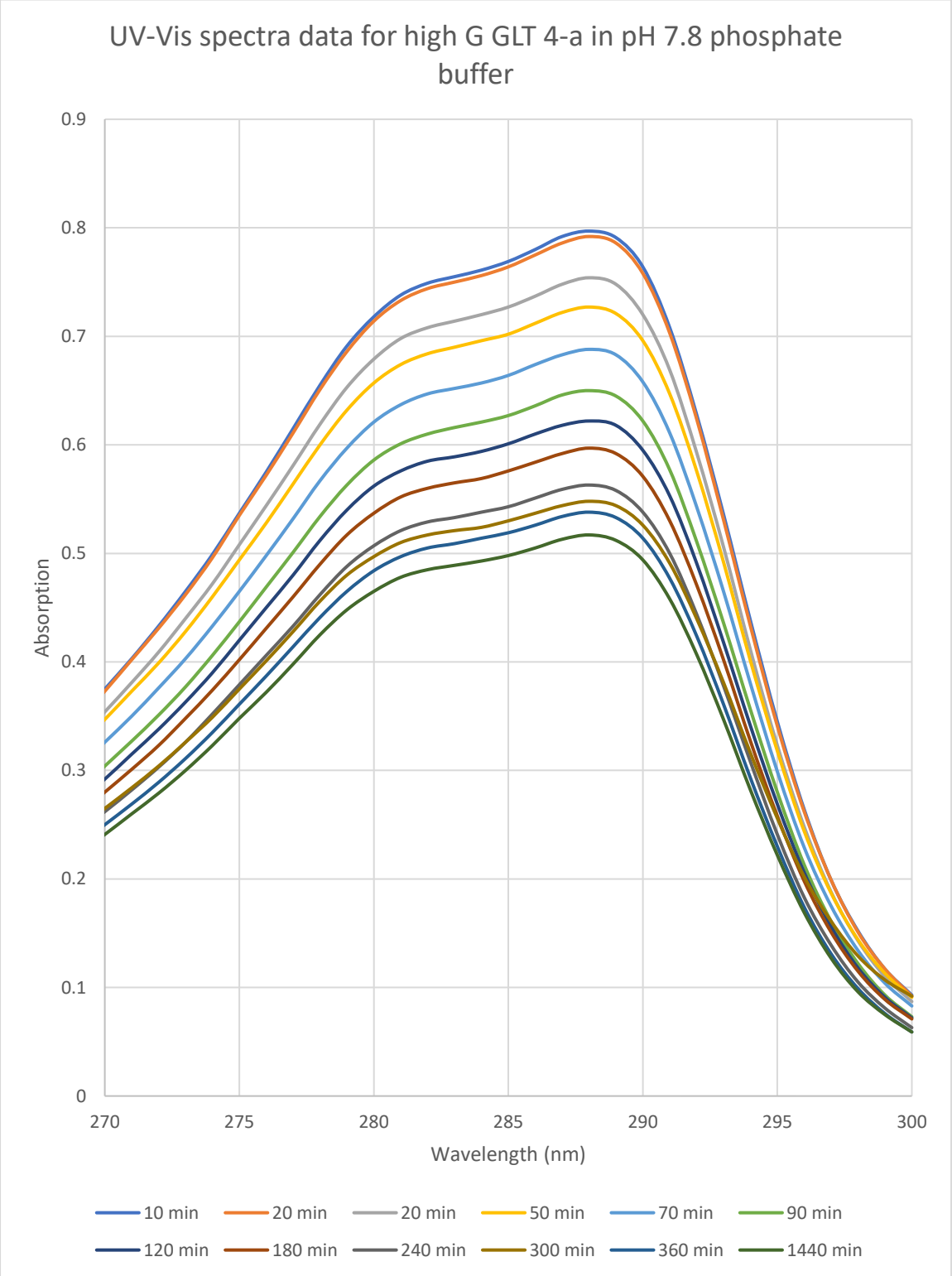

Figure 6- 36: UV-Vis spectra data for the first release of galantamine HBr over 24 hours, in pH 7.8 phosphate buffer solution, from a high G GLT 4 film.

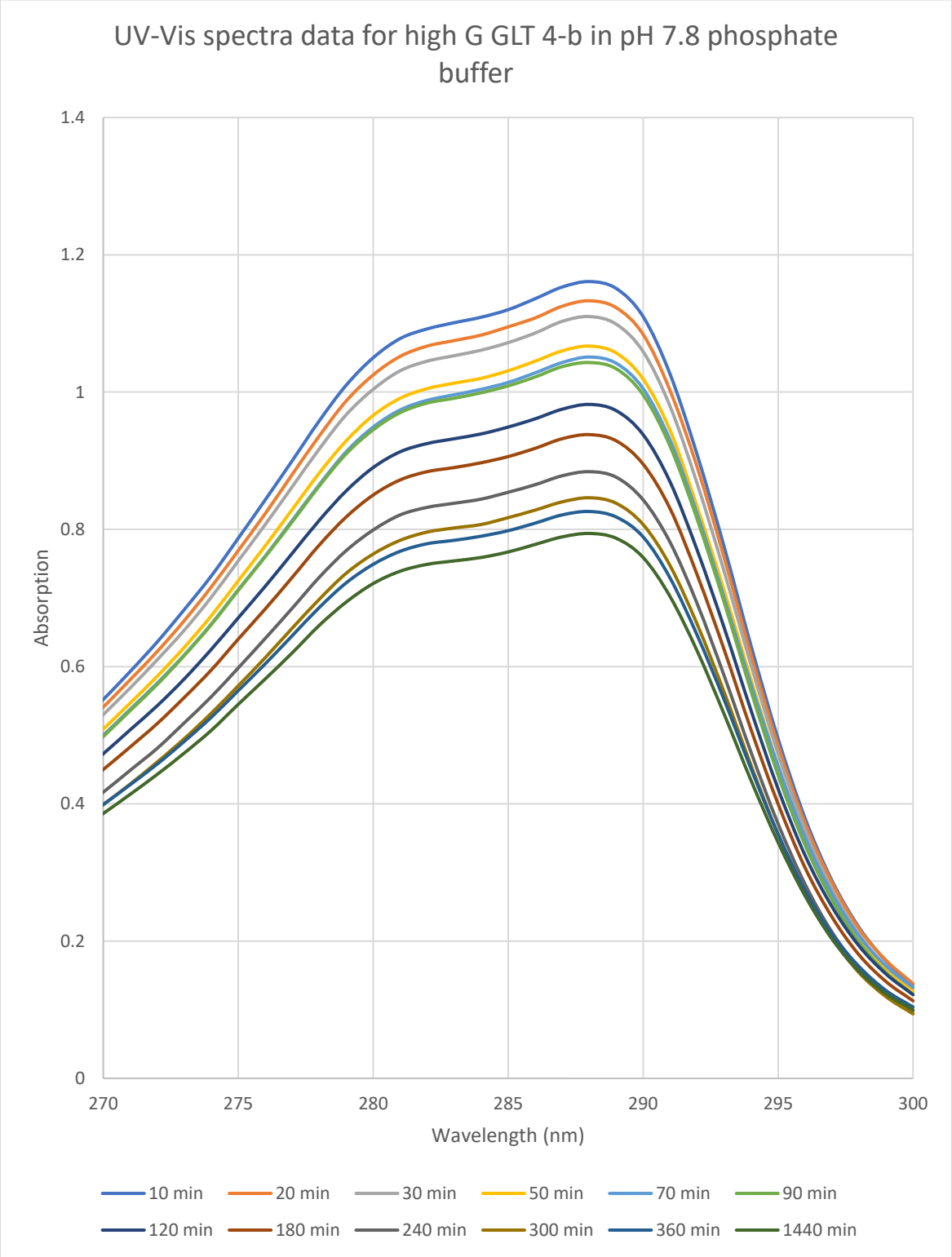

Figure 6- 37: UV-Vis spectra data for the second release of galantamine HBr over 24 hours, in pH 7.8 phosphate buffer solution, from a high G GLT 4 film.

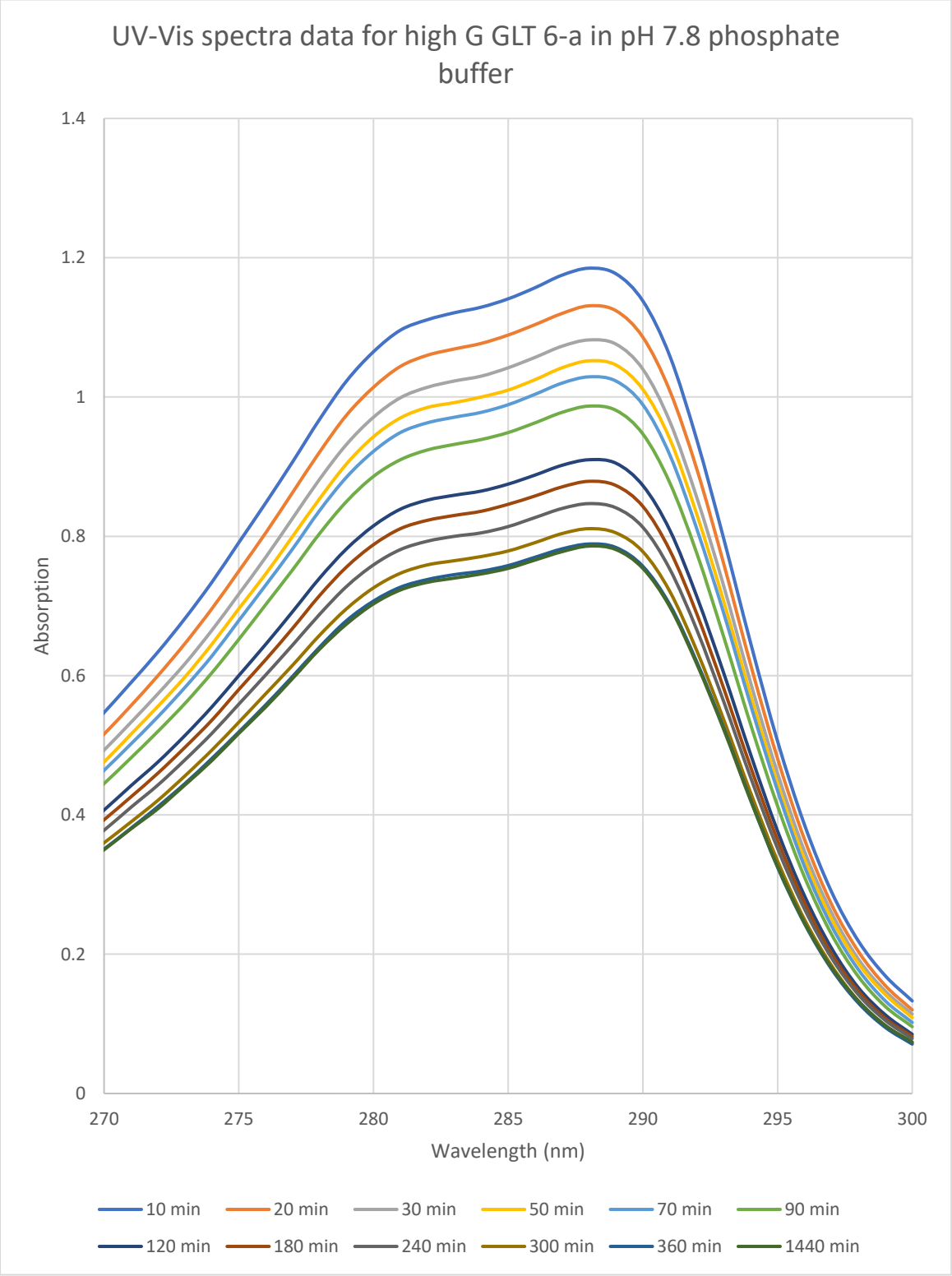

Figure 6- 38: UV-Vis spectra data for the first release of galantamine HBr over 24 hours, in pH 7.8 phosphate buffer solution, from a high G GLT 6 film.

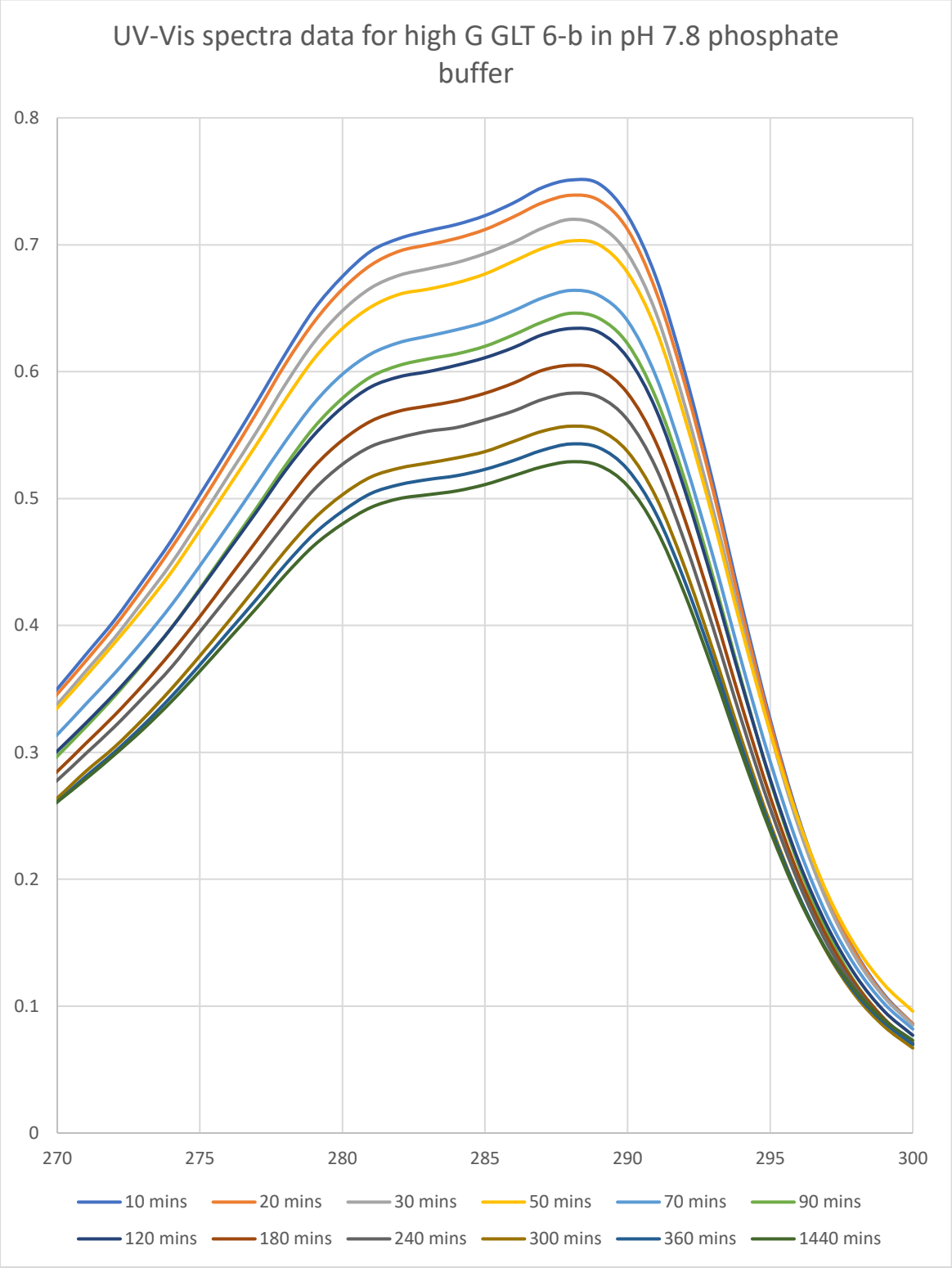

Figure 6- 39: UV-Vis spectra data for the second release of galantamine HBr over 24 hours, in pH 7.8 phosphate buffer solution, from a high G GLT 6 film.

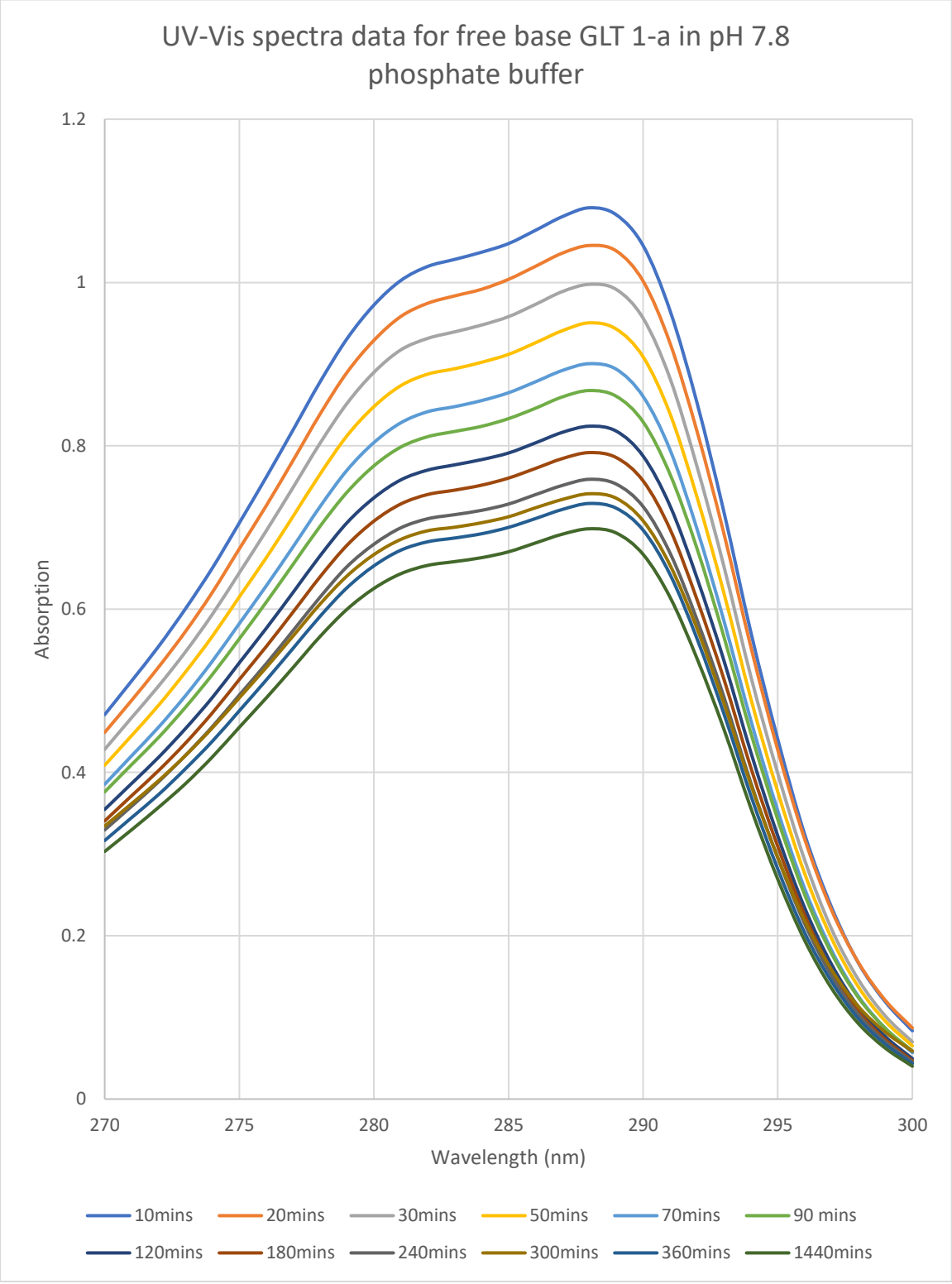

Figure 6- 40: UV-Vis spectra data for the first release of free base galantamine HBr over 24 hours, in pH 7.8 phosphate buffer solution, from a GLT 1 film.

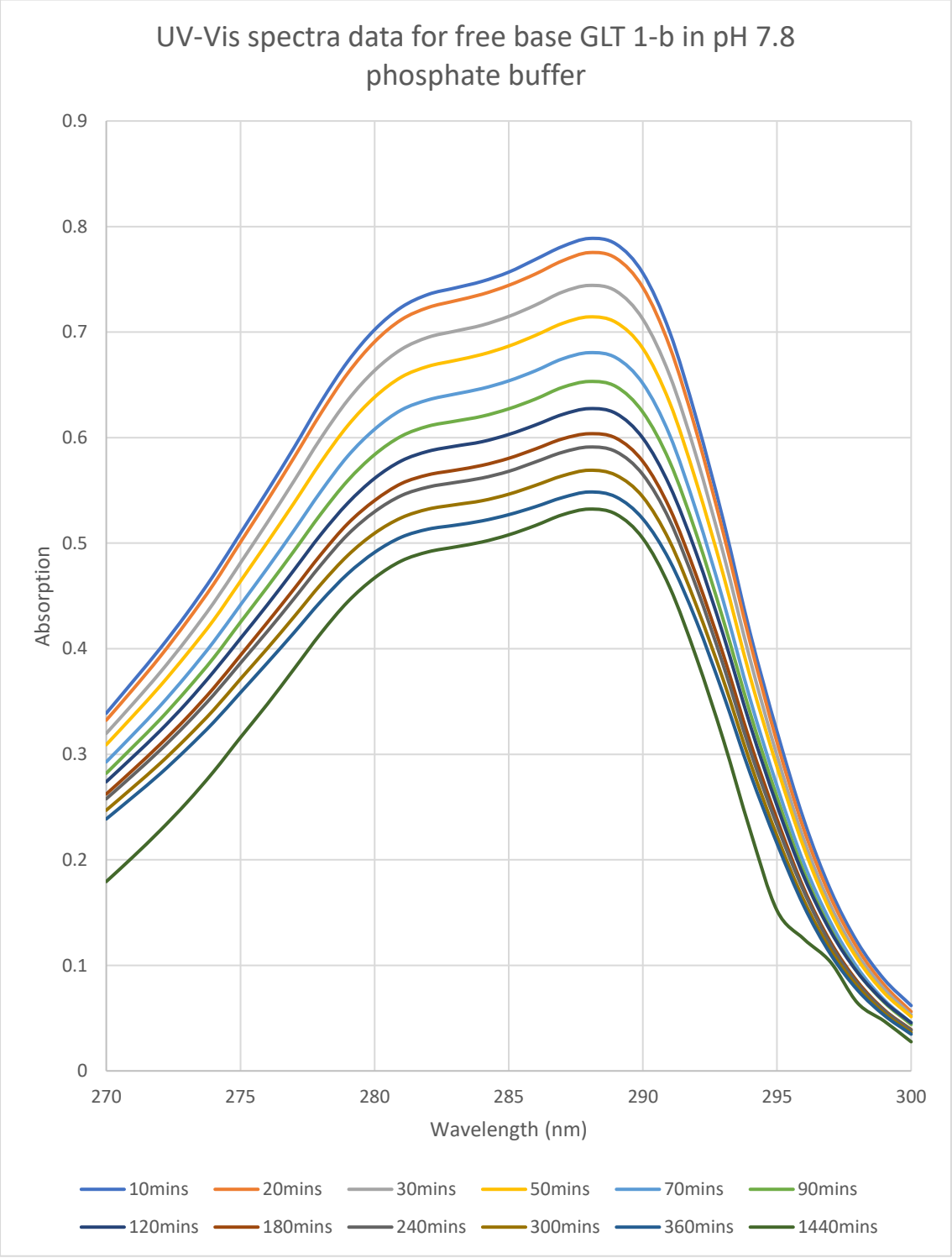

Figure 6- 41: UV-Vis spectra data for the second release of free base galantamine HBr over 24 hours, in pH 7.8 phosphate buffer solution, from a GLT 1 film.

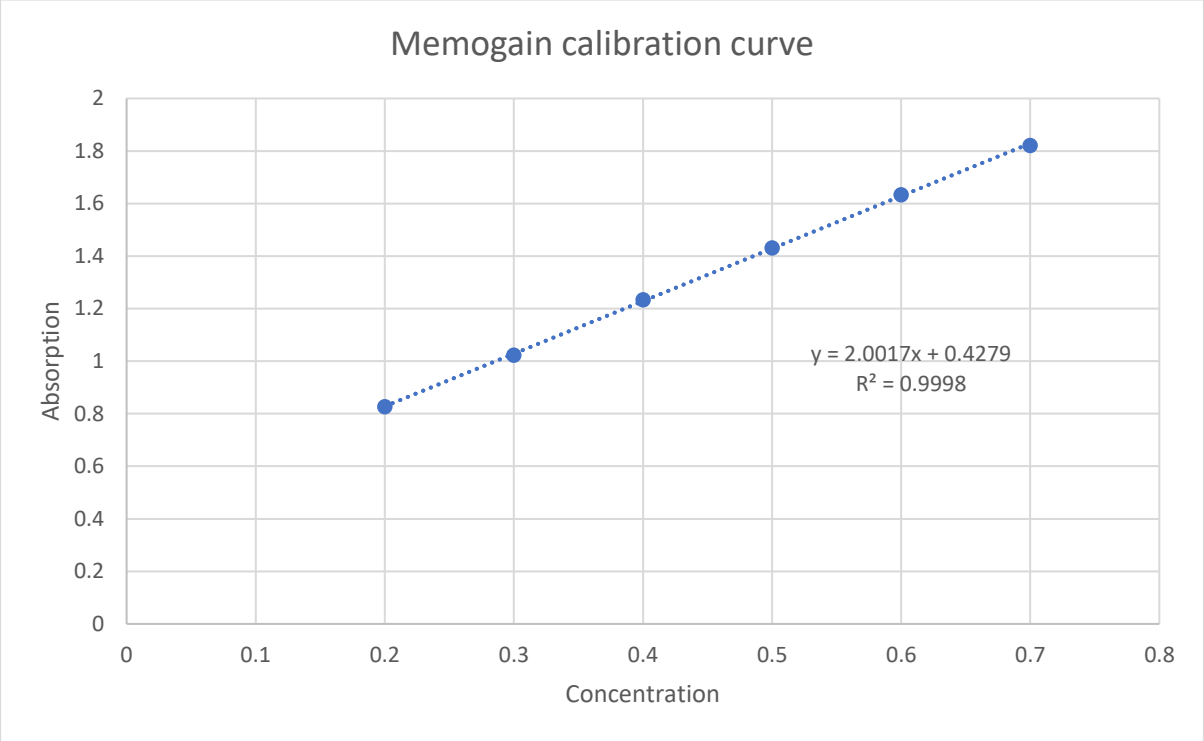

Figure 6- 42: Calibration curve for memogain.

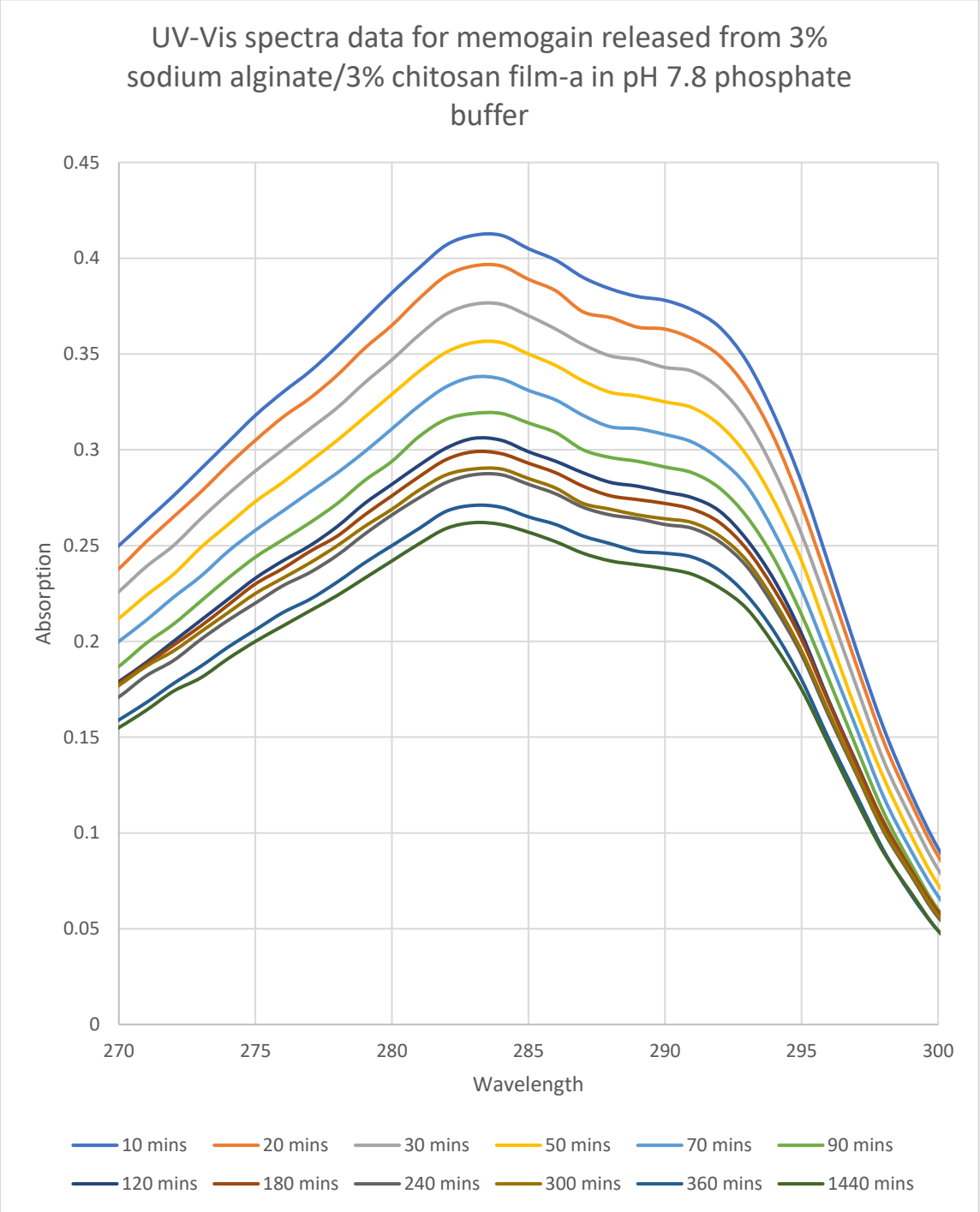

Figure 6- 43: UV-Vis spectra data for the first release of memogain over 24 hours, in pH 7.8 phosphate buffer solution, from a 3% sodium alginate and 3% chitosan film.

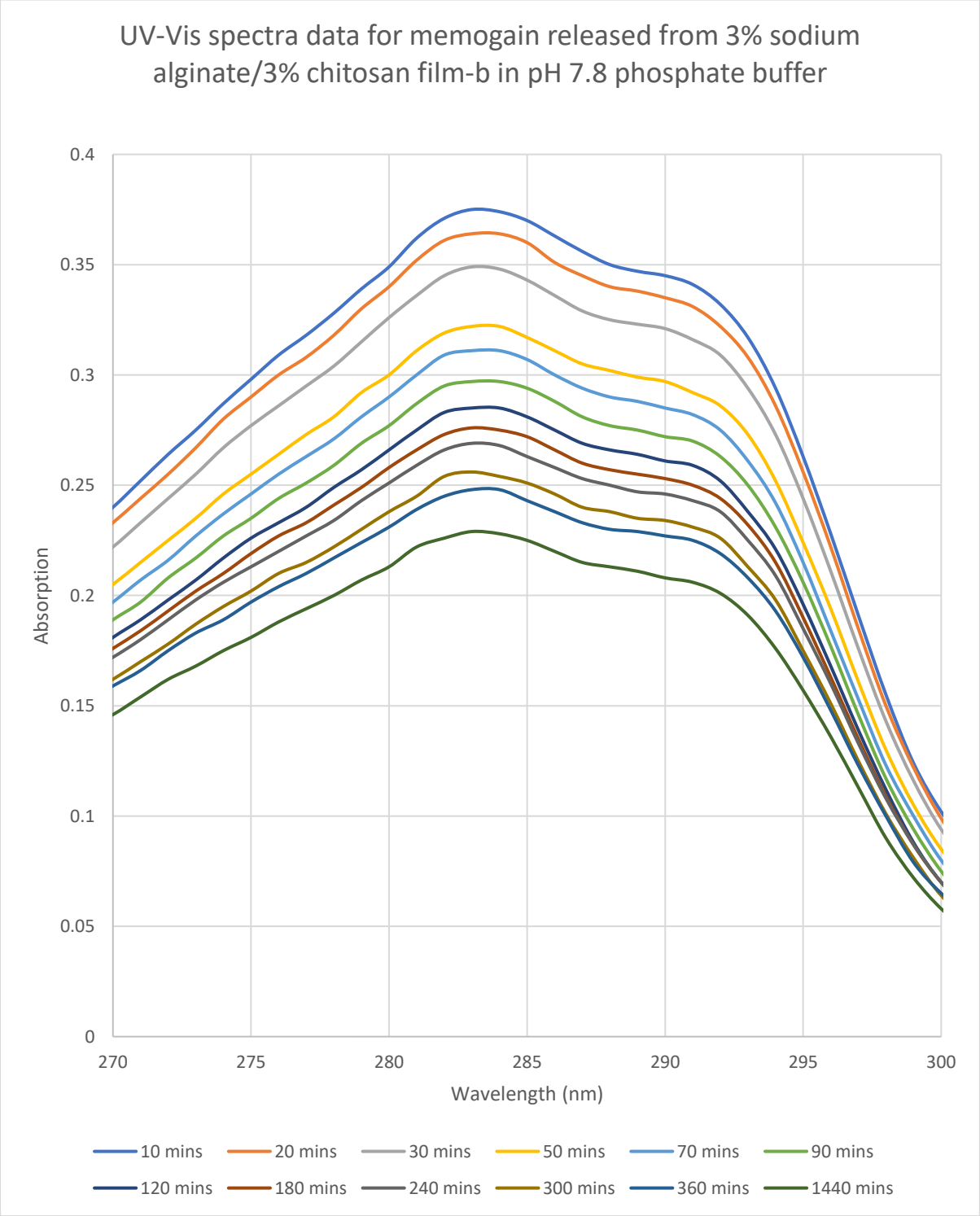

Figure 6- 44: UV-Vis spectra data for the second release of memogain over 24 hours, in pH 7.8 phosphate buffer solution, from a 3% sodium alginate and 3% chitosan film.

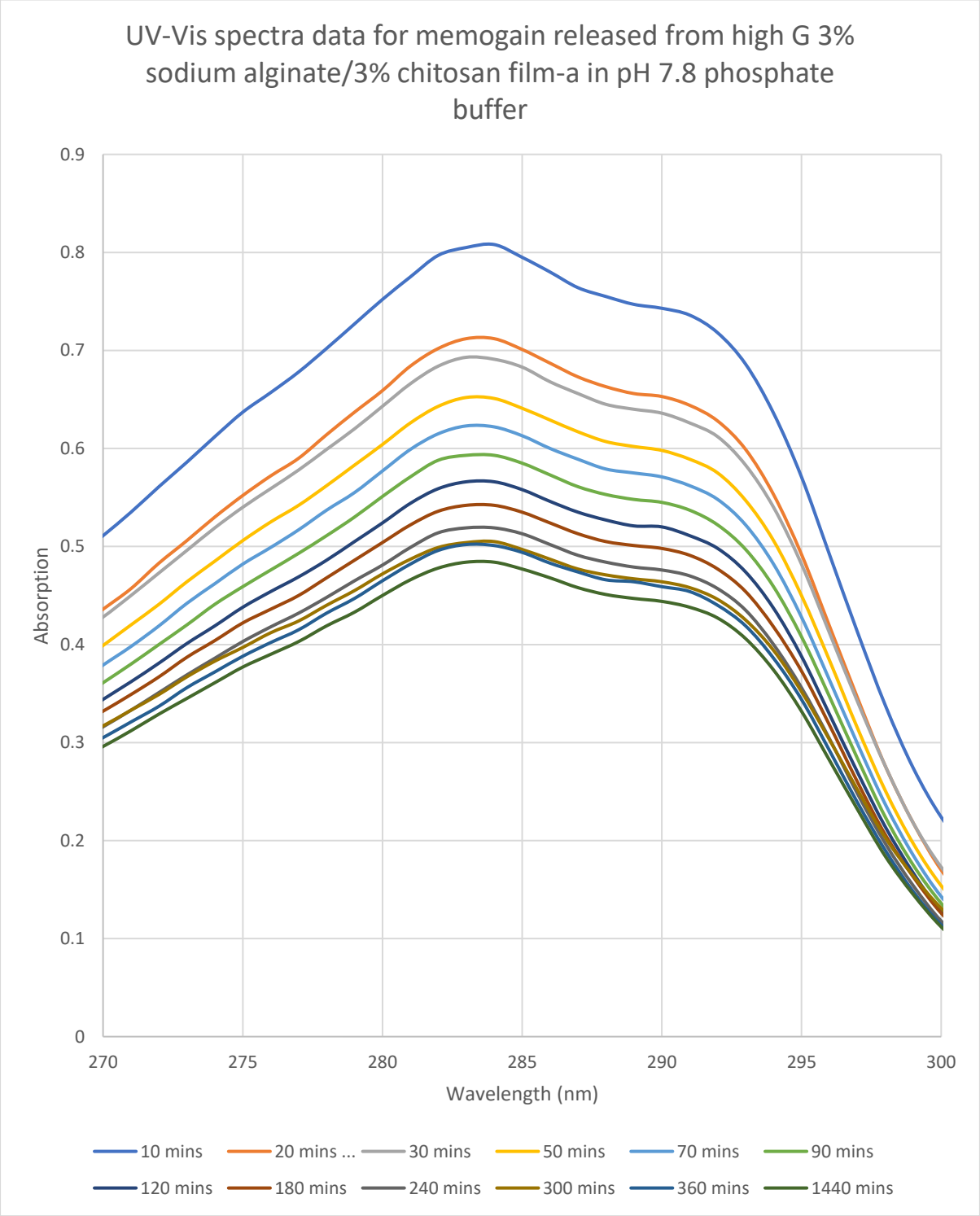

Figure 6- 45: UV-Vis spectra data for the first release of memogain over 24 hours, in pH 7.8 phosphate buffer solution, from a high G 3% sodium alginate and 3% chitosan film.

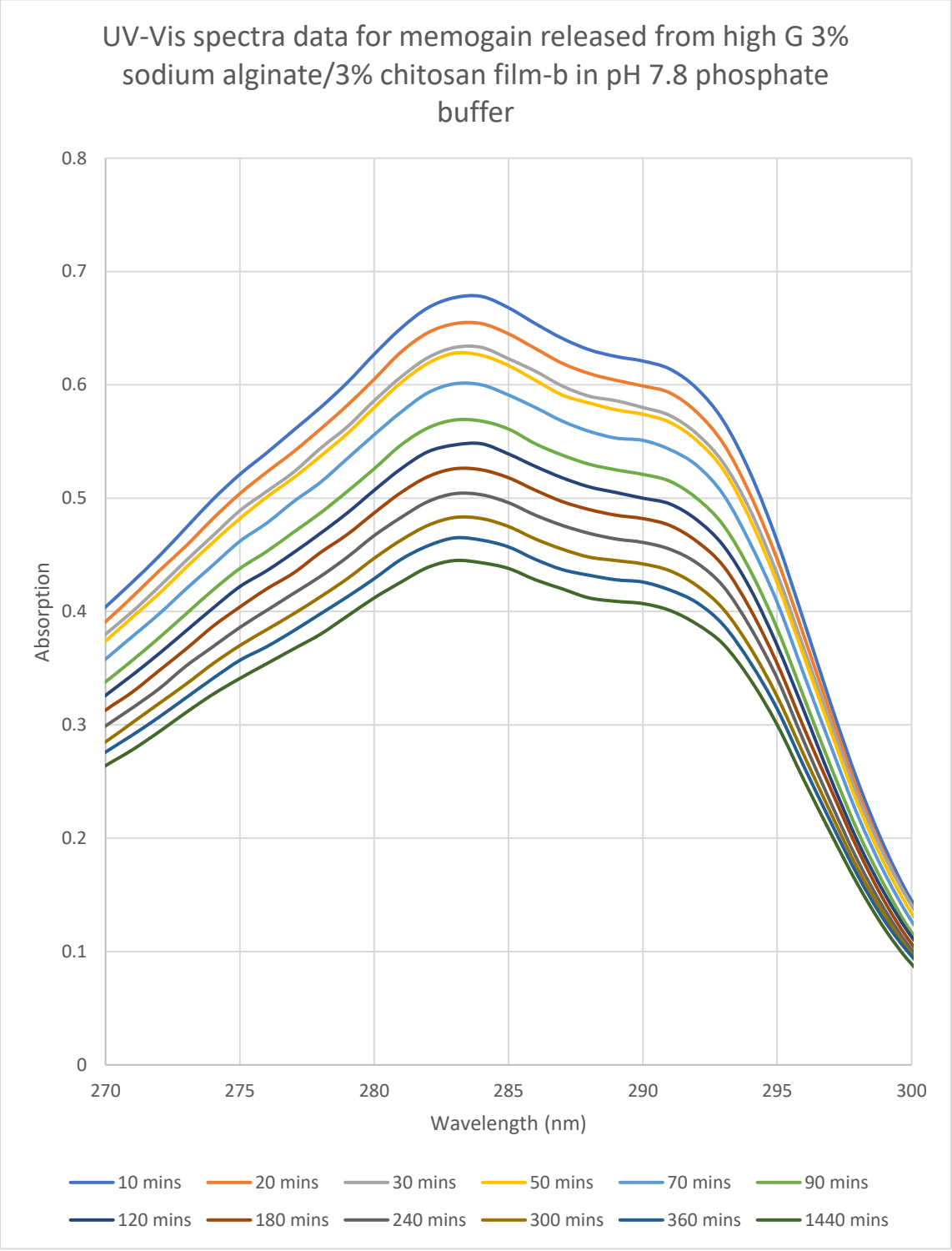

Figure 6- 46: UV-Vis spectra data for the second release of memogain over 24 hours, in pH 7.8 phosphate buffer solution, from a high G 3% sodium alginate and 3% chitosan film.

Table 6- 2: Weights of GLT films and the mass of galantamine HBr loaded in the film.

Film Name	Film Weight (mg)	Mass of Galantamine HBr in Film (mg)
GLT 1-a pH 7.8 PBS	74.26	15.66
GLT 1-b pH 7.8 PBS	86.20	18.07
GLT 1-a pH 4.0 PBS	28.20	6.21
GLT 1-b pH 4.0 PBS	31.91	6.97
GLT 1-a pH 9.2 PBS	43.83	9.61
GLT 1-b pH 9.2 PBS	37.92	8.37
GLT 2-a pH 7.8 PBS	66.11	9.79
GLT 2-b pH 7.8 PBS	56.29	8.38
GLT 3-a pH 7.8 PBS	79.08	8.45
GLT 3-b pH 7.8 PBS	54.37	5.90
GLT 4-a pH 7.8 PBS	59.24	6.47
GLT 4-b pH 7.8 PBS	60.89	6.59
GLT 5-a pH 7.8 PBS	44.81	4.85
GLT 5-b pH 7.8 PBS	49.92	5.41
GLT 6-a pH 7.8 PBS	84.60	17.93
GLT 6-b pH 7.8 PBS	72.34	17.45
GLT 7-a pH 4.0 PBS	37.11	6.53
GLT 7-b pH 4.0 PBS	113.28	18.88
GLT 8-a pH 7.8 PBS	41.24	9.02
GLT 8-b pH 7.8 PBS	30.93	6.80
GLT 9-a pH 7.8 PBS	57.49	6.08
GLT 9-a pH 7.8 PBS	51.39	5.45
High G GLT 1-a pH 7.8 PBS	63.51	13.57
High G GLT 1-b pH 7.8 PBS	70.04	14.96
High G GLT 4-a pH 7.8 PBS	92.76	9.66
High G GLT 4-b pH 7.8 PBS	140.55	14.06
High G GLT 6-a pH 7.8 PBS	116.82	23.74
High G GLT 6-b pH 7.8 PBS	96.61	20.71

Free Base GLT 1-a pH 7.8 PBS	66.94	14.09
Free Base GLT 1-b pH 7.8 PBS	46.80	10.10

Table 6- 3: Weights of memogain loaded galantamine and chitosan bio-based polymer films and the mass of memogain loaded in the film.

Film Name	**Film Weight (mg)**	**Mass of Galantamine HBr in Film (mg)**
3% Sodium Alginate/3% Chitosan, Low G - a	51.62	11.35
3% Sodium Alginate/3% Chitosan, Low G - b	51.65	11.18
3% Sodium Alginate/3% Chitosan, High G - a	55.30	11.80
3% Sodium Alginate/3% Chitosan, High G - b	44.54	9.45

6.8 Disulfanediylbis(ethane-2,1-diyl) diacrylate' (DSDA) monomer synthesis

6.8.1 Materials and quantities:

Table 6- 4: The materials and quantities used for the synthesis and purification of the DSDA monomer.

Material	Quantity
Triethylamine	22.3 mL
Chloroform	100 mL
2-hydroxyethyl disulfide	6.16 g
Acyl Chloride	12.6 mL
Water	750 mL
Na_2HCO_3	3.78 g
NaCl	0.88 g
$MgSO_4$	10.00 g
Dichloromethane (DCM)	150 mL

6.8.2 Synthesis Procedure of DSDA

2-hydroxyethyl disulfide (6.16 g, 39.94 mmol), chloroform (100 mL) and triethylamine (22.25 mL, 0.32 mol) were added into a 250 mL two-neck round bottom flask, cooled in ice bath while purged with nitrogen for 20 minutes. Acryloyl chloride (25.8 mL, 0.32 mol) was then added dropwise over 30 minutes, then the mixture sealed, and stirred for 36 hours under nitrogen atmosphere. A viscous yellow liquid was observed.

6.8.3 Purification Procedure of DSDA

The solution was filtered via vacuum filtration in order to remove salt by-product, and the filtrate was washed sequentially with water (2 x 75 mL), then with Na_2HCO_3 solution (6 x 75 mL, 0.1 M) and with NaCl solution (2 x 75 mL, 0.10 M) in a separating funnel. Upon visual observation of 2 clear layers, the organic layer was dried over magnesium sulphate, filtered and evaporated via rotary evaporation. The oil obtained was passed through an aluminium oxide column eluting with DCM (300 mL). After evaporation of the eluant a viscous dark brown liquid was obtained (8.45 g, 36.70 mmol) in 61% yield.

6.9 RAFT polymerization of '2-(diethylamino)ethyl methacrylate' (DMAEMA) with DSDA

3 polymers of different ratios of DMAEMA:DSDA ratios were synthesized using reversible addition-fragmentation chain transfer (RAFT) polymerization. RAFT agent used was '4-cyano-5-(((dodecylthio)carbonothioyl)thio)-4-methylpentanoic acid' (CDCTMA). Initiator used is 'azobis(isobutyronitrile)' (AIBN).

Table 6- 5: The materials and quantities used for the synthesis of the three PDMAEMA:DSDA copolymers.

Material	**Polymer Ratio and Material Quantity**		
	99:1	**95:5**	**9:1**
DMAEMA	5.36 g	5.36 g	5.36 g
DSDA	0.07 g	0.37 g	0.79 g
CDCTMA	0.11 g	0.59 g	1.25g
AIBN	0.05 g	0.23 g	0.49 g
THF	5.00 mL	5.00 mL	5.00 mL
Final % Yield	83.02%	78.06%	66.46%

The synthesis of the PDMAEMA:DSDA copolymers was achieved using the same method for each polymer ratio. The desired amounts of DMAEMA, DSDA, CDCTMA, AIBN and THF were added to a round bottom flask, and purged with nitrogen for 20 minutes. The reaction was then stirred for 16 hours at 60˚C. 2 mL of THF was added to each sample to dissolve polymers in order to allow for easier extraction from the round bottom flask. Polymer precipitation was achieved by pouring the reaction mixture into a 50 mL solution of stirring 7:1 hexane:diethyl ether. The solvent solution was then decanted, removing any unreacted monomers. The Polymers were purified further by re-dissolved in 6 mL of THF, then precipitated again into 80 mL 7:1 hexane:diethyl ether. The solvent solution was again decanted, removing any unreacted monomers. The solid products were dried in a vacuum oven at 40˚C, and 150atm for 24 hours.

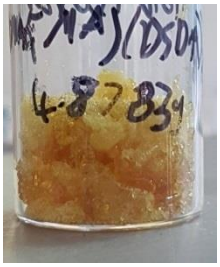

Figure 6- 47: 95:5 P(DMAEMA-co-DSDA) polymer after drying.

Observations:

Increasing the amount of DSDA increased the viscosity of the polymer and caused the yellow colouring to deepen.

99:1, a viscous pale yellow solid.

95:5, a very viscous yellow solid.

9:1, an extremely viscous deep yellow solid.

6.10 NIPAM Chain Extension

The 3 polymers of varying ratios (99:1, 95:5 and 9:1) chains were extended with NIPAM via RAFT polymerization. 2 g of each polymer were mixed with NIPAM (2 g, 16.67 mmol) and initiator '4,4'-azobis(4-cyanovalericacid)' (ACVA) (0.04 g, 0.35 mmol) in a round bottom flask. The synthesis of the PDMAEMA:DSDA:NIPAM copolymers was achieved using the same method for each polymer ratio. The desired amounts of DMAEMA, DSDA, CDCTMA, AIBN and THF were added to a round bottom flask, and purged with nitrogen for 20 minutes. The reaction was then stirred for 14 hours at 60˚C. 2 mL of THF was added to each sample to dissolve polymers in order to allow for easier extraction from the round bottom flask. Polymer precipitation was achieved by pouring the reaction mixture into a 50 mL solution of stirring 7:1 hexane:diethyl ether. The solvent solution was then decanted, removing any unreacted monomers. The Polymers were purified further by re-dissolved in 6 mL of THF, then precipitated again into 80 mL 7:1 hexane:diethyl ether. The solvent solution was again decanted, removing any unreacted monomers. The solid products were dried in a vacuum oven at 40˚C, and 150 atm for 24 hours.

Figure 6- 48: 95:5:95 P(DMAEMA-co-DSDA)-PNIPAM polymer after drying.

6.10.1 Observations and Percentage Yields

99:1:99, a clumpy pale yellow solid.	% Yield = 83.02%
95:5:95, a flaky yellow solid.	% Yield = 72.47%
9:1:9, an extremely viscous deep yellow solid.	% Yield = 70.32%

6.11 Solubility Testing Procedure

Two 10 mg samples of each polymer were subjected to basic and acidic conditions. The polymers were dissolved in 0.1 M NaOH solutions, but did not dissolve in 0.1 M HCl solutions. pH solutions of pKa 6.0, 6.8, 7.4 and 8.0 were produced using very dilute HCl (0.01 M) and NaOH (0.01 M) solutions, and adding the solutions dropwise to 250 mL deionlised H_2O. pH was determined by use of a calibrated pH meter in the solution at 21˚C.

Four 10 mg samples of each polymer were tested for their solubility in 1 mL of each pH solution at 21˚C.

Observation:

The polymers were dissolved in acidic pH solutions. Polymers did not dissolve in alkiline pH solutions. 99:1 PDMAEMA:DSDA polymer partially dissolved at pH 7.4.

6.12 LCST Testing

All 24 samples were individually heated to 50 ˚C. Samples which had previously dissolved precipitated back out at different temperatures. Upon precipitation, the LCST was recorded as the temperature at which precipitation occurred. Samples dissolved upon cooling to room temperature.

Observation:

No change for polymers in alkaline pH's. Cloudy white precipitation for polymers in acidic pH's.

Figure 6- 49: The 99:1 P(DMAEMA-co-DSDA) polymer in pH 6.0 solution upon precipitation at its LCST of 35.5 ˚C.

6.13 UV Testing of PDD and PDDN Polymers

A 17.5 mL solution of pH 6.8 was prepared by adding dilute HCl (0.01 M) dropwise to H_2O solution. pH was determined by use of a calibrated pH meter in the solution at 21˚C. Carmoisine dye solutions were prepared by adding carmoisine (3.5 mg) to 17.5 mL of pH 6.8 H_2O solution. Carmoisine solutions (2.5 mL) were added to seven separate sample vials. Six for each polymer, and one for a blank sample. Three PDMAEMA:DSDA, and the three PDMAEMA:DSDA:NIPAM 10 mg polymer samples were prepared and individually added to six of the sample vials containing carmoisine solution. The solution's heated to 50˚C to achieve precipitation. The samples were left for 1 hour for precipitations to settle at the bottom of the sample vials. Samples of 0.5 mL of each polymer/carmoisine solution were added to quartz cuvettes. A blank solution was run in UV spectrometer for wavelengths between 380 nm-700 nm (Visible spectrum). Samples were run in UV spectrometer for wavelengths between 380 nm-700 nm.

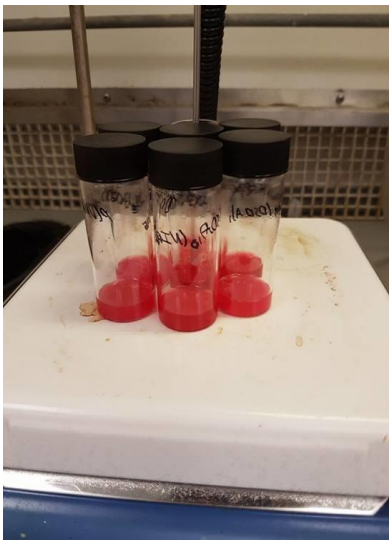

Figure 6- 50: The six carmoisine infused polymer solutions after heating to 50 ˚C.

6.14 PDD and PDDN NMR

Polymer samples were dissolved in $CDCl_3$ and analysed at 400 MHz.

^1H NMR obtained. Peaks were consistent in all NMR's. Intensities differed depending on polymer ratios.

PDD ^1H NMR σ [ppm] (400 MHz, $CDCl_3$): 0.89 (d, J 5.7Hz, **3H**), 1.05 (s, 3**H**), 1.26 (s, 8x**2H**), 1.34 (s, **2H**), 1.53 (s, **3H**), 1.82 (s, **2H**), 1.90 (s, **2H**), 2.12 (s, **2H**), 2.28 (s, 2x**3H**), 2.41 (s, **2H**), 2.57 (t, 4.0HZ, **2H**), 2.72 (s, **2H**), 2.89 (t, J 6.0Hz, **2H**), 3.35 (s, **2H**), 4.06 (t, J 6.0Hz, **2H**), 4.21 (s, **H**), 4.34 (t, J 6.0Hz, **2H**), 5.45 (s, **H**), 6.07 (s, H), 6.68 (s, **H**), 12.20 (s, **H**).

PDDN ^1H NMR σ [ppm] (400 MHz, $CDCl_3$): 0.89 (d, J 5.7Hz, **3H**), 1.05 (s, **3H**), 1.14 (d, J 4.0 Hz, **3H**), 1.19 (s, 8x**2H**), 1.25 (s, **2H**), 1.54 (s, **3H**), 1.85 (s, **2H**), 1.90 (s, **2H**), 2.12 (s, **2H**), 2.28 (s, 2x**3H**), 2.41 (s, **2H**), 2.58 (t, J 6.0Hz, **2H**) 2.72 (s, **2H**), 3.00 (t, J 6.0Hz, **2H**), 3.47 (s, **2H**), 3.74 (t, J 6.0Hz, **2H**), 3.85 (m, J 24.0Hz, **H**), 4.05 (m, J 20Hz, **H**), 4.35 (t, J 6.0Hz, **2H**), 5.45 (s, **H**), 6.07 (s, **H**),6.23 (s, **H**), 8.38 (s, **H**), 6.68 (s, **H**), 12.21 (s, **H**).

6.15 Mass Spectrometry Data

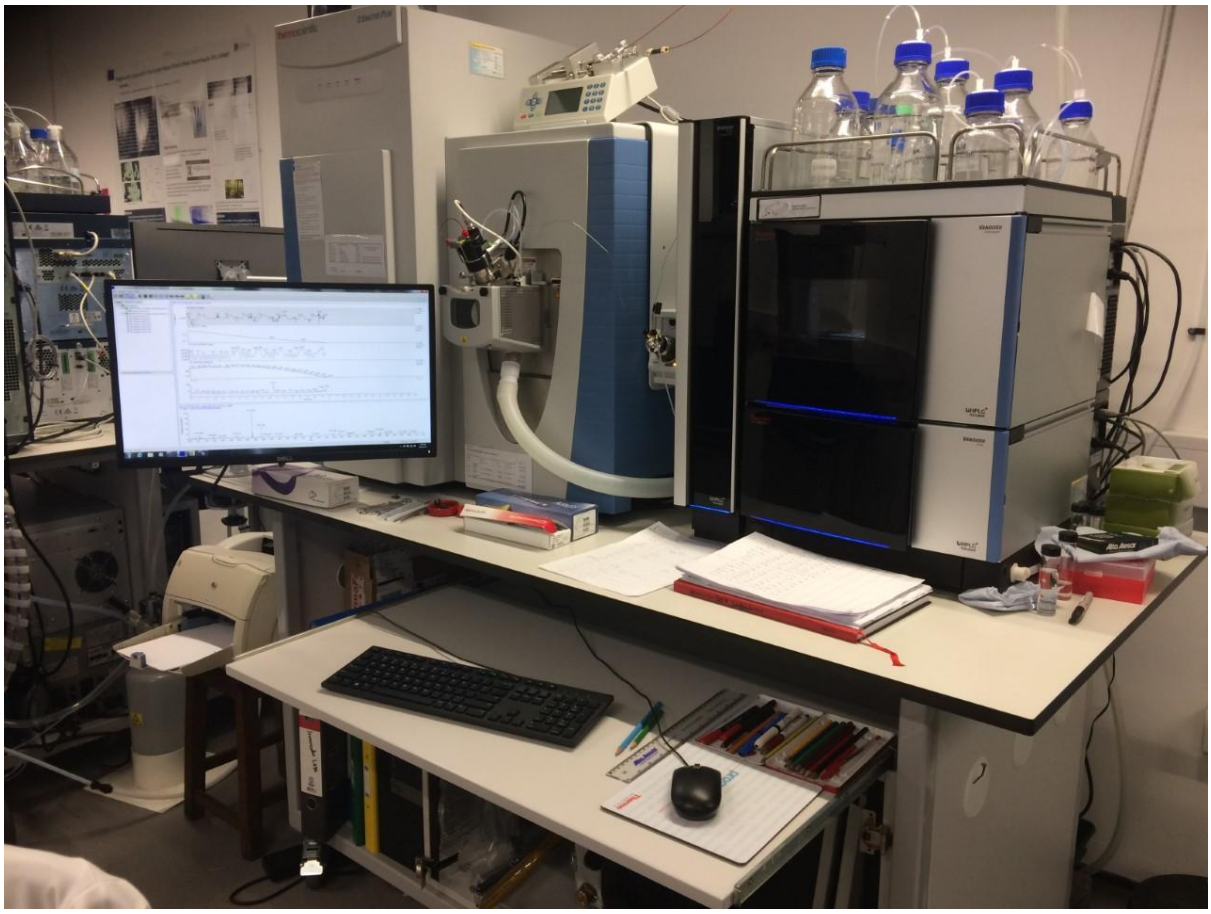

Figure 6- 51: All MS samples were analysed using the Thermo Fisher Q Exactive Plus mass spectrometer.

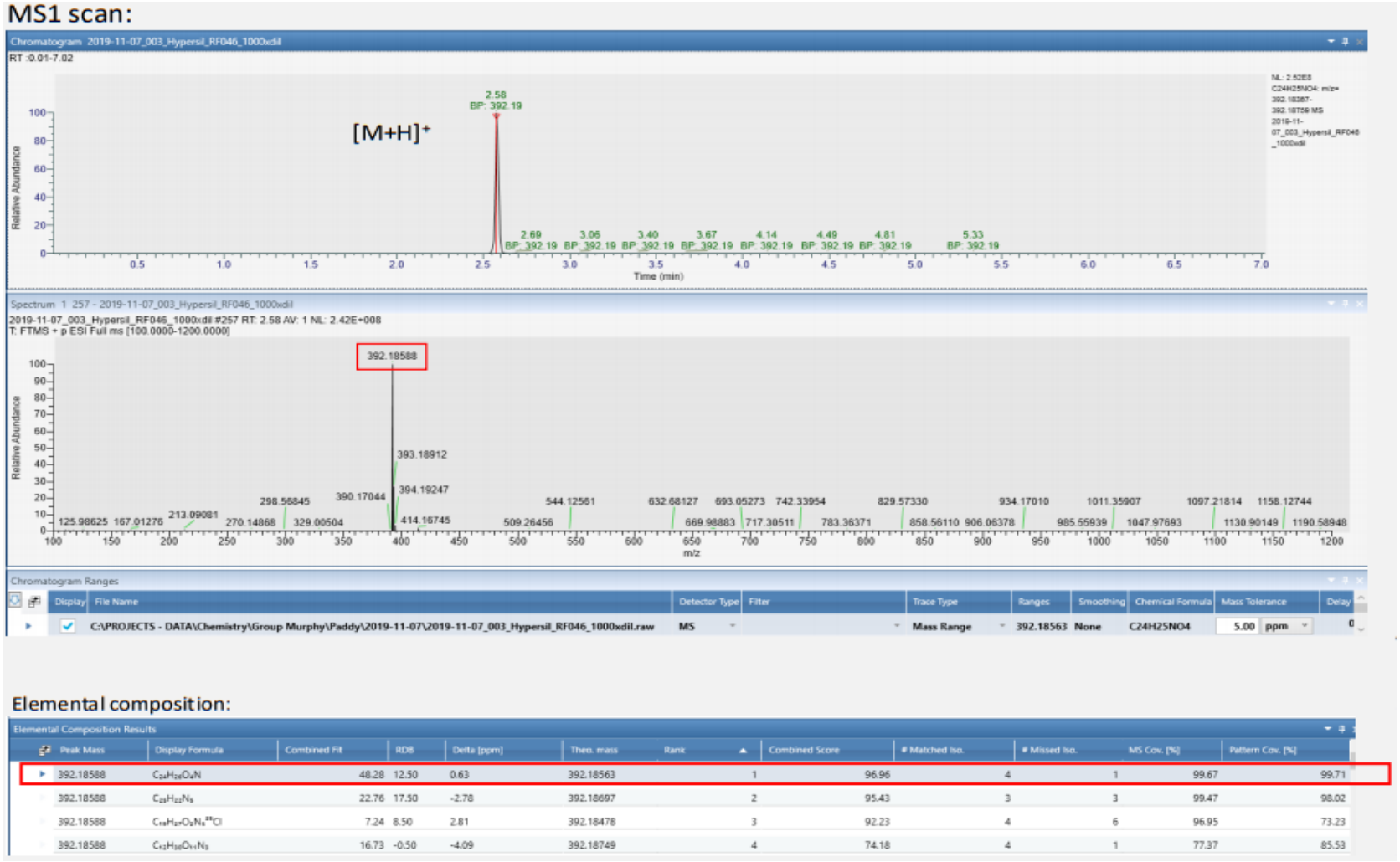

Figure 6- 52: Mass spectrometry data for memogain.